

DIELECTRIC STUDIES OF RIGID AND FLEXIBLE
MOLECULES IN VARIOUS MEDIA

A Thesis Submitted To
Lakehead University
Thunder Bay, Ontario, Canada

by

© MOHAMMED SABER AHMED

in partial fulfillment of the
requirements for the degree of

MASTER OF SCIENCE

1984

ProQuest Number: 10611697

All rights reserved

INFORMATION TO ALL USERS

The quality of this reproduction is dependent upon the quality of the copy submitted.

In the unlikely event that the author did not send a complete manuscript and there are missing pages, these will be noted. Also, if material had to be removed, a note will indicate the deletion.



ProQuest 10611697

Published by ProQuest LLC (2017). Copyright of the Dissertation is held by the Author.

All rights reserved.

This work is protected against unauthorized copying under Title 17, United States Code
Microform Edition © ProQuest LLC.

ProQuest LLC.
789 East Eisenhower Parkway
P.O. Box 1346
Ann Arbor, MI 48106 - 1346

"If anyone wishes to search out the truth of things in serious earnest, he ought not to select special science; for all sciences are co-joined with each other and interdependent"...

Descartes, rules for the direction
of the mind

TO MY PARENTS

ABSTRACT

This thesis investigates mainly the molecular and intramolecular relaxation processes of some aromatic and aliphatic molecules containing rotatable polar groups and some analogous rigid molecules dispersed in (a) atactic polystyrene matrices and (b) cis-decalin. Sample preparations and the dielectric measurements using General Radio 1615A and 1621 Capacitance bridges with appropriate temperature controllable cells have been described. The glass transition temperature (T_g) measurements using the Glass Transition Apparatus have also been described. The experimental data as a function of frequency at different temperatures were subject to analysis by a series of computer programs written in APL language. The activation energy barriers opposing the dielectric relaxation processes were obtained by the application of the Eyring rate equation.

Of the spherically shaped rigid polar molecules examined in cis-decalin, both β - and α -relaxations are detected in most of the compounds. Dielectric data for α -relaxations are described by the Cole-Davidson skewed arc function. The ΔH_E values of the β -process increase appropriately with molecular size but are largely in-

dependent of the glassy medium. The β -processes for these systems are attributed to molecular relaxation which may possibly occur in a "solvent cavity".

Of the aromatic flexible molecules, a variety of anisoles have been studied in cis-decalin. In the systems studied methoxy group relaxation except for the para-fluoro-anisole. The barrier to methoxy group rotation is independent of para-substitution and the choice of solvent.

In the long chain polar molecules of the types $\text{CH}_3(\text{CH}_2)_n\text{X}$ (where $\text{X} = -\text{CH}_2\text{Br}$, $-\text{COCH}_3$ and $-\text{NH}_2$) and $[\text{CH}_3(\text{CH}_2)_n]_2\text{Y}$ (where $\text{Y} = \begin{array}{c} \text{O} \\ \parallel \\ \text{C} \end{array}$, S , O and $\text{N} \begin{array}{l} \diagup \\ \diagdown \end{array} \text{H}$) where n lies in the range between 2 to 20 two distinct relaxation processes are found for molecules with $n < 6$ in a polystyrene matrix. Both ΔH_E and relaxation time are found to increase with the increase in the number of carbon atoms in the chain for the low temperature absorption. The nature of polar end groups has negligible influence on the relaxation time and ΔH_E values for the low temperature absorption of molecules of the type $\text{CH}_3(\text{CH}_2)_n\text{X}$. The low temperature absorption which is insensitive to the viscosity of the media identified as the intramolecular rotation about the C-C bonds involving the movement of the polar group. The high temperature absorption is attributed to

molecular rotation. The location of dipole away from the chain end has negligible influence on the relaxation time and ΔH_E values for the low temperature absorption of long chain amines and ketones.

The data for the long chain polar molecules may be successfully analyzed in terms of a model which involves a molecular relaxation process (governed by a μ_m movement) and segmental motion involving movement of the polar group (characterized by a μ_s dipole moment). The extrapolated values of μ_m and μ_s at 330 K lead to a molecular dipole moment in reasonable agreement with literature values.

ACKNOWLEDGEMENTS

It gives me great pleasure to express my sincere appreciation and great admiration to Professor S. Walker, my research supervisor, for stimulating freedom of thought and constant encouragement throughout the course of this work, which will inspire me always. I am especially indebted to him for many invaluable suggestions and critical comments, and for being available at any time for discussion, involving much of his valuable time, particularly in reviewing the manuscript of this thesis.

I am grateful to Dr. M. A. Saleh of the Department of Chemistry, University of Chittagong, Bangladesh, formerly a post-doctoral fellow in the Department of Chemistry at Lakehead University for encouragement and helpful discussions in this regard. I am thankful to fellow research colleagues Dr. M. A. Desando, Mr. D. L. Gourlay, Mr. M. A. Kashem, Mr. M. S. Hossain, Miss J. C. N. Chao, Mr. M. E. Huque and Mr. M. A. Siddiqui for various important discussions.

Thanks are also due to Mrs. J. Parnell for her work in typing this thesis in a very short time, to Mr. B. K. Morgan for his invaluable technical assistance and

to all members of this department for their co-operation. I gratefully acknowledge financial support for this work by the Lakehead University through teaching assistantships and by the National Research Council of Canada for research assistantships during 1982-1984.

Finally and very importantly, with special gratitude to my wife, Dr. Taslima, I acknowledge her helping me in computer analyses, exceptional patience and understanding in allowing me to devote sufficient time and the privilege of working mostly in the laboratory, when she looked after the household work.

Thunder Bay

Author

August 1, 1984

CONTENTS

	<u>PAGE</u>
TITLE PAGE.....	i
ABSTRACT.....	iii
ACKNOWLEDGEMENTS.....	vi
LIST OF TABLES.....	xi
LIST OF FIGURES.....	xv
CHAPTER I: INTRODUCTION AND BASIC THEORY.....	1
Introduction.....	2
Basic Theory.....	8
References.....	24
CHAPTER II: EXPERIMENTAL MEASUREMENTS.....	26
Introduction.....	27
Three Terminal Co-axial Cells.....	29
The General Radio Bridges.....	33
Sample Preparations and Dielectric Measurements.....	35
Glass Transition Apparatus.....	38
Analysis of Experimental Data.....	40
References.....	45
CHAPTER III: α - and β -RELAXATIONS OF SOME RIGID POLAR MOLECULES IN cis-DECALIN.....	46
Introduction.....	47
Experimental Results.....	49
Discussion.....	50
References.....	64

	<u>PAGE</u>
CHAPTER IV: DIELECTRIC RELAXATION OF SOME ANISOLES IN cis-DECALIN.....	96
Introduction.....	97
Experimental Results.....	101
Discussion.....	102
References.....	108
CHAPTER V: DIELECTRIC RELAXATION OF SOME 1-BROMOALKANES IN A POLYSTYRENE MATRIX.....	123
Introduction.....	124
Experimental Results.....	127
Discussion.....	129
References.....	143
CHAPTER VI: DIELECTRIC RELAXATION OF SOME BROMOSUBSTITUTED ALKANES IN POLYSTYRENE AND POLYPROPYLENE MATRICES.....	166
Introduction.....	167
Experimental Results.....	171
Discussion.....	173
References.....	185
CHAPTER VII: DIELECTRIC RELAXATION OF SOME 2-ALKANONES AND 1-AMINOALKANES IN A POLYSTYRENE MATRIX.....	215
Introduction.....	216
Experimental Results.....	222
Discussion.....	224
References.....	236

	<u>PAGE</u>
CHAPTER VIII: DIELECTRIC RELAXATION OF SOME SYMMETRICALLY SUBSTITUTED ETHERS, KETONES, SULFIDES AND AMINES IN A POLYSTYRENE MATRIX.....	272
Introduction.....	273
Experimental Results.....	279
Discussion.....	283
References.....	295
CHAPTER IX: CONCLUSIONS AND SUGGESTIONS FOR FURTHER WORK.....	335
Conclusions.....	336
Suggestions for further work.....	345
PUBLICATIONS.....	347

LIST OF TABLES

	<u>PAGE</u>
TABLE III-1: Eyring analysis Results for β -relaxation of rigid polar molecules in cis-decalin.....	66
TABLE III-2: Eyring analysis results for α -relaxation of rigid polar molecules in cis-decalin.....	68
TABLE III-3: Fuoss-Kirkwood analysis parameters for rigid polar molecules in cis-decalin.....	69
TABLE IV-1: Eyring analysis results for some anisoles in cis-decalin...	110
TABLE IV-2: Fuoss-Kirkwood parameters for some anisoles in cis-decalin...	111
TABLE V-1: Eyring analysis results for the low temperature absorption of 1-bromoalkanes.....	145
TABLE V-2: Eyring analysis results for the higher temperature absorption of 1-bromoalkane in a polystyrene matrix.....	146
TABLE V-3: μ_s , μ_m and μ_{eff} for 1-bromoalkane in a polystyrene matrix.....	147
TABLE V-4: ΔE_0 values for 1-bromoalkane in a polystyrene matrix.....	148

List of Tables continued...

	<u>PAGE</u>
TABLE V-5: Fuoss-Kirkwood analysis parameters, ϵ_{∞} and μ at various temperatures for l-bromoalkanes.....	149
TABLE VI-1: Eyring parameters for the low temperature absorption of bromooctanes.....	186
TABLE VI-2: Eyring parameters for the high temperature absorption of bromooctanes.....	187
TABLE VI-3: Eyring activation parameters for some bromoheptanes and bromopentanes in a polystyrene matrix.....	188
TABLE VI-4: Comparison of Eyring activation parameters for l-bromoalkanes and α,ω -dibromoalkanes in a polystyrene matrix.....	189
TABLE VI-5: Maximum loss factors for some molecules in polystyrene and polypropylene at 50.2 Hz.....	190
TABLE VI-6: μ_s , μ_m and μ_{eff} for some bromo-substituted alkanes in a polystyrene matrix.....	191
TABLE VI-7: Fuoss-Kirkwood parameters, ϵ_{∞} and μ at various temperatures for some bromoalkanes in a polystyrene matrix..	192
TABLE VII-1: Relaxation time and Eyring activation parameters for the low temperature absorption of $CH_3(CH_2)_2X$ (where X = $-CH_2OH$, $-CH_2Br$, $-COCH_3$ and $-NH_2$) in a polystyrene matrix.....	237

List of Tables continued...

	<u>PAGE</u>	
TABLE VII-2:	Relaxation time and Eyring activation parameters for the higher temperature absorption of $\text{CH}_3(\text{CH}_2)_n\text{X}$ (where X = $-\text{CH}_2\text{Br}$, $-\text{CH}_2\text{OH}$, $-\text{COCH}_3$ and $-\text{NH}_2$) in a polystyrene matrix..	240
TABLE VII-3:	μ_s , μ_m and μ_{eff} for $\text{CH}_3(\text{CH}_2)_n\text{COCH}_3$ in a polystyrene matrix..	243
TABLE VII-4:	μ_s , μ_m and μ_{eff} for $\text{CH}_3(\text{CH}_2)_n\text{NH}_2$ in a polystyrene matrix....	244
TABLE VII-5:	ΔE_0 values for $\text{CH}_3(\text{CH}_2)_n\text{X}$ (where X = $-\text{COCH}_3$ and $-\text{NH}_2$) in a polystyrene matrix.....	245
TABLE VII-6:	Fuoss-Kirkwood parameters, ϵ_∞ and μ at various temperatures for 2-alkanones and 1-aminoalkanes in a polystyrene matrix.....	246
TABLE VIII-1:	Eyring activation parameters for the low temperature absorption of $[\text{CH}_3(\text{CH}_2)_n]_2\text{X}$ (where X = $\begin{array}{c} \text{O} \\ \\ \text{C} \end{array}$, S , O , and $\text{N} \begin{array}{l} \diagup \\ \diagdown \end{array} \text{H}$) in a polystyrene matrix.....	296
TABLE VIII-2:	Comparison of Eyring activation parameters for $\text{CH}_3(\text{CH}_2)_n\text{COCH}_3$ and $[\text{CH}_3(\text{CH}_2)_n]_2\text{CO}$ for a given total number of carbon atoms in a polystyrene matrix.....	299

List of Tables continued...

	<u>PAGE</u>
TABLE VIII-3: Comparison of Eyring activation parameters for $\text{CH}_3(\text{CH}_2)_n\text{NH}_2$ and $[\text{CH}_3(\text{CH}_2)_n]_2\text{NH}$ in a polystyrene matrix.....	300
TABLE VIII-4: Eyring activation parameters for the high temperature absorption of $[\text{CH}_3(\text{CH}_2)_n]_2\text{CO}$ in a polystyrene matrix.....	301
TABLE VIII-5: μ_s , μ_m and μ_{eff} for $[\text{CH}_3(\text{CH}_2)_n]_2\text{CO}$ in a polystyrene matrix.....	302
TABLE VIII-6: ΔE_0 values for $[\text{CH}_3(\text{CH}_2)_n]_2\text{CO}$ in a polystyrene matrix.....	303
TABLE VIII-7: Fuoss-Kirkwood parameters, ϵ_∞ and μ at various temperatures for $[\text{CH}_3(\text{CH}_2)_n]_2\text{X}$ (where X = $\begin{matrix} \text{O} \\ \parallel \\ \text{C} \end{matrix}$, O , S and $\text{N} \begin{matrix} \text{H} \\ \diagup \end{matrix}$) in a polystyrene matrix.....	304
TABLE IX-1: Summaries of the results of long chain polar molecules in a polystyrene matrix (low temperature absorption).....	343
TABLE IX-2: Summaries of the results of long chain polar molecules in a polystyrene matrix (high temperature absorption).....	344

LIST OF FIGURES

	<u>PAGE</u>
FIGURE I-1: Loss tangent curve.....	13
FIGURE I-2: Plot of total polarization versus log frequency.....	14
FIGURE I-3a: Potential energy diagram for dipole rotating in a solid with energy barrier ΔG_E and equilibrium positions of equal energy.....	21
FIGURE I-3b: Potential diagram for rotating dipole with unequal potential minima.....	21
FIGURE II-1: Three terminal co-axial cell....	32
FIGURE II-2: Parallel plate capacitor cell...	32
FIGURE II-3: Glass Transition Temperature Measurement Apparatus.....	39
FIGURE III-1: Plot of $\log T\tau$ versus $1/T$ (K^{-1}) for methyl iodide in cis-decalin.	74
FIGURE III-2: Cole-Cole plots for methyl- iodide in cis-decalin.....	75

List of Figures continued...

	<u>PAGE</u>
FIGURE III-3: Plots of ϵ'' versus T(K) for 1,1,1-trichloroethane in cis-decalin.....	76
FIGURE III-4: Plots of ϵ'' versus T(K) for 2,2-dichloropropane in cis-decalin.....	77
FIGURE III-5: Plot of ϵ'' versus T(K) for 2-methyl-2-chloropropane in cis-decalin.....	78
FIGURE III-6: Plots of ϵ'' versus T(K) for 2-methyl-2-bromopropane in cis-decalin.....	79
FIGURE III-7: Plot of $\log T\tau$ versus $1/T$ (K^{-1}) for 2-methyl-2-bromopropane in cis-decalin.....	80
FIGURE III-8: Plots of ϵ'' versus T(K) for methyl trichlorosilane in cis-decalin.....	81
FIGURE III-9: Plots of ϵ'' versus log frequency for bromoform in cis-decalin....	82
FIGURE III-10: Plots of $\log T\tau$ versus $1/T$ (K^{-1}) for bromoform in o-terphenyl, polyphenyl ether polystyrene and cis-decalin.....	83
FIGURE III-11: Plots of ϵ'' versus T(K) for o-dichlorobenzene in G.O.T.P., P.S., S.V. and cis-decalin.....	84

List of Figures continue...

	<u>PAGE</u>
FIGURE III-12: Plots of $\log T\tau$ versus $1/T$ (K^{-1}) for o-dichlorobenzene in P.S., G.O.T.P., S.V. and cis-decalin.....	85
FIGURE III-13: Plots of ϵ'' versus $T(K)$ for o-bromo-chlorobenzene in cis-decalin.....	86
FIGURE III-14: Plots of ϵ'' versus $T(K)$ for o-bromotoluene in cis-decalin.....	87
FIGURE III-15: Plots of ϵ'' versus $T(K)$ for 4-methylpyridine in cis-decalin..	88
FIGURE III-16: Cole-Cole plots for 4-methylpyridine in cis-decalin.....	89
FIGURE III-17: Plots of ϵ'' versus $T(K)$ for trichloroethylene in cis-decalin.	90
FIGURE III-18: ϵ'' versus $\log \nu$ plots for 2,2-dichloropropane in cis-decalin...	91
FIGURE III-19: Plots of $\log T\tau$ versus $1/T$ (K^{-1}) for (a) t-butylisothiocyanate, (b) t-butylcyanide, (c) nitrobenzene, and (d) trichloroethylene in cis-decalin.....	92
FIGURE III-20: Cole-Cole plots for 2-methyl-2-chloropropane in cis-decalin.....	93
FIGURE III-21: Cole-Cole plots for (a) 2-methyl-2-chloropropane, (b) 2,2-dichloropropane, and (c) 2-methyl-2-bromopropane in cis-decalin...	94

List of Figures continued...

	<u>PAGE</u>
FIGURE III-22: ϵ'' versus T(K) plots for o-xylene in cis-decalin.....	95
FIGURE IV-1: Plot of $\log T\tau$ versus $1/T$ (K^{-1}) for para-methylanisole in cis-decalin.....	113
FIGURE IV-2: ϵ'' versus T(K) plot for 2,5- dimethylanisole in cis-decalin..	114
FIGURE IV-3: ϵ'' versus $\log \nu$ plots for 3,5- dimethylanisole in cis-	115
FIGURE IV-4: Plot of $\log T\tau$ versus $1/T$ (K^{-1}) for 3,5-dimethylanisole in cis-decalin.....	116
FIGURE IV-5: ϵ'' versus T(K) plots for para- chloroanisole in cis-decalin....	117
FIGURE IV-6: ϵ'' versus T(K) plots for para- bromoanisole in cis-decalin.....	118
FIGURE IV-7: Plot of ϵ'' versus T(K) plot for para-iodoanisole in cis-decalin.	119
FIGURE IV-8: Cole-Cole plots for para- chloroanisole in cis-decalin....	120
Figure IV-9: Plot of ϵ'' versus T(K) for para-fluoroanisole in poly- styrene.....	121

List of Figures continued...

	<u>PAGE</u>
FIGURE IV-10: ϵ'' versus $\log \nu$ plots for para-fluoroanisole in polystyrene.....	122
FIGURE V-1: ϵ'' versus T(K) plots for some 1-bromoalkanes in a polystyrene matrix.....	158
FIGURE V-2: Plots of ϵ'' versus $\log \nu$ for 1-bromodocosane in a polystyrene matrix.....	159
FIGURE V-3: ϵ'' versus $\log \nu$ plots for 1-bromoheptane in a polystyrene matrix.....	160
FIGURE V-4: $\tau_{150\text{ K}}$ versus n (number of methylene groups) for the low temperature absorption of 1-bromoalkanes.....	161
FIGURE V-5: Plot of ΔS_E versus ΔH_E for the low temperature absorption of 1-bromoalkanes in a polystyrene matrix.....	162
FIGURE V-6: $\tau_{300\text{ K}}$ versus n (number of methylene groups) for the higher temperature absorption of 1-bromoalkanes in a polystyrene matrix.....	163
FIGURE V-7: Plot of ΔS_E versus ΔH_E for the higher temperature absorption of 1-bromoalkanes in a polystyrene matrix.....	164

List of Figures continued...

	<u>PAGE</u>
FIGURE V-8: Plots of $\log T\tau$ versus $1/T$ (K^{-1}) for the higher temperature absorption of some 1-bromoalkanes in a polystyrene matrix.....	165
FIGURE V-9: Potential energy diagram for unequal potential minima....	138
FIGURE V-10: Potential energy diagram for dipole rotating in a polystyrene matrix with energy barrier ΔH_E and equilibrium positions of equal energy.....	139
FIGURE VI-1 ϵ'' versus $T(K)$ for some bromooctanes in a polystyrene matrix.....	198
FIGURE VI-2: $\tau_{100 K}$ and $\tau_{200 K}$ versus location of the bromine atom along the n-octane chain in a polystyrene matrix.....	199
FIGURE VI-3: ϵ'' versus $\log \nu$ plots for the higher temperature absorption of 4-bromooctane in polystyrene.	200
FIGURE VI-4: Plots of ϵ'' versus $T(K)$ for 4-bromooctane in polypropylene..	201
FIGURE VI-5: ϵ'' versus $T(K)$ plots for 3-bromopentane and 1-bromopentane in a polystyrene matrix.....	202

List of Figures continued...

	<u>PAGE</u>
FIGURE VI-6: ϵ'' versus T(K) plots for 4-bromoheptane and 1-bromoheptane in a polystyrene matrix.....	203
FIGURE VI-7: ϵ'' versus $\log \nu$ plots for the high temperature absorption of 4-bromoheptane in a polystyrene matrix.....	204
FIGURE VI-8: Plot of ϵ'' versus $\log \nu$ for the low temperature absorption of 4-bromoheptane in a polystyrene matrix.....	205
FIGURE VI-9: ϵ'' versus T(K) plots for 4-bromoheptane in a polypropylene matrix.....	206
FIGURE VI-10: ϵ'' versus T(K) plots for 1,6-dibromohexane in a polystyrene matrix.....	207
FIGURE VI-11: ϵ'' versus T(K) plot for 1,10-dibromodecane in a polystyrene matrix.....	208
FIGURE VI-12: Cole-Cole plot for 1,6-dibromohexane at 117 K in polystyrene..	209
FIGURE VI-13: Cole-Cole plot for 1,6-dibromohexane at 232.2 K in polystyrene.....	210
FIGURE IV-14: Plots of $\log T\tau$ versus $1/T$ (K^{-1}) for the low temperature absorption of some bromooctanes in a polystyrene and polypropylene matrix.....	211

List of Figures continued...

	<u>PAGE</u>
FIGURE VI-15: Plots of $\log T\tau$ versus $1/T$ (K^{-1}) for the high temperature absorption of some bromooctanes in polystyrene and polypropylene matrices.....	212
FIGURE VI-16: Plots of ϵ'' versus $\log \nu$ for the high temperature absorption of 4-bromoheptane in polypropylene.....	213
FIGURE VI-17: Plots of ϵ'' versus $\log \nu$ for the high temperature absorption of 4-bromooctane in polypropylene.....	214
FIGURE VII-1: ϵ'' versus $T(K)$ plots for $CH_3(CH_2)_nCOCH_3$ in a polystyrene matrix.....	258
FIGURE VII-2: ϵ'' versus $T(K)$ plots for $CH_3(CH_2)_nNH_2$ in a polystyrene matrix.....	259
FIGURE VII-3: $\tau_{150 K}$ versus n (number of methylene groups) for the low temperature absorption of $CH_3(CH_2)_nCOCH_3$ in a polystyrene matrix.....	260
FIGURE VII-4: $\tau_{150 K}$ versus n (number of methylene groups) for the low temperature absorption of $CH_3(CH_2)_nNH_2$ in a polystyrene matrix.....	261

List of Figures continued...

	<u>PAGE</u>
FIGURE VII-5: Plot of ΔH_E versus n (number of methylene groups) for the low temperature absorption of $\text{CH}_3(\text{CH}_2)_n\text{COCH}_3$ in a polystyrene matrix.....	262
FIGURE VII-6: Plot of ΔH_E versus n (number of methylene groups) for the low temperature absorption of $\text{CH}_3(\text{CH}_2)_n\text{NH}_2$ in a polystyrene matrix.....	263
FIGURE VII-7: Plot of ΔS_E versus ΔH_E for the low temperature absorption of $\text{CH}_3(\text{CH}_2)_n\text{COCH}_3$ in a polystyrene matrix.....	264
FIGURE VII-8: Plot of ΔS_E versus ΔH_E for the low temperature absorption of $\text{CH}_3(\text{CH}_2)_n\text{NH}_2$ in a polystyrene matrix.....	265
FIGURE VII-9: Plot of ΔS_E versus ΔH_E for the higher temperature absorption of $\text{CH}_3(\text{CH}_2)_n\text{X}$ (where X = $-\text{COCH}_3$, $-\text{CH}_2\text{Br}$, $-\text{NH}_2$ and $-\text{CH}_2\text{OH}$) in a polystyrene matrix.	266
FIGURE VII-10: Plots of $\log T\tau$ versus $1/T$ (K^{-1}) for the low temperature absorption of $\text{CH}_3(\text{CH}_2)_n\text{X}$ (where X = $-\text{COCH}_3$ and $-\text{NH}_2$) in a polystyrene matrix.....	267

List of Figures continued...

	<u>PAGE</u>
FIGURE VII-11: Plots of $\log T\tau$ versus $1/T$ (K^{-1}) for the high temperature absorption of $CH_3(CH_2)_n X$ (where $X = -COCH_3$ and $-NH_2$) in a polystyrene matrix.....	268
FIGURE VII-12: Plots of ϵ'' versus $\log \nu$ for the low temperature absorption of $CH_3(CH_2)_{14}COCH_3$ in a polystyrene matrix.....	269
FIGURE VII-13: ϵ'' versus $\log \nu$ plots for the high temperature absorption of $CH_3(CH_2)_6COCH_3$ in a polystyrene matrix.....	270
FIGURE VII-14: ϵ'' versus $\log \nu$ plots for the low temperature absorption of $CH_3(CH_2)_{11}NH_2$ in a polystyrene matrix.....	271
FIGURE VII-15: ϵ'' versus $\log \nu$ plots for the high temperature absorption of $CH_3(CH_2)_5NH_2$ in a polystyrene matrix.....	272
FIGURE VIII-1: Plots of ϵ'' versus $T(K)$ for $[CH_3(CH_2)_n]_2CO$ in a polystyrene matrix.....	317
FIGURE VIII-2: Plots of ϵ'' versus $T(K)$ for $[CH_3(CH_2)_n]_2NH$ in a polystyrene matrix.....	318

List of Figures continued...

	<u>PAGE</u>
FIGURE VIII-3: Plots of ϵ'' versus T(K) for $[\text{CH}_3(\text{CH}_2)_n]_2\text{S}$ in a polystyrene matrix.....	319
FIGURE VIII-4: Plots of ϵ'' versus T(K) for $[\text{CH}_3(\text{CH}_2)_n]_2\text{O}$ in a polystyrene matrix.....	320
FIGURE VIII-5: $\tau_{150\text{ K}}$ versus n (number of methylene groups) for the low temperature absorption of $[\text{CH}_3(\text{CH}_2)_n]_2\text{CO}$ in a polystyrene matrix.....	321
FIGURE VIII-6: Plot of $\tau_{150\text{ K}}$ versus n (number of methylene groups) for the low temperature absorption of $[\text{CH}_3(\text{CH}_2)_n]_2\text{NH}$ in a polystyrene matrix.....	322
FIGURE VIII-7: Plot of $\tau_{150\text{ K}}$ versus n (number of methylene groups) for the low temperature absorption of $[\text{CH}_3(\text{CH}_2)_n]_2\text{S}$ in a polystyrene matrix.....	323
FIGURE VIII-8: $\tau_{150\text{ K}}$ versus n (number of methylene groups) plot for the low temperature absorption of $[\text{CH}_3(\text{CH}_2)_n]_2\text{O}$ in a polystyrene matrix.....	324

List of Figures continued...

	<u>PAGE</u>
FIGURE VIII-9: ΔH_E versus n (number of methylene groups) for the low temperature absorption of $[\text{CH}_3(\text{CH}_2)_n]_2\text{X}$ in a polystyrene matrix.....	325
FIGURE VIII-10: Plot of ΔS_E versus ΔH_E for the low temperature absorption of $[\text{CH}_3(\text{CH}_2)_n]_2\text{S}$ in a polystyrene matrix.....	326
FIGURE VIII-11: $\tau_{300\text{ K}}$ versus n (number of methylene groups) for the high temperature absorption of $[\text{CH}_3(\text{CH}_2)_n]_2\text{CO}$ in a polystyrene matrix.....	327
FIGURE VIII-12: Plots of $\log T\tau$ versus $1/T$ (K^{-1}) for the low temperature absorption of $[\text{CH}_3(\text{CH}_2)_n]_2\text{X}$ (where $\text{X} = \begin{array}{c} \diagup \text{O} \diagdown \\ \diagup \text{S} \diagdown \\ \text{C} \end{array}$ and $\begin{array}{c} \diagup \text{N} \diagdown \\ \text{H} \end{array}$) in a polystyrene matrix.....	328
FIGURE VIII-13: Plots of $\log T\tau$ versus $1/T$ (K^{-1}) for the high temperature absorption of $[\text{CH}_3(\text{CH}_2)_n]_2\text{CO}$ in a polystyrene matrix.....	329

List of Figures continued...

	<u>PAGE</u>
FIGURE VIII-14: Plots of ϵ'' versus $\log \nu$ for the low temperature absorption of $[\text{CH}_3(\text{CH}_2)_{10}]_2\text{CO}$ in a polystyrene matrix.....	330
FIGURE VIII-15: Plots of ϵ'' versus $\log \nu$ for the high temperature absorption of $[\text{CH}_3(\text{CH}_2)_2]_2\text{CO}$ in a polystyrene matrix.....	331
FIGURE VIII-16: ϵ'' versus $\log \nu$ plots for the low temperature absorption of $[\text{CH}_3(\text{CH}_2)_7]_2\text{NH}$ in a polystyrene matrix.....	332
FIGURE VIII-17: Plots of ϵ'' versus $\log \nu$ for the low temperature absorption of $[\text{CH}_3(\text{CH}_2)_{11}]_2\text{S}$ in a polystyrene matrix.....	333
FIGURE VIII-18: ϵ'' versus $\log \nu$ plots for the low temperature absorption of $[\text{CH}_3(\text{CH}_2)_5]_2\text{O}$ in a polystyrene matrix.....	334
FIGURE VIII-19: Two sites symmetric barrier model for $[\text{CH}_3(\text{CH}_2)_n]_2\text{X}$ (where $\text{X} = \begin{array}{c} \text{O} \\ \parallel \\ \text{C} \end{array}$, O , S and $\begin{array}{c} \text{H} \\ \diagup \\ \text{N} \end{array}$) in a polystyrene matrix..	290

CHAPTER I

INTRODUCTION AND BASIC THEORY

CHAPTER I

INTRODUCTION

Dielectric investigations are becoming an increasingly important tool for studying the molecular and/or intramolecular motions of molecules containing rotatable polar groups. The dielectric absorption of aromatic molecules which contain a rotatable polar group at microwave frequency may contain contributions from whole molecule and intramolecular group reorientations. These types of studies were mostly performed either as pure liquids or in non-polar solvents. In the vast majority of cases, however, the dielectric absorption of the group and the molecule itself are nearly always overlapped (2) so that it is difficult to attain reliable results for the energy barriers associated with the relaxations. Group relaxation times, obtained by Budó analyses of the loss data, and the activation enthalpies for internal rotation generally contain appreciable errors.

In recent years, the dielectric absorption studies of polar solutes dispersed in a polymer-matrix such as polystyrene, polypropylene and polyethylene matrix

have received considerable attention in the literature. It has been found to yield reasonable reliable intramolecular energy barriers (3,4) as compared to other relaxation techniques (n.m.r. and ultrasonic)(4). One of the great advantages of polymer-matrix techniques is that for a system with a flexible polar molecule, where both the molecular and intramolecular process overlap at microwave frequency around room temperature, the relaxation time for the former can be increased to such an extent either it may be considerably slowed down or may even be eliminated owing to highly viscous surrounding medium, so either or both the processes may be studied independently. Such a technique appeared more straightforward in comparison to the dielectric solution approach, since in solution studies complications are frequently met owing to overlap of different types of processes which for their separation require a Budó analyses which in a number of cases, is now known to be unsatisfactory (4). Moreover, the frequency and temperature ranges accessible to the solution studies are fairly limited, and hence relaxation parameters cannot be obtained with reasonable accuracy. However, these limitations may be overcome in the polymer matrix techniques, since different instruments can be used to cover a wide frequency range of investigations over a

broad temperature range i.e. from liquid nitrogen temperature [~ 80 K] to the glass transition temperature of the matrix system. Thus, it seemed that the technique can be used more reliably for determining the activation parameters comparable to those determined by other direct relaxation methods.

One of the most commonly used polymer solvents is polystyrene. Polystyrene is used as the solvent for a matrix, which contains the cavities within which the solute molecules can be trapped (3,5). Since polystyrene is almost a non-polar solvent, studies in which polar molecules are monomolecularly dispersed in the matrix are simplified by the very low loss of polystyrene. Samples of polystyrene have low losses which are less than 1×10^{-3} over the frequency range 100 Hz to 1 GHz.

Most recently, three other molecular glass forming solvent systems, o-terphenyl, polyphenyl ether and cis-decalin have been used by polymer-matrix technique. o-Terphenyl is a non-polar solvent which melts at 328.7 K and the liquid may be cooled to a glass with an apparent glass transition at 243 K (6). Polyphenylether is a six-ring meta-linked bis(m(m-phenoxy phenoxy)phenyl)ether with a glass transition at about 270 K (6). cis-Decalin is

a weakly polar solvent having the glass transition temperature at about 131 K (6). It has very little dielectric loss of its own (less than 1×10^{-3} over the frequency range 10 Hz to 100 kHz) below its glass transition temperature. The polyphenyl ether differs from o-terphenyl, cis-decalin and polystyrene in that it is more polar since it contains polar ether linkages and has a comparatively large loss, α -process just above its T_g , but the absorption in the glassy state is of the order of $(1 - 1.5 \times 10^{-3})$ which is quite small (16).

There is now a considerable amount of literature available for the dielectric absorption studies of aromatic molecules having a rotatable polar group whose dipole is not directed along a molecular axis and in which the intramolecular process has been completely separated from the molecular one in a polystyrene matrix (7-10).

Aliphatic long chain polar molecules are far more flexible and may exist in a variety of molecular conformations; intramolecular rotation may occur about many bonds and involve molecular segments of different size. If barriers for rotation of various groups are

not very different, overlapping absorptions then ensue with broad absorption curves and a wide distribution of relaxation times. At microwave frequency the long-chain polar molecules as pure liquids and in non-polar solvents are unresolved and display some distribution of relaxation times (11-14). Utilization of restrictive media (polystyrene, polypropylene and compressed solids) has now permitted the observation and characterization of a number of relaxation modes (i.e. around C-C bonds) common to long-chain organic molecules. A successful separation of intramolecular process from the large segmental and/or molecular one for the long-chain aldehydes in a polystyrene matrix has recently been reported in the literature (15).

The research work which is presented in this thesis concerns itself primarily with relaxation studies of long-chain polar molecules of the types, $\text{CH}_3(\text{CH}_2)_n\text{X}$ ($\text{X} = -\text{CH}_2\text{Br}, -\text{COCH}_3$ and $-\text{NH}_2$) and $[\text{CH}_3(\text{CH}_2)_n]_2\text{X}$ ($\text{X} =$
 $\begin{array}{c} \text{O} \\ \parallel \\ \text{C} \end{array}$, $\begin{array}{c} \text{S} \\ \diagdown \\ \text{C} \end{array}$, $\begin{array}{c} \text{O} \\ \diagdown \\ \text{C} \end{array}$ and $\begin{array}{c} \text{H} \\ \diagup \\ \text{N} \end{array}$) mainly in a polystyrene matrix, although a few has been examined in polypropylene and o-terphenyl as well. The aim was to separate completely the absorption peaks of some or any of the relaxation processes and characterize by means of its Eyring

activation parameters.

A number of dipolar solutes, both rigid and flexible, have also been studied in cis-decalin in order to make possible comparisons between Eyring parameters observed for molecular and intramolecular motions in other solvents.

BASIC THEORY

Two fundamental types of dielectric materials are recognized that are characterized by the absence of free charge able to move through the material under the influence of an applied electric field. In non-polar dielectrics, all electrons are bound, and so the only motion possible in the presence of an electric field is a very limited displacement of positive and negative charge in opposite directions. The non-polar molecules normally possess induced dipole moments and the material is said to be polarized. A polar dielectric material is one which has a permanent electric dipole moment.

The total polarization (P_T) of a dielectric material in an applied electric field can be described by the Clausius - Mossotti - Debye theories (17) as:

$$\begin{aligned}
 P_T &= P_E + P_A + P_O \\
 &= \frac{4\pi N}{3} (\alpha_E + \alpha_A + \frac{\mu^2}{3kT}) \\
 &= \frac{\epsilon_o - 1}{\epsilon_o + 2} \left(\frac{M}{d} \right) \qquad \text{I-1}
 \end{aligned}$$

where ϵ_0 ... static dielectric constant
 M ... gram molecular weight
 d ... density of the material
 N ... Avogadro's number
 μ ... electric dipole moment
 K ... Boltzman Constant
 T ... absolute temperature

From the equation (I-1), it is seen that three different processes contribute to the total polarization (P_T).

(i) Electronic polarization, P_E , (or deformation of electron cloud) which means the electron density is drawn away from the nuclei.

(ii) Atomic polarization, P_A , (or displacement of ions) due to changes in the mean position of the ($\delta+$) atoms and the ($\delta-$) atoms or due to the change of the relative angles of polar links.

(iii) Orientation polarization, P_O (or orientation of electric dipoles) of a permanent dipole moment of a polar molecule. In order to achieve minimum energy, the dipole moment tends to align itself along the field.

The quantity $(\epsilon_0 - 1)M/(\epsilon_0 + 2)d$ is known as the molar polarization. From the equation (I-1), the following conclusions can be made. For a non-polar

material the molar polarizability should be a constant independent of the temperature and pressure. An increase in the density leads to an increase in permitivity. For a polar substance the molar polarizability falls with increasing temperature, because the thermal agitation decreases the dipolar polarization. If a plot of molar polarizability versus the reciprocal of temperature is made, a straight line is obtained, from whose slope the dipole moment of the molecule can be found.

The Clausius - Mossoti - Debye theories are applicable to gases, but are often inadequate when applied to polar liquids, due to the inability of the Lorentz field used in these theories to represent adequately the local field in a dipolar dielectric.

In order to give a theory which would extend the relation between permitivity and dipole moment to liquids and solids, Onsager (2) developed a theory on the assumption that there exists a cavity which is a sphere in a homogeneous medium of static dielectric constant, ϵ_0 ,

$$\frac{(\epsilon_0 - \epsilon_\infty)(2\epsilon_0 + \epsilon_\infty)}{\epsilon_0(\epsilon_\infty + 2)^2} \cdot \frac{M}{d} = \frac{4\pi N\mu^2}{9kT} \quad \text{I-2}$$

where ϵ_{∞} is the dielectric constant at very high frequency when the orientation polarization vanishes. Hence equation I-1 becomes,

$$\frac{\epsilon_{\infty} - 1}{\epsilon_{\infty} + 2} \frac{M}{d} = \frac{4\pi N (\alpha_E + \alpha_A)}{3} \quad \text{I-3}$$

From equation I-1 and I-3, Debye equation follows:

$$\frac{3 (\epsilon_0 - \epsilon_{\infty})}{(\epsilon_0 + 2)(\epsilon_{\infty} + 2)} \frac{M}{d} = \frac{4\pi N \mu^2}{9kT} \quad \text{I-4}$$

From equation I-2 and I-4, we can obtain a relationship of dipole moment between the Onsager and the Debye equation as follows:

$$\frac{\mu^2 (\text{Onsager})}{\mu^2 (\text{Debye})} = \frac{2 (\epsilon_0 + \epsilon_{\infty}) (\epsilon_0 + 2)}{3 \epsilon_0 (\epsilon_{\infty} + 2)} \quad \text{I-5}$$

For gases at low pressure ϵ_0 and ϵ_{∞} are practically identical and thus the Onsager equation is reduced to the Debye equation.

When an insulating material is placed in an electric field it becomes polarized, due to the relative displacement of positive and negative electric charges in the material. The ratio of the field strength

without any dielectric to that in the presence of the dielectric is called the static dielectric constant (relative permittivity) ϵ_0 of the material. For majority of normal-sized polar molecules in non-polar solvents, the three components of P_T , namely P_E , P_O and P_A , can all reach their equilibrium values when the applied field is of the order of 10^8 Hz or less. As the frequency of the applied field increases, the dipoles begin to lag behind and the polarization (P_O) falls off so that its contribution to the total permittivity decreases. It is this decrease in polarization and permittivity and the resultant absorption of energy which describes the dielectric dispersion. The phase difference between the applied field and the dipole reorientation causes a dissipation of energy known as Joule heating which is measured by the dielectric loss (ϵ'') defined below as

$$\epsilon'' = \epsilon' \tan\delta \quad \text{I-6.}$$

where ϵ' is the real component of the complex term of the dielectric constant and $\tan\delta$ is the loss tangent or energy dissipation factor.

The complex quantity of the dielectric constant in the dispersion region can be represented by the

following equation and diagram,

$$\epsilon^* = \epsilon' - i\epsilon'', \text{ where } i = \sqrt{-1} \text{ -----I-7}$$

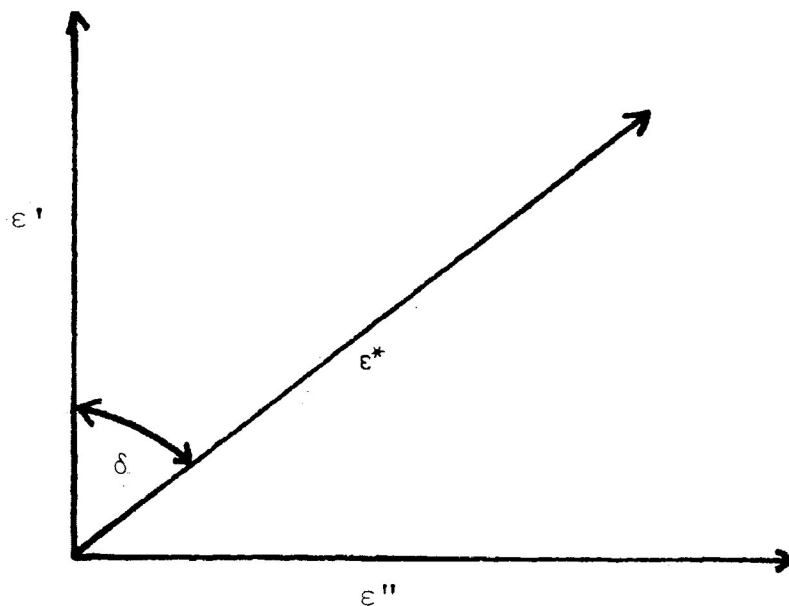


Figure I-1, Loss tangent curve

The absorption region associated with different mechanisms of polarization occurs in different parts of the electromagnetic spectrum, as shown in fig. I-2.

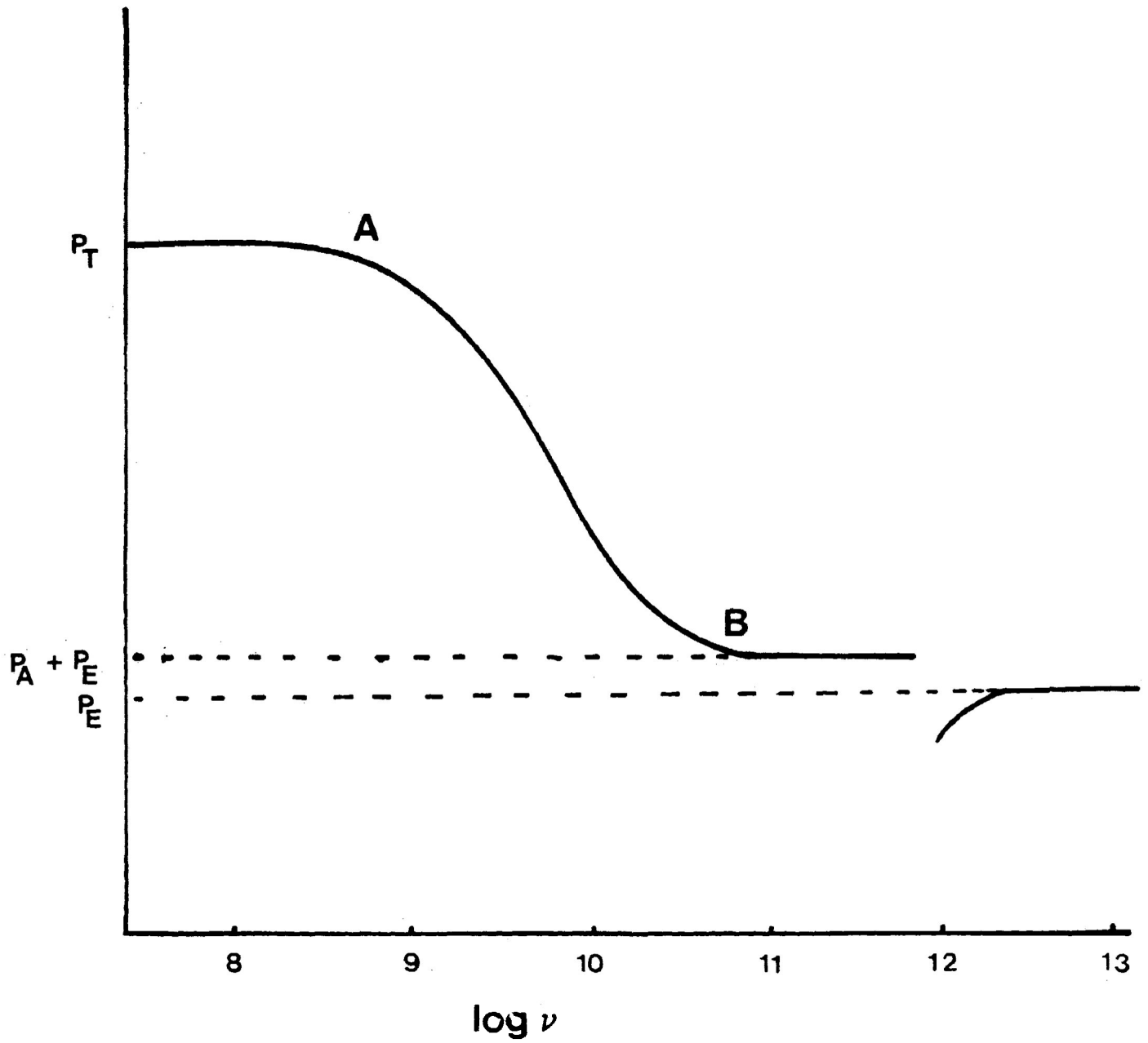


Figure I-2. Total polarization versus log frequency curve

Between points A and B on figure I-2 the total polarization (P_T) decreases expectedly as the frequency increases and the dielectric constant becomes complex. It is over the region A to B that the dipole moment begins to lag behind the applied field. When the applied frequency is beyond that of molecular reorientation, atomic polarization arises at frequencies of 10^{12} to 10^{14} Hz, corresponding to the infra red region of the electromagnetic spectrum. The electronic polarization occurs with a frequency of about 10^{15} Hz which corresponds to frequencies in the ultraviolet region. The time required for the orientation polarization response depends in part on the frictional resistance of the medium to the change in molecular orientation. In a highly viscous medium a molecule will encounter more frictional drag as it rotates than in a low viscosity medium. This will result in a longer period for molecular reorientation in a more viscous medium. Small molecules in liquids of low viscosity reorientate themselves in a period of 10^{-11} s to 10^{-12} s with frequencies of 10^{11} to 10^{12} Hz. These frequencies corresponds to the microwave region.

Dielectric relaxation is the exponential decay of the polarization with time in a dielectric when an external field is removed. The relaxation time, τ is defined

as the time (t) during which the polarization is reduced to $1/e$ times its original value (P_0), therefore,

$$P(t) = P_0 \exp(-t/\tau) \quad \text{I-8}$$

where $P(t)$ is the specific polarization at time, t in an electric field.

The frequency dependence of the permittivity (ϵ') and the dielectric loss (ϵ'') in the region of dielectric absorption for a system is characterized by the Debye equation.

$$\epsilon^* = \epsilon_\infty + \frac{\epsilon_0 - \epsilon_\infty}{1 + i\omega\tau} \quad \text{I-9}$$

where ω is the angular frequency in rad.s^{-1} and ϵ_0 and ϵ_∞ are the static and infinite frequency permittivities respectively. Separation of equation I-9 into its real and imaginary parts gives equations (17,19) I-10 and I-11.

$$\epsilon' = \epsilon_\infty + \frac{\epsilon_0 - \epsilon_\infty}{1 + \omega^2\tau^2} \quad \text{I-10}$$

$$\epsilon'' = \frac{\omega\tau(\epsilon_0 - \epsilon_\infty)}{1 + \omega^2\tau^2} \quad \text{I-11}$$

The relaxation time, τ of a system can also

be obtained from the following equations:

$$\begin{aligned}\omega\tau &= 1 \\ \omega &= 2\pi\nu_m \\ \tau &= \frac{1}{\omega} = \frac{1}{2\pi\nu_m}\end{aligned}\tag{I-12}$$

The maximum permitivities (ϵ'_{\max}) and maximum loss (ϵ''_{\max}) can now be obtained by putting $\omega\tau=1$ in equations I-10 and I-11 respectively.

$$\epsilon'_{\max} = \frac{\epsilon_0 + \epsilon_\infty}{2}\tag{I-13}$$

$$\epsilon''_{\max} = \frac{\epsilon_0 - \epsilon_\infty}{2}\tag{I-14}$$

Elimination of $\omega\tau$ from equations I-10 and I-11 gives equation I-15,

$$\left(\epsilon' - \frac{\epsilon_0 + \epsilon_\infty}{2}\right)^2 + \epsilon''^2 = \left(\frac{\epsilon_0 - \epsilon_\infty}{2}\right)^2\tag{I-15}$$

This is the equation of a circle with the centre lying on the abscissa. This function leads to a Cole-Cole plot of semi-circle of radius $\frac{\epsilon_0 - \epsilon_\infty}{2}$ when ϵ'' is plotted against ϵ' at the same frequencies.

Debye equation, I-9 is valid only when there is single relaxation process. Since many molecules exhibit a range of relaxation times, rather than single relaxation time, Cole and Cole modified equation I-9 to consider a symmetrical distribution of relaxation times about the mean relaxation time, τ_0 :

$$\epsilon^* = \epsilon_\infty + \frac{\epsilon_0 - \epsilon_\infty}{1 + (i\tau_0\omega)^{1-\alpha}} \quad \text{I-16}$$

where α is the distribution parameter which may have values between 0 and 1. When $\alpha=0$, the Debye equation is obtained.

Similarly, equation (I-16) can be separated into real and imaginary parts to yield analogous Cole-Cole plot where the centre of the semi-circle lies below abscissa:

$$\epsilon' = \epsilon_\infty + \frac{(\epsilon_0 - \epsilon_\infty)(1 + (\omega\tau_0)^{1-\alpha} \sin(\alpha\pi/2))}{1 + 2(\omega\tau_0)^{1-\alpha} \sin(\alpha\pi/2) + (\omega\tau_0)^{2(1-\alpha)}} \quad \text{I-17}$$

$$\epsilon'' = \frac{(\epsilon_0 - \epsilon_\infty)(\omega\tau_0)^{1-\alpha} \cos(\alpha\pi/2)}{1 + 2(\omega\tau_0)^{1-\alpha} \sin(\alpha\pi/2) + (\omega\tau_0)^{2(1-\alpha)}} \quad \text{I-18}$$

A number of functions have been considered for non-Debye type of absorption. Cole and Davidson have formulated a function which describes right-skewed arcs (21)

$$\epsilon^* = \epsilon' - i\epsilon'' = \epsilon_\infty + \frac{\epsilon_0 - \epsilon_\infty}{(1+i\omega\tau)^\beta} \quad \text{I-19}$$

where β is the asymmetric distribution co-efficient whose value lies in the range $0 < \beta < 1$.

Fuoss and Kirkwood (22) also developed a theory regarding the distribution of relaxation times. The equation is

$$\cosh^{-1} \left(\frac{\epsilon''_{\max}}{\epsilon''} \right) = 2.303\beta \log \left(\frac{\nu_{\max}}{\nu} \right)$$

-20

where β is a significant empirical parameter whose inverse measures the width of the absorption relative to the Debye process ($\beta = 1$).

In some cases where the molecules are flexible, the dielectric absorption can be characterized by two discrete relaxation processes which corresponds to molecular and intramolecular rotation. For such systems Budó (23) developed the following equation which sums up

the Debye terms.

$$\frac{\epsilon^* - \epsilon_\infty}{\epsilon_0 + \epsilon_\infty} = \sum_{K=0}^N \frac{C_k}{1 + 2\omega\tau_k} \quad \text{I-21}$$

where k is the relaxation time for the k th mode of relaxation and C_k is a factor (called weight factor) representing the proportion of contribution of the k th mode to the total dispersion. Thus for a system having two discrete processes with relaxation times τ_1 and τ_2 the following equations can be deduced:

$$\epsilon' = \epsilon_\infty + (\epsilon_0 - \epsilon_\infty) \left\{ \frac{C_1}{1 + (\omega\tau_1)^2} + \frac{C_2}{1 + (\omega\tau_2)^2} \right\}$$

$$\epsilon'' = (\epsilon_0 - \epsilon_\infty) \left\{ \frac{C_1 \omega\tau_1}{1 + (\omega\tau_1)^2} + \frac{C_2 \omega\tau_2}{1 + (\omega\tau_2)^2} \right\}$$

Where C_1 and C_2 are the weight factors and $C_1 + C_2 = 1$. When C_1/C_2 is small, an almost symmetrical Cole-Cole plot is obtained. Systems with significantly large τ_1/τ_2 and C_1/C_2 ratios may have two processes separated into two distinct absorption regions.

A number of models have been suggested to account for the relaxation processes of molecules. Debye (1) has suggested a simple relaxation mechanism. In his theory each dipole has two equilibrium positions

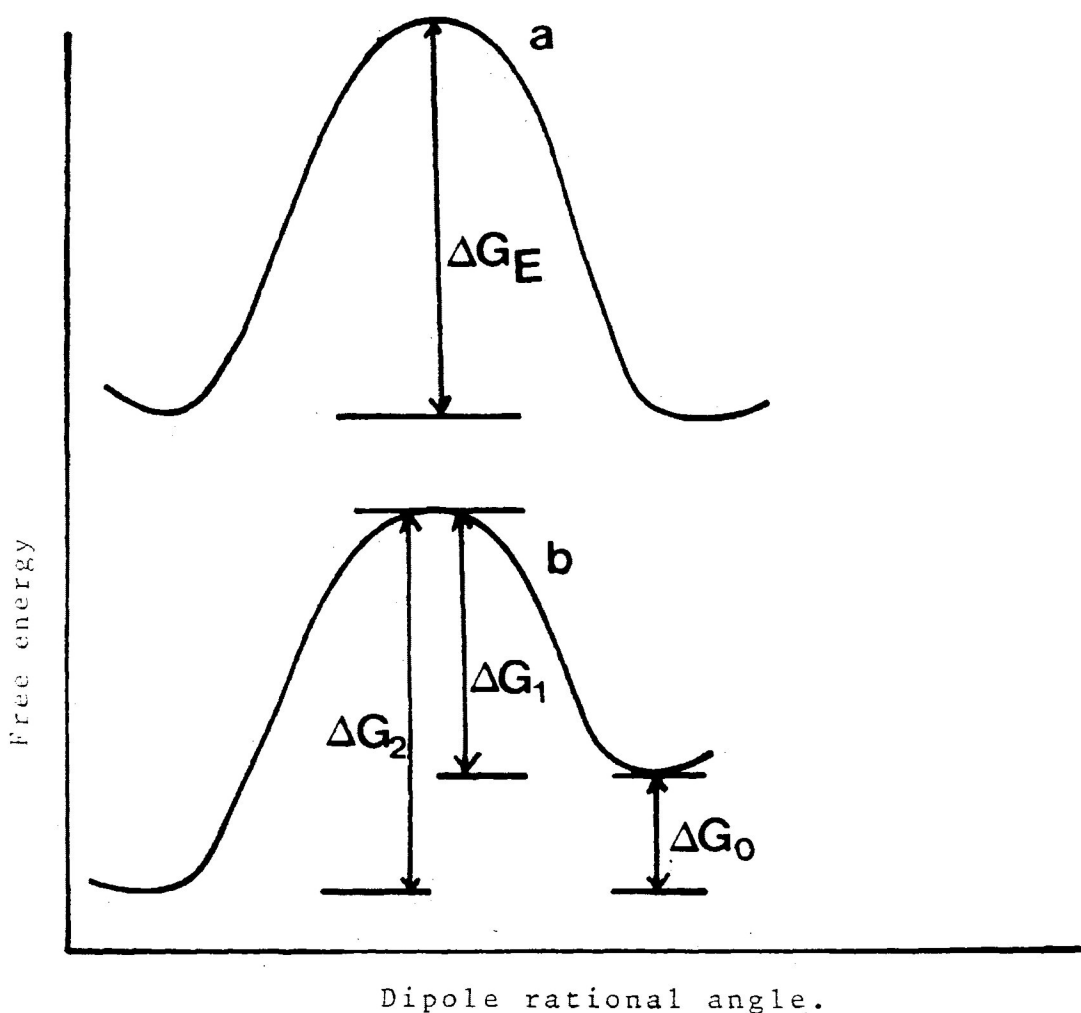


Figure I-3 Energy barrier diagram for a rotating dipole.

which are equal in energy and opposite in direction. The two equilibrium positions are separated by an energy barrier, ΔG_E . This is illustrated in Figure I-3a. In such

a situation the dipole will oscillate with a frequency f_0 to within the potential minima, and sometimes acquire enough energy to jump over the barrier. However, at any instant in time there are equal numbers of dipoles in each equilibrium position in the absence of an external field.

The energy barrier between the equilibrium positions of the dipoles can be obtained from the temperature dependence of the frequency of maximum absorption, f_{\max} by means of the equation (8),

$$f_{\max} = \frac{1}{2\pi\tau} = \frac{f_0}{\pi} \exp(-\Delta G_E/RT)$$

I-24

where R is the universal gas constant and T is the absolute temperature. In many molecular systems, particularly solids, the equilibrium positions are unequal as shown in figure I-3b.

Eyring has treated the dipole rotation by a comparison with chemical rate process (7). The more commonly used equation is

$$\frac{1}{\tau} = \frac{kTK}{h} \exp(-\Delta G_E/RT)$$

I-25

Where h is the Planck's constant, k is Boltzman's constant, and K is the transmission co-efficient normally taken to be 1. now,

$$\Delta G_E = \Delta H_E - T\Delta S_E \quad \text{I-26}$$

where ΔH_E is the enthalpy of activation and ΔS_E is the entropy of activation, thus:

$$\tau = \frac{h}{kT} \exp(\Delta H_E/RT) \exp(-\Delta S_E/RT) \quad \text{I-27}$$

from equation I-23 it is evident that a plot of $\log(\tau)$ versus $1/T$ should give a straight line.

The value of ΔH_E and ΔS_E may be obtained from the slope and intercept respectively.

REFERENCES

1. C. P. Smyth, Ad. Mol. Int. Relax. Proc. 1, 1(1967).
2. J. Crossley, S. P. Tay & S. Walker, Ad. Mol. Int. Relax. Proc. 6, 29(1974).
3. M. Davies and J. Swain, Trans. Fara. Soc., 67, 1637(1971).
4. S. P. Tay, S. Walker & E. Wyn-Jones, Ad. Mol. Int. Relax. Proc. 13, 47(1978).
5. M. Davies and A. Edwards, Trans. Fara. Soc., 63, 2163(1967).
6. M. S. Ahmed, J. Crossley, M.S. Hossain, M. A. Saleh & S. Walker. J. Chem. Phys., 81, (448(1984)).
7. C. K. McLellan & S. Walker, Can. J. Chem., 55, 583(1977).
8. A. Lakshmi, S. Walker & N.A. Weir, Trans. Fara. Soc., 74, 727(1978).
9. A. Lakshmi, S. Walker, N.A. Weir & J.H. Calderwood, Ad. Mol. Int. Relax. Proc., 13, 287(1978).
10. J. Crossley, M.A. Mazid, C.K. McLellan, P.F. Mountain & S. Walker. J. Chem. Phys., 56, 567(1978).
11. J. Crossley. Ad. Mol. Int. Relax. Proc., 6, 39(1974).
12. J. Crossley & N. Koizumi, J. Chem. Phys., 60, 4800 (1974).
13. Y. Yano, R. Minami and A. Takahasi, Bull. Chem. Soc. Japan, 53, 642(1980).
14. M. A. Desando, S. Walker & J.H. Calderwood, J. Chem. Phys., 78, 3238(1983).
15. H.A. Khwaja & S. Walker. Ad. Mol. Int. Relax. Proc., 22, 27(1982).
16. J. Crossley, A. Heravi & S. Walker, J. Chem. Phys., 75, 418(1981).

17. P. Debye, "Polar Molecules". Chemical Catalog Co., New York, (1929).
18. L. Onsager, J. Am. Chem. Soc. 58, 1486(1936).
19. H. Fröhlich, "Theory of Dielectrics" Oxford University Press, Amen House, London E.C.4, England (1949).
20. K.S. Cole and R.H. Cole. J. Chem. Phys., 9, 341(1941).
21. D.W. Davidson and R.H. Cole, J. Chem. Phys., 19, 1484 (1951)
22. R.M. Fuoss and J.G. Kirkwood, J. Am. Chem. Soc., 63, 385(1941)
23. A. Budo^o Z. Phys., 39 706(1938).
24. S. Glasstone, K.J. Laidler, and H. Eyring, "The Theory of Rate processes", McGraw-Hill, New York, (1941).

CHAPTER II

EXPERIMENTAL MEASUREMENTS

INTRODUCTION

In this thesis most of the chemical systems studied were experimentally examined as solutes dissolved in (a) cis-decalin, and (b) atactic polystyrene. The solutes were either polar liquids or solids. cis-Decalin and atactic polystyrene were purchased from the Aldrich Chemical Co. and the Division of Haven Industries, Inc., Philadelphia, U.S.A. (Lot. No. 700-228-20) respectively. Liquids were measured in a three terminal co-axial cell and solid disks in a parallel plate capacitor cell.

Dielectric measurements were performed by the use of General Radio 1615A capacitance bridge and the General Radio 1621 Precision Capacitance Measurement system. The glass transition temperature, T_g of some of the Chemical systems, were measured by the use of the Glass Transition Measurement Apparatus. This instrument has been designed by Mr. B.K. Morgan of this laboratory.

Dielectric properties of a polar material can conveniently be considered by assuming it to be situated between the parallel plates of a condenser such that the dielectric constant (ϵ) of the material may be defined by the equation:

$$\epsilon = \frac{C}{C_0} \quad \text{II-1}$$

where C and C_0 are the capacitance values for the condenser with the dielectric material and with vacuum respectively. When a sinusoidal potential of amplitude ϵ and frequency ω rad s⁻¹ is applied to the capacitor, the current, I , flowing through the circuit is given by:

$$I = E\omega C = E\omega C_0 (\epsilon' - \epsilon'') \quad \text{II-2}$$

In this equation the real component $E\omega C_0 \epsilon'$, known as charging current is 90° out of phase with the applied potential and therefore, does not involve any electrical work. The imaginary component, $E\omega C_0 \epsilon''$, known as the loss current, is, however, in phase with the applied potential and is related to the energy dissipated as heat since it causes some electrical work to be done by the dot product, $EI = E^2 \omega C_0 \epsilon''$. As was given by equation I-6, the resulting phase displacement (δ), (i.e., the angle between the total current and charging currents is related to the dielectric loss factor (ϵ'') as:

$$\begin{aligned} \tan \delta &= \frac{\text{loss current}}{\text{charging current}} \\ &= \frac{E\omega C_0 \epsilon''}{E\omega C_0 \epsilon'} \\ &= \frac{\epsilon''}{\epsilon'} \end{aligned} \quad \text{II-3}$$

where ϵ' is the observed dielectric constant according to equation II-1. These are the basic principles of the dielectric measurements.

THREE-TERMINAL COAXIAL CELLS

The cells, designed by Mr. B.K. Morgan of this laboratory, were described earlier by previous workers. However, the cells which were used for this work are illustrated in the following figures (reproduced by the courtesy of D.L. Gourlay (1)). Figure II.1 and Figure II.2 represent the two three-terminal coaxial cells. The cell shown in Figure II.1 is circular and has concentric stainless steel electrodes, A and B. Their shape permits the rapid transfer of heat to or from the solid aluminium case, C. The undersides of the electrodes are insulated from the case by a 0.25 cm thick teflon disk. A 0.50 cm thick teflon sleeve insulated the outer circumference of electrode B. The fringe field is practically eliminated by the presence of the grounded case below and a grounded guard ring, E, above. The circular teflon cap, F, fits closely into the top of electrode B to prevent the escape of liquid vapours.

The liquid sample can conveniently be introduced

into the 0.50 cm gap between electrodes A and B by a disposable pipette which should first be pushed to the bottom of the semicircular hole cut vertically in the edge of electrode A. Tests have shown that if the gap between the electrodes is filled from the bottom all the air will be expelled. One and one-half milliliters is enough to fill the cell. To empty it the sample is sucked up with a dropper and the electrodes are flushed with solvents (first acetone and then with cyclohexane) several times. To dry the electrodes a cotton swab is pushed down the filling hole. Any remaining liquid is removed by wiping around the electrode gap with 2.50 cm wide strips of cardboard. Hot air is also blown to dry the cell completely.

The lid of cell G is secured to the case by five recessed bolts. The surface between G and C is coated with heat conductive grease of the type used with semiconductor heat-sinks.

The outer cell wall is insulated by a ring of micro cellular polystyrene foam which is flush with the top of G. The insulation has a wall thickness of 5 cm. The cell's underside is also insulated with a 23 cm diameter and 5 cm thick disk of polystyrene.

The cell can be rapidly cooled by replacing a 3 litre flat-bottomed aluminium container of liquid nitrogen to cover the lid, G. The vertical sides of the nitrogen container are insulated with polystyrene foam. When the desired temperature is reached an appropriate number of sheets of paper is placed between the nitrogen container and the lid to reduce the rate of cooling. Equilibrium is maintained by a Thermo Electric thermo-regulator model 3814021133 connected via a variac transformer to heater H. This heater is a 300 watt 110 V ARI Industries heater, model number BXA-06F-40-4K, but we run it at about 60 V. The temperature is measured by a Newport 264-3 digital platinum resistance pyrometer. Its probe, J, is partly insulated from the heater by a Teflon sleeve. The upper temperature limit of the cell is about 368 K, just below the temperature at which the polystyrene deforms.

Connections are made to electrodes A and B through screws insulated by teflon sleeves and mica washers. The beads of the screws are screened by a 2.5 cm wide aluminium block with three 1.25 cm diameter holes cut into it. The screw from electrode A is connected to a miniature coaxial cable which enters through the side of the block. The cable has Teflon insulation (type number - RG-316/U). A similar coaxial connection is made to one of the screws

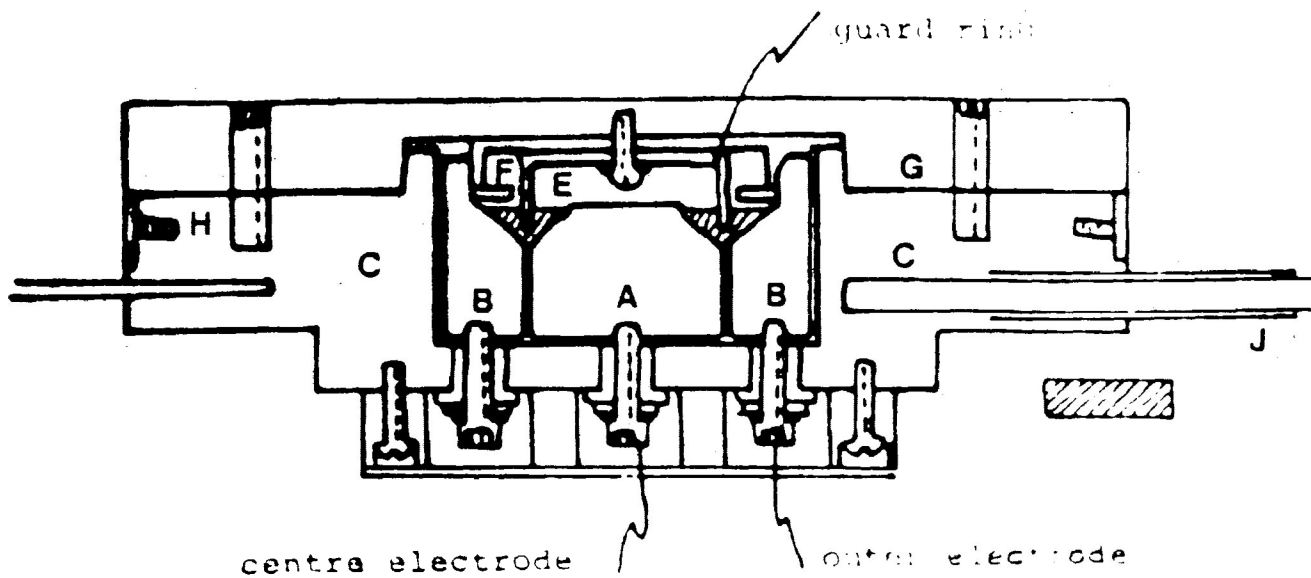


FIGURE:- II-1 Three terminal coaxial cell

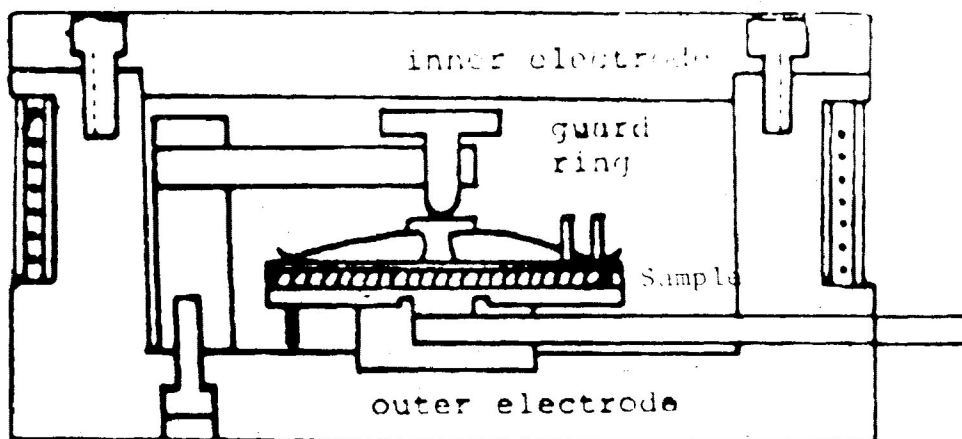


FIGURE:- II-2 Parallel plate capacitor cell

from electrode B. The cables are connected to the GR Bridges via extension cables if required.

The principal merits of this cell are its thermal characteristics which allow the sample to reach equilibrium temperature quickly. The rigidly fixed coaxial electrode design gives a very stable cell constant with a very small stray capacitance. Finally, the cell uses only a small volume of liquid and is easy to clean.

Another type of cell, parallel plate capacitor cell, used for solid disks, also designed by Mr. Morgan is shown in Figure II.2.

THE GENERAL RADIO BRIDGES

The GR1615-A Capacitance bridge and the GR1621 Precision Capacitance Measurement system are manufactured by the General Radio Company, Concord, Massachusetts, U.S.A. The GR1615-A bridge allows measurement of the capacitance and conductivity of a sample to be made at frequencies ranging from 50 Hz to 10^5 Hz. This system consists of GR1310-B sine wave signal generator and 1232-A tuneable amplifier - null detector, while the GR1621 system consists of the GR1616 Precision Capacitance bridge with

the GR1316 Oscillator and the GR1238 Detector. This GR1621 system measures the capacitance and conductivity of a capacitor more precisely in the frequency range of 10 Hz to 10^5 Hz. After warm-up the frequency stability is typically within $\pm 0.001\%$ for a few minutes. Also, with the help of this later system a wide range of capacitance can be measured, extending from the resolution limit of 0.1 aF (10^{-7} picofarad) to a maximum of 10 μ F (10 microfarad), with internal standards, or farther with external standards.

This GR bridge measures the capacitance and conductivity of the capacitor, which can be related to the components of the complex permittivity by the following equations (2):

$$\epsilon' = C/C_0 \quad \text{II-4}$$

and

$$\epsilon'' = G/\omega C_0 \quad \text{II-5}$$

where G is the conductivity of the system and the other forms have their usual meaning, mentioned previously. Actual measurements were made by bringing the bridge into balance as indicated by null-detector for solutions studied in different three-terminal co-axial and parallel-plate capacitance cells.

SAMPLE PREPARATIONS AND DIELECTRIC MEASUREMENTS

Liquid samples were used in the co-axial cells. The solutions were prepared by adding a given quantity of solvent such that the resultant solution had a weight/weight concentration of about 8% or less depending upon the magnitude of the dipole moment of the solute and, in certain cases, on the solubility of the solute in the solvent. The two main solvents used in these studies were cis-decalin and polystyrene. The solutions were then left for about twenty-four hours to ensure a homogeneous solution.

For a chemical system, the dielectric characteristics of which were unknown, the sample was cooled to near liquid nitrogen temperature and slowly heated up to the glass transition temperature while capacitance and dissipation (conductance in the case of GR1621) at recorded temperatures were taken periodically. From the resultant plot of loss factor (ϵ'') versus temperature (K) at a fixed frequency, suspected areas of dielectric absorption were identified. The system was then heated again to 295 K and cooled quickly to some temperature well below the temperature at which the absorption process was expected to begin from the lowest frequency of the measurement. Full frequency dielectric measurements at specific temperatures were then

carried out so as to obtain as broad a $\log f_{\max}$ range as possible. The temperature was recorded to an accuracy of $\pm 0.1^\circ\text{C}$ with the help of a Newport 264-3 platinum resistance thermometer.

In the case of solutions of polar solvents trapped in atactic polystyrene, the samples were prepared by employing the procedure similar to that described by Davies and Swain (3). The desired amount of solute (0.15-0.25 g) and polystyrene pellets (nearly 2.5 g to make about 4-8% of the former) were dissolved in 10 ml of 1,2-trans-dichloroethylene, in a porcelain crucible. The mixture was stirred thoroughly, until it dissolved completely, followed by evaporation in a drying oven at about 80°C . The plastic mass was then placed in a stainless steel die, removed, trimmed to size and its average thickness was measured. The weight of the disk was also noted, and the molar concentration of the solute in the matrix was calculated according to the formula given by Tay and Walker (4) as:

$$\text{concentration} = \frac{\text{wt. of solute used}}{\text{mol wt. of solute}} \quad \times$$

$$\frac{\text{wt. of disk}}{\text{wt. of PS + Solute}} \quad \times \quad \frac{1000}{\text{vol. of disk}}$$

The polystyrene matrix disk was clamped between the two

electrodes of the parallel plate capacitance cell and the dielectric measurement carried out in the previously described way.

The dissipation or conductivity factors and capacitance were measured with the General Radio bridge. The product of the frequency and dissipation factor gives loss tangent value, $\tan\delta$. With these values obtained experimentally and the following relations, it was possible to determine dielectric loss values for the parallel plate capacitance cell.

$$\epsilon'' = \epsilon' \tan\delta \quad \text{II-6}$$

$$\epsilon' = \frac{cd}{0.08842A} \quad \text{II-7}$$

$$\epsilon'' = \frac{\epsilon'G}{\omega C} \quad \text{II-8}$$

where C is the capacitance of the cell with the sample in picofarads, d is the spacing of the capacitance plates (in cm), A is the effective area of the plates (in cm^2), G is the conductivity of the system in picomhos.

The effective area of the electrode plates, A, had been determined by measuring the capacitance of the cell containing a standard quartz disk having a diameter of 2.0 in

and a thickness measuring 0.0538 in (supplied by the Rutherford Research Products Co., New Jersey, USA) with a dielectric constant of 3.819.

The co-axial cells were also calibrated, to determine relevant constants, with purified cyclohexane at room temperature.

GLASS TRANSITION APPARATUS

This apparatus which measures the linear expansion of solid or frozen liquid samples was also devised by Mr. B.K. Morgan of this laboratory. When the sample A is heated, it causes the inner pyrex tube to move upwards relative to the outer pyrex tube. This movement is transmitted from the cup of the inner tube to the core of transducer B. Movement of the core causes a change in the electromagnetic coupling between the input and output coils of the transducer. The output coil is connected to a strip chart recorder which displaces a rising trace as the sample is heated towards the glass transition temperature. Near the glass transition temperature the trace levels off and then begins to fall as the sample softens. There are two interchangeable sample holders with the apparatus. The sample holder, C, is for samples which are solid at room

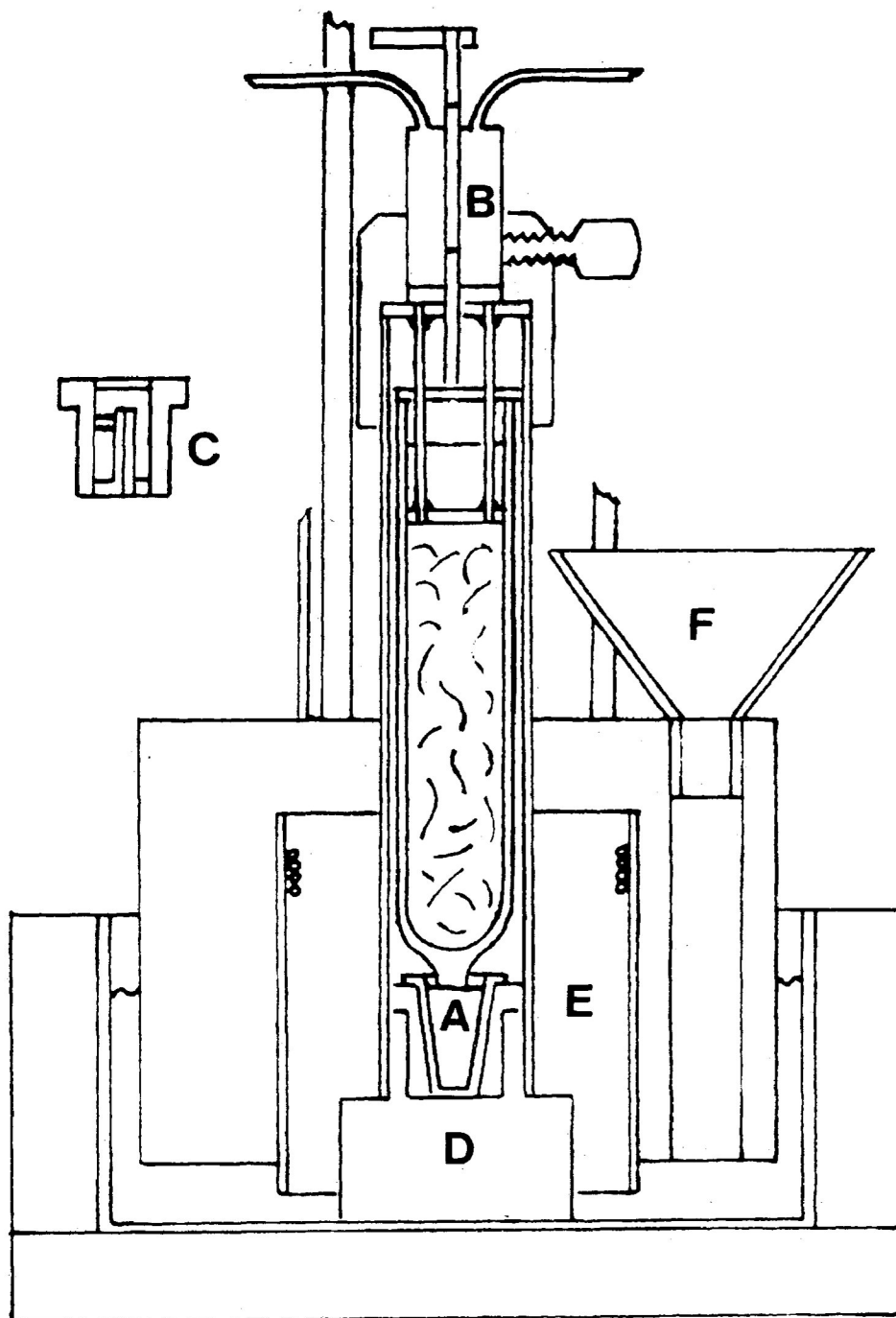


Figure 11-3 Glass Transition Temperature Measurement Apparatus.

temperature while A is for samples which are liquid at room temperature. The idea for this apparatus was suggested by Dr. N. Koizumi of Kyoto University, Japan. The solid sample was prepared in the form of a strip roughly 20 mm by 8 mm and 1 to 2 mm thick. The sample was secured at one end by a small screw in a slotted rod which fits freely in a sample holder, C.

ANALYSIS OF EXPERIMENTAL DATA

The experimental data, obtained by dielectric measurements, were analysed by a series of calculator and computer programs. The programs were written in the APL language. The dielectric loss of the sample solution was calculated using the Texas Instruments SR59 programmable calculator and Radio Shack TRS-80, pocket computer.

$$\Delta\epsilon''_{\text{solute}} = \epsilon''_{\text{solution}} - \epsilon''_{\text{solvent}}$$

For each measurement of temperature, the data of dielectric loss factor as a function of frequency were analysed by the computer according to the Fuoss-Kirkwood equation (6) the linear form of which is

$$\cosh^{-1} \frac{\epsilon''_{\text{max}}}{\epsilon''} = 2.303\beta(\log v_{\text{max}} - \log v) \quad \text{II-9}$$

by a procedure employed by Davies and Swain (3). By iteration the computer program finds that the value of ϵ''_{\max} provides the best linear fit to the plot of $\cosh^{-1} (\epsilon''_{\max} / \epsilon'')$ against $\log v$; the slope of this straight line gives the β -value and the v_{\max} is obtained from the slope and intercept.

The Fuoss-Kirkwood equation does not consider the real part of the complex permittivity nor does it with the limiting values at low and high frequencies, ϵ_0 and ϵ_α , respectively, except that the total dispersion is given by the equation:

$$\Delta\epsilon = \epsilon_0 - \epsilon_\alpha = \frac{2\epsilon''_{\max}}{\beta} \quad \text{II-10}$$

The Cole-Cole distribution parameter, α , may be obtained from the Fuoss-Kirkwood distribution parameters, β , by the equation:

$$\beta = \frac{1 - \alpha}{\sqrt{2} \cos\left(\frac{\pi(1 - \alpha)}{4}\right)} \quad \text{II-11}$$

The program entitled EINF was used to find the value of ϵ_0 at various temperatures. Equations I-17 and I-18, with experimental values of ϵ' of various frequencies

at each temperature, were fed into the computer; ϵ_α came out as an output with an estimate of error involved.

The results from the foregoing analysis were used for the calculation of the effective dipole moments involved in the relaxation process from both the Debye (5) equation (II-12) and the Onsager (6) equation (II-13):

$$\mu^2 = \frac{27000 \text{ kT} (\epsilon_0 - \epsilon_\alpha)}{4\pi\text{NC}(\epsilon' + 2)^2} \quad \text{II-12}$$

$$\mu^2 = \frac{9000 \text{ kT} (2\epsilon_0 + \epsilon_\alpha)(\epsilon_0 - \epsilon_\alpha)}{4\pi\text{NC}\epsilon_0 (\epsilon_\alpha + 2)} \quad \text{II-13}$$

where:

$$\epsilon_0 - \epsilon_\alpha = \frac{2\epsilon''_{\text{max}}}{\beta}$$

ϵ' is the value of ϵ' at ν_{max} , that is
 $(\epsilon_\alpha + \epsilon_0)/2$

ϵ_0 is the static dielectric constant derived from ϵ_α and equation II-10.

N is the Avogadro Number, 6.023×10^{23} molecules/mol

C is the concentration in mol/litre

k is the Boltzman constant, 1.38×10^{-16}
erg K⁻¹, and

T is the temperaure in K.

These equations yielded μ in units of e.s.u. - cm,
but commonly this parameter is expressed in Debye units, where:

$$1 \text{ D} = 1 \times 10^{-18} \text{ e.s.u. - cm.}$$

The energy barrier which must be surmounted in
the motion of the dipole was evaluated in terms of the
Eyring enthalpy of activation, ΔH_E by using the Eyring rate
expression equation (II-14), a procedure commonly used
in dielectric work (3,7):

$$\tau = \frac{h}{kT} \exp\left(\frac{\Delta H_E}{RT}\right) \exp\left(\frac{-\Delta S_E}{R}\right)$$

which can be rearranged to the linear form as:

$$\ln(T\tau) = \frac{\Delta H_E}{RT} - \left(\frac{\Delta S_E}{R}\right) + \ln\left(\frac{h}{k}\right) \quad \text{II-14}$$

The plot of $\log(T\tau)$ against $1/T$ yielded good straight lines, and from the slope and intercept of these lines the value of the enthalpy of activation, ΔH_E , and the entropy of activation, ΔS_E , respectively were evaluated with the help of a computer program. The computer program also calculates relaxation times ' τ ' and free energies of activation, ΔG_E , at different temperatures by employing the equations II-15 and II-16, respectively.

$$\tau = \frac{h}{RT} e^{\Delta G/RT} \quad \text{II-15}$$

$$\Delta G_E = \Delta H_E - T\Delta S_E \quad \text{II-16}$$

Standard statistical techniques (8) provide a means of estimating errors in fitting a straight line to a set of graph points. The Fuoss computer program calculated errors in $\log v_{\max}$ and β for the 90%, 95%, 98%, and 99% confidence intervals. The 95% confidence interval was chosen as a good representation of experimental error, typical values for $\log_{10}(v_{\max})$ being ± 0.05 to 0.10 .

The same technique was adopted to calculate the 95% confidence intervals for both ΔH_E and ΔS_E . In the present work, the maximum error in ΔH_E is hardly greater than $\pm 10\%$ or $\pm 3 \text{ kJ mol}^{-1}$ whichever be the greater.

REFERENCES

1. D.L. Gourlay, M.Sc. Thesis, Lakehead University, Thunder Bay, Canada, 1982.
2. C.P. Smyth, "Dielectric Behaviour and Structure", McGraw-Hill Book Co., New York, 1955.
3. M. Davies and J. Swain, Trans. Faraday Soc., 67, 1637, (1971).
4. S.P. Tay and S. Walker, J. Chem. Phys., 63, 1634, (1975).
5. N.E. Hill, W.E. Vaughan, A.H. Price and M. Davies, "Dielectric Properties and Molecular Structure", Van Nostrand-Reinhold, London, England, 272, (1969).
6. C.J.F. Böttcher, "Theory of Electric Polarization", Elsevier Publishing Co., Amsterdam, Netherlands, 323(1952).
7. M. Davies and A. Edwards, Trans. Faraday Soc., 63, 2163 (1967).
8. B. Ostle, "Statistics in Research", (2nd ed.), Iowa State University Press, Ames, Iowa, U.S.A., (1963).

CHAPTER III

α - AND β -RELAXATIONS OF SOME RIGID POLAR
MOLECULES IN *cis*-DECALIN

INTRODUCTION

The rotation of simple dipolar organic molecules as pure liquids or in non-polar solvents at room temperature gives rise to dielectric dispersion at microwave frequencies (1). Dipole reorientation may be slowed down to such an extent that the absorption occurs in the kHz region by the employment of a glassy forming solvent (2). At temperatures just above the glass transition, the relaxation involves a highly co-operative process characterized by a large apparent activation enthalpy, ΔH_E . A relaxation process often persists on cooling into the glassy state (3). These secondary relaxations, which have a much smaller ΔH_E , are observed for rigid molecules which cannot undergo reorientation by an intramolecular process. They may also be observed for flexible molecules.

α and β -processes have been observed for various systems which form glasses and these include:

- (a) pure o-terphenyl (2,4)
- (b) cis-decalin (2,4)
- (c) solutes in cis-decalin (2,6,7,9)
- (d) various other supercooled liquids (2,4,5)

- (e) mixtures of polar liquids (2,4,8)
- (f) amorphous polymers (7).

A variety of studies has been made on the glassy forming substances, cis-decalin and o-terphenyl. In both cases solutes have been added (usually at high concentration) and α and β processes have been detected above and below the T_g in both cases. The precise nature of the β -process in these systems has never been identified. The analogy which is made to the behaviour of solid polymers is appealing - especially with respect to the α -process. However, for the β -process the relaxation may be somewhat vague - especially since the precise nature of the β -process in most polymers has never been established.

Various interpretations of the β -process in glasses of rigid molecules have been made, and most of these have been considered by Johari and Goldstein (4), Johari (10) and Williams (2).

The present work examines twelve rigid nearly spherical dipolar solutes in cis-decalin. It was considered worthwhile to attempt to relate the results obtained in the solvent media, cis-decalin, o-terphenyl and Santovac, with those in polystyrene where it had been well established

that for a rigid molecule at low concentration the relaxation process is a molecular one (11,12,13). This was first established by Davies and Edward (11). A suitable parameter to carry out this comparison of the low temperature (β -) process in all four media is the enthalpy of activation.

EXPERIMENTAL RESULTS

The dielectric measurements of seventeen dipolar rigid molecules have been made in cis-decalin as well as cis-decalin in the pure supercooled state in the frequency range 10 Hz to 10^5 Hz by 1621 General Radio Precision bridge and 1615A General Radio bridge. Some of these molecules studied in polystyrene matrices by several workers in this laboratory are also recorded in this chapter for comparison with the results obtained in the cis-decalin medium.

Figures III.1, 7, 10, 12 and 19 show the plots of $\log T\tau$ versus $1/T$. Figures III.2, 16, 20 and 21 show the Cole-Cole plot. Sample plots of dielectric loss ($=\epsilon''_{\text{obs}} - \epsilon''_{\text{solv.}}$) versus $T(K)$ are shown in Figures III.3, 4, 5, 6, 8, 11, 13, 14, 15, and 16. Figures III.9 and 18 show the sample plots of ϵ'' versus $\log \nu$ in cis-decalin.

DISCUSSION

A. β -Relaxation

The low temperature absorptions which appeared in the twelve rigid molecules (Table III.1) are termed as β -relaxation. The Fuoss-Kirkwood analysis parameters for twelve rigid dipolar molecules have been given in Table III-3.

Methyliodide

Methyliodide shows a β -relaxation in the temperature range 80-95 K. The Eyring plot of $\log T\tau$ versus $1/T$ is shown in Figures III.1 which gives ΔH_E and ΔS_E values of $7.6 \pm 1.3 \text{ kJ mol}^{-1}$ and $-49.7 \pm 15 \text{ J K}^{-1} \text{ mol}^{-1}$, respectively. The Cole-Cole plot is symmetric and broad indicating a wide spectrum of relaxation times (Figure III-2). The low relaxation time, $1.8 \times 10^{-6} \text{ s}$ at 100 K, and the corresponding low activation enthalpy suggests molecular rotation.

1,1,1-Trichloroethane

The β -relaxation in this molecule has been

studied in the temperature range 79-97 K. The plot of ϵ'' versus T is given in Figure III.3. The ΔH_E and ΔS_E values for this molecule are $8.7 \pm 1.7 \text{ kJ mol}^{-1}$ and $-28 \pm 20.4 \text{ J K}^{-1} \text{ mol}^{-1}$, respectively. Since the molecule is nearly spherical, the volume swept out by the molecule will be small and hence and so will the energy barrier. The intramolecular process about the C-C bond is dielectrically inactive, because there is no perpendicular dipole moment component and the only dipole moment is along the perpendicular axis. Clearly, the β -relaxation for 1,1,1-trichloroethane is a molecular process.

2,2,-Dichloropropane

The plot of ϵ'' versus T is given in Figure III.4. The enthalpy of activation and the entropy of activation for 2,2-dichloropropane are $9.3 \pm 1.2 \text{ kJ mol}^{-1}$ and $-17.9 \pm 14.5 \text{ J K}^{-1} \text{ mol}^{-1}$, respectively. The relaxation time and the free energy of activation at 100 K are $3.0 \times 10^{-7} \text{ s}$ and 11.1 kJ mol^{-1} , respectively, which are comparable with the similar sized molecule 1,1,1-trichloroethane, $5.2 \times 10^{-7} \text{ s}$ and 11.6 kJ mol^{-1} , respectively.

An n.m.r. study of this molecule in the solid state indicates $E_a = 12.5 \text{ kJ mol}^{-1}$ for molecular tumbling. Thus,

$\Delta H_E \cong 9.3 \text{ kJ mol}^{-1}$ obtained by the dielectric method compares reasonably within experimental error with that obtained by the n.m.r. method (14). Hence, the β -relaxation in 2,2-dichloropropane is due to molecular rotation.

2-Methyl-2-chloropropane and 2-methyl-2-bromopropane

A dielectric β -relaxation process seems to be present in *t*-butylchloride near the liquid nitrogen temperature (Figure III.5). At 82 K the free energy of activation was found to be 10.2 kJ mol^{-1} .

For *t*-butylbromide, which is slightly greater sized than *t*-butylchloride, the absorption process shifts to a higher temperature region (Figure III.6). The Eyring rate plot $\log T\tau$ versus $1/T$ is given in Figure III.7, which gives ΔH_E and ΔS_E values, $10.6 \pm 1.2 \text{ kJ mol}^{-1}$ and $-7.5 \pm 14.5 \text{ J K}^{-1} \text{ mol}^{-1}$, respectively, which is comparable with the ΔH_E and ΔS_E values of the similar-sized molecule, 2,2-dichloropropane, $9.3 \pm 1.2 \text{ kJ mol}^{-1}$ and $-17.9 \pm 14.5 \text{ J K}^{-1} \text{ mol}^{-1}$, respectively. Thus, it is reasonable to assign this lower temperature absorption of *t*-butylbromide to a molecular process. *t*-Butylchloride is more spherical than *t*-butylbromide and so the rotation of the molecule

should be less hindered. Moreover, the measured ΔG_E value of t-butylchloride is at a lower temperature (82 K). Since the lower temperature absorption of t-butylbromide may be attributed to a molecular relaxation, it seems reasonable to assign the lower temperature relaxation of t-butylchloride to a molecular one.

Methyltrichlorosilane

One temperature region of absorption has been found in this molecule and studied from 105-128 K. The ϵ'' versus T plot is broad and asymmetric (Figure III.8). The ΔH_E and ΔS_E values are $23.4 \pm 1.5 \text{ kJ mol}^{-1}$ and $46.6 \text{ J K}^{-1} \text{ mol}^{-1}$, respectively. The ΔH_E value and relaxation time at 100 K are three times and 10^4 times greater than that of the slightly lower sized molecule, 1,1,1-trichloroethane (Table III.1). The broad asymmetric absorption curves and the ΔH_E and ΔS_E values for methyl trichlorosilane suggest that there is appreciable overlapping between α - and β -processes.

Bromoform

The low temperature absorption for bromoform in cis-decalin has been studied from 87-100 K. The symmetric

and broad ϵ'' versus $\log f$ curves are given in Figure III.9. Kashem (18) studied bromoform in polystyrene matrix, o-terphenyl and polyphenyl ether. The Eyring plots in various media are shown in Figure III.10. The ΔH_E (kJ mol^{-1}) values in cis-decalin, polystyrene matrix, o-terphenyl and polyphenyl ether are respectively, 12.2 ± 0.9 , 7.9 ± 0.7 , 10.4 ± 0.8 and 8.8 ± 0.5 . It is clear that the ΔH_E value of bromoform in four glassy media is similar within the limits of experimental error. The β -values for bromoform are in the range 0.17-0.34, which is similar to what has been found by Davies and Swain (10) for the molecular rotation in a polystyrene matrix. Therefore, it is quite reasonable that the low temperature absorption of bromoform in cis-decalin is a molecular rotation.

o-Dichlorobenzene, o-xylene, o-bromochlorobenzene and bromotoluene

O-Dichlorobenzene has been studied in the temperature range 100 - 124 K in cis-decalin. o-Dichlorobenzene has also been studied in polystyrene (10), o-terphenyl and Santovac (18). In all four glassy media the ϵ'' versus T curves are symmetric and broad and appear almost in the similar temperature range (Fig. III-11). The plot of $\log T\tau$ versus $1/T$ is shown in Figure III-12. The ΔH_E and ΔS_E values for o-dichlorobenzene in cis-decalin,

polystyrene, o-terphenyl and polyphenyl ether are 12.9 ± 0.8 and -31.7 , 11.2 ± 0.6 and $21.4 \pm 6-9$, 13.4 ± 0.7 kJ mol^{-1} and -17.4 ± 7.8 $\text{J K}^{-1} \text{mol}^{-1}$ respectively. The very similar ΔH_E and ΔS_E values for o-dichlorobenzene in different glassy media indicates that the same mechanism is operative in all the glassy solvent. In polystyrene matrix it has been established that the β -process is due to molecular rotation. Therefore, it is obvious that the β -relaxation in cis-decalin for o-dichlorobenzene is a molecular one.

o-Xylene has been studied in cis-decalin in the temperature range 101-119 K. The ϵ'' versus T plot (Fig. 22) is symmetric and broad. The enthalpy and entropy of activation for o-xylene are 14.3 kJ mol^{-1} and -40.3 $\text{J K}^{-1} \text{mol}^{-1}$ respectively. Generally, the size of the methyl group is reckoned as the size of a chlorine atom. Therefore, the size of o-xylene is similar to o-dichlorobenzene. The enthalpy and entropy of activation for o-xylene are in excellent agreement with the enthalpy and entropy of activation of o-dichlorobenzene ($\Delta H_E = 12.9$ kJ mol^{-1} and $\Delta S_E = -31.7$ $\text{J K}^{-1} \text{mol}^{-1}$) in cis-decalin. So the dielectric absorption in o-xylene is due to molecular rotation.

o-Bromochlorobenzene has been studied in

the temperature range 128-152 K in cis-decalin. The plot of ϵ'' versus T is broad and asymmetric (Fig. III.13). The ΔH_E and ΔS_E values are $18.9 \pm 0.7 \text{ kJ mol}^{-1}$ and $4.9 \pm 4.9 \text{ J K}^{-1} \text{ mol}^{-1}$, respectively. The ΔH_E and ΔS_E values in polystyrene matrix are 16.0 kJ mol^{-1} and $8 \text{ J K}^{-1} \text{ mol}^{-1}$, respectively. But the relaxation time at 150 K in cis-decalin is 10^2 times greater than that of polystyrene. This, together with the broad and asymmetric nature of the loss curve, suggest that the β -relaxation overlapped with the α -process.

o-Bromotoluene, which is similar in size to o-bromochlorobenzene, absorbs in the similar temperature range (130-150 K). The ϵ'' versus T plot is also broad and asymmetric (Fig. III-4). From Table III-1 it is seen that the ΔG_E and τ (s) at 100 K are 18.5 kJ mol^{-1} and 2.2×10^{-3} which are considerably greater than that of o-bromochlorobenzene in polystyrene which has been interpreted as molecular rotation. This consideration led to the conclusion of overlapping of β -relaxation with α -relaxation.

Pyridine

The low temperature absorption of pyridine

absorbs in the temperature range 103-119 K in cis-decalin. The ΔH_E and ΔS_E values are $14.2 \pm 2.9 \text{ kJ mol}^{-1}$ and $-14.2 \text{ J K}^{-1} \text{ mol}^{-1}$, respectively. Kashem (18) studied pyridine in o-terphenyl and the ΔH_E and ΔS_E values are $8.4 \pm 1.1 \text{ kJ mol}^{-1}$ and $-43.9 \pm 7.5 \text{ J K}^{-1} \text{ mol}^{-1}$ respectively. The large variation in ΔH_E value from cis-decalin to o-terphenyl is not properly understood.

4-Methylpyridine

The low temperature absorption for 4-methylpyridine appears in the temperature region 103-119 K in cis-decalin. The ϵ'' versus T plot is given in Fig. III-15. The Cole-Cole plots at various temperatures are shown in Fig. III-16. On comparison of ΔH_E (kJ mol^{-1}) values (Table III-1), we find that they are for 4-methylpyridine, (i) in a polystyrene matrix, 14 (ii) in o-terphenyl, 16.0 ± 0.9 , (iii) in polyphenyl ether 17.2 ± 0.7 and in (iv) cis-decalin 15.8 ± 1.5 . In polystyrene matrix, the β -process of 4-methyl pyridine has been explained by the molecular rotation. Hence the β -relaxation for 4-methylpyridine in cis-decalin is a molecular one.

From the above discussion we see that except

in the case of methyltrichlorsilane, o-bromochlorobenzene and o-bromotoluene, in all other rigid dipolar molecules, the β -relaxation has been completely separated from the α -relaxation. In the latter three rigid dipolar molecules, probably α - and β -relaxations overlapped.

The β -relaxation has been found to possess the following characteristics;

- (i) takes place below T_g
- (ii) broad and asymmetric loss curves
- (iii) linear Eyring plot
- (iv) low activation enthalpy
- (v) relaxation time decreases with the increase of temperature

Three compounds, o-dichlorobenzene, 4-methylpyridine and bromoform have been studied in four solvents (Table III-1). For both of these solutes, for similar concentrations, the activation enthalpy and the intensity of absorptions are similar for each solute in various solvents (Fig. III-11).

In general, the ΔH_E values for each solute in a particular solvent show an increase with increased molecular size, and the similarity in behaviour of mono-

halobenzenes in polystyrene, o-terphenyl and Santovac appears significant. All of the solutes are incapable of exhibiting dielectrically active intramolecular motion. The fact that ΔH_E is essentially independent of the solvent implies that there is little influence upon the rotation of the dipolar solute. For the solute in polystyrene matrix at these low concentrations, the β -relaxation is well established as molecular rotation (11) where the solute molecules are monomolecularly dispersed in the polystyrene cavities (1). The virtual identity of the ΔH_E values for o-dichlorobenzene in cis-decalin, o-terphenyl and Santovac and their correspondence with the polystyrene matrices indicate the molecular nature of the β -relaxation. This is supported by similar studies on 4-methylpyridine and bromoform in all four solvents (Table III-1).

It is striking that for each of the polar solute molecules in the somewhat diverse glassy materials, a similar ΔH_E value results and that the ΔH_E value increases with size appropriately.

It is tempting to extend the concept of the single solute (at low concentration) in the polystyrene cavity to that of the other solvents, the model being that there is a solute molecule (in what is effectively a

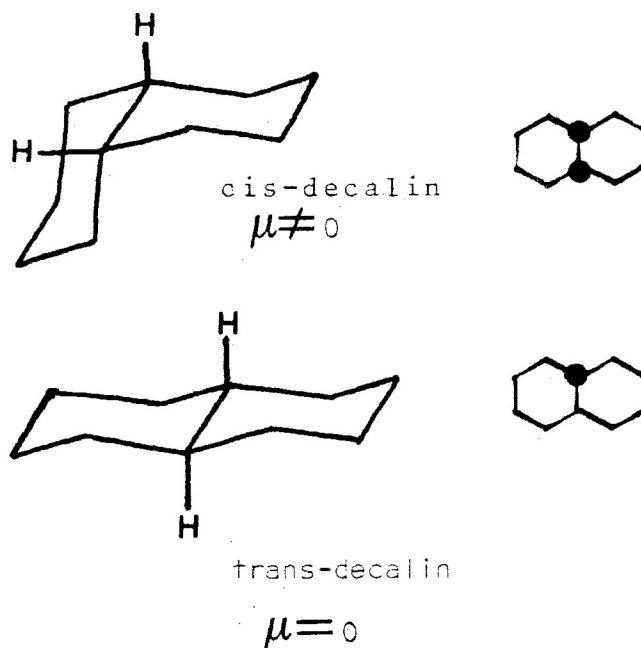
cavity) where molecular relaxation takes place between equilibrium positions. On the time scale of relaxation processes the solvent cavity does not need to alter appreciably to permit a solute molecule to rotate.

It must be stressed, however, that our findings are for simple rigid molecules in four glassy forming solids. Our concentrations are low compared with most of those employed by the previous investigations on α - and β -processes such as mixtures of polar compounds (4,8). Furthermore, the work on pure supercooled liquids may present a somewhat different case.

A more all-embracing model which leads to a β -relaxation in these various systems is one by Johari (10) where he postulates that a potential exists within the region of the solute molecule which resists the local rearrangement and leads to relative fixedness of the molecules in that region. Hence, β -relaxation processes take place over this energy barrier. Our systems, which seem to lead to a "solvent-cavity" model, for somewhat limited types of systems, would seem in harmony with the more general model conceived by Johari.

B. α -Relaxation

The main relaxations appeared near or above their respective T_g for the compounds listed in Table III-2 are termed α -relaxation. cis-Decalin is a weakly polar liquid and exhibits α -relaxation just above its glass transition temperature ($T_g \approx 136$ K) (19). But trans-decalin is non-polar by virtue of its symmetry and does not yield a α -process detectable by dielectric absorption studies.



The addition of chlorobenzene to trans-decalin reveals an α -process where the polar solute acts as a probe to reveal the co-operative motion of the dispersion medium. This was also observed for chlorobenzene in the non-polar cyclohexane.

The α -relaxation for the rigid dipolar molecules are found to possess the following characteristics:

- (1) absorption at high temperature (Table III-2)
- (2) broad asymmetric loss curves (Figs. 17 and 18)
- (3) large apparent enthalpy of activation (Table III-2)
- (4) a curved Eyring plot (Fig. III-19)
- (5) absorption at and above T_g
- (6) Cole-Cole plot is asymmetric (Fig. III-20 and III-21).

The α -process is due to co-operative motion of solvent and solute molecules (15). Co-operative relaxation is usually described by a Cole-Davidson skewed arc function. Higasi et al (17) made dielectric studies of a number of molecules in supercooled o-terphenyl over the temperature range 283-303 K. Their dielectric data were represented by the asymmetric Davidson-Cole function.

Johari and Goldstein (4) studied the dielectric microbrownian relaxation with the activation

enthalpy in the range 230-293 kJ mol^{-1} in a large number of supercooled systems involving molecules smaller in size. An apparent activation enthalpy about 200 kJ mol^{-1} was found for some small molecules in the supercooled o-terphenyl (7). The activation energy of around 300 kJ mol^{-1} was observed for the co-operative process of di-n-butyl phthalate in polystyrene (15), which is close to that commonly found for the glass transition process in amorphous polymers and for polystyrene in particular (16).

Johari and Smyth (6) studied some rigid molecules in cis-decalin in the supercooled state. They obtained an asymmetric Cole-Cole plot with activation enthalpy from 80-290 kJ mol^{-1} .

Our results for the α -relaxation shows that the Cole-Cole plot, loss curves are asymmetric and Eyring rate plot is non-linear. These considerations suggest that these α -relaxations which take place above the glass transition temperature are co-operative motions of solute and solvent molecules.

Recently, Mansingh et al (20) showed that the α -relaxation in cis-decalin takes place in the amorphous state above T_g and the β -relaxation takes place in the glassy state below T_g .

REFERENCES

1. N.E. Hill, W.E. Vaughan, A.H. Price and M. Davies. "Dielectric Properties and Molecular Behaviour", Van-Nostrand-Reinhold, London, 1969.
2. G. Williams in "Dielectric and Related Molecular Processes". (ed. M. Davies). Specialist Periodical reports, Chemical Society, London, Vol. 2, 1975.
3. L. Hayer and M. Goldstein, J. Chem. Phys., 66, 4736(1977).
4. G.P. Johari and M. Goldstein. J. Chem. Phys., 53, 2372(1970).
5. G.P. Johari and M. Goldstein. J. Chem. Phys., 55, 4245(1971).
6. G.P. Johari and C.P. Smyth. J. Chem. Phys., 56, 4411(1972).
7. G. Williams and P.J. Hains, J.C.S., Faraday Symp., 6, 14(1972).
8. G.P. Johari, J. Phys. Chem., 74, 2034(1970).
9. M.S. Ahmed, M.A. Kashem and S. Walker. J. Phys. Chem. (submitted)
10. G.P. Johari. Annals, N.Y. Acad. Sci., 279, 117(1976).
11. M. Davies and S. Swain. Trans. Faraday Soc., 67, 1637(1971).
12. M. Davies and A. Edwards. Trans. Faraday Soc. 63, 2163(1967).
13. H.A. Khwaja and S. Walker. Adv. Mol. Relax. Processes, 19, 418(1981).
14. E.O. Stejskal, D.E. Woessner, T.C. Farrar, and H.S. Gutowsky, J. Chem. Phys., 31, 55(1959).

15. P.J. Hains and G. Williams, *Polymer*, 16, 725(1975).
16. N.G. McCrum, B.E. Read, and G. Williams, "Anelastic and Dielectric effects in Polymer Solids", John Wiley, N.Y., 1967.
17. M. Nakamura, H. Takahashi and K. Higasi, *Bull. Chem. Soc. Jpn.*, 47, 1593(1974).
18. M.A. Kashem, M.Sc. Thesis, Lakehead University, 1982.
19. M.S. Ahmed, J. Chao, J. Crossley, M.S. Hossain and S. Walker. *J. Chem. Soc. Faraday*. (In press)
20. A. Mansingh, C.B. Agarwal and R. Singh, *Chem. Phys. Letts.* 68, 101(1980).

TABLE III-1:

EYRING ANALYSIS RESULTS FOR β -PROCESS OF RIGID POLAR MOLECULES IN CIS-DECALIN

MOLECULE	MEDIUM	T (K)	Relaxation Times τ (s)		ΔG_E (kJ mol ⁻¹)		ΔH_E kJ mol ⁻¹	ΔS_E J K ⁻¹ mol ⁻¹
			100 K	150 K	100 K	150 K		
methyl iodide ¹	cis-decalin	80-95	1.8×10^{-6}	1.0×10^{-6}	12.6	15.8	7.6±1.3	-49.7±15.1
1,1,1-trichloroethane	cis-decalin	79-97	5.2×10^{-7}	1.1×10^{-8}	11.6	12.8	8.7±1.7	-28.3±20.4
2,2-dichloropropane	cis-decalin	80-86	3.0×10^{-7}	4.8×10^{-9}	11.1	12.0	9.3±1.2	-17.9±14.5
2-bromo-2-methylpropane	cis-decalin	81-87	3.9×10^{-7}	3.8×10^{-9}	11.3	12.2	10.6±1.2	-7.5±14.5
2-chloro-2-methylpropane	cis-decalin	82			10.4			
methyl trichlorosilane	cis-decalin	105-128	3.2×10^{-3}	1.8×10^{-7}	18.8	16.5	23.4±1.5	46.6±10.2
cyclohexanone	cis-decalin	107-128	1.2×10^{-3}	2.1×10^{-7}	18.0	16.7	20.5±4.7	25.5±4.3
bromoform	cis-decalin	87-100	1.1×10^{-4}	5.6×10^{-7}	16.0	17.9	12.2±0.9	-38.5±10.6
bromoform ²	P.S.	99-135	1.6×10^{-4}	4.5×10^{-6}	16.3	20.5	7.9±0.7	-84.3±6.2
bromoform ²	G.O.T.P.	107-144	1.7×10^{-3}	1.7×10^{-5}	18.2	22.2	10.4±0.8	-78.4±6.2
Bromoform ²	Santovac	100-139	2.1×10^{-4}	4.0×10^{-6}	16.5	20.4	8.8±0.5	-77.1±4.6
o-dichlorobenzene	cis-decalin	100-124	1.2×10^{-4}	4.4×10^{-8}	16.0	17.6	12.9±0.8	-31.7±5.6
o-dichlorobenzene ³	P.S.	80-103	4.3×10^{-6}	3.3×10^{-8}	13.3	14.4	11.2±0.6	-21.4±6.9
o-dichlorobenzene ²	G.O.T.P.	80-114	2.4×10^{-6}	1.7×10^{-7}	14.7	16.4	11.4±0.6	-33.8±6.4
o-dichlorobenzene ²	Santovac	80-114	3.8×10^{-5}	1.2×10^{-7}	15.1	16.0	13.4±0.7	-17.4±7.8
o-bromochlorobenzene	cis-decalin	128-152	6.0×10^{-3}	2.0×10^{-7}	19.3	19.5	18.9±0.6	-4.93±4.9
o-bromochlorobenzene ⁴	P.S.	88-120	3.6×10^{-5}	4.1×10^{-8}	15.1	14.7	16.0	8.0
o-bromotoluene	cis-decalin	130-150	2.2×10^{-3}	1.6×10^{-6}	18.5	19.3	17.0±2.3	-15.5±18.2
pyridine	cis-decalin	103-119	1.2×10^{-5}	1.6×10^{-7}	15.7	16.4	14.2±2.9	-14.2±13.0
4-methylpyridine	cis-decalin	82-106	7.1×10^{-5}	8.3×10^{-8}	15.6	15.5	15.8±1.5	1.9±16.8

TABLE III-1 continued....

MOLECULE	MEDIUM	ΔT (K)	Relaxation Times τ (s)		ΔG_E (kJ mol ⁻¹)		ΔH_E	ΔS_E
			100 K	150 K	100 K	150 K	kJ mol ⁻¹	J K ⁻¹ mol ⁻¹
4-methylpyridine ⁴	P.S.	88-124	8.5×10^{-5}	2.1×10^{-7}	15.8	16.7	14.0	-19.0
4-methylpyridine ²	G.O.T.P.	105-154	5.8×10^{-3}	6.3×10^{-6}	19.3	20.9	16.0 \pm 1.0	-33.0 \pm 7.5
4-methylpyridine ²	Santovac	110-152	1.0×10^{-2}	2.0×10^{-6}	18.8	19.8	17.2 \pm 0.8	-26.0 \pm 6.0
o-xylene	cis-decalin	101-119	1.8×10^{-3}	3.8×10^{-6}	18.3	20.3	14.3 \pm 1.4	-40.3 \pm 12.3

1 - reproduced courtesy of Dr. M.A. Saleh, Post-doctoral Research Fellow, 1981-82, Lakehead University

2 - reproduced courtesy of M.A. Kashem, M.Sc. Thesis, 1982, Lakehead University.

3 - Davies and Swain, J. Chem. Soc. Faraday, Trans. (II), 67, 1637(1971)

4 - reproduced courtesy of M.A. Mazid, M.Sc. Thesis, 1978, Lakehead University.

TABLE III-2:

EYRING ANALYSIS RESULTS OF α -PROCESSES OF RIGID POLAR MOLECULES IN CIS-DECALIN

MOLECULE	T (K)	Relaxation Times τ (s)		ΔG_E (kJ mol ⁻¹)		ΔH_E	ΔS_E
		150 K	150 K	150 K	150 K	kJ mol ⁻¹	J K ⁻¹ mol ⁻¹
cis-decalin ¹	140-147	1.2×10^{-6}		18.8		118.6±8.5	665±59
methyl iodide ¹	138-143	1.0×10^{-8}		12.9		137.6±25.5	832±178
2-chloro-2-methylpropane ¹	140-145	9.0×10^{-8}		15.6		141.8±25.3	840±176
1,1,1-trichloroethane ¹	140-147	2.7×10^{-7}		17.0		138.9±32.7	812±228
2,2-dichloropropane ¹	140-146	3.9×10^{-8}		14.6		166.4±40.1	730±55
trichloroethylene ¹	137-144	1.2×10^{-8}		13.1		138.5±330.3	836±208
t-butylisothiocyanate ¹	145-154	4.9×10^{-5}		23.5		105.6±10.7	546±66
t-butylcyanide ¹	143-150	2.5×10^{-6}		19.8		148.7±29.0	859±200
nitrobenzene	141-148	3.8×10^{-7}		17.5		145.9±47.1	856±325
2-methyl-2-nitropropane ¹	147-150	4.4×10^{-5}		23.3		156.3±110.8	885±740

TABLE III-3: Fuoss-Kirkwood Analysis Parameters for some Rigid Polar Molecules in cis-decalin

T (K)	$10^6 \tau$ (s)	$\log v_{\max}$	β	$10^3 \epsilon''_{\max}$	ϵ_{∞}	μ (D)
<u>0.84 M Methyl iodide</u>						
83.5	12.6	4.10	0.19	11.22	2.498	0.56
87.8	7.95	4.30	0.20	11.87	2.435	0.52
91.2	4.40	4.55	0.21	12.46	2.435	0.53
94.2	3.46	4.66	0.23	12.75	2.424	0.55
101.0	2.35	4.83	0.25	12.94	2.454	0.54
<u>0.84 M Methyl iodide</u>						
136.1	700.0	2.35	0.22	36.31	2.611	1.06
137.9	176.0	2.96	0.26	31.13	2.620	0.99
138.7	73.5	3.34	0.29	35.88	2.628	0.94
139.4	35.4	3.65	0.32	35.32	2.642	0.89
140.3	16.5	3.98	0.37	35.12	2.652	0.82
141.2	9.5	4.23	0.43	34.68	2.667	0.76
141.8	6.9	4.36	0.45	34.56	2.670	0.75
142.7	4.7	4.53	0.53	33.72	2.689	0.68
<u>0.75 M 2-bromo-2-methylpropane</u>						
87.6	3.13	4.70	0.21	71.47	2.218	1.37
86.0	3.54	4.65	0.20	70.94	2.200	1.38
85.5	3.84	4.61	0.20	70.48	2.190	1.38
84.8	4.52	4.54	0.19	69.79	2.196	1.37
84.3	5.17	4.48	0.20	69.43	2.197	1.36
82.8	6.88	4.36	0.19	68.30	2.182	1.36
81.2	8.72	4.26	0.19	67.21	2.160	1.36
<u>0.75 M 2-bromo-2-methylpropane</u>						
138.0	440.0	2.55	0.13	32.27	3.058	1.25
138.5	301.0	2.72	0.13	33.16	3.062	1.25
139.5	143.0	3.04	0.14	34.77	3.063	1.26
140.5	66.5	3.37	0.15	35.79	3.007	1.25
141.5	23.8	3.82	0.17	36.68	3.086	1.24
142.5	12.6	4.10	0.19	36.94	3.108	1.11
143.6	5.7	4.44	0.22	36.97	3.126	1.04
144.6	3.5	4.66	0.27	36.85	3.158	0.94

TABLE III-3: continued...

T(K)	$10^6 \tau$ (s)	$\log v_{\max}$	β	$10^3 \epsilon''_{\max}$	ϵ_{∞}	μ (D)
<u>0.74 M 2,2-dichloropropane</u>						
80.6	5.60	4.45	0.19	88.40	1.536	1.45
81.5	4.62	4.53	0.19	89.13	1.535	1.45
81.9	4.39	4.55	0.19	89.21	1.514	1.43
83.0	8.59	4.64	0.20	90.75	1.534	1.46
89.1	3.13	4.71	0.21	91.70	1.516	1.44
85.3	2.28	4.83	0.21	92.29	1.527	1.45
<u>0.74 M 2,2-dichloropropane</u>						
139.9	1512.0	2.02	0.12	31.01	3.230	
140.6	417.0	2.58	0.13	33.33	3.972	
141.5	78.2	3.31	0.17	30.68	3.224	
142.0	46.2	3.54	0.17	30.60	3.213	
142.5	26.2	3.78	0.21	30.75	3.241	
143.7	10.1	4.20	0.26	30.65	3.260	
144.2	7.9	4.30	0.29	30.54	3.274	
144.9	5.2	4.48	0.34	30.11	3.289	
145.6	4.7	4.53	0.37	29.80	3.296	
<u>0.78 M 2-chloro-2-methylpropane</u>						
140.8	189.0	2.92	0.14	24.38	3.060	1.03
141.4	98.0	3.20	0.16	24.62	3.060	1.00
142.5	30.8	3.712	0.18	24.89	3.075	0.93
143.6	12.6	4.10	0.23	25.04	3.091	0.85
144.1	9.3	4.23	0.25	25.07	3.098	0.82
145.0	5.9	4.42	0.29	24.70	3.112	0.75
<u>0.76 M 1,1,1,-trichloroethane</u>						
79.8	8.63	4.26	0.18	57.80	2.361	1.27
80.3	8.21	4.28	0.19	58.58	2.370	1.25
81.1	7.51	4.32	0.18	58.70	2.380	1.27
82.0	6.80	4.36	0.19	59.25	2.399	1.26
82.9	5.79	4.43	0.19	59.56	2.382	1.29
83.6	5.30	4.47	0.19	59.72	2.394	1.27
84.8	3.73	4.63	0.20	60.51	2.397	1.27
86.2	3.09	4.71	0.20	60.41	2.391	1.27

TABLE III-3: continued....

T(K)	$10^6 \tau$ (s)	$\log v_{\max}$	β	$10^3 \epsilon''_{\max}$	ϵ_{∞}	μ (D)
<u>0.76 M 1,1,1-trichloroethane</u>						
140.3	921.00	2.23	0.15	15.98	2.905	0.86
141.2	577.00	2.44	0.13	15.51	2.891	0.92
141.9	137.00	3.06	0.14	15.33	2.891	0.87
142.9	42.61	3.57	0.17	15.24	2.899	0.79
143.9	17.90	3.95	0.22	15.18	2.909	0.71
144.7	9.90	4.20	0.27	15.09	2.917	0.64
145.3	8.96	4.27	0.31	15.04	2.933	0.60
146.5	4.87	4.51	0.36	14.81	2.926	0.56
147.3	4.41	4.55	0.44	14.07	2.936	0.49
<u>0.76 M methyltrichlorosilane</u>						
103.8	1014.0	2.19	0.16	76.62	2.358	1.63
106.1	597.0	2.42	0.16	77.89	2.350	1.66
107.3	363.0	2.64	0.17	78.92	2.356	1.64
110.1	180.8	2.94	0.18	80.75	2.356	1.66
113.0	84.9	3.55	0.19	84.60	2.353	1.68
118.6	24.3	3.81	0.20	86.62	2.373	1.66
122.1	12.0	4.11	0.22	89.06	2.387	1.66
127.1	4.1	4.58	0.25	92.47	2.122	1.57
<u>0.56 M t-butylcyanide</u>						
143.7	475.54	2.52	0.25	3.62		
144.8	167.50	2.97	0.27	3.60		
145.6	48.18	3.27	0.28	3.58		
146.5	42.99	3.56	0.29	3.52		
147.5	22.19	3.85	0.35	3.50		
148.4	13.02	4.08	0.39	3.37		
149.4	10.18	4.19	0.42	3.18		
<u>0.65 M trichloroethylene</u>						
137.2	812.34	2.29	0.18	27.55		
137.6	339.31	2.67	0.20	27.32		
138.3	140.09	3.05	0.22	27.50		
139.2	46.37	3.53	0.26	27.80		
140.7	12.37	4.10	0.34	28.39		
141.5	7.45	4.32	0.40	28.79		
142.7	4.23	4.57	0.46	29.20		
143.6	3.24	4.69	0.51	28.93		

TABLE III-3: continued...

T(K)	$10^6 \tau$ (s)	$\log \nu_{\max}$	β	$10^3 \epsilon''_{\max}$	ϵ_{∞}	μ (D)
<u>0.45 M Pyridine</u>						
103.1	50.52	3.50	0.23	12.76		
104.8	41.17	3.58	0.22	13.17		
107.0	23.98	3.82	0.25	13.64		
109.9	13.81	4.06	0.28	14.29		
118.1	4.35	4.56	0.36	15.64		
<u>0.85 M o-bromotoluene</u>						
118.2	91.35	3.24	0.32	5.19		
121.9	44.76	3.55	0.31	5.65		
126.5	23.35	3.83	0.29	6.17		
129.0	15.27	4.02	0.28	6.43		
132.6	10.77	4.17	0.25	6.78		
141.2	4.09	4.59	0.23	7.21		
<u>0.65 M 2-methyl-2-nitropropane</u>						
147.0	642.39	2.39	0.24	5.15		
147.7	440.03	2.55	0.22	4.91		
148.6	82.37	3.28	0.30	3.88		
149.4	52.84	3.47	0.36	2.92		
150.3	52.84	3.47	0.36	2.92		
<u>0.51 M o-dichlorobenzene</u>						
103.6	63.32	3.40	0.29	13.53		
107.4	44.35	3.55	0.27	14.54		
110.4	25.50	3.79	0.27	15.49		
111.2	22.18	3.86	0.27	15.87		
115.0	12.59	4.10	0.29	17.15		
119.9	75.40	4.33	0.29	18.75		
<u>0.45 M bromoform</u>						
87.0	1203.02	2.12	0.17	0.3		
88.7	726.05	2.34	0.18	0.3		
90.5	54.77	2.46	0.19	0.3		
92.2	39.46	2.60	0.21	0.3		
94.3	27.99	2.75	0.22	0.3		
96.6	19.30	2.91	0.22	0.3		
99.3	12.35	3.11	0.21	0.3		

TABLE III:3 continued...

$T(K)$	$10^6 \tau (s)$	$\log v_{\max}$	β	$10^3 \epsilon''_{\max}$	ϵ_{∞}	$\mu (D)$
<u>0.35 M o-xylene</u>						
101.4	1300.94	2.09	0.28	0.30		
103.0	1300.94	2.18	0.28	0.30		
106.2	578.49	2.44	0.28	0.30		
109.0	397.86	2.60	0.30	0.30		
111.0	289.79	2.74	0.31	0.30		
114.2	179.68	2.95	0.32	0.30		
118.6	90.65	3.24	0.33	0.30		
<u>pure cis-decalin</u>						
140.8	726.62	2.34	0.20	1.07		
141.2	462.81	2.53	0.29	1.09		
142.5	173.03	2.96	0.30	1.15		
143.5	91.11	3.24	0.31	1.18		
144.7	38.65	3.62	0.34	1.22		
145.4	23.51	3.83	0.36	1.23		
146.4	14.57	4.04	0.40	1.23		

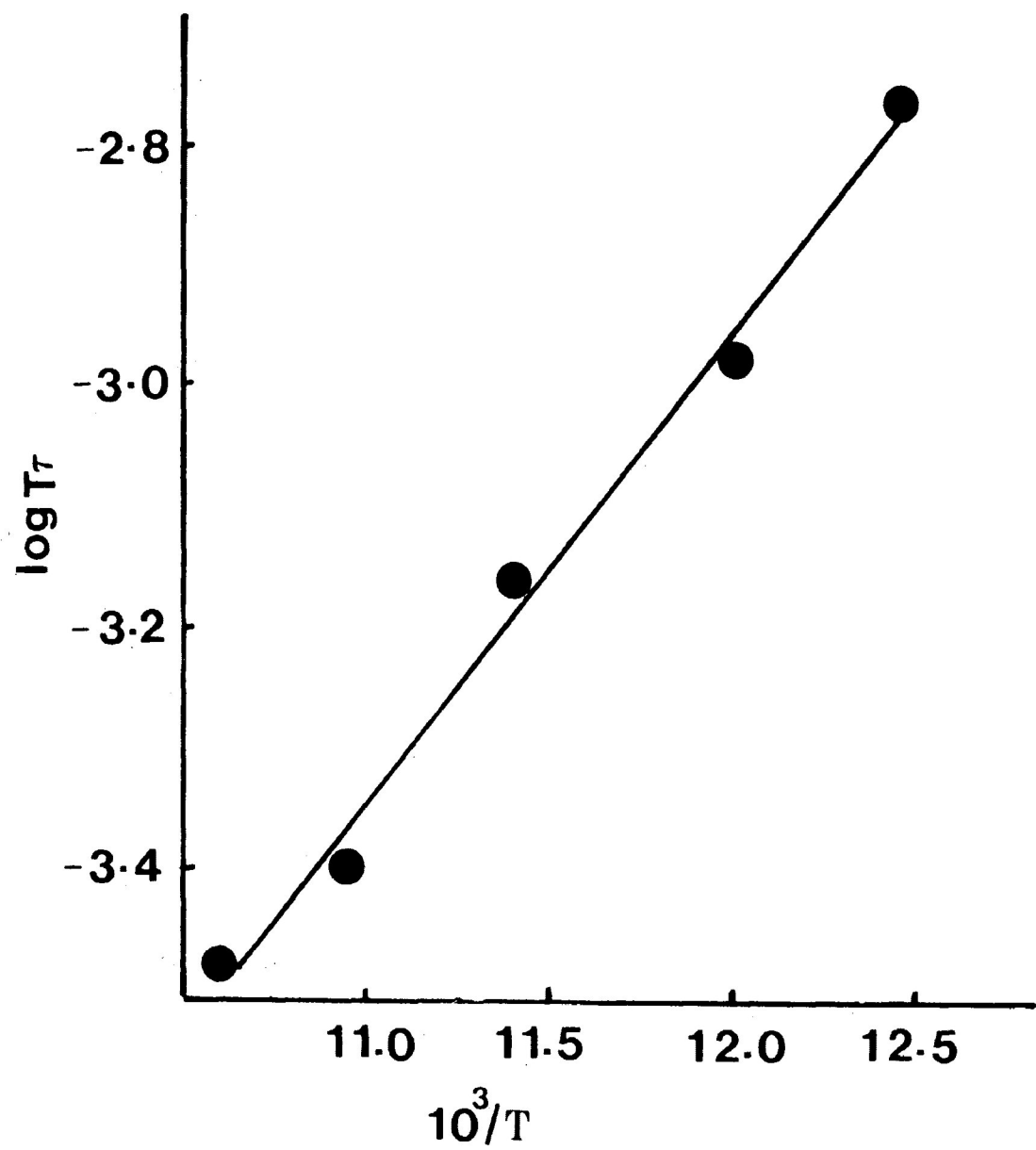


FIGURE III-1: Eyring rate plot of $\log T\tau$ versus $1/T$ (K^{-1}) for methyl iodide in cis-decalin

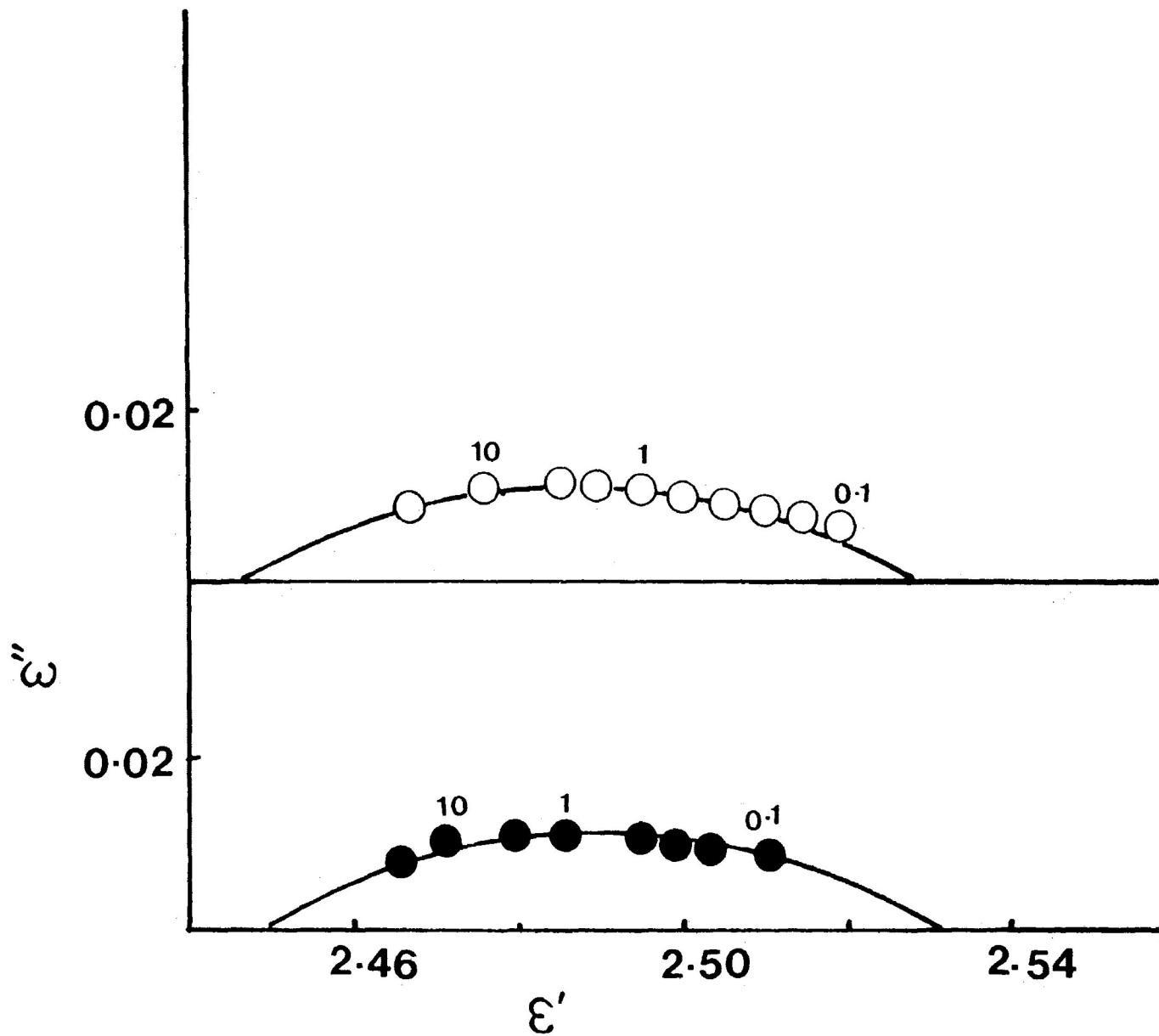


FIGURE III-2: Cole-Cole plots for methyl iodide in cis-decalin at 80.2 K (lower) and 83 K (upper). The numbers beside the points are frequencies in kHz

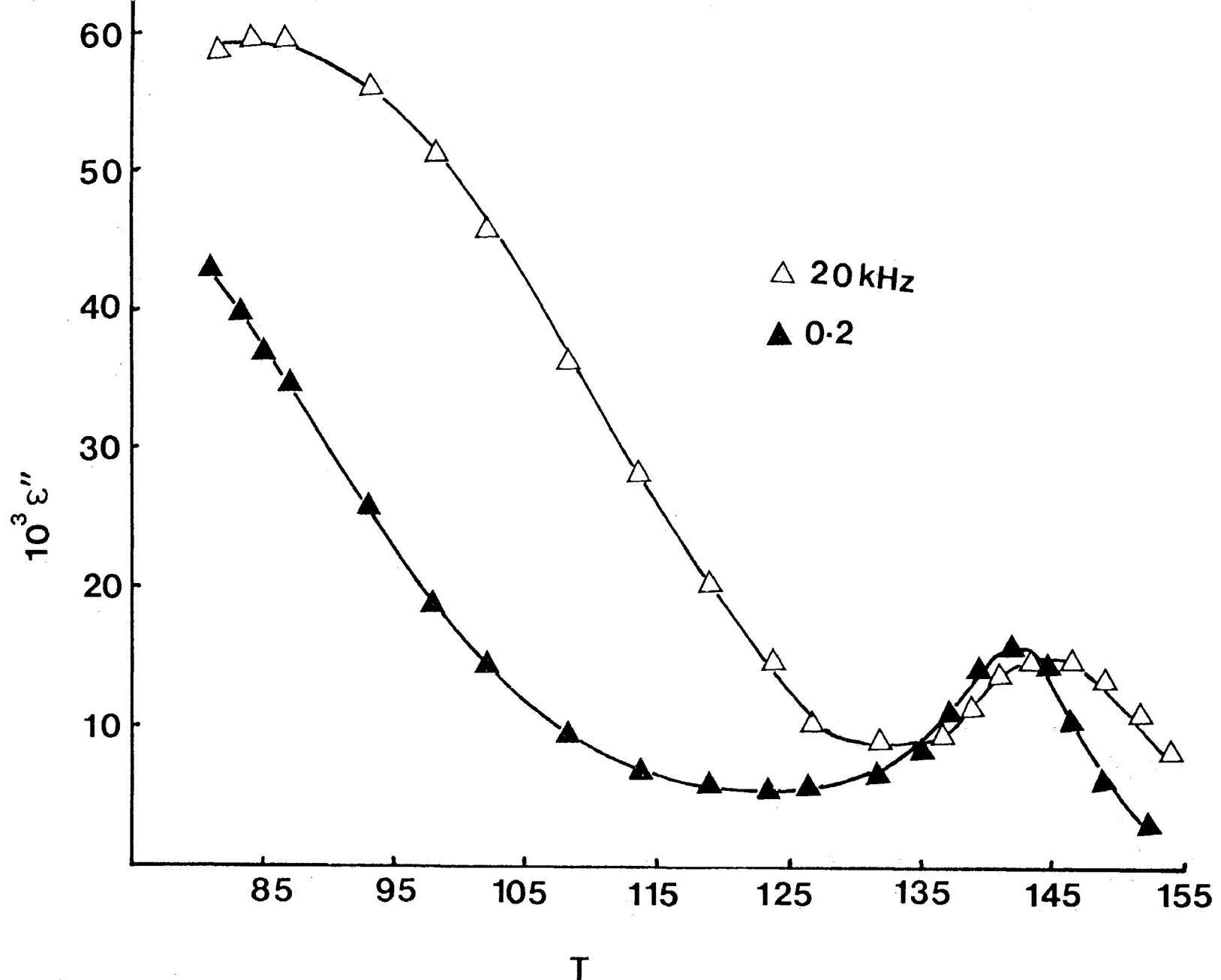


FIGURE III-3: Dielectric loss factor, ϵ'' versus temperature (K) for 1,1,1-trichloroethane in cis-decalin

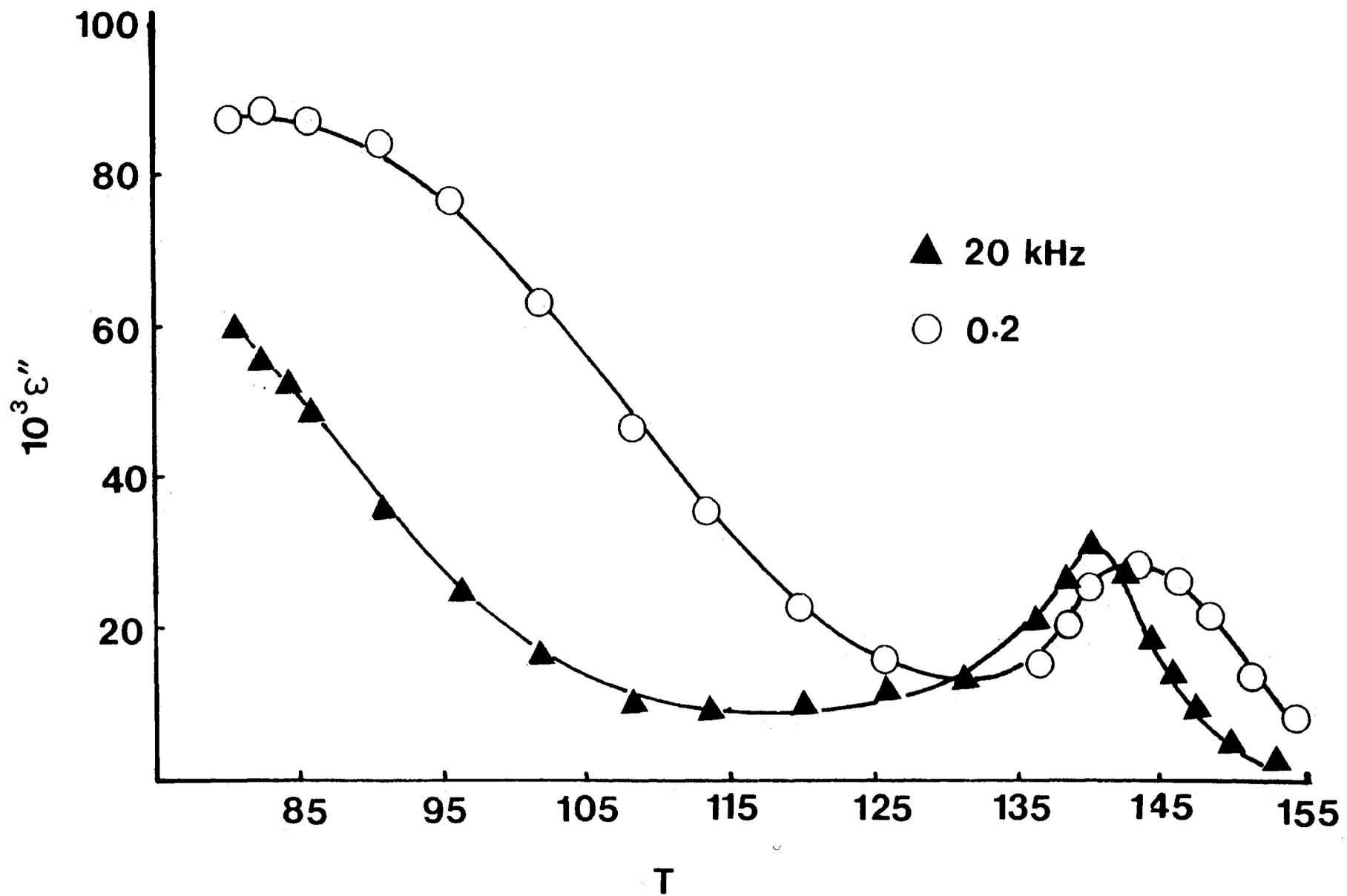


FIGURE III-4: Dielectric loss factor, ϵ'' versus temperature (K) for 2,2-dichloropropane in cis-decalin

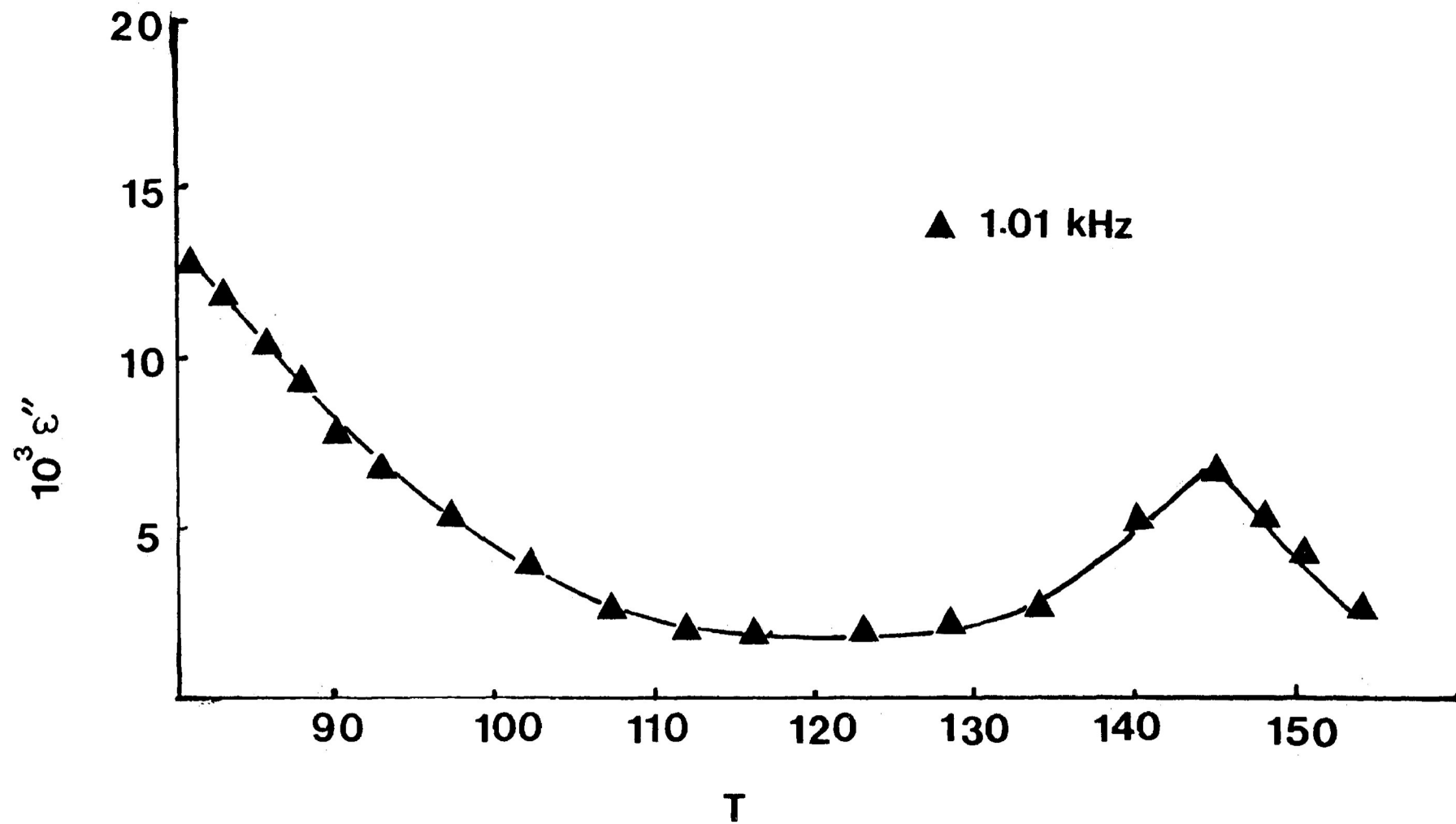
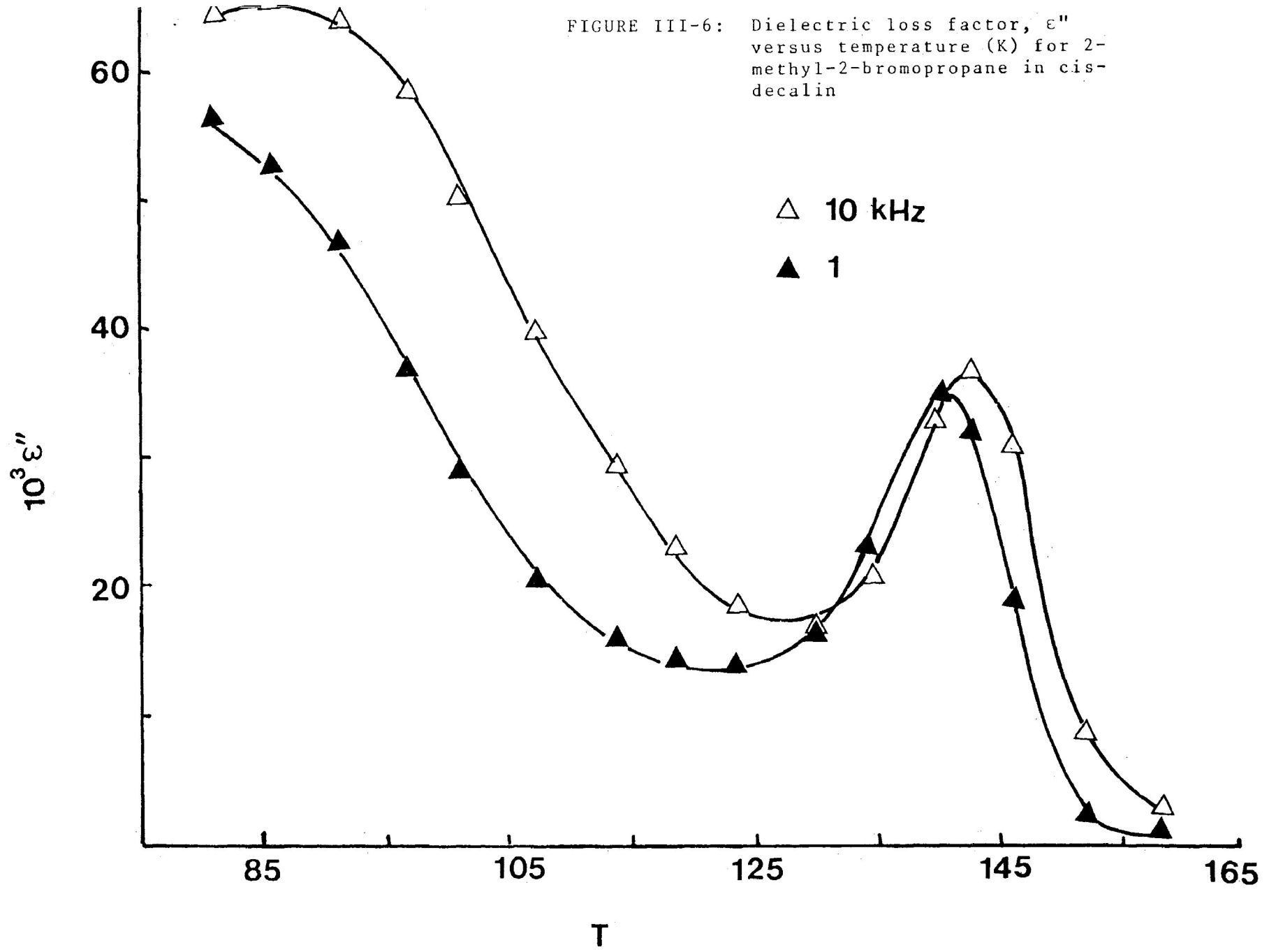


FIGURE III-5: Dielectric loss factor, ϵ'' versus temperature (K) for 2-methyl-2-chloropropane in cis-decalin

FIGURE III-6: Dielectric loss factor, ϵ'' versus temperature (K) for 2-methyl-2-bromopropane in cis-decalin



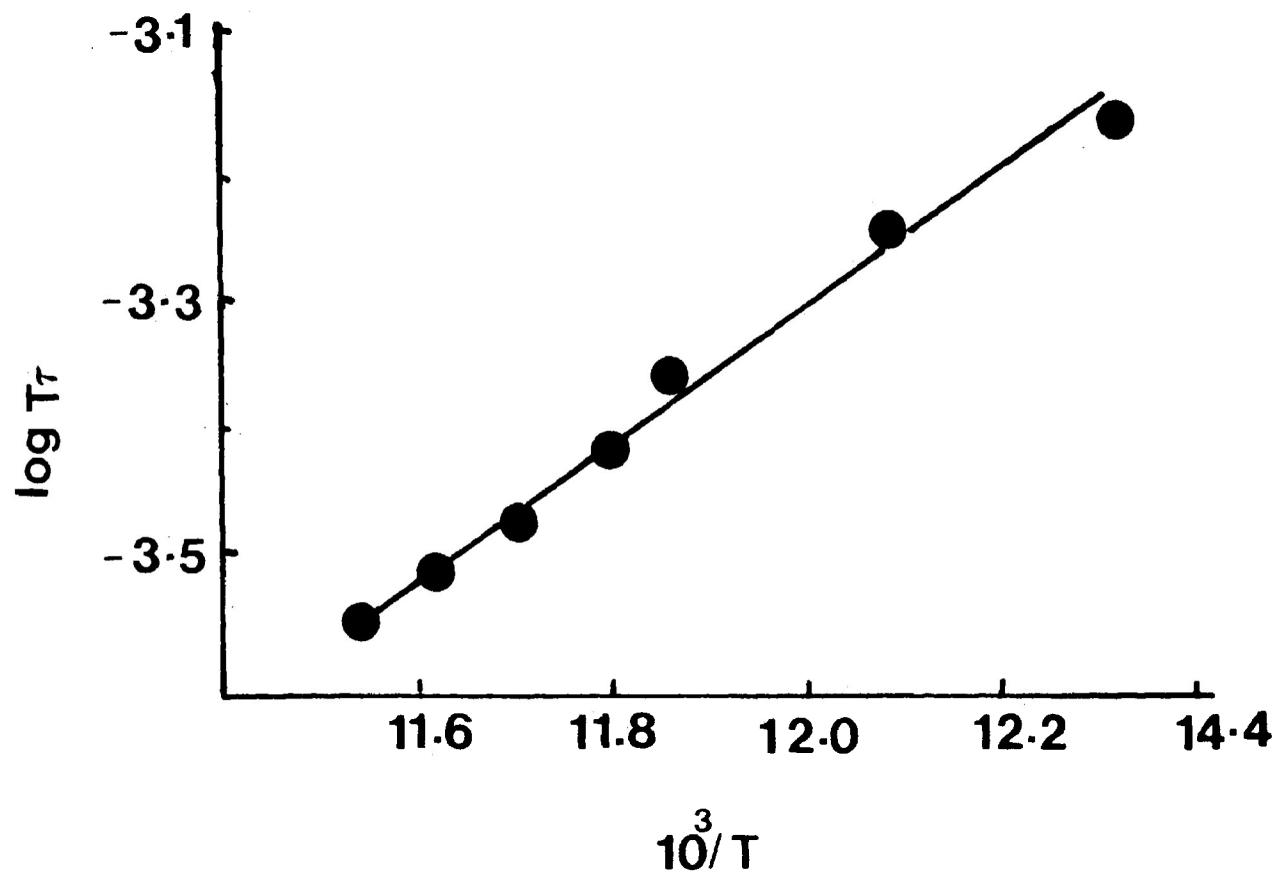


FIGURE III-7: Eyring rate plot of $\log T\tau$ versus $1/T$ (K^{-1}) for 2-methyl-2-bromopropane in cis-decalin

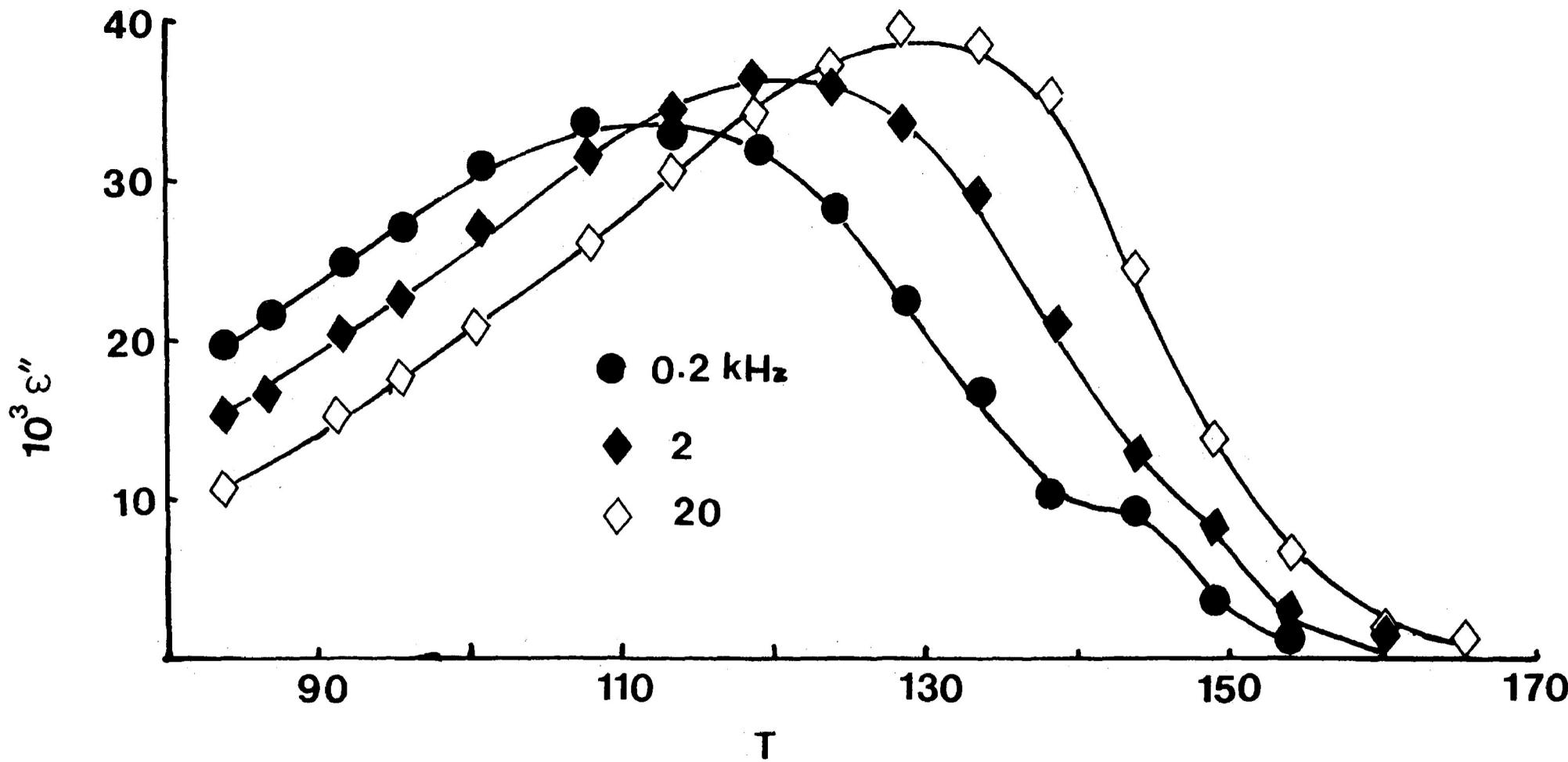


FIGURE III-8: Dielectric loss factor, ϵ'' versus temperature (K) for methyl trichlorosilane in cis-decalin

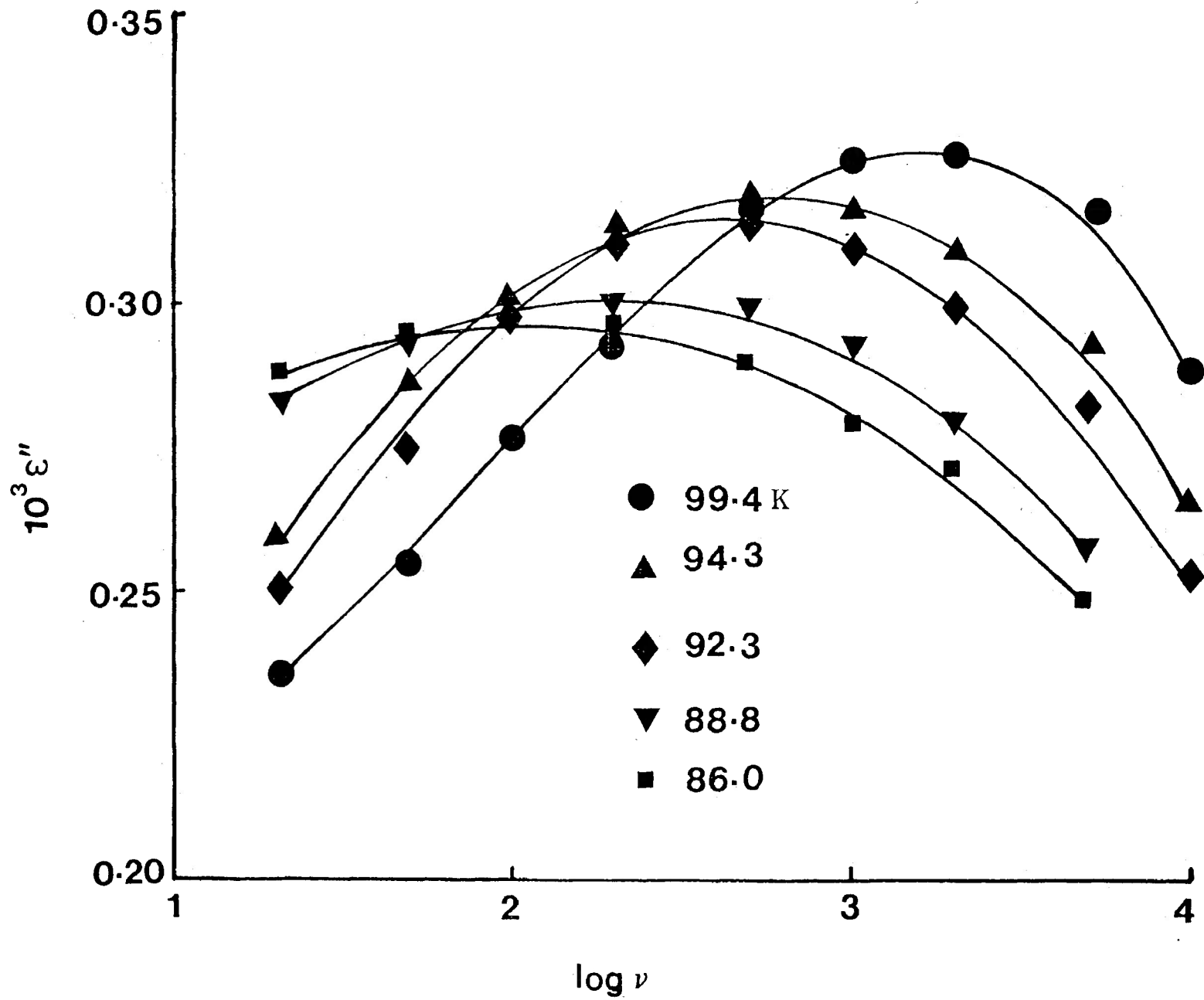


FIGURE III-9: Dielectric loss factor, ϵ'' versus $\log \nu$ for bromoform in cis-decalin

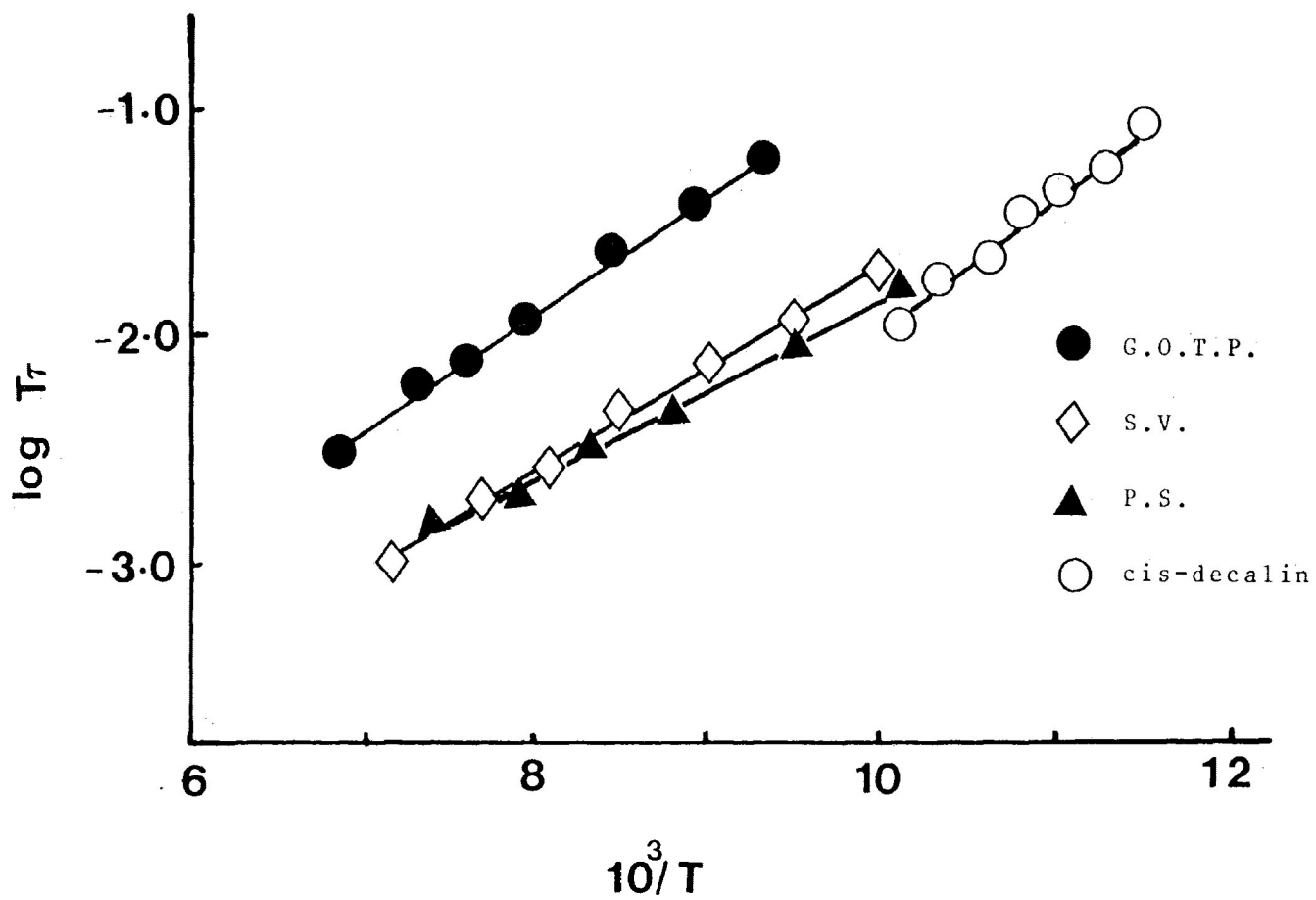


FIGURE III-10: Eyring rate plots of $\log T_r$ versus $1/T$ (K^{-1}) for bromoform in o-terphenyl, polyphenyl ether, polystyrene and cis-decalin

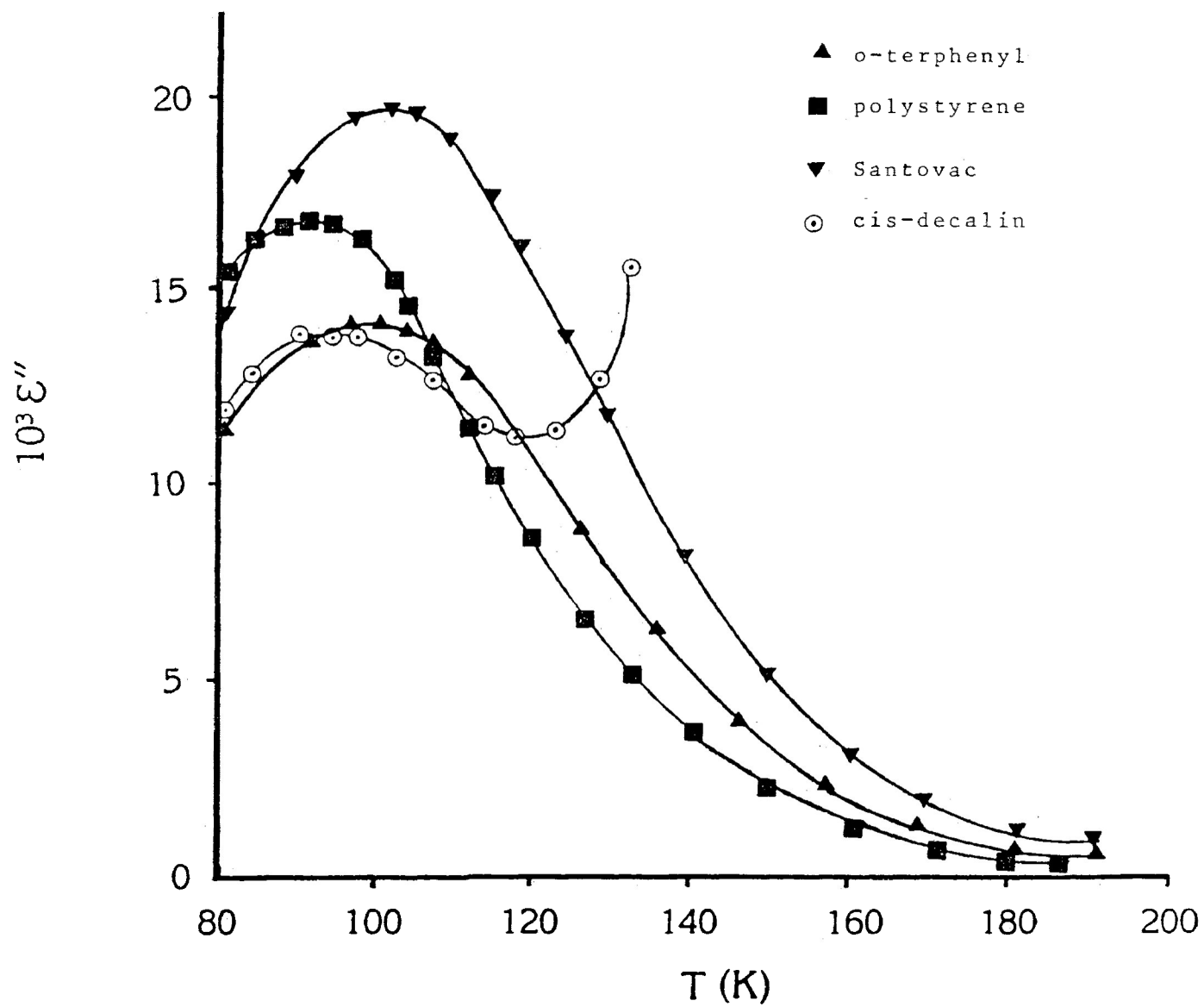
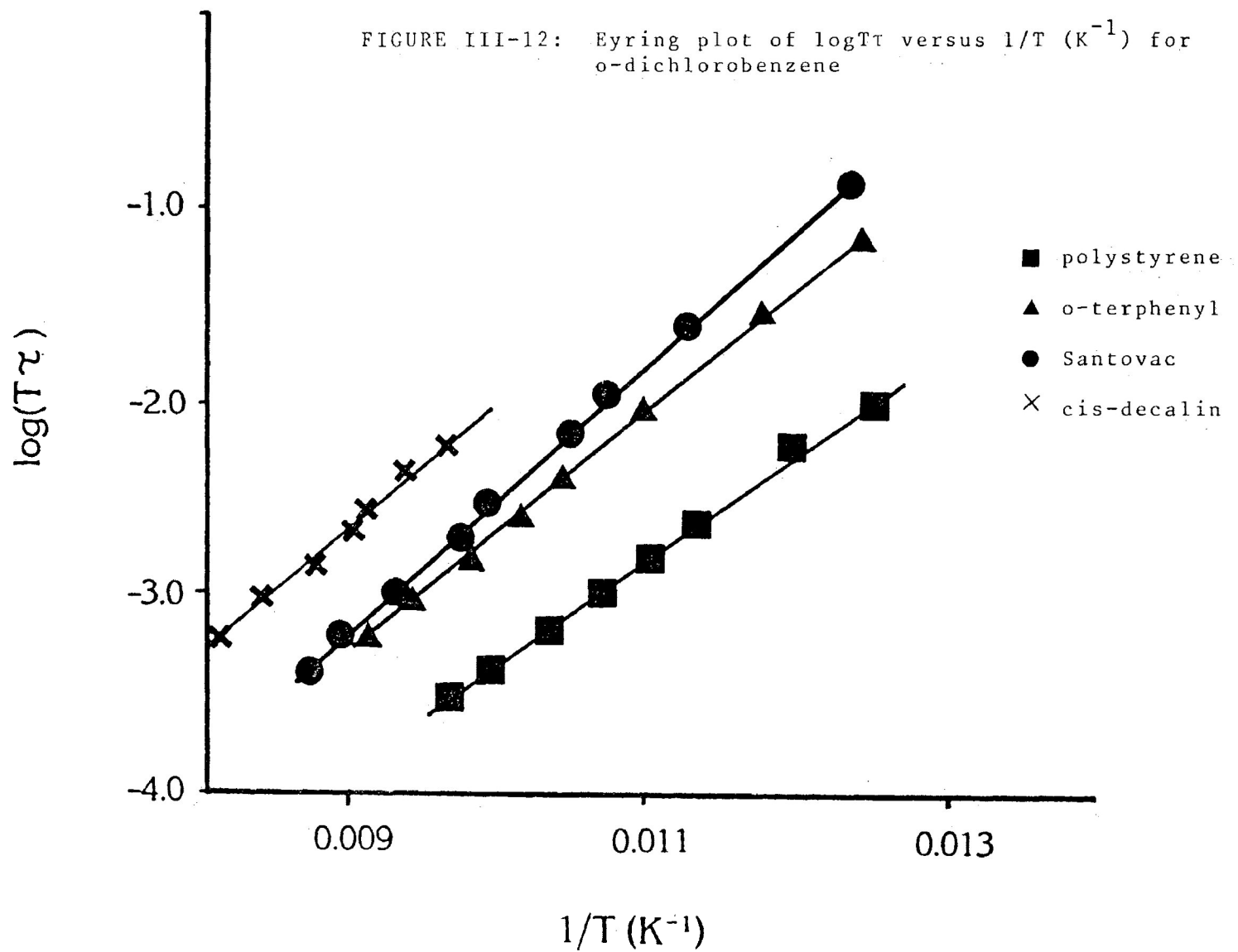


FIGURE III-11: Dielectric loss factor, ϵ'' versus temperature (K) for o-dichlorobenzene at 1.01 kHz

FIGURE III-12: Eyring plot of $\log T\tau$ versus $1/T$ (K^{-1}) for o-dichlorobenzene



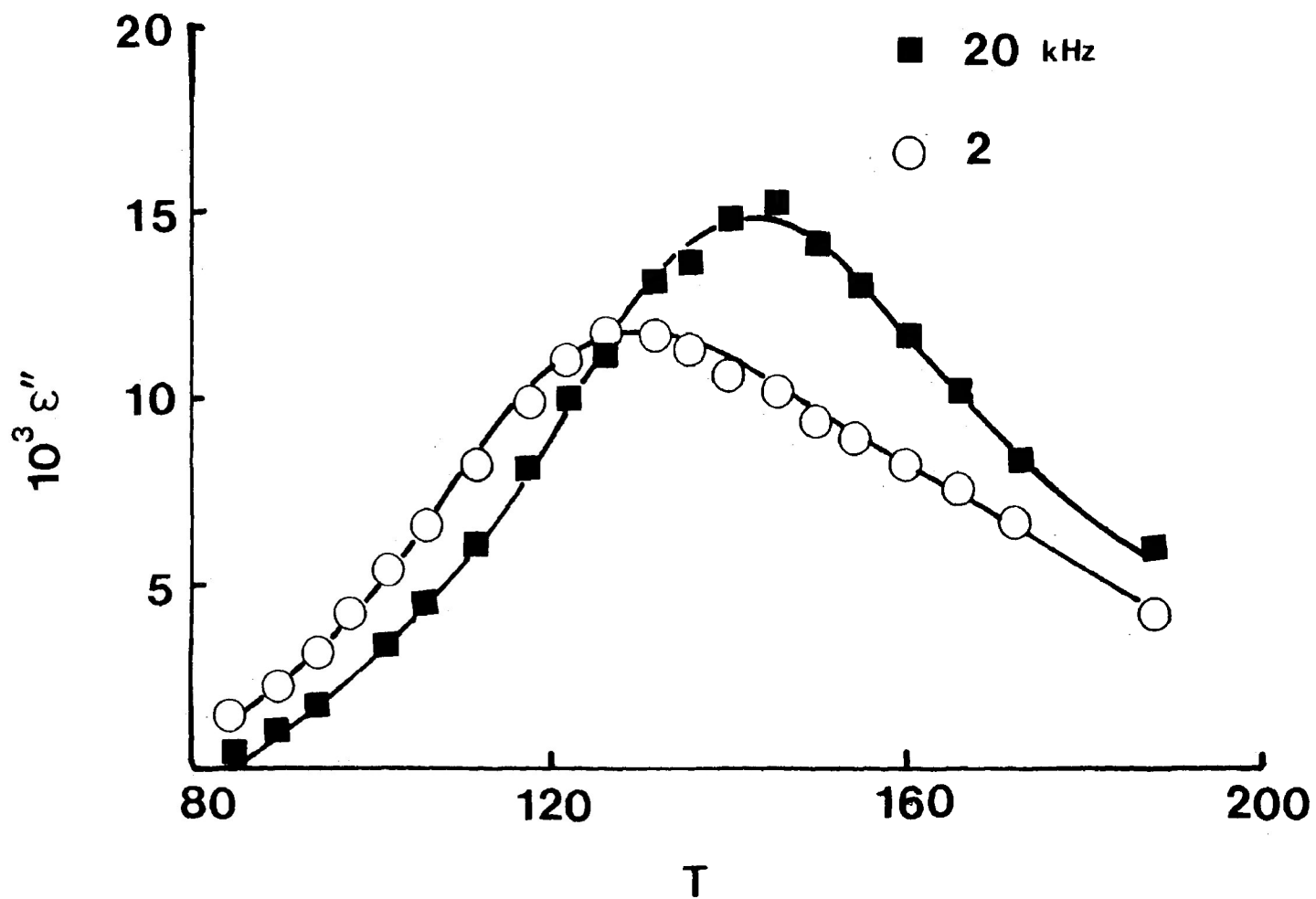


FIGURE III-13: Dielectric loss factor, ϵ'' versus temperature (K) for o-bromochlorobenzene in cis-decalin

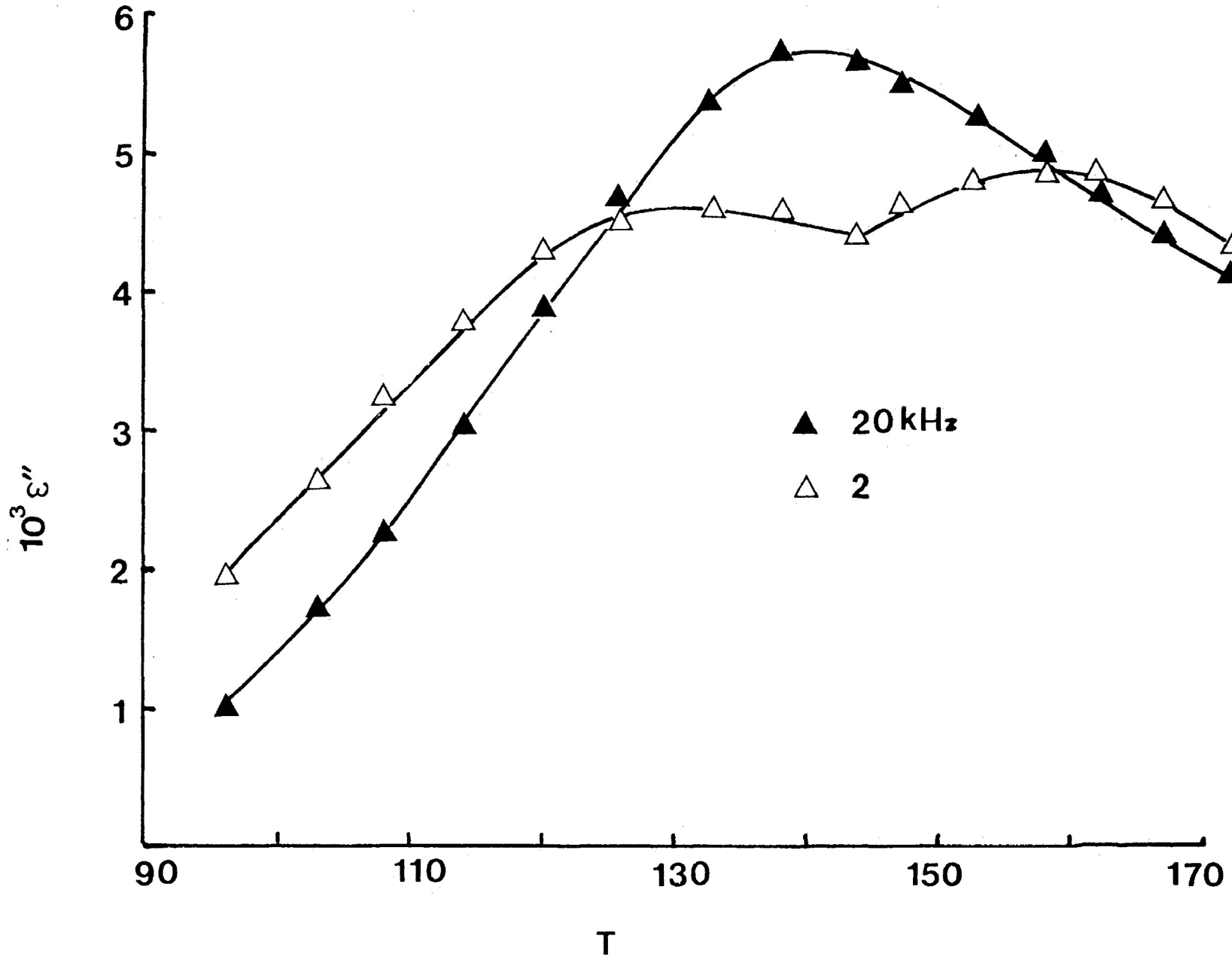


FIGURE III-14: Dielectric loss factor, ϵ'' versus temperature (K) for o-bromotoluene in cis-decalin

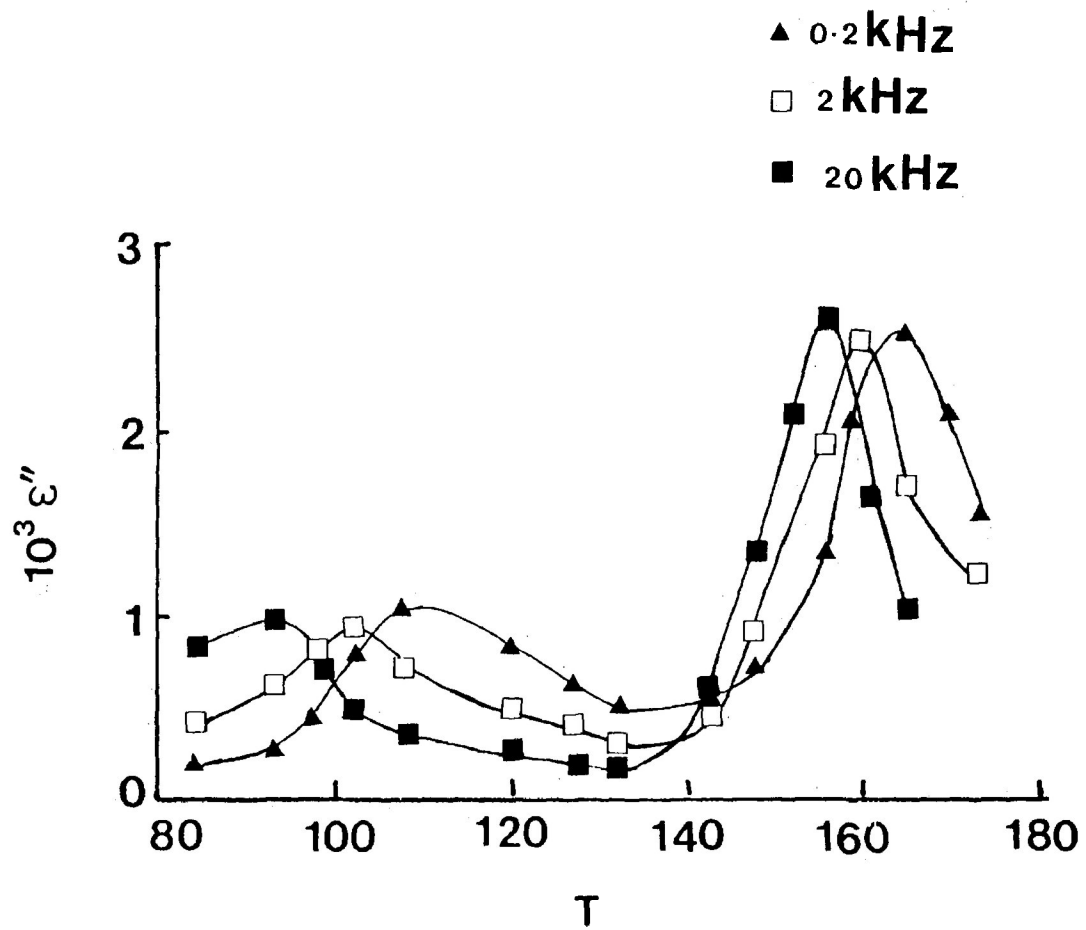


FIGURE III-15: Dielectric loss factor, ϵ'' versus temperature (K) for 4-methylpyridine in cis-decalin

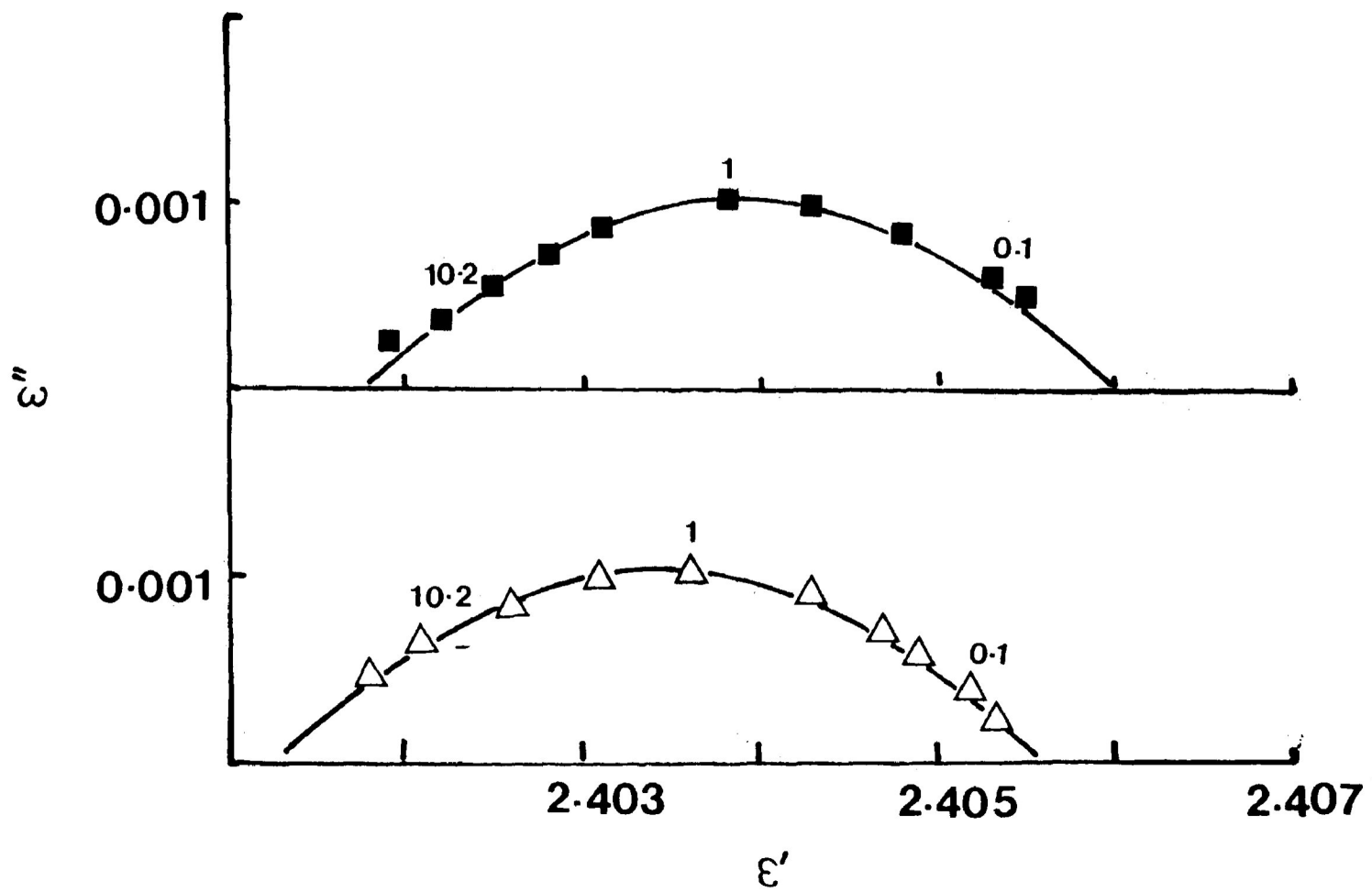


FIGURE III-16: Cole-Cole plots for 4-methylpyridine in cis-decalin at 93.0 K (lower) and 88.1 K (upper)

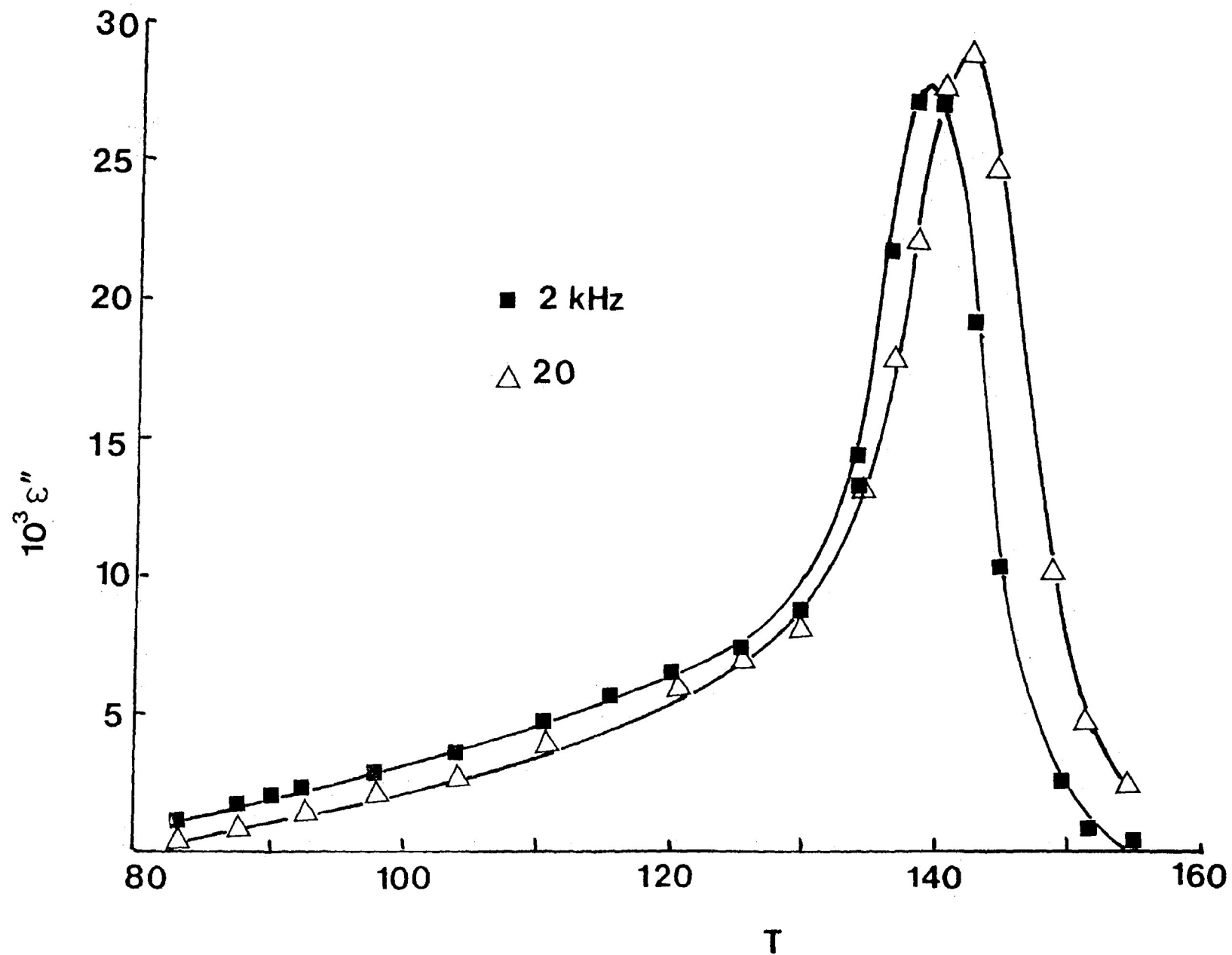


FIGURE III-17: Dielectric loss factor, ϵ'' versus $T(K)$ for trichloroethylene in cis-decalin

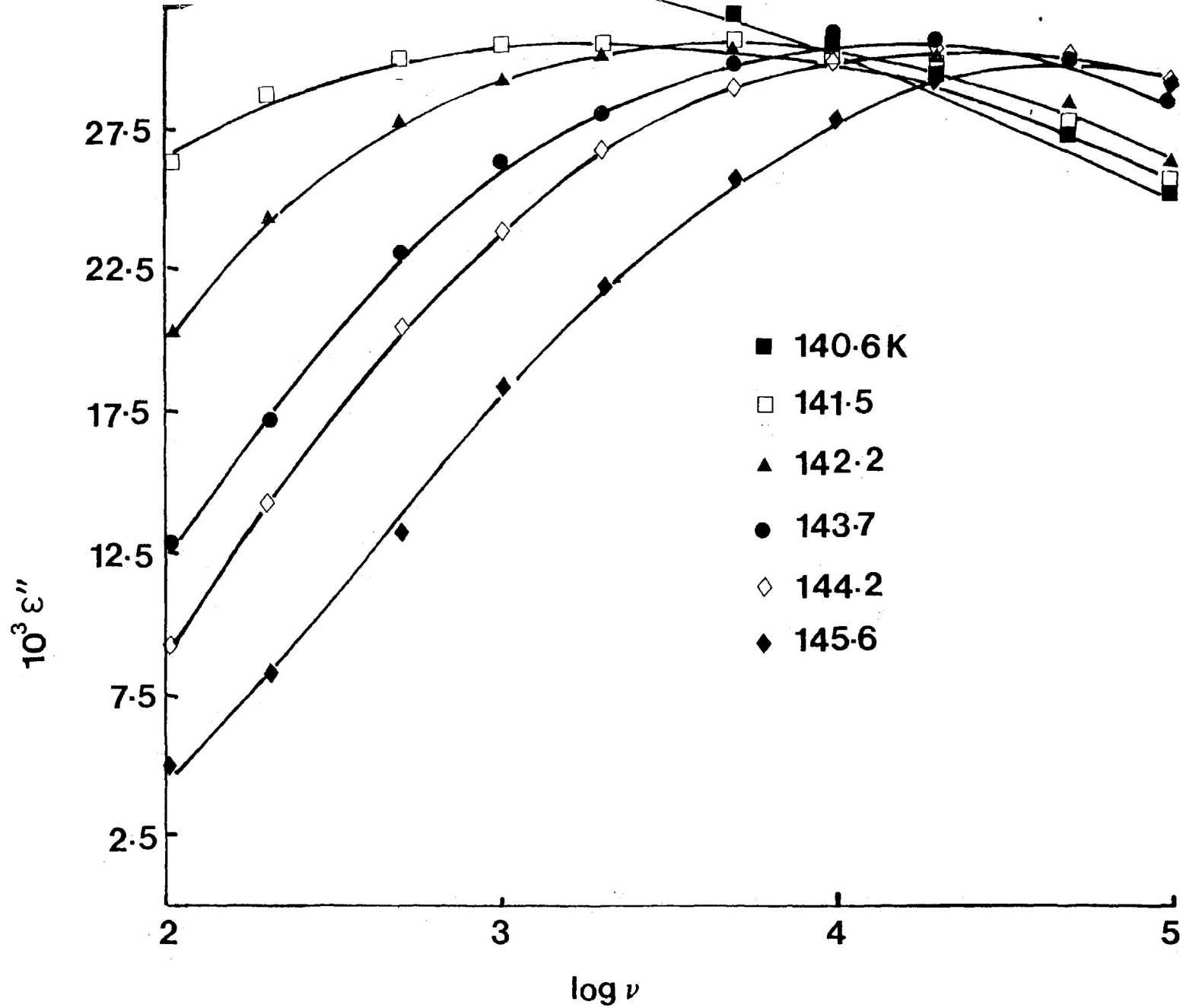


FIGURE III-18: Dielectric loss factor, ϵ'' versus $\log \nu$ for 2,2-dichloropropane in cis-decalin

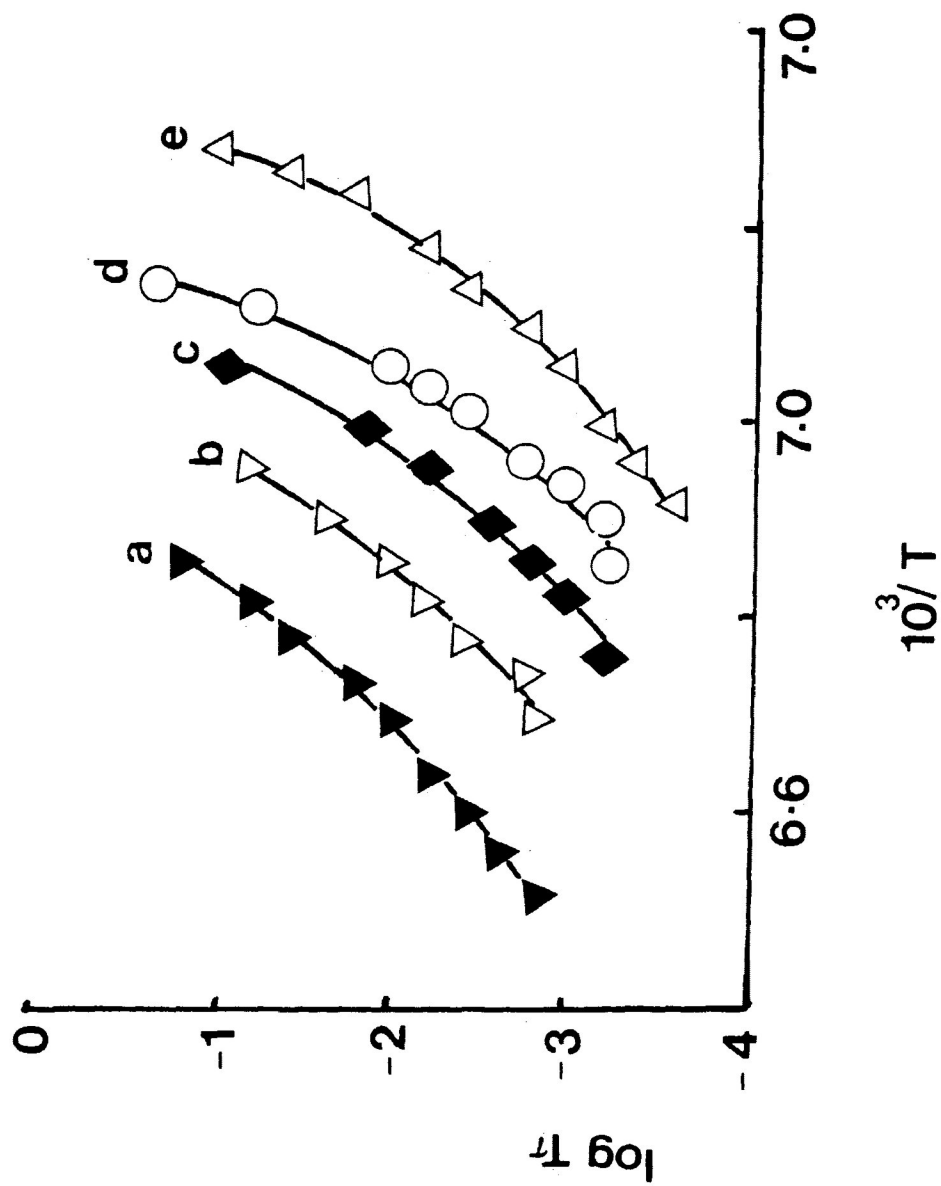


FIGURE 111-19: Eyring plots of $\log \tau_4$ versus $1/T$ (K^{-1}) in *cis*-decalin
 a) *t*-butylisothiocyanate, b) *t*-butyleyanide, c) nitrobenzene
 d) 2,2-dichloropropane and e) trichloroethylene

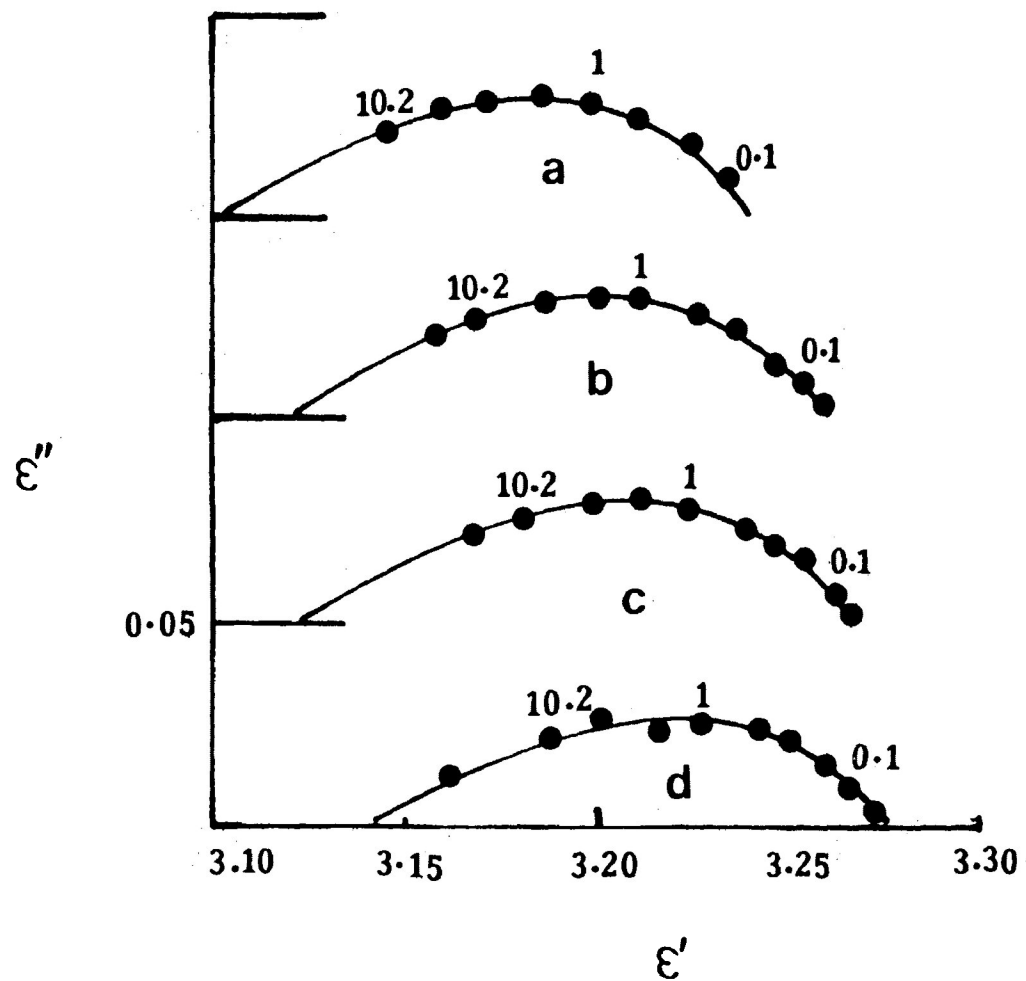


FIGURE III-20: Cole-Cole plots for 2-methyl-2-chloropropane in cis-decalin
 a) 140.8 K, b) 143.6 K, c) 144.1 K and d) 145.0 K

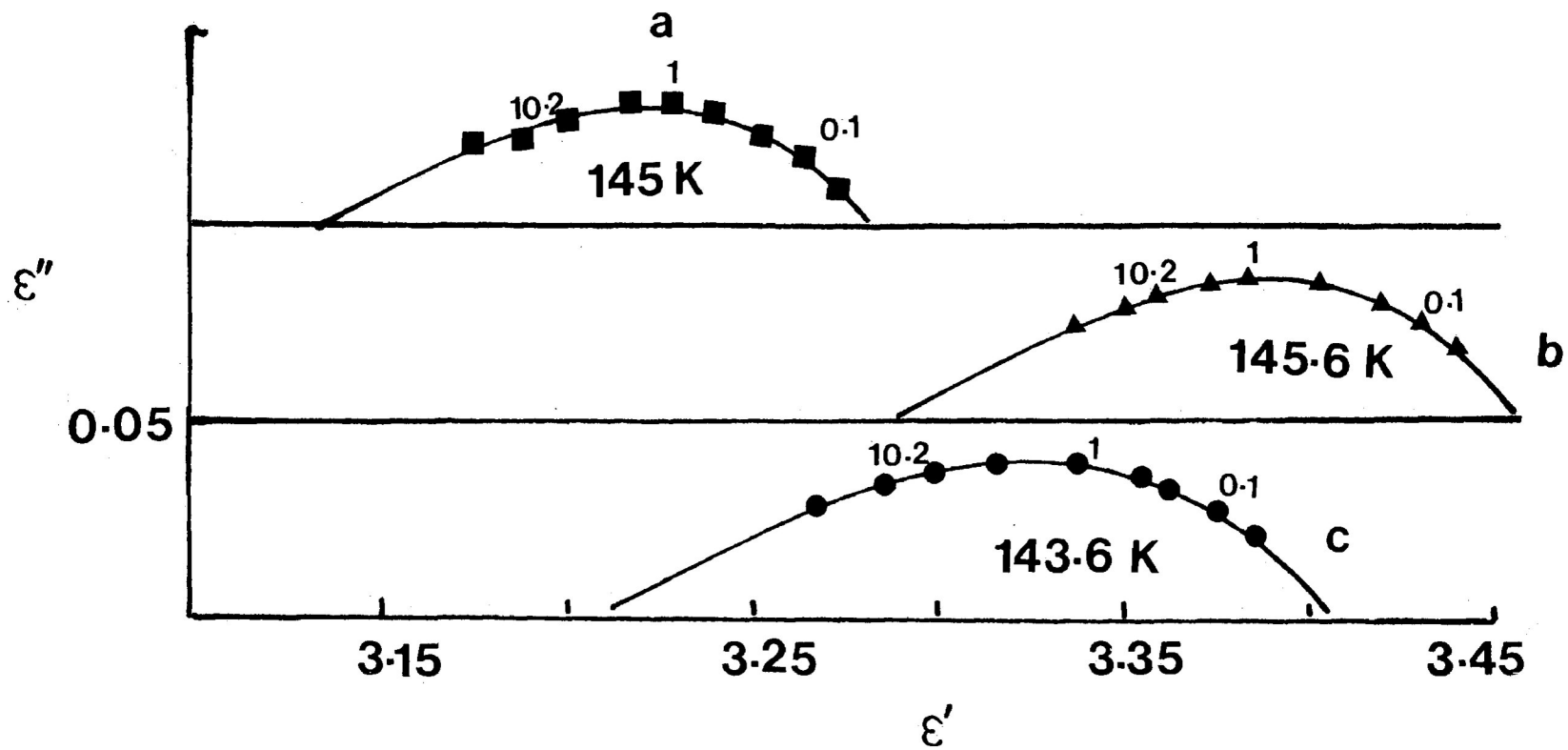


FIGURE III-21: Cole-Cole plots for a) 2-methyl-2-chloropropane at 145.0 K; b) 2,2-dichloropropane at 145.6 K, and c) 2-methyl-2-bromopropane at 143.6 K in cis-decalin

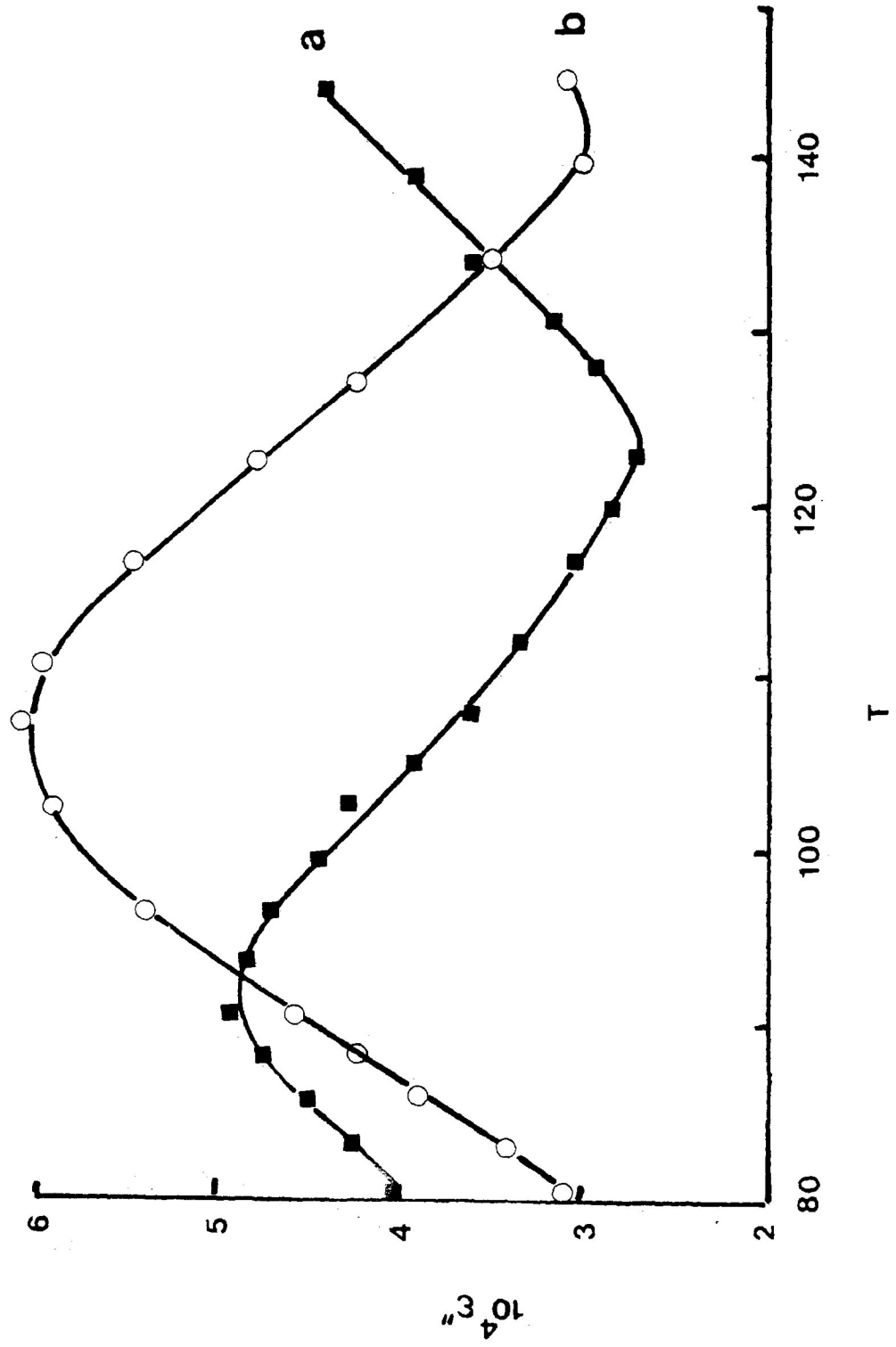


FIGURE III-22: Dielectric loss factor, ϵ'' versus temperature (K) for o-xylene in cis-decalin: a) 0.0502 kHz; b) 1.01 kHz

CHAPTER IV

DIELECTRIC RELAXATION OF SOME ANISOLES

IN *cis*-DECALIN

CHAPTER IV

INTRODUCTION

Dielectric absorption techniques have previously been used for the study of molecular and/or intramolecular motions of numerous molecules containing rotatable polar groups, particularly in dilute solutions of non-polar solvents. Such studies have normally been complicated by the overlap of the molecular and the intramolecular processes, requiring a Budó analysis which in a number of cases is known to be unsatisfactory (1) for the evaluation of relaxation data. However, by dispersing the polar molecules in a polymer matrix such as in polystyrene, Davies et al (2,3) and Walker et al (4-14) have found that the intramolecular absorption process can be separated completely from the molecular relaxation in a few instances owing to different influences of the high viscosity of the medium on the molecular and intramolecular relaxation times.

Molecules having a methoxy group attached to an aromatic ring have been widely studied by dielectric techniques (15-17). In the main, they have been examined either as a pure liquid or as a solute in a dilute solution

of a non-polar solvent, and the absorption observed in the microwave region. Normally the molecular and group absorptions have overlapped, while relaxation time obtained for the group rotation (deduced from a Budo analysis (1)) indicates that the methoxy group has a high degree of mobility. Recently, from their dielectric studies in a polystyrene matrix, Walker et al (8) concluded that "in the absence of appreciable steric, or mutual conjugative effects the barrier to methoxy group relaxation, attached to a conjugated system, is low and of the order of 10 kJ mol^{-1} ."

Kashem (18) studied the dielectric absorptions of anisoles, p-methylanisole, 3,5-dimethylanisole, p-dimethoxyanisole and p-chloro-, bromo- and iodoanisole in a variety of viscous solvents such as polystyrene, o-terphenyl and polyphenyl ether. He concluded that the energy barrier to methoxy group rotation is insensitive to para-substitution and viscosity of the medium. The barrier to rotation about the C-O bond is low and virtually remains the same (i.e. of the order of 8 kJ mol^{-1}).

It, therefore, seemed desirable to make a dielectric absorption study of molecules containing a rotatable methoxy

groups in a variety of anisoles in cis-decalin to compare Eyring and relaxation parameters with that of these molecules in polystyrene, glassy o-terphenyl and polyphenyl ether.

An additional aspect of this study is that the solvents are glassy media and have a glass transition temperature T_g which may be lowered somewhat by the dispersion of a solute in the medium. The T_g values for the pure glasses employed in this work and in the previous investigation (18), polystyrene (19), Santovac® (20), o-terphenyl (20) and cis-decalin (24), are 370 K, 270 K, 243 K and 136 K, respectively.

Just above T_g the solvents exhibit a process which is generally agreed to involve large scale rearrangements in a viscous medium and is regarded as co-operative in nature (20,22,23). When a polar solute is inserted into the glassy medium, it acts as a probe on the motions of the weakly polar solvent (20,22,23).

For a wide variety of systems at a significantly lower temperature than the T_g of the mixture another process is found, and this has been termed a β -process and has been subject to several interpretations including

a molecular relaxation process (22), an intramolecular process (23), or a process which results from the relaxation of the molecules in the interstices between the clusters (24), or a molecular rotation in the "solvent cavity" for some limited types of systems (25).

There is, however, as yet no all-embracing theory which accounts for the β -process in these various glassy forming media. Thus, an object of the present work is to explore in detail the nature of a possible β -process of one type of molecule where the polar molecules are dispersed at low concentrations in the glassy medium. The study has centred around the examination of molecules with a flexible methoxy group.

EXPERIMENTAL RESULTS

The dielectric measurements of para-methyl-anisole, 3,5-dimethyl, para-chloro, para-bromo- and para-bromoanisole in a polystyrene matrix have been made in the frequency range of 10 to 10^5 Hz by the use of General Radio 1615-A and 1621 capacitance bridges.

Sample plots of loss factor, ϵ'' versus temperature, T (K) are shown in Figures IV-2, IV-5, IV-6 IV-7 and IV-9 while Figures IV-3 and IV-10 show the plots of loss factor, ϵ'' versus logarithm (frequency). Figures IV-1, IV-4 and IV-8 show the sample plots of $\log T\tau$ versus $1/T$ and dielectric loss versus dielectric constant, for some of the anisoles studied here.

Table IV-1 lists the Eyring and relaxation parameters while Table IV-2 summarizes the Fuoss-Kirkwood parameters.

DISCUSSION

para-Methylanisole has been chosen as a key molecule for this study because the methyl group moment is directed into the ring and opposes the resultant fixed component of the moment from the anisole part of the molecule on the long axis. Thus, this molecule has virtually no component of the dipole moment along this axis and consequently, the intramolecular process predominates. Farmer and Walker (15), from their dielectric studies of para-methyl anisole in para-xylene at 25°C at microwave frequencies indicated that methoxy group rotation predominates in this molecule. Only one absorption process was detected for para-methylanisole in both a polystyrene matrix and cis-decalin, but two absorption processes were found in both o-terphenyl and polyphenyl ether. Figure IV-1 gives the $\log T\tau$ versus $1/T$ for para-methylanisole in cis-decalin. Eyring analysis results are given in Figure IV-1. The process in the liquid nitrogen temperature region is common in all four media and yielded almost identical values of ΔH_E , $\Delta G_{E(100 K)}$, $\tau_{100 K}$ and ΔS_E (see Table IV-1). These observed values of ΔH_E ($\sim 8 \text{ kJ mol}^{-1}$) and other parameters for this molecule are too low for the molecular process when compared to corresponding values obtained for para-chlorotoluene, a rigid molecule of slightly smaller size (see Table IV-1). Mazid et al (8) obtained

ΔH_E values of 10 kJ mol^{-1} for methoxy group rotation in substituted anisoles. Thus, the enthalpies of activation ($\Delta H_E = \sim 8 \text{ kJ mol}^{-1}$) obtained for para-methylanisole for the low temperature process are consistent with the values reported by Mazid et al (8) indicating that the process is methoxy group rotation and that the ΔH_E of the process hardly varies amongst the four media.

The higher temperature absorption process of para-methylanisole in o-terphenyl and polyphenyl ether has been attributed to the co-operative motion of the α -process (18).

Figure IV-2 shows the plot of dielectric loss (ϵ'') versus temperature, T (K) at 1.01 kHz frequency for 3,5-dimethylanisole in cis-decalin. From Figure IV-2 it is evident that the absorption process appears near the liquid nitrogen temperature for the frequency range used. The absorption curves are symmetrical and broad (Figure IV-3). An Eyring rate plot of the data is given in Figure IV-4 which yields a $\Delta H_E = 12.9 \pm 1.6 \text{ kJ mol}^{-1}$. Within the limits of experimental error, Table IV-1 shows that the Eyring and relaxation parameters are almost similar to the corresponding values obtained for methoxy group rotation in para-methylanisole.

This is another case where the moment between 1 and 4 atoms of the rings is negligible (15).

para-Chloro-, para-bromo- and para-iodoanisoles have been studied in both cis-decalin and o-terphenyl. Figures IV-5, IV-6 and IV-7 show the plots of dielectric loss (ϵ'') versus temperature, T(K) at 1.01, 2 and 0.2 kHz frequencies for para-chloro-, para-bromo-, para-iodoanisole in cis-decalin, respectively. The Cole-Cole plots at various temperatures for para-chloroanisole, are given in Figure IV-8. Table IV-1 shows that para-chloro-, para-bromo- and para-iodoanisole in both cis-decalin and o-terphenyl absorbed nearly in the same temperature region and yielded identical values of Eyring parameters within the limits of experimental error. The temperature region and the values of ΔH_E , $\Delta G_E(100\text{ K})$, and $\tau_{100\text{ K}}$ for these para-haloanisoles are of the same order of magnitude for group rotation in para-methylanisole.

para-Fluoroanisole was examined in polystyrene matrices from 80 to 200K. Figure IV-9 shows the plot of dielectric loss (ϵ'') versus temperature, T(K), at 1.01 kHz frequency for para-fluoroanisole in a polystyrene matrix but indicates no clear cut absorption peak in the liquid

nitrogen temperature region but a process between 136 and 165 K. Further, Table IV-1 shows that the values of ΔH_E , $\Delta G_E(200 \text{ K})$ and ΔS_E are the most similar in magnitude to the corresponding values obtained for para-chlorotoluene (a rigid molecule of identical size) in the same medium (26). Thus, this observed dielectric relaxation process of para-fluoroanisole in a polystyrene matrix is most likely attributed to rotation of the whole molecule. The absence of an intramolecular absorption process for this molecule in a polystyrene matrix may be attributed to either weak absorptions or merging of the process into the low temperature side of the tail -end of the molecular relaxation process.

It would seem likely that methoxy group rotation is the predominant contributor to the dielectric relaxation of the above mentioned anisoles. In addition, the results of para-methyl- and para-chloro-, bromo- and iodoanisoles clearly indicate that the barrier to methoxy group rotation is insensitive to para-substituents and virtually remains the same (i.e. of the order of 8 kJ mol^{-1}). The most striking point, though, is that the barrier for rotation of this small group is scarcely influenced by variation of the identity of the highly viscous dispersion media.

For all the flexible molecules which exhibit just an intramolecular process below the glass transition temperature this process may be regarded as a β -process since it has the universal features ascribed to such a process:

- (a) a low energy barrier
- (b) symmetrical absorption curves
- (c) a broad distribution of relaxation times
which increases with decreasing temperature
- (d) a linear Eyring plot

Thus, for such molecules, the β -process may be ascribed to methoxy group relaxation. This specific case is opposed to the more general one considered by Johari and Goldstein (27) in that the presence of secondary relaxations should be considered as a characteristic property of the molecule in or near the glassy state and do not require specific intramolecular mechanisms for their existence.

CONCLUSION

For most of these various anisoles dispersed at low concentrations in glassy media the work establishes that:

1. methoxy group relaxation is the main contributor to the dielectric relaxation and these rotations are almost independent of para-substitution and the choice of solvent.
2. in the simple cases for the methoxy group molecule, the lowest temperature relaxation process (often termed a β -process) is an intramolecular one. Various mechanisms have been involved (4,22) to account for the β -process in organic glasses and one has been an intramolecular one (2). However, another viewpoint is that β -processes do not require specific intramolecular mechanisms for their existence (27). This does not apply to the case considered here, nor is it necessary to invoke a mechanism such as re-orientation of polar solutes in interstitial positions (24). Methoxy group relaxation alone is quite adequate to explain the main results in the glassy media considered here.

REFERENCES

1. J. Crossley, S. P. Tay and S. Walker, Adv. Mol. Relax. Proc., 6(1974)79.
2. M. Davies and A. Edwards, Trans. Faraday, Soc., 63(1967)2163.
3. M. Davies and J. Swain, Trans. Faraday Soc., 67(1971)1637.
4. C. K. McLellan and S. Walker, Can. J. Chem., 55(1977)583.
5. S. P. Tay, S. Walker and E. Wyn-Jones, Adv. Mol. Relax. Inter. Proc., 13(1978)47.
6. J. Crossley, M. A. Mazid, C. K. McLellan, P. F. Mountain and S. Walker, Can. J. Chem., 56(1978)567.
7. Ibid., Adv. Mol. Relax. Inter. Proc., 12(1978)239.
8. M. A. Mazid, J. P. Shukla and S. Walker, Can. J. Chem., 56(1978)1800.
9. A. Lakshmi, S. Walker, N.A. Weir and J. H. Calderwood, J. Phys. Chem., 82(1978)1091.
10. Ibid., J. Chem. Soc. Trans. Faraday II, 74 (1978)727.
11. M. A. Mazid, S. Walker and N. A. Weir, Adv. Mol. Relax. Inter. Proc., 19(1981)249.
12. H. A. Khwaja, M. A. Mazid and S. Walker. Z. Phys. Chem. Neuefloge, 128(1981)147.
13. H. A. Khwaja and S. Walker, Adv. Mol. Relax. Inter. Proc., 22(1982)27.
14. J. P. Shukla, J. Warren and S. Walker, Z. Phys. Chem. Neufloge, 125(1981)67.
15. D. B. Farmer and S. Walker, Can. J. Chem., 47(1967)4645.

16. D. M. Roberti and C. P. Smyth, J. Am. Chem. Soc., 82(1960)406.
17. E. Forrest and C. P. Smyth, J. Am. Chem. Soc. 86(1964)3474.
18. M. A. Kashem, M.Sc. Thesis, Lakehead University, Thunder Bay, Ontario, Canada, 1982.
19. S. K. Garg and C. P. Smyth, J. Chem. Phys., 46(1967)373.
20. G. Williams in "Dielectric and Related Molecular Processes" (ed. M. Davies). Specialist Periodical Reports, Chemical Society, London, Vo. 2, 1975.
21. A. J. Barlow, J. Lamb and N. S. Taskopiulu, J. Acoust. Soc. Am., 46(1969)569.
22. G. P. Johari and M. Goldstein, J. Chem. Phys., 53(1970)2372.
23. G. P. Johari, N. Y. Acad. Sci., 279(1976)117.
24. L. Hayler and M. Goldstein, J. Chem. Phys., 66(1977)4736.
25. M. S. Ahmed, J. Crossley, M. S. Hossain, M. A. Kashem, M. A. Saleh and S. Walker, J. Chem., Phys., 81, 448(1984).
26. H. A. Khwaja, M.Sc. Thesis, Lakehead University, Thunder Bay, Ontario, Canada, 1977.
27. G. P. Johari and M. Goldstein, J. Chem. Phys., 55(1971)4245.

TABLE IV-1:

Relaxation time and Eyring Data for some Anisoles in a variety of Organic Glasses

Molecule	Medium	Temperature Range (K)	Relaxation Time τ (s)			ΔG_E (kJ mol ⁻¹)			ΔH_E kJ mol ⁻¹	ΔS_E J K ⁻¹ mol ⁻¹
			100 K	200 K	300 K	100 K	200 K	300 K		
para-methylanisole	polystyrene ¹⁸ matrix	79-111	1.7x10 ⁻⁵	6.1x10 ⁻⁷		14.4	21.7		7.2±0.5	-73±5
	o-terphenyl ¹⁸	70-110 200-213	9.9x10 ⁻⁶	3.4x10 ⁻⁸ 1.7x10 ⁻³	2.5x10 ⁻⁵	14.0	19.7 37.6	30.4	8.3±0.4 ~210	-57±5 ~710±5
	polyphenyl ¹⁸ ether	80-107 257-268	1.0x10 ⁻⁵	3.3x10 ⁻⁸ 2.4x10 ⁻²	4.5x10 ⁻⁵	14.0	19.7 45.6	33.6	8.4±0.6 ~213	-56±8 ~651
	cis-decalin	83-98	2.8x10 ⁻⁶	6.4x10 ⁻⁹		12.9	16.9		819±3.1	-40±34
para-chloroanisole	o-terphenyl	80-110	2.6x10 ⁻⁵	1.5x10 ⁻⁷		14.8	22.2		7.5±0.6	-74±7
	cis-decalin	80-107	2.8x10 ⁻⁴	2.7x10 ⁻⁷		16.8	23.1		10.4±1.6	-64±17
para-bromoanisole	o-terphenyl	87-118	3.9x10 ⁻⁵	1.3x10 ⁻⁷		15.2	22.0		8.3±0.3	-68±3
	cis-decalin	85-109	6.9x10 ⁻⁴	8.4x10 ⁻⁷		17.5	25.0		10.0±3.1	-75±14
para-iodoanisole	o-terphenyl	79-111	4.1x10 ⁻⁵	2.3x10 ⁻⁷		15.2	22.9		7.5±0.4	-77±5
	cis-decalin	83-101	5.9x10 ⁻⁵	8.4x10 ⁻⁸		15.4	21.2		9.7±2.2	-57±25
	polyphenyl ether	79-104	6.3x10 ⁻⁶	1.1x10 ⁻⁷		13.6	21.7		5.4±0.4	-81±4
3,5-dimethylanisole	cis-decalin	84-106	2.3x10 ⁻⁴	4.7x10 ⁻⁸		16.7	20.3		12.9±2.6	-37±28
para-fluoroanisole	polystyrene matrix	136-163	1.9x10 ⁻⁴	8.3x10 ⁻⁷		26.0	25.0		27.1±2.1	10±14
para-chlorotoluene	polystyrene ²⁶ matrix	163-196		1.6x10 ⁻³	5.8x10 ⁻⁶		28.0	29.0	26.0	-9.0
	o-terphenyl	205-241		8.5x10 ⁻³	2.0x10 ⁻³		35.7	38.0	28.8±3.0	-25±12
	polyphenyl ether	197-240		8.8x10 ⁻¹	9.1x10 ⁻⁴		35.7	36.7	32.9±2.6	10±8

TABLE IV-3: Fuoss-Kirkwood parameters for some anisoles in cis-decalin

T(K)	$10^6 \tau$ (s)	$\log v_{\max}$	β	$10^3 \epsilon''_{\max}$	ϵ_{∞}	μ (D)
<u>0.58 M p-iodoanisole</u>						
83.8	656.01	2.38	0.35	0.38		
86.1	484.76	2.51	0.35	0.38		
85.1	547.90	2.46	0.35	0.38		
89.6	206.83	2.88	0.31	0.39		
93.9	193.28	2.91	0.44	0.40		
100.7	49.41	3.50	0.40	0.39		
<u>0.79 M p-chloroanisole</u>						
85.4	2657.20	1.77	0.34	0.21		
87.3	2440.60	1.81	0.26	0.22		
90.4	1379.30	2.06	0.27	0.23		
94.0	610.68	2.40	0.34	0.24		
96.1	449.12	2.54	0.33	0.25		
97.1	335.57	2.67	0.31	0.25		
103.6	219.51	2.86	0.46	0.27		
107.8	108.73	3.16	0.39	0.27		
<u>0.68 M p-bromoanisole</u>						
87.8	2089.01	1.88	0.77	0.08		
91.0	1862.41	1.93	0.60	0.08		
93.9	1087.40	2.16	0.87	0.09		
103.3	513.02	2.49	0.56	0.09		
106.5	303.43	2.71	0.47	0.10		
108.2	231.74	2.83	0.43	0.10		

TABLE IV-3: continued...

T (K)	$10^6 \tau$ (s)	$\log v_{\max}$	β	$10^3 \epsilon''_{\max}$	ϵ_{∞}	μ (D)
<u>0.68 M 3,5-dimethylanisole</u>						
84.5	4360.90	1.56	0.63	0.38	2.322	1.86
86.6	3588.20	1.64	0.51	0.41	2.334	2.15
89.7	1769.71	1.95	0.49	0.42	2.333	2.26
95.9	378.96	2.62	0.49	0.44	2.333	2.40
99.4	207.13	2.88	0.50	0.45	2.333	2.41
105.7	120.24	3.12	0.62	0.43	2.334	2.24
<u>0.75 M p-methylanisole</u>						
83.1	25.88	3.78	0.50	1.04		
87.4	20.83	3.88	0.61	1.08		
89.5	9.65	4.21	0.51	1.03		
92.5	7.47	4.32	0.51	0.94		
95.0	5.42	4.46	0.51	0.90		
97.9	3.43	4.66	0.47	0.78		
<u>0.45 M para-fluoroanisole (polystyrene)</u>						
136.5	2117.80	1.88	0.18	7.12		
140.9	1177.20	2.13	0.17	7.35		
144.1	605.67	2.42	0.18	7.57		
148.4	356.76	2.65	0.18	7.82		
151.2	227.03	2.85	0.18	7.96		
154.3	133.64	3.08	0.17	8.09		
163.8	33.81	3.67	0.19	8.67		

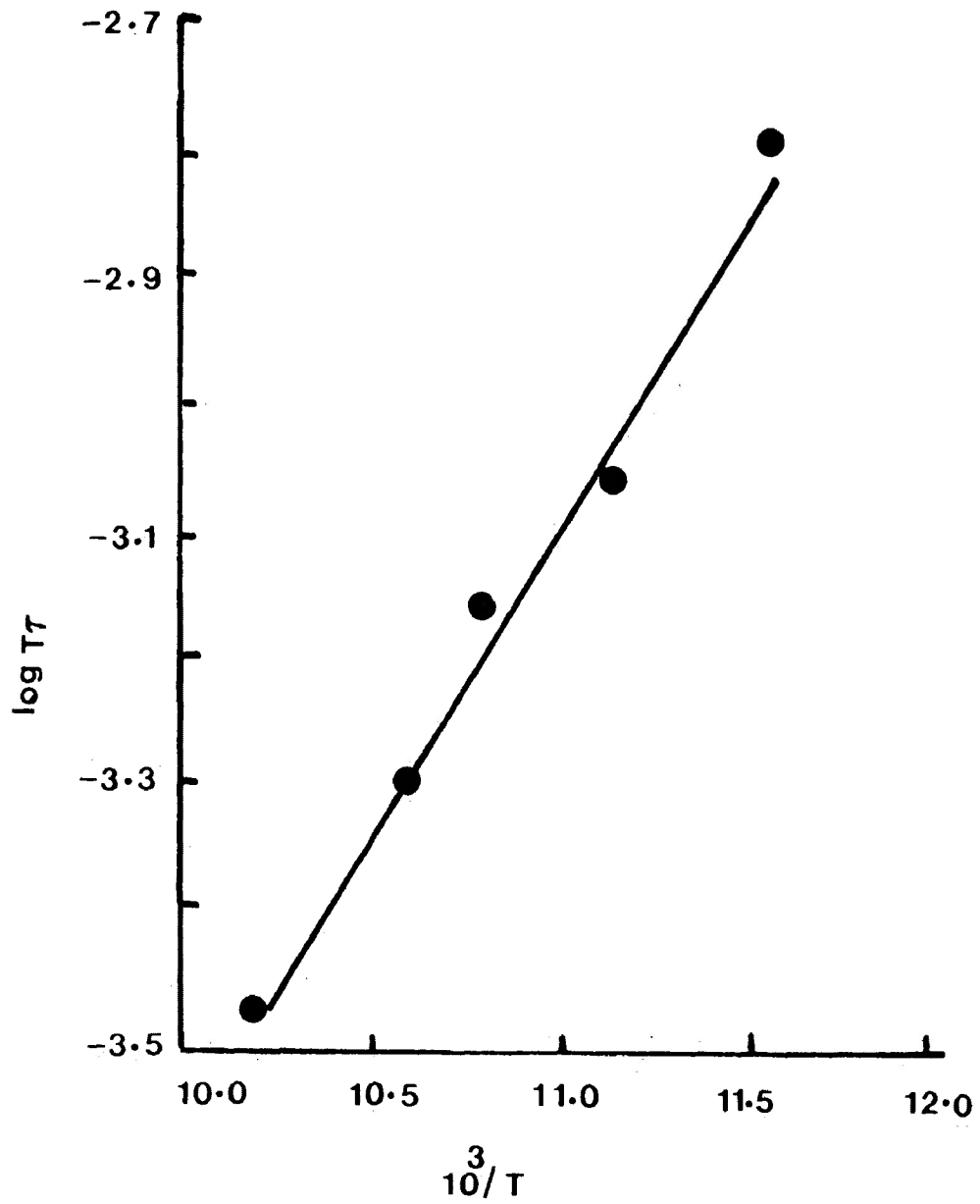


FIGURE IV-1: Eyring plot of $\log T\tau$ versus $1/T$ (K^{-1}) for para-methylanisole in cis-decalin

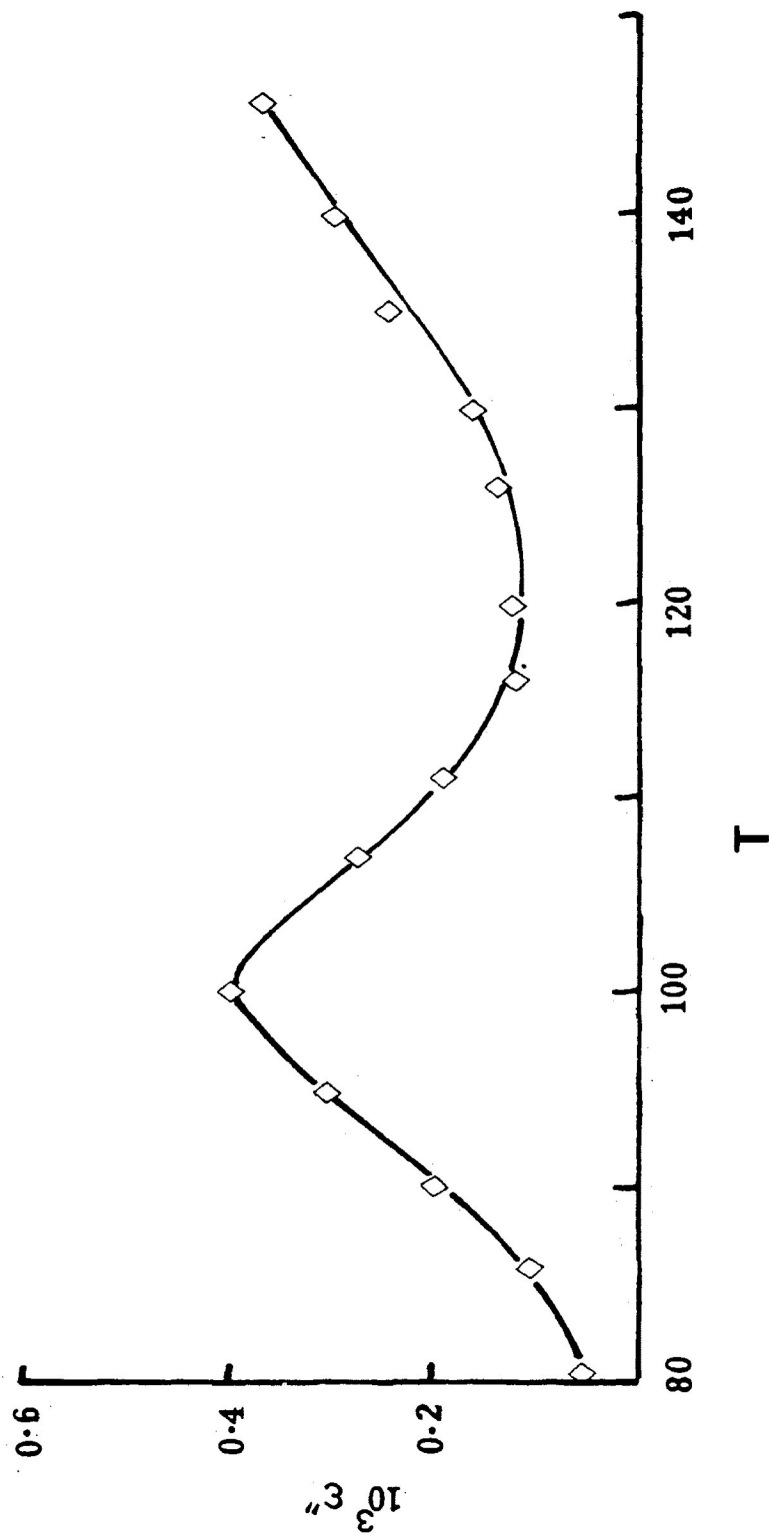


FIGURE IV-2: Dielectric loss factor, ϵ'' versus temperature (K) for 3,5-dimethyl-anisole in cis-decalin at 1.01 kHz

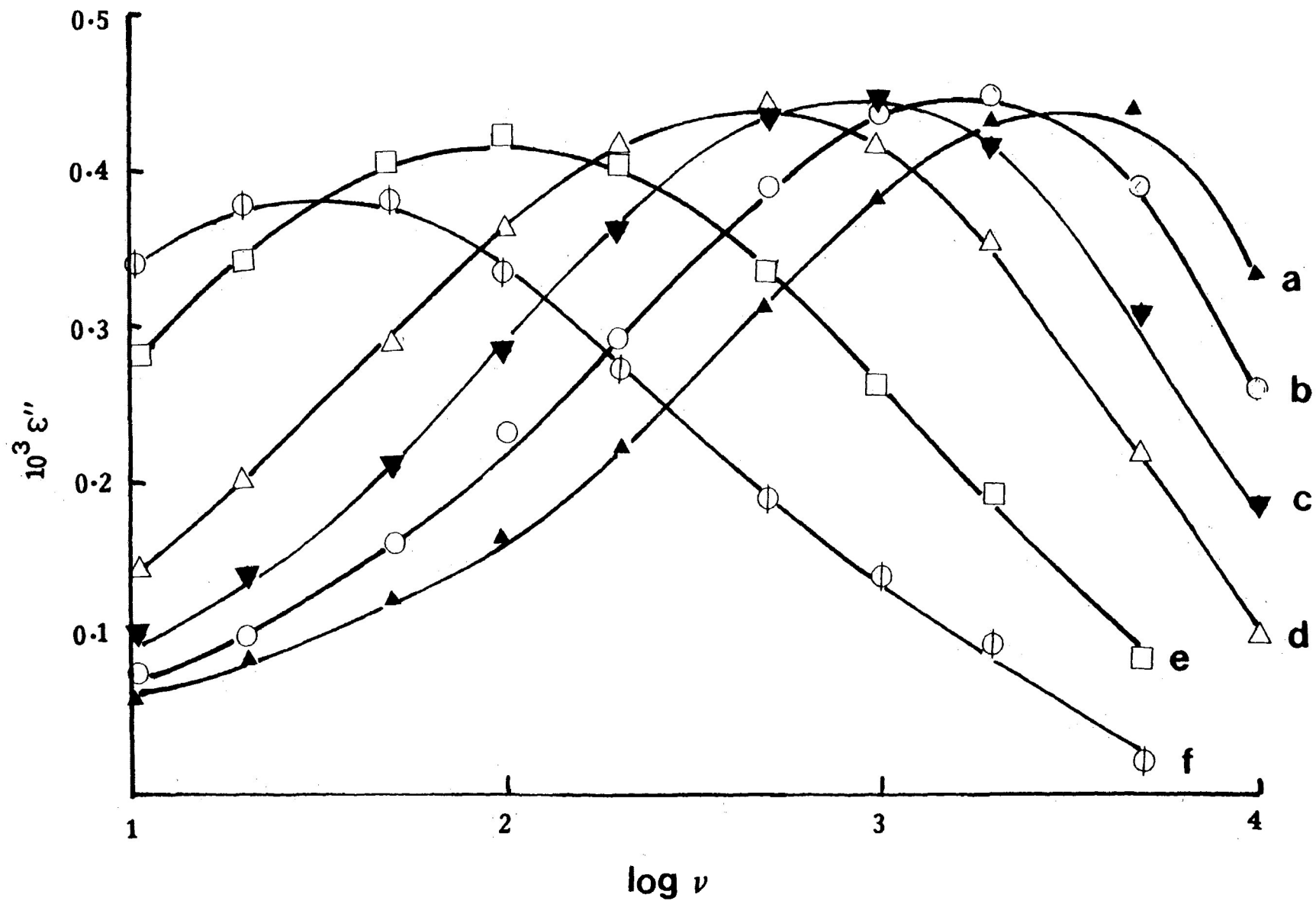


FIGURE IV-3: Dielectric loss factor, ϵ'' versus $\log \nu$ for 3,5-dimethylanisole in cis-decalin
 a) 105.7 K; b) 99.4 K; c) 95.9 K; d) 89.7 K; e) 86.6 K and f) 84.5 K.

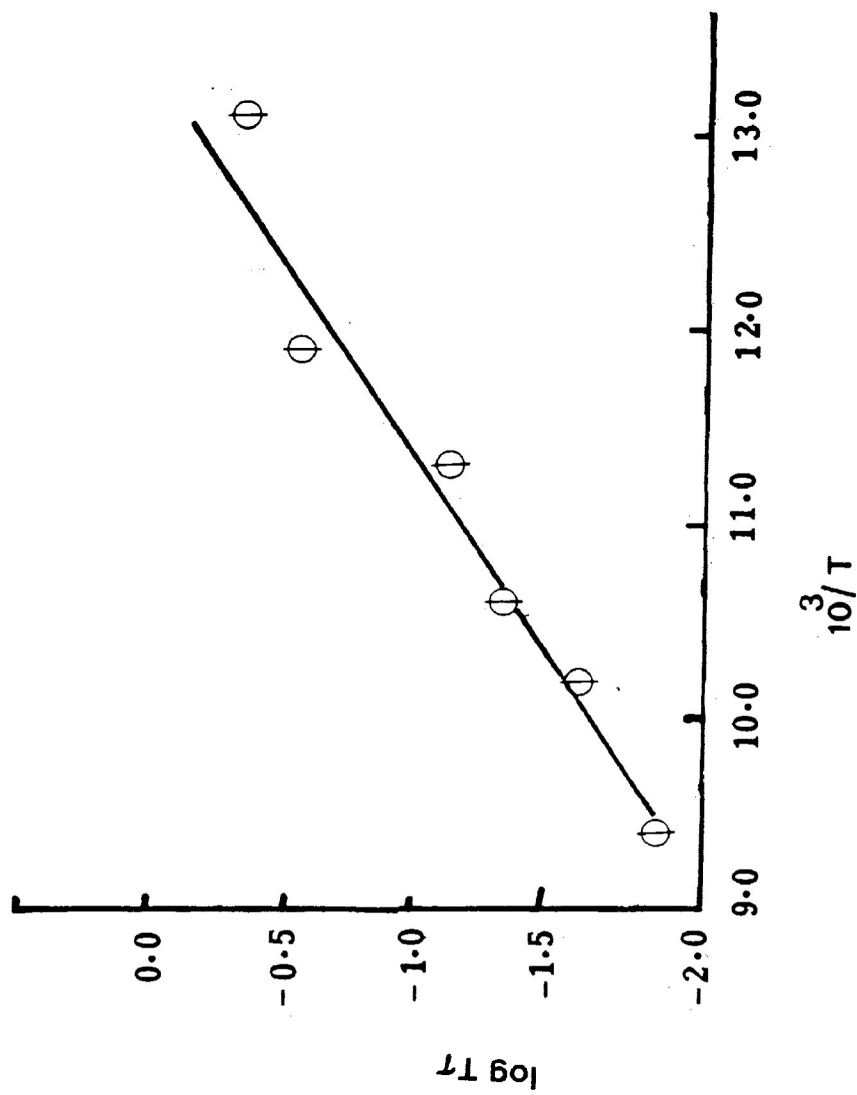


FIGURE IV-4: Eyring plot of $\log T_1$ versus $1/T$ (K^{-1}) for 3,5-dimethylanisole in cis-decalin

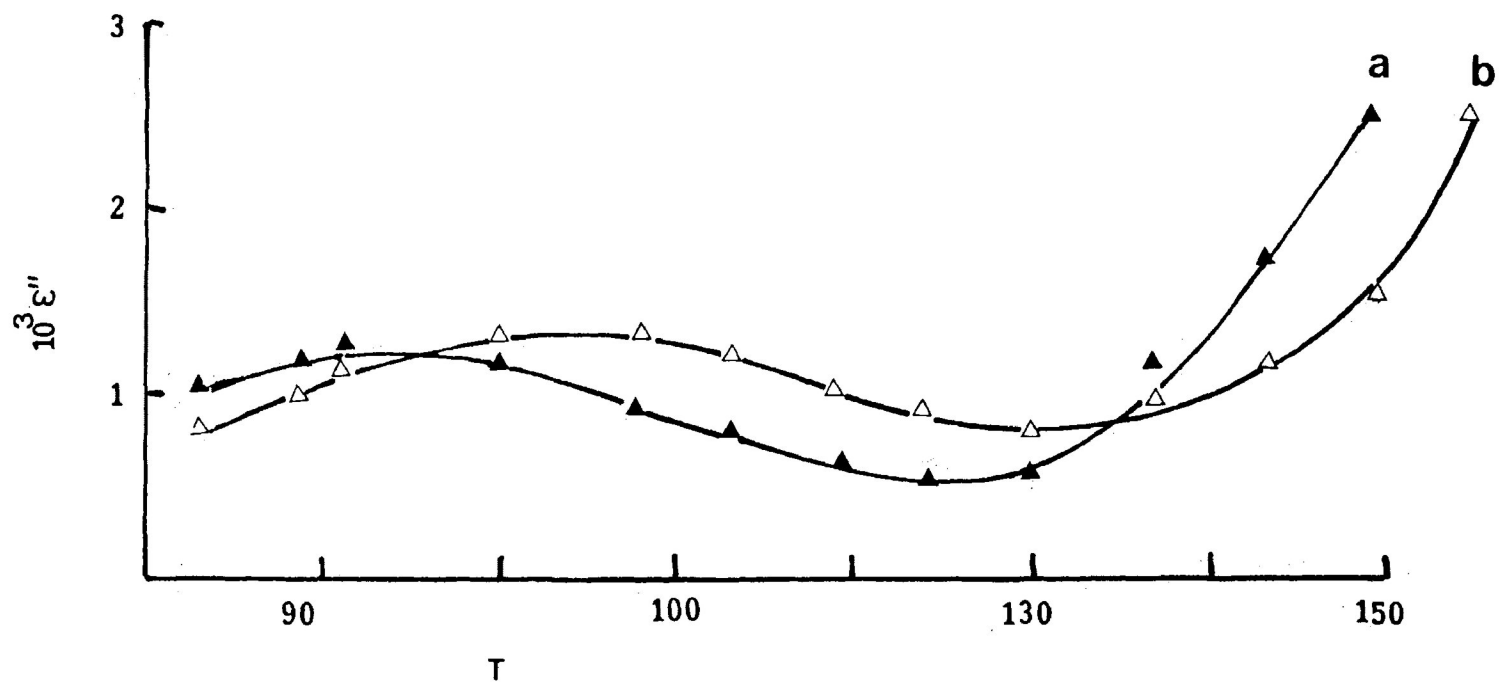


FIGURE IV-5: Dielectric loss factor, ϵ'' versus temperature (K) for para-chloroanisole in cis-decalin. a) 0.2 kHz, b) 2 kHz

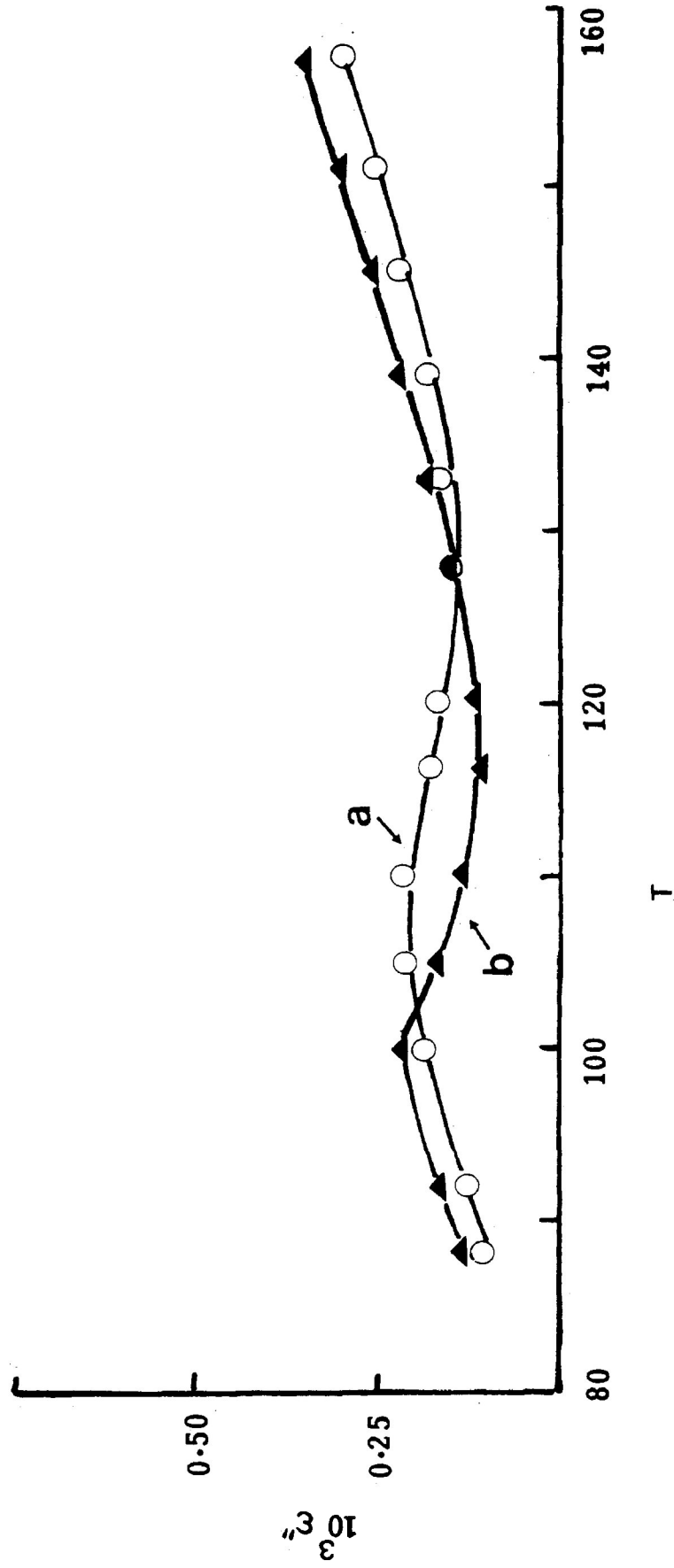


FIGURE IV-6: Dielectric loss factor, $10^3 \epsilon''$ versus temperature (K) for para-bromoanisole in cis-decalin. a) 0.2 kHz, b) 2 kHz

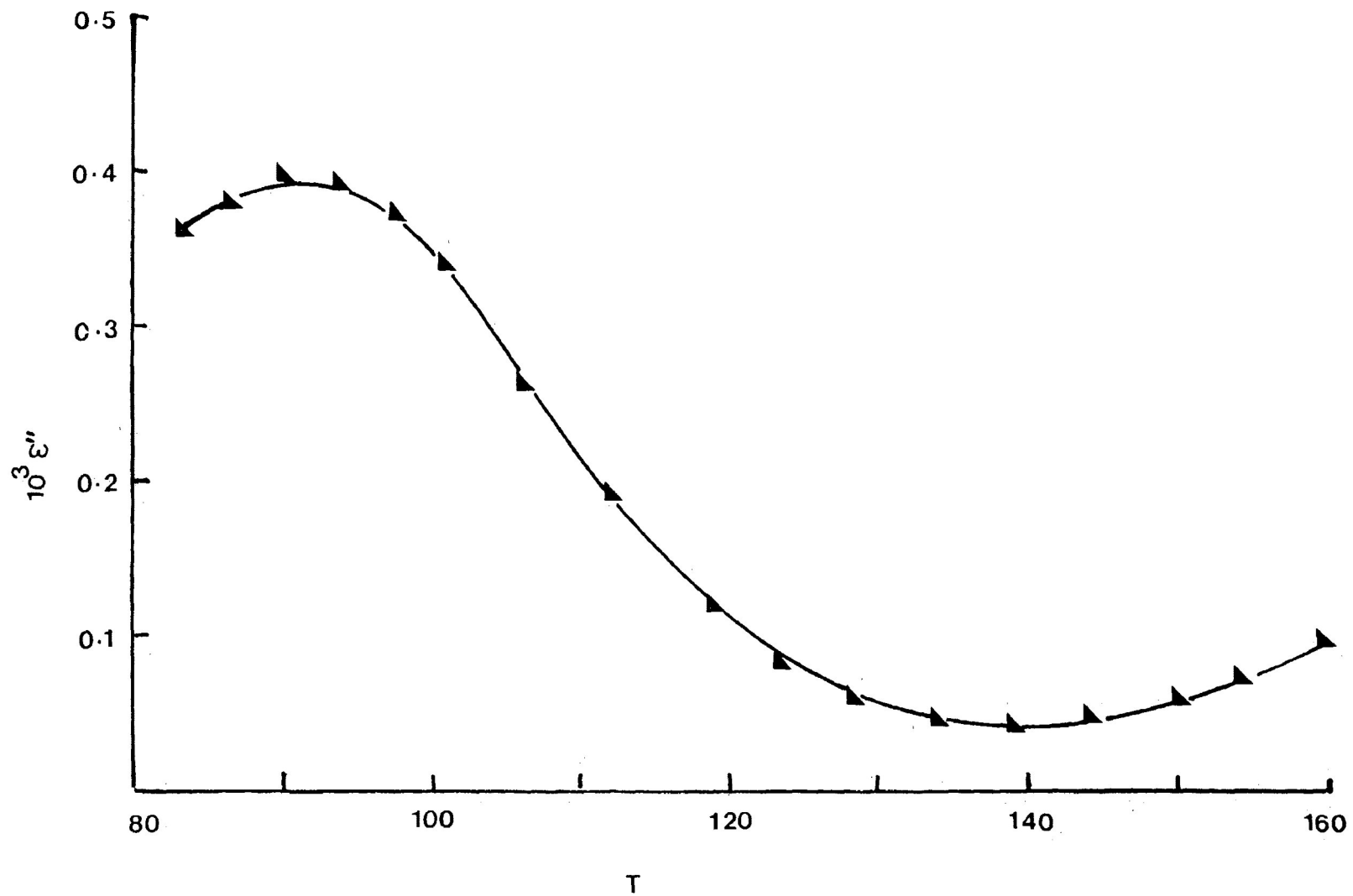


FIGURE IV-7: Dielectric loss factor, ϵ'' versus temperature (K) for paraiodoanisole in cis-decalin at 1.01 kHz

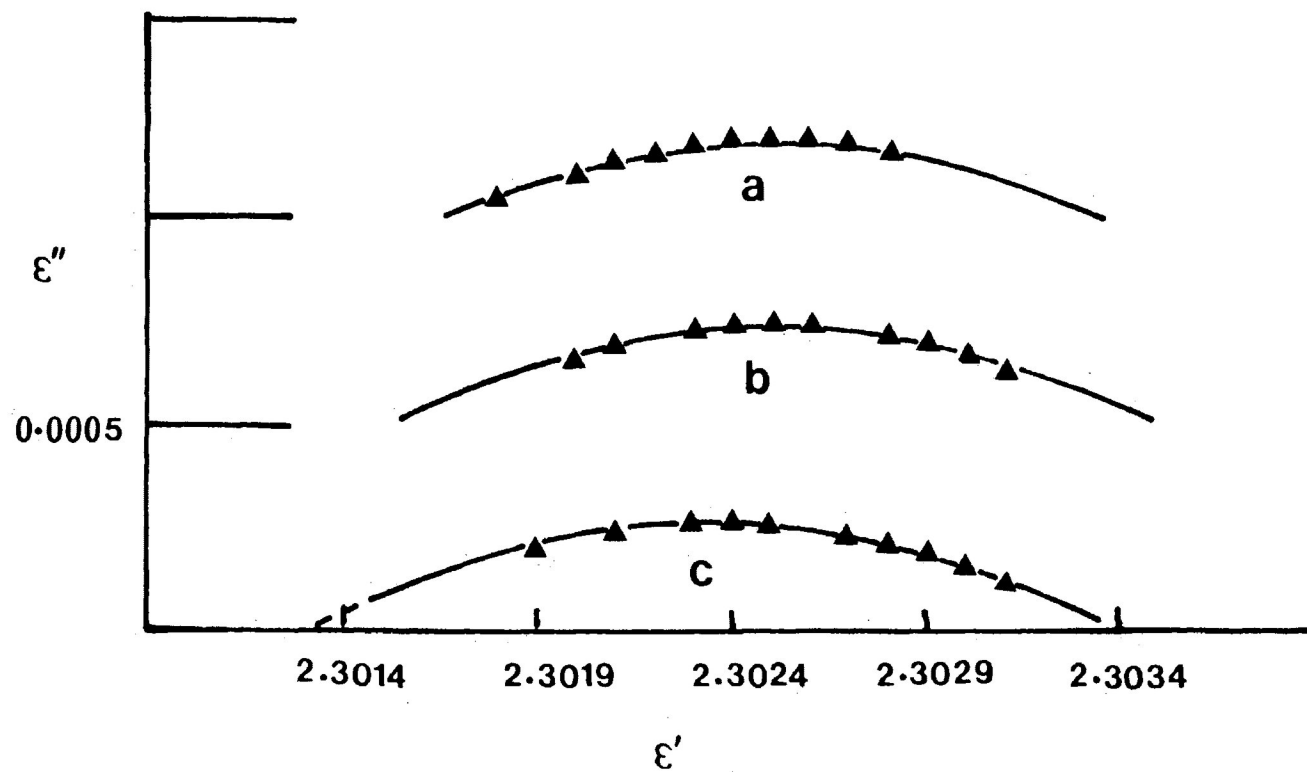


FIGURE IV-8: Cole-Cole plots for para-chloroanisole in cis-decalin
 a) 94 K, b) 97 K, and c) 107 K.

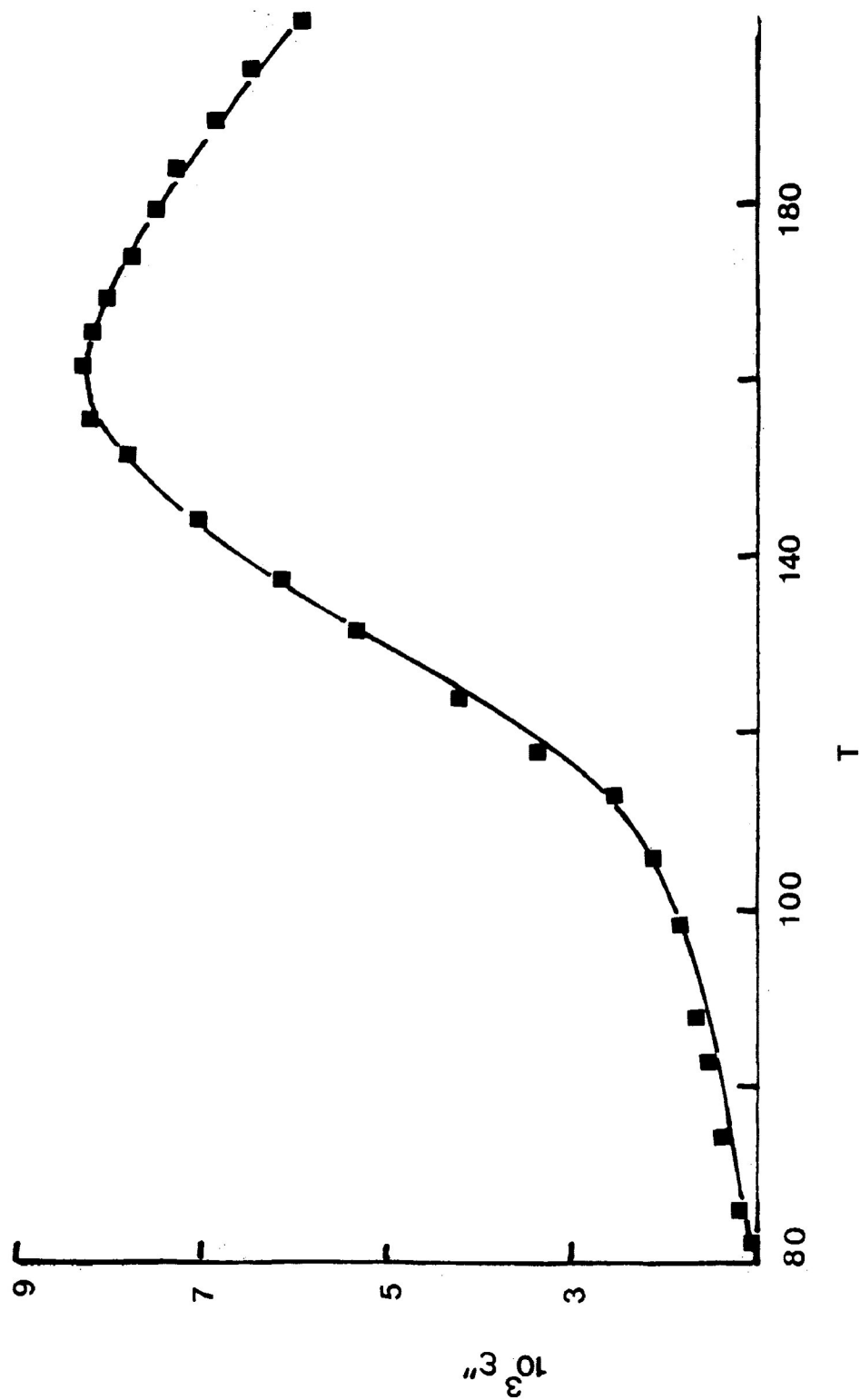


FIGURE IV-9: Dielectric loss factor, ϵ'' versus temperature (K) for para-fluoroanisole in a polystyrene matrix at 1.01 kHz

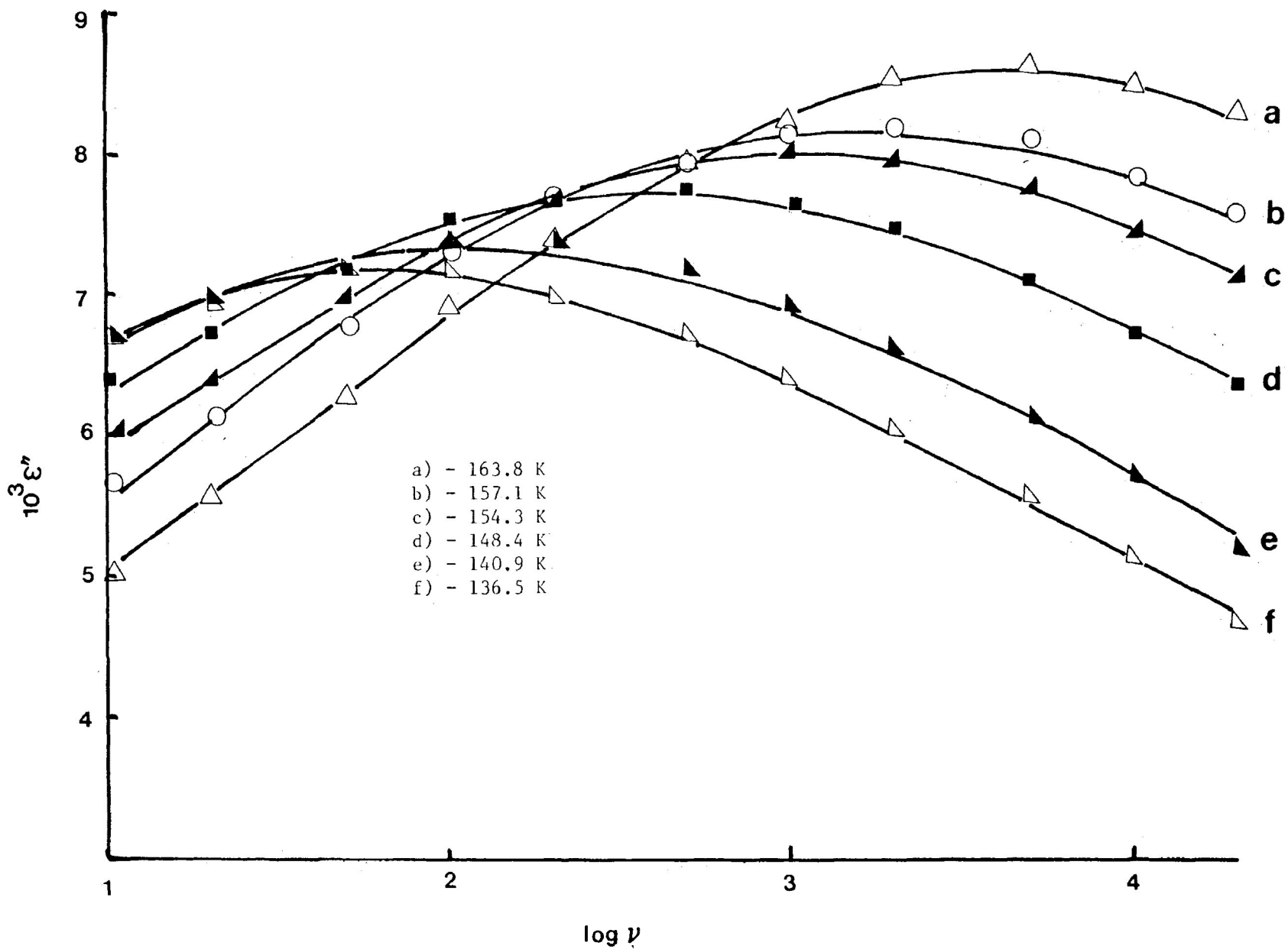


FIGURE IV-10: Dielectric loss factor, ϵ'' versus $\log \nu$ for para-fluoroanisole in polystyrene

CHAPTER V

DIELECTRIC RELAXATION OF 1-BROMOALKANES
IN A POLYSTYRENE MATRIX

INTRODUCTION

Dielectric relaxation studies have been reported for aliphatic polar compounds in the solid, pure liquid states, as well as in a variety of non-polar solvents. The aliphatic bromides appear to have received considerable attention. Smyth and co-workers (1-3) measured dielectric constants and losses of twenty-seven organic halides, mostly n-alkylbromides as pure liquids at microwave frequencies. The mean relaxation times and Cole-Cole distribution parameters increased with increased chain length, and decreased with increased temperature. They inferred that the large distribution parameters for the long chain alkyl bromides result from segmental reorientations about the C-C bonds, with a maximum rotating unit rarely larger than the segment of a chain extending ten to twelve carbon atoms from the dipole.

Just over a decade later, Higasi, Bergmann & Smyth (4) analyzed the dielectric data for bromoalkanes in terms of a distribution of relaxation times between two limiting values. The lower limit was attributed to the relaxation time for the rotation of the terminal $-\text{CH}_2\text{Br}$ group and the upper limit was considered to represent the

relaxation time of the largest segmental unit, usually end-over-end rotation of the molecule as a whole. Later, Johari, Crossley & Smyth (5) examined n-octylbromide in n-heptane at microwave frequency. The Cole-Cole plot was adequately represented by the depressed centre semicircular arc. They were unable to find a successful analysis of the dielectric data in terms of two relaxation times.

Subsequently, Tay and Crossley (6) studied the dielectric relaxation of eight alkylbromides in cyclohexane solution at 298 K. The Cole-Cole plots were adequately represented by the depressed centre semicircular arcs. The mean relaxation times were found to increase with the increase of chain length. They were unable to obtain any sensible analysis of the data in terms of two discrete relaxation times. Their results suggested (a) the polar end group rotation is not as dominant a mechanism of dipole reorientation for bromoalkanes as it is for primary amines and 2-alkanones, (b) the mean relaxation time lengthens only slightly with increased molecular size from 1-bromodecane to 1-bromooctadecane, (c) the contribution from intramolecular rotation, especially for the larger molecules, is not negligible, (d) the intramolecular reorientation is dominated by the smaller segments.

The aim of the present investigation is to gain insight into the types of relaxation processes which can take place. The interpretations of previous investigations have been based largely on arguments from mean relaxation time and distribution parameter values and resolution of these data into two limiting relaxation times or from Budó analyses which sometimes may be quite deceptive. Our present intent was to separate completely the absorption peaks of some or any of the relaxation processes. A separation into molecular and intramolecular processes has previously been achieved for a series of long chain aldehydes in a polystyrene matrix (7). This is to be contrasted with the work on R-X (X = $-\text{CH}_2\text{Br}$, $-\text{NH}_2$, $-\text{COCH}_3$, $-\text{SCH}_3$, etc.) solutes in non-polar solvents which have been studied dielectrically in the microwave region. In no case has a complete separation of the two processes been attained in the liquid phase. Our present aim was to achieve such a separation by dispersing the 1-bromoalkanes in highly viscous media where the molecular relaxation time would likely be lengthened much more than the intramolecular one.

EXPERIMENTAL RESULTS

The following compounds were included in the present study:

<u>Number</u>	<u>Name</u>	<u>Structural Formula</u>
1	1-bromopropane	$\text{CH}_3(\text{CH}_2)_1\text{CH}_2\text{Br}$
2	1-bromohexane	$\text{CH}_3(\text{CH}_2)_4\text{CH}_2\text{Br}$
3	1-bromoheptane	$\text{CH}_3(\text{CH}_2)_5\text{CH}_2\text{Br}$
4	1-bromooctane	$\text{CH}_3(\text{CH}_2)_6\text{CH}_2\text{Br}$
5	1-bromodecane	$\text{CH}_3(\text{CH}_2)_8\text{CH}_2\text{Br}$
6	1-bromododecane	$\text{CH}_3(\text{CH}_2)_{10}\text{CH}_2\text{Br}$
7	1-bromotetradecane	$\text{CH}_3(\text{CH}_2)_{12}\text{CH}_2\text{Br}$
8	1-bromohexadecane	$\text{CH}_3(\text{CH}_2)_{14}\text{CH}_2\text{Br}$
9	1-bromooctadecane	$\text{CH}_3(\text{CH}_2)_{16}\text{CH}_2\text{Br}$
10	1-bromoeicosane	$\text{CH}_3(\text{CH}_2)_{18}\text{CH}_2\text{Br}$
11	1-bromodoeicosane	$\text{CH}_3(\text{CH}_2)_{20}\text{CH}_2\text{Br}$

All of the compounds were obtained commercially.

Table V-1 and Table V-2 collect the values of ΔH_E , ΔS_E along with ΔG_E and τ values for the low and high temperature absorptions respectively.

Table V-3 lists the extrapolated dipole moment

at 330 K ($\mu_{330\text{ K}}$), effective dipole moment (μ_{eff}) and literature dipole moments (μ_{lit}). The energy differences between the equilibrium positions of the dipoles are given in Table V-4.

The Fuoss-Kirkwood analyses parameters, ϵ_{∞} and μ at various temperatures are given in Table V-5. Figures V-1 to V-8 show the dielectric loss factor versus temperature plots, absorption curves, relaxation time versus number of methylene groups, ΔS_E versus ΔH_E and Eyring rate plots of some of the 1-bromoalkanes.

DISCUSSION

Aliphatic bromides of the general formula $\text{CH}_3 \cdot (\text{CH}_2)_n \text{CH}_2 \text{Br}$ where $n = 4, 5, 6, 8, 12, 14, 16, 18$ and 20 , dispersed in polystyrene, exhibited two distinct absorption maxima when the loss factor was plotted against the temperature at a fixed frequency (see Figure V-1). The low temperature peak occurs somewhere in the 90-150 K region, and the higher temperatures are between 160 and 300 K. The temperature maximum for each peak increases within the range as the molecular weight increases. In the case of $n = 1$ only a low temperature absorption peak was detected.

Low temperature dielectric absorption

From Figure V-1 it is evident that the half-width $\Delta T_{\frac{1}{2}}$ (which measures the breadth of the loss peak at half of the loss maximum in the ϵ'' versus T plot at a fixed frequency) of the low temperature absorption peak is approximately the same and lies in the range 40-58 K whereas the $\Delta T_{\frac{1}{2}}$ for the high temperature absorption peaks increases slightly and lies in the range 90-150 K. The relatively narrow half-widths for the low temperature absorption compared with that of high temperature absorption peaks suggests an intramolecular process for the former. Table V-1 gives the Fuoss-Kirkwood

distribution parameter, β , which does not change significantly when n varies from 4 to 20 and lies between 0.18-0.35. Such a large β -value as 0.35 in the low temperature region bears out the intramolecular nature of the low temperature absorption. Comparison may be made of the β -values for $\text{CH}_3(\text{CH}_2)_n\text{CH}_2\text{Br}$ with those for intramolecular relaxation in molecules containing similar types of bonds, for example, β -values for intramolecular relaxation in long chain aldehydes $[\text{CH}_3(\text{CH}_2)_n\text{CHO}]$ (7) where β lies in the range 0.22-0.36 at 85-140 K. In this case the lower temperature was interpreted as segmental rotation involving the $-\text{CHO}$ group. There is considerable similarity between the behaviour of the long chain bromides and aldehydes. However, the previous study on the aldehydes was not so comprehensive as the present one. The intramolecular nature of the low temperature absorption is also borne out by similar β -values (0.23-0.34) for intramolecular relaxation of some symmetrically substituted diaryl ether compounds in the temperature range 83-141 K (10). Sample plots of ϵ'' versus $\log \nu$ for 1-bromodocosane and 1-bromoheptane at different temperatures are given in Figures V-2 and V-3 respectively.

Shukla et al (11) studied benzyl bromide in a polystyrene matrix and obtained an enthalpy of activation, 12 kJ mol^{-1} for the $-\text{CH}_2\text{Br}$ rotation. The potential barrier, V , for group rotation in $\text{CH}_3-\text{CH}_2\text{Br}$ has been reported to be 14.9 kJ mol^{-1} (12). Schaeffer et al (13) employing the n.m.r.

technique in addition to molecular orbital calculations estimated the lower limit for the energy barrier to group rotation in benzyl bromide to be 13 kJ mol^{-1} . Padmanabhan (14) obtained the enthalpy of activation, 14.9 kJ mol^{-1} , for n-propylbromide by the ultrasonic relaxation technique for cis-trans isomerization involving the CH_3CH_2- and $-\text{CH}_2\text{Br}$ groups. The smallest molecule we have been able to study is $n = 1$, and the enthalpy of activation is 18.3 kJ mol^{-1} . The high temperature absorption has not been detected for n-propylbromide; the low temperature absorption is either the intramolecular process (where the molecular process occurs below that of liquid nitrogen temperature) or an overlapping of the molecular and intramolecular processes. The $\Delta H_E = 18.3 \text{ kJ mol}^{-1}$ is of the same order as that obtained by Padmanabhan by the ultrasonic technique (14) for n-propylbromide and Flanagan et al (12) in $\text{CH}_3-\text{CH}_2\text{Br}$ for group rotation by microwave spectra. The higher barrier for $-\text{CH}_2\text{Br}$ rotation in n-propylbromide could be accounted for by the introduction of the CH_3 group in ethylbromide and an enhanced steric effect. Again, in benzylbromide the steric effect would be less than n-propylbromide and may account for the low value of 13 kJ mol^{-1} estimated by Schaeffer et al (13) for benzylbromide.

Figure V-4 shows that the relaxation time, τ_{150} ,

increases as the number of carbon atoms in the molecule increases and becomes almost linear between $n = 14$ and $n = 20$. This clearly indicates that the intramolecular process involves increasing segmental motion as n increases. Since an alkyl segmental relaxation on its own could not account for the substantial absorption, then the segmental motion must be detected through corresponding movement of the terminal $-\text{CH}_2\text{Br}$ dipole.

A linear relationship between ΔS_E and ΔH_E appears when ΔS_E is plotted against ΔH_E for the low temperature absorption (Figure V-5). For intramolecular processes there appears to be no specific relationship between ΔS_E and ΔH_E . However, for a particular type of intramolecular process, a linear correlation may exist between ΔS_E and ΔH_E . For example, Davies et al (9) established the relationships ΔS_E ($\text{J K}^{-1} \text{ mol}^{-1}$) = $4.2 \Delta H_E$ (kJ mol^{-1}) - 173 for the "butterfly flapping"-type of intramolecular motion in thianthrene-type structures, and Desando et al (10) found the relationship $\Delta S_E = 4.1 \times \Delta H_E - 110$ for the intramolecular relaxation of symmetrically substituted diaryl ethers and sulfides in a polystyrene matrix. These relationships are to be strongly contrasted with one found by Khwaja and Walker (17) for rigid molecules in a polystyrene matrix which is:

$$\Delta S_E = 2.2 \Delta H_E - 72$$

Within experimental error there is a reasonable fit of the $\Delta S_{E(\text{obsd})}$ values for intramolecular rotation of the 1-bromoalkanes to the relation, $\Delta S_E = 4.1 \Delta H_E - 70$. The sole rotation of the terminal $-\text{CH}_2\text{Br}$ postulated by some investigators cannot account for the appreciable variation in ΔH_E with increasing chain length, nor for the relationships between ΔS_E and ΔH_E which favours an intramolecular process rather than a molecular one.

In order to investigate the lower temperature process more thoroughly, 1-bromoalkanes with $n = 6, 12, 14$ and 16 have been studied in *o*-terphenyl. Glassy *o*-terphenyl as with polystyrene has been used with success to separate relaxation processes which normally overlap at microwave frequencies around room temperature. Between 77 and 230 K glassy *o*-terphenyl shows negligible dielectric loss ($\epsilon'' \sim 10^{-4}$) and, therefore, is particularly useful as a restrictive medium for the study of intramolecular motions (15,16). There may, however, be difficulty in detecting the molecular process of the solute when it occurs around the glass transition temperature of *o*-terphenyl ($T_g \sim 250$ K). In fact, only low temperature absorption has been detected for the systems examined. The higher temperature process is most likely enveloped by the α -process of the dispersion medium.

Similar ΔG_E and also ΔH_E values are obtained for the low temperature process for a given solute in the different dispersion media (e.g. the 1-bromoalkane with $n = 10$ yields ΔH_E and ΔG_E values of 23.9 kJ mol^{-1} and 20.0 kJ mol^{-1} in a polystyrene matrix and 23.3 kJ mol^{-1} and 19.1 kJ mol^{-1} in a polypropylene matrix).

The similarity of the ΔH_E values of a particular 1-bromoalkane in polystyrene, polypropylene, and glassy o-terphenyl, strongly confirms the intramolecular nature of the low temperature process (see Table V-1).

Higher temperature dielectric absorption

All the 1-bromoalkanes except $n = 1$ display a second absorption in the temperature range 165-300 K in a polystyrene matrix. A representative curve for ϵ'' versus $\log \nu$ is given in Figure V-3).

A survey of the Fuoss-Kirkwood distribution parameters shows low values lying in the range 0.13-0.22, and these testify to the wide range of relaxation times. Rigid molecules, for example para-halotoluenes and para-halobiphenyls, absorb with similar β values (0.17-0.24) in the similar

temperature range, 160 - 330 K (17). These low β -values which are reflected in the broad loss curves (see Figures V-1 and V-3) would be appropriate for whole molecule rotation.

The relaxation time, $\tau_{300\text{ K}}$, increases almost linearly with the increase of carbon atoms in the chain (see Figure 6). This indicates that the size of the reorientating unit also increases with the number of carbon atoms in the chain.

The data (see Table V-2) for the higher temperature absorption processes follow the relationship:

$$\Delta S_E = 2.1 \Delta H_E - 60$$

within experimental error. This is virtually identical to the one Khwaja and Walker found for the molecular relaxation of rigid molecules in a polystyrene matrix (17). For molecular rotation there may be considerable disturbance to the surroundings of the dipole; and thus there is greater disorder in the system, and this is reflected in the large positive ΔS_E values for the higher temperature processes for the molecules which possess the largest values of n .

Thus, it seems reasonable to assume that the higher temperature absorption may be attributed to molecular

reorientation. This is borne out by the fact that the molecule with $n = 10$ dispersed in a polypropylene matrix yields significantly different Eyring parameters ($\Delta H_E = 67$ kJ mol^{-1} , $\Delta S_E = 158$ $\text{J K}^{-1} \text{mol}^{-1}$) than that in a polystyrene matrix ($\Delta H_E = 52$ kJ mol^{-1} and $\Delta S_E = 32$ $\text{J K}^{-1} \text{mol}^{-1}$).

The higher temperature absorption cannot be attributed to the co-operative motion of the solute and solvent since the glass transition temperature, for example, of 1-bromoeicosane ($n = 18$) in polystyrene was found to be ~ 340 K which is considerably higher than the high temperature absorption region of the 1-bromoalkanes (165-300 K).

Altogether, the present work for 1-bromoalkanes in viscous media bears out what was previously inferred by Smyth et al (1-4) for the dielectric absorption of such molecules as pure liquids. The conclusions differ, however, in that segmental reorientation does not appear to be limited to ten or twelve carbon atoms from the $-\text{CH}_2\text{Br}$ dipole. Our results seem to be in contrast with Tay et al (5) who concluded that the dielectric absorption in bromoalkanes in cyclohexane solution is dominated by the terminal $-\text{CH}_2\text{Br}$ rotation. In the glassy media, however, the intramolecular process has been completely separated from the molecular one and characterized by means of its Eyring activation parameters

whereas the work in the microwave region led to a mean relaxation time resulting from the overlap of molecular and intramolecular relaxation processes. It is quite apparent from the ϵ''_{\max} values in Figure V-1 that the contributions from the higher and lower temperature processes are very similar.

Since our results appear to be accounted for by an intramolecular (segmental) process and a molecular one, we adopt the model that the dipole moment is composed of two components, μ_m (molecular) and μ_s (segmental), which governs the effective dipole moment (μ_{eff}) where:

$$\mu_{\text{eff}} = [\mu_m^2 + \mu_s^2]^{\frac{1}{2}}$$

In line with the procedure adopted by Swain and Davies (9) for flexible molecules the μ_s may be taken to be the extrapolated value of the dipole moment at 330 K for the higher temperature absorption. Therefore, the estimated value of the total dipole moment for 1-bromooctane in polystyrene at 330 K is $[(1.46)^2 + (1.25)^2]^{\frac{1}{2}} = 1.9_2$ D which is in good agreement with the literature values 1.88 D at 298 K (19). Estimates of $\mu_{(\text{eff})}$ for the other molecules are given in Table 3. On the whole, the agreement is adequate to support the model especially since

the μ_s values had to be extrapolated over a range of 150 K.

The intensities of the two peaks should be in the approximate ratio of μ_m^2 / μ_s^2 and for 1-bromooctane $\mu_m^2 / \mu_s^2 = 1.25^2 / 1.46^2 = 0.73$. This corresponds closely with the loss factor maxima ratio in Figure 1 which gives a value of 0.74.

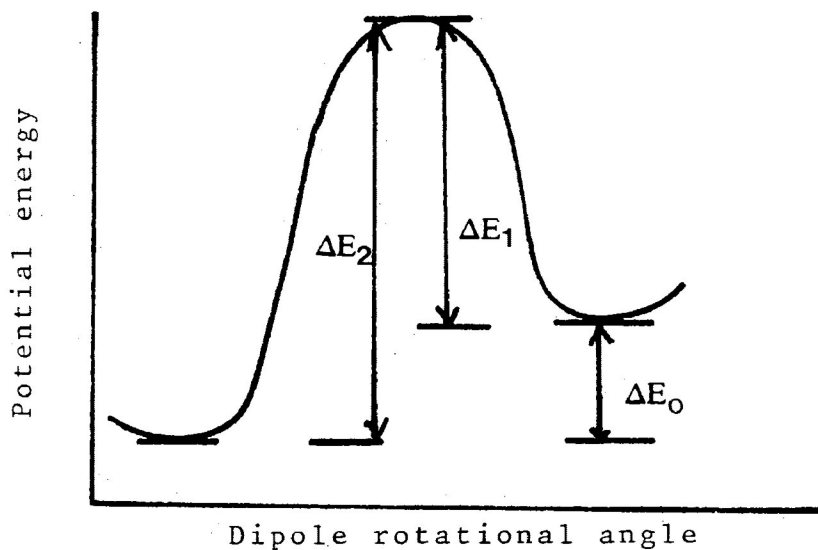
The energy differences, ΔE_0 , between the equilibrium positions of the dipoles in 1-bromoalkanes in a polystyrene matrix calculated from the equation (2)

$$\ln(\epsilon''_{\max} \cdot T) = \text{constant} - \frac{\Delta E_0}{RT}$$

are given in Table V-3. The ΔE_0 values for the chain molecules as in the pure state are high and lie between 8 to 21 kJ mol⁻¹ (21,22). The two sites, unsymmetrical barrier model in which the dipole rotates from one equilibrium position to the other through an angle much

FIGURE V-9:

Potential energy diagram for unequal potential minima



smaller than 180° has been suggested. The high ΔE_0 values for these molecules have been attributed to the end-to-end interaction between the molecule in the crystal lattice. Meakins (20) found the ΔE_0 values for the solid solution of long chain polar molecules in long chain hydrocarbons to be smaller. He adopted the two sites, symmetrical barrier model in which the dipoles rotate from one equilibrium position to the other through an angle of 180° .

In the case of long chain bromides in a polystyrene matrix, we found ΔE_0 values either zero or very small for both the low and high temperature absorptions. Therefore, we adopt the two sites symmetrical barrier model (see Figure V-10) for both the low and high temperature absorptions. The reason for the low

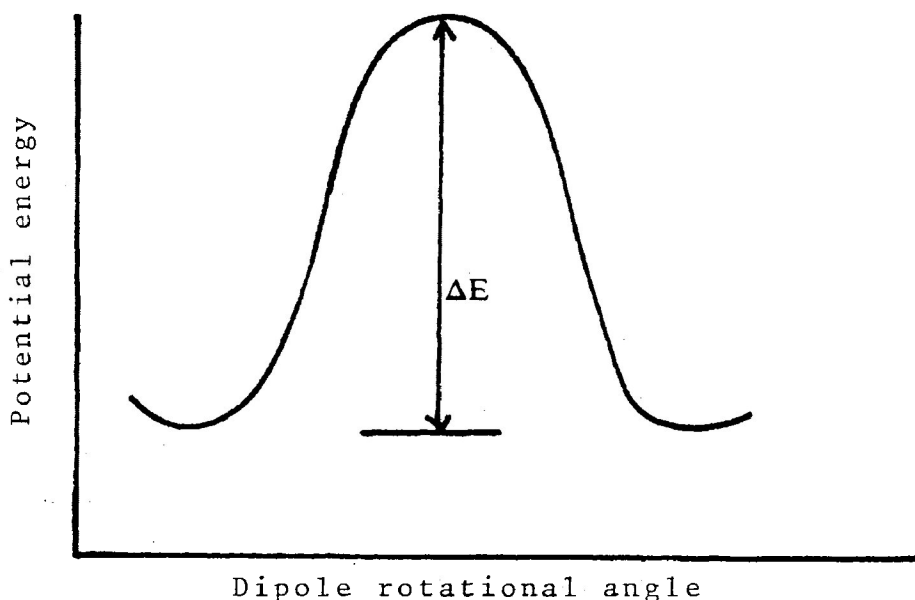


FIGURE V-10: Potential energy diagram for dipole rotating in a polystyrene matrix with energy barrier ΔE and equilibrium positions of equal energy

E_0 values for the long chain bromides in a polystyrene matrix compared to long chain polar compounds in the pure solid state is that in a polystyrene matrix, the molecules are monomolecularly dispersed in the cavities (23). Thus, the packing and molecular interactions are negligible.

CONCLUSION

Our experimental data answer directly the speculations of some of the previous workers as was discussed in our introduction, e.g.:

- (1) there are at least two relaxation processes (see Figure V-1).
- (2) the magnitude of the processes (if there are just two) is of the same order (see Figure V-1), and the relaxation times of each of these processes lengthens with the number of carbon atoms in the chain (See Figures V-4 and V-6).
- (3) both the enthalpies and the entropies of activation increase with the number of carbon atoms in the chain (see Figures V-5 and V-7). Further, for the higher temperature process, ΔH_E and ΔS_E are linearly related by the same equation which is obeyed for rigid molecules in a polystyrene matrix.
- (4) The two sites, symmetrical barrier model seems adequate for the long chain bromides in a polystyrene matrix.

Our dipole moments calculated on the basis of the model of two relaxation processes are in reasonable agreement with the literature values from more direct methods. Thus, μ_m may be identified with molecular rotation while μ_s involves rotation of the segments which leads to movement of the main group moment ($-\text{CH}_2\text{Br}$). Strictly this motion is composed of several relaxation motions involving different

chain lengths, although it is, of course, always the μ_s component which governs the lower temperature absorption. This more refined model then accounts for the lengthening of the relaxation time with increased chain length (see Figure V-4) for the lower temperature absorption.

REFERENCES

1. W.M. Heston, Jr., E.J. Hennelly, and C.P. Smyth, J. Am. Chem. Soc., 1948, 70, 4093.
2. H.L. Lacquer and C.P. Smyth, ibid., 1948, 70, 4097.
3. E.J. Hennelly, W.M. Heston, Jr., and C.P. Smyth, ibid., 1948, 70, 4102.
4. K. Higasi, K. Bergmann, C.P. Smyth, J. Phys. Chem., 1960, 64, 880.
5. G.P. Johari, J. Crossley & C.P. Smyth. J. Am. Chem. Soc., 1969, 91, 5197.
6. S.P. Tay and J. Crossley, Can. J. Chem., 1972, 50, 2031.
7. H.A. Khwaja and S. Walker. Adv. Mol. Interact. and Relax. Processes, 1982, 22, 27.
8. S.P. Tay & S. Walker. J. Chem. Phys. 1975, 63, 1634.
9. M. Davies and J. Swain, Trans. Faraday Soc., 1971, 67, 1637.
10. J. Chao, M.A. Desando, D.L. Gourlay, D.E. Orr, and S. Walker. J. Phys. Chem. , 1984, 88, 711.
11. J.P. Shukla, J. Warren and S. Walker. Adv. Mol. Relax. and Interact. Processes, 1980, 17, 107.
12. W. Gordy and R.L. Cook, "Microwave Molecular Spectra", in W. West, Ed., Chemical Applications of Spectroscopy", Vol. 9, Part II, (Interscience, 1970), pp. 476.
13. T. Schaeffer, L.J. Kruczynski and W.J.E. Parr, Can. J. Chem., 1970, 54, 3210.
14. R.A. Padmanabhan, J. Sci. Ind. Res. (India), 1960, 19B, 336.

15. M.A. Desando, D.L. Gourlay, and S. Walker, J. Chem. Soc., Faraday, Trans. II, 1983, 2, 79, 559.
16. J. Crossley, D. Gourlay, M. Rujimethabas, S.P. Tay, and S. Walker. J. Chem. Phys., 1979, 71, 4095.
17. H.A. Khwaja and S. Walker, Adv. Mol. Relax. and Interact. Processes, 1981, 19, 1.
18. H. Fröhlich, "Theory of Dielectrics", Oxford University Press (1949).
19. A.L. McClellan, "Experimental Dipole Moments". W.H. Freeman and Company, 1963.
20. R. J. Meakins, Trans. Faraday, Soc., 159, 55, 1701.
21. J. S. Dryden and H.K. Welsh, Austral. J. Sci. Res., A, 1951, 4, 616.
22. J. S. Cook and R.J. Meakins, J. Chem. Phys., 1959, 30, 787.
23. M. Davies and A. Edwards, J. Chem. Soc. Faraday, Trans., 1967, 63, 2163.

TABLE V-1:

Eyring activation parameters for the higher temperature absorption of 1-bromoalkanes in a polystyrene matrix

n	Medium	Temperature Range (K)	Relaxation Time τ (s)		ΔG_E (kJ mol ⁻¹)		ΔH_E	ΔS_E
			100 K	150 K	100 K	150 K	kJ mol ⁻¹	J K ⁻¹ mol ⁻¹
1	P.S. [‡]	90-109	3.40×10^{-4}	1.50×10^{-7}	16.9	16.3	18.3	13
4	P.S.	95-117	3.66×10^{-4}	1.00×10^{-7}	17.0	15.8	19.5	24
5	P.S.	96-116	1.10×10^{-3}	2.80×10^{-7}	17.9	17.0	19.6	17
6	P.S.	98-124	1.68×10^{-3}	6.23×10^{-7}	18.3	18.1	18.7	4.0
6	GOTP [‡]	102-125	4.37×10^{-3}	8.24×10^{-7}	19.1	18.4	20.4	13.1
8	P.S.	106-130	1.15×10^{-2}	1.13×10^{-6}	19.9	18.8	22.0	21.4
10	P.S.	114-136	6.12×10^{-2}	2.83×10^{-6}	21.3	20.0	23.8	26.2
10	P.P.*	107-124	2.37×10^{-2}	1.38×10^{-6}	20.4	19.1	23.3	28
12	P.S.	114-135	1.36×10^{-1}	4.20×10^{-6}	21.9	20.4	24.9	29.6
12	GOTP	120-149	1.27×10^{-1}	2.38×10^{-5}	21.9	22.6	20.4	-14
14	P.S.	116-144	4.24×10^{-1}	6.76×10^{-6}	22.9	21.0	26.5	36.7
14	GOTP	117-150	1.07×10^{-1}	9.14×10^{-6}	21.7	21.4	22.4	6.4
16	P.S.	119-147	5.25×10^{-1}	9.63×10^{-6}	23.1	21.5	26.2	31.4
16	GOTP	112-147		1.87×10^{-5}		22.3	19.0	-22
18	P.S.	121-146		1.32×10^{-5}		21.4	27.4	37
20	P.S.	125-146		1.66×10^{-5}		22.2	29.6	49

‡ Dispersion medium polystyrene (P.S.)

‡ Dispersion medium glassy o-terphenyl (GOTP)

* Dispersion medium polypropylene

TABLE V-2:

Eyring activation parameters for the higher temperature absorption of 1-bromoalkanes in a polystyrene matrix

n	Medium	Temperature Range (K)	Relaxation Time τ (s)		ΔG_E (kJ mol ⁻¹)		ΔH_E	ΔS_E
			200 K	300 K	200 K	300 K	kJ mol ⁻¹	J K ⁻¹ mol ⁻¹
4	P.S.	168 - 204	6.60×10^{-5}		32.3		31.5	-3.7
5	P.S.	189 - 213	6.05×10^{-4}		36.0		35.4	-2.9
6	P.S.	205 - 249	5.00×10^{-3}		39.5		39.3	-1.2
8	P.S.	220 - 260	4.14×10^{-2}		43.0		46.9	19.3
10	P.S.	236 - 261	2.50×10^{-1}		46.0		52.4	32
10	P.P.	192 - 207	4.80×10^{-4}		35.6		67.4	158
12	P.S.	237 - 280	5.40×10^{-1}	6.2×10^{-6}	47.3	43.6	54.7	37.3
14	P.S.	238 - 279	1.30×10^1	6.70×10^{-6}	48.8	43.8	58.8	50.0
16	P.S.	245 - 299	2.98×10^1	8.70×10^{-6}	50.1	44.4	61.6	57.7
18	P.S.	262 - 299	6.20×10^1	1.24×10^{-5}	55.2	46.8	72.0	84
20	P.S.	264 - 297	2.09×10^2	1.67×10^{-5}	57.2	46.0	79.5	111.6

TABLE V-3: μ_m and μ_s values extrapolated to 330 K
 and μ_{eff} from $\mu_{\text{eff}} = (\mu_m^2 + \mu_s^2)^{\frac{1}{2}}$

n	μ_{lit} (D)	$\mu_m(330 \text{ K})$ (D)	$\mu_s(330 \text{ K})$ (D)	μ_{eff} (D)
4	1.99	1.3 ₈	1.4 ₇	2.0 ₂
5	1.90	1.1 ₈	1.5 ₉	1.9 ₈
6	1.98	1.2 ₅	1.4 ₆	1.9 ₂
8	1.92	1.3 ₇	1.4 ₈	2.0 ₂
10	-	1.4 ₉	1.2 ₂	1.9 ₃
12	1.92	1.2 ₉	1.3 ₄	1.7 ₃
14	1.87	1.4 ₃	1.3 ₉	1.9 ₉
16	-	1.3 ₃	1.4 ₁	1.9 ₇
18	-	1.3 ₆	1.2 ₇	1.8 ₀
20	-	1.3	1.1	1.7 ₉

TABLE V-4: Energy differences between the equilibrium positions of the dipoles in a polystyrene matrix.

n	Temperature region of absorption	ΔE_0 kJ mol ⁻¹
1	LTA	3.8
4	LTA ‡	0.67
4	HTA *	~0.12
5	LTA	5.94
5	HTA	0.67
6	LTA	0.55
6	HTA	0.25
8	LTA	0.53
8	HTA	0.52
10	LTA	0.50
10	HTA	0.35
12	LTA	0.55
12	HTA	0.48
14	LTA	0.48
14	HTA	0.25
16	LTA	0.27
16	HTA	0.45
18	LTA	0.25
18	HTA	0.03
20	LTA	0.19
20	HTA	0.10

LTA ‡ = Low temperature absorption

HTA * = High temperature absorption

TABLE V-5: Fuoss-Kirkwood parameters, ϵ_{∞} and μ , at various temperatures for 1-bromoalkanes in a polystyrene matrix

T(K)	$10^6 \tau$ (s)	$\log v_{\max}$	β	$10^3 \epsilon''_{\max}$	ϵ_{∞}	μ (D)
<u>0.85 M n-propylbromide (lower temperature process)</u>						
90.6	3766.96	1.62	0.24	3.24		
92.2	2161.39	1.86	0.25	3.30		
94.0	1360.71	2.06	0.26	3.60		
97.3	627.49	2.40	0.27	3.42		
100.4	299.62	2.72	0.28	3.49		
104.0	138.45	2.06	0.28	3.50		
108.2	58.31	3.43	0.30	3.59		
<u>0.50 M 1-bromohexane (lower temperature process)</u>						
95.0	1221.02	2.11	0.22	5.9	2.876	0.45
97.7	625.57	2.40	0.22	6.1	2.874	0.47
100.6	331.27	2.68	0.22	6.2	2.873	0.47
105.0	118.20	3.12	0.21	6.4	2.869	0.50
107.8	61.55	3.41	0.21	6.6	2.866	0.52
110.0	35.82	3.64	0.21	6.8	2.864	0.54
116.6	9.83	4.20	0.21	6.9	2.861	0.55
<u>0.50 M 1-bromohexane (higher temperature process)</u>						
168.0	2506.84	1.80	0.16	8.8	2.878	0.85
171.6	1653.31	1.98	0.17	9.0	2.878	0.85
175.7	1118.29	2.15	0.16	9.1	2.875	0.88
179.7	677.41	2.37	0.16	9.2	2.873	0.89
185.8	333.39	2.67	0.17	9.4	2.870	0.91
189.3	235.51	2.82	0.16	9.5	2.867	0.93
194.1	121.34	3.11	0.16	9.5	2.862	0.96
197.1	85.39	3.27	0.16	9.6	2.859	0.97
199.6	62.36	3.40	0.16	9.6	2.858	0.98
203.2	42.82	3.57	0.16	9.7	2.857	0.98

TABLE V-5: continued...

T(K)	$10^6 \tau$ (s)	$\log v_{\max}$	β	$10^3 \epsilon''_{\max}$	ϵ_{∞}	μ (D)
<u>0.60 1-bromoheptane (lower temperature process)</u>						
96.0	3762.40	1.62	0.22	9.0	2.873	0.51
98.0	1610.06	1.99	0.24	9.2	2.873	0.50
100.2	995.75	2.20	0.24	9.4	2.872	0.51
103.0	473.29	2.52	0.25	9.7	2.872	0.52
106.0	287.38	2.74	0.25	9.9	2.870	0.53
109.0	146.23	2.03	0.25	10.0	2.879	0.54
112.8	63.91	3.39	0.26	10.4	2.869	0.55
116.0	39.67	3.60	0.26	10.6	2.826	0.56
<u>0.60 1-bromoheptane (higher temperature process)</u>						
189.1	1945.46	1.91	0.19	15.2	2.793	1.02
190.7	1708.96	1.96	0.18	15.2	2.807	1.04
193.0	1404.39	2.05	0.18	15.3	2.804	1.05
195.7	1024.52	2.19	0.17	15.4	2.866	1.06
199.0	691.66	2.36	0.17	15.4	2.980	1.06
201.7	530.06	2.47	0.17	15.5	2.796	1.11
204.0	410.46	2.58	0.17	15.6	2.794	1.13
208.4	254.71	2.79	0.16	15.6	2.800	1.18
212.2	143.34	3.04	0.15	15.6	2.789	1.21
<u>0.52M 1-bromooctane (lower temperature process)</u>						
98.0	2532.52	1.79	0.25	8.0	2.858	0.49
99.4	1536.69	2.01	0.26	8.2	2.858	0.49
101.8	1275.18	2.09	0.24	8.4	2.856	0.52
104.4	721.52	2.34	0.25	8.6	2.854	0.52
108.5	293.09	2.73	0.26	8.9	2.852	0.53
112.8	112.27	3.15	0.26	9.1	2.850	0.55
115.7	61.71	3.41	0.28	9.4	2.849	0.55
119.0	37.71	3.62	0.29	9.6	2.849	0.55
123.1	19.87	3.90	0.30	9.9	2.848	0.56

TABLE V-5: continued...

T(K)	$10^6 \tau$ (s)	$\log v_{\max}$	β	$10^3 \epsilon''_{\max}$	ϵ_{∞}	μ (D)
0.52 M 1-bromooctane (higher temperature process)						
205.2	2120.69	1.87	0.18	11.0	2.871	0.98
208.6	1643.17	1.98	0.18	11.1	2.867	1.01
212.0	1276.13	2.09	0.16	11.1	2.863	1.04
217.1	814.95	2.29	0.16	11.2	2.856	1.08
222.8	461.01	2.53	0.16	11.3	2.855	1.09
227.4	300.79	2.72	0.15	11.3	2.850	1.13
233.2	151.05	3.02	0.14	11.3	2.834	1.17
237.2	113.71	3.14	0.15	11.3	2.842	1.16
243.8	50.90	3.49	0.15	11.3	2.836	1.19
248.7	32.93	3.68	0.15	11.3	2.766	1.19
0.50 M 1-bromodecane (lower temperature process)						
106.3	2075.58	1.88	0.26	10.5	2.846	0.59
109.4	1111.08	2.15	0.26	10.7	2.845	0.61
113.7	412.26	2.58	0.27	11.1	2.842	0.62
116.6	239.44	2.82	0.28	11.4	2.845	0.62
119.4	124.83	3.10	0.29	11.5	2.841	0.62
122.7	67.54	3.37	0.30	11.8	2.840	0.63
125.6	39.89	3.60	0.32	12.1	2.840	0.63
129.4	21.62	3.86	0.33	12.4	2.839	0.63
0.50 M 1-bromodecane (higher temperature process)						
220.0	2153.19	1.86	0.18	12.9	2.870	1.10
223.4	1756.81	1.95	0.18	12.8	2.867	1.12
228.0	1190.35	2.12	0.17	12.9	2.863	1.16
233.6	661.96	2.38	0.17	12.8	2.857	1.19
237.4	469.52	2.53	0.16	12.8	2.854	1.22
241.8	296.46	2.72	0.16	12.8	2.851	1.23
246.8	181.98	2.94	0.16	12.7	2.846	1.25
253.1	76.52	3.31	0.15	12.6	2.837	1.29
259.1	42.93	3.56	0.16	12.6	2.836	1.28
0.47 M 1-bromododecane (lower temperature process)						
114.8	1293.99	2.08	0.27	11.5	2.840	0.66
117.0	772.93	2.31	0.28	11.7	2.841	0.66
119.4	497.37	2.50	0.28	11.8	2.841	0.66
122.5	256.05	2.79	0.29	12.1	2.834	0.67
126.0	125.07	3.10	0.30	12.3	2.842	0.67
129.6	64.01	3.39	0.32	12.6	2.839	0.67
132.6	38.52	3.61	0.33	12.8	2.839	0.67
136.6	20.62	3.88	0.35	13.1	2.883	0.66

TABLE V-5: continued...

T(K)	$10^6 \tau$ (s)	$\log v_{\max}$	β	$10^3 \epsilon''_{\max}$	ϵ_{∞}	μ (D)
<u>0.47 M 1-bromododecane (higher temperature process)</u>						
231.4	2651.89	1.77	0.18	11.9	2.887	1.14
234.4	1902.57	1.92	0.18	12.0	2.885	1.15
237.7	1481.63	2.03	0.18	12.2	2.889	1.14
241.5	1040.49	2.18	0.15	11.9	2.877	1.24
247.0	587.16	2.43	0.15	12.0	2.823	1.27
251.0	388.50	2.61	0.15	11.9	2.866	1.30
256.0	201.52	2.89	0.13	11.8	2.856	1.38
261.0	95.95	3.22	0.13	11.8	2.851	1.39
<u>0.44 M 1-bromotetradecane (lower temperature process)</u>						
114.0	2813.11	1.75	0.27	10.6	2.803	0.65
116.5	1642.59	1.98	0.27	11.0	2.801	0.67
118.5	1119.57	2.15	0.27	11.1	2.801	0.67
120.5	678.75	2.37	0.28	11.3	2.799	0.68
123.0	337.88	2.67	0.29	11.6	2.799	0.69
126.1	223.21	2.85	0.29	11.8	2.798	0.69
129.5	109.38	3.16	0.30	11.9	2.796	0.70
134.8	42.40	3.57	0.33	12.4	2.799	0.70
<u>0.44 M 1-bromotetradecane (higher temperature process)</u>						
236.9	2101.12	1.87	0.19	9.8	2.828	1.05
241.7	1449.14	2.04	0.18	9.8	2.862	1.08
247.0	878.92	2.25	0.17	9.7	2.862	1.14
254.0	417.17	2.58	0.16	9.7	2.812	1.19
262.0	213.35	2.87	0.15	9.7	2.803	1.25
269.6	67.61	3.37	0.14	9.6	2.790	1.30
274.5	42.96	3.56	0.14	9.6	2.787	1.30
279.4	33.10	3.68	0.15	9.5	2.788	1.27
<u>0.34 M 1-bromohexadecane (lower temperature process)</u>						
116.1	4762.98	1.52	0.25	10.2	2.835	0.76
118.5	2273.42	1.84	0.26	10.5	2.819	0.76
120.8	1399.89	2.05	0.26	10.7	2.814	0.77
122.5	938.37	2.22	0.27	10.8	2.813	0.77
124.1	659.34	2.38	0.27	11.0	2.812	0.78
125.6	495.08	2.50	0.28	11.1	2.842	0.78
128.7	255.30	2.79	0.29	11.3	2.812	0.78
133.4	102.57	3.19	0.34	11.6	2.810	0.79
136.7	56.16	3.45	0.32	11.9	2.811	0.78
143.7	18.78	3.92	0.34	12.3	2.809	0.80

TABLE V-5: continued...

T(K)	$10^6 \tau$ (s)	$\log v_{\max}$	β	$10^3 \epsilon''_{\max}$	ϵ_{∞}	μ (D)
<u>0.34 M 1-bromohexadecane (higher temperature process)</u>						
238.0	2888.12	1.74	0.19	9.6	2.839	1.21
241.1	2294.45	1.84	0.19	9.7	2.836	1.20
243.0	1786.45	1.94	0.19	9.7	2.833	1.22
247.0	1258.45	2.10	0.18	0.6	2.830	1.25
254.7	629.90	2.40	0.17	9.5	2.824	1.30
258.4	373.26	2.62	0.17	9.5	2.820	1.31
265.1	199.27	2.90	0.16	9.4	2.813	1.37
269.0	134.44	3.07	0.14	9.3	2.825	1.43
274.2	55.36	3.45	0.15	9.2	2.800	1.43
279.0	32.72	3.68	0.15	9.2	2.807	1.44
<u>0.39 M 1-bromooctadecane (lower temperature process)</u>						
119.1	2778.93	1.75	0.25	8.5	2.824	0.65
121.1	1789.85	1.94	0.26	8.7	2.845	0.65
125.0	747.74	2.32	0.27	8.9	2.822	0.66
130.1	273.89	2.76	0.28	9.3	2.821	0.67
134.4	116.14	3.13	0.30	9.4	2.819	0.67
138.4	55.55	3.45	0.32	9.7	2.819	0.67
143.4	26.55	3.77	0.34	10.0	2.819	0.66
146.1	17.98	3.94	0.34	10.0	2.818	0.67
<u>0.39 M 1-bromooctadecane (higher temperature process)</u>						
245.7	2049.10	1.89	0.20	9.6	2.833	1.09
251.4	1266.61	2.09	0.19	9.6	2.828	1.13
256.7	775.51	2.31	0.18	9.6	2.822	1.17
260.7	441.18	2.55	0.19	9.6	2.841	1.16
265.3	260.09	2.78	0.18	9.5	2.816	1.19
270.6	126.38	3.10	0.17	9.3	2.809	1.22
275.3	77.62	3.31	0.17	9.2	2.804	1.23
282.5	37.73	3.62	0.17	9.0	2.825	1.24
284.0	33.70	3.67	0.17	8.8	2.797	1.22
288.8	25.81	3.78	0.17	8.7	2.888	1.23
291.8	21.17	3.87	0.17	8.6	2.918	1.22
298.2	8.70	4.26	0.16	8.4	2.982	1.28

TABLE V-5: continued...

T(K)	$10^6 \tau$ (s)	$\log v_{\max}$	β	$10^3 \epsilon''_{\max}$	ϵ_{∞}	μ (D)
<u>0.67 M 1-bromoeicosane (lower temperature process)</u>						
120.9	2955.22	1.73	0.25	8.09	2.835	0.49
123.6	1758.91	1.95	0.25	8.37	2.834	0.50
126.5	1015.0	2.19	0.25	8.53	2.832	0.51
130.1	465.01	2.53	0.26	8.72	2.831	0.51
132.7	262.01	2.78	0.28	8.92	2.828	0.51
136.5	121.09	3.11	0.29	9.05	2.821	0.51
140.5	57.93	3.43	0.30	9.30	1.827	0.52
145.7	26.99	3.77	0.33	9.62	2.831	0.51
<u>0.67 M 1-bromoeicosane (higher temperature process)</u>						
262.0	1718.62	1.96	0.17	6.40	2.827	0.78
264.7	1193.11	2.12	0.16	6.39	2.854	0.79
266.6	932.80	2.23	0.16	6.36	2.823	0.80
273.0	590.82	2.43	0.16	6.32	2.821	0.79
275.9	409.98	2.58	0.15	6.29	2.816	0.82
277.3	290.10	2.73	0.15	6.23	2.813	0.84
280.0	172.38	2.96	0.14	6.14	2.806	0.87
289.2	72.17	3.34	0.14	6.14	2.800	0.88
293.0	43.85	3.56	0.14	6.11	2.792	0.86
299.0	25.12	3.80	0.15	6.04	2.775	0.89
<u>0.38 M 1-bromodocosane (lower temperature process)</u>						
124.6	2330.81	1.83	0.24	8.4	2.858	0.68
126.0	1831.32	1.93	0.24	8.5	2.880	0.68
128.7	1022.61	2.19	0.25	8.7	2.855	0.69
132.1	471.19	2.52	0.26	8.9	2.854	0.69
135.3	235.54	2.82	0.27	9.1	2.854	0.70
138.6	118.34	3.12	0.28	9.3	2.853	0.69
141.7	65.59	3.38	0.30	9.4	2.852	0.69
145.6	36.43	3.64	0.32	9.7	2.853	0.68

TABLE V-5: continued...

T(K)	$10^6 \tau$ (s)	$\log v_{\max}$	β	$10^3 \epsilon''_{\max}$	ϵ_{∞}	μ (D)
<u>0.38 M 1-bromodocosane (higher temperature process)</u>						
263.1	1755.61	1.95	0.15	6.5	2.855	1.10
267.0	1037.37	2.18	0.14	6.5	2.848	1.12
271.4	541.92	2.46	0.15	6.4	2.846	1.10
276.0	282.81	2.75	0.15	6.4	2.841	1.12
281.0	130.39	3.08	0.14	6.3	2.833	1.16
286.5	66.29	3.38	0.14	6.4	2.828	1.16
291.0	45.66	3.54	0.15	6.3	2.824	1.15
296.9	29.10	3.73	0.15	6.2	2.819	1.09
<u>1-bromooctane (G.O.T.P.) (6.5% by weight)</u>						
102.6	2049.60	1.89	0.31	1.79		
107.0	903.57	2.24	0.31	1.88		
109.4	506.54	2.49	0.32	1.94		
112.5	270.06	2.77	0.34	1.98		
115.3	147.12	3.03	0.33	1.99		
117.8	90.55	3.24	0.34	2.08		
118.8	75.38	3.32	0.34	2.04		
119.9	57.90	3.43	0.35	2.07		
122.9	37.06	3.63	0.36	2.10		
124.7	27.41	3.76	0.35	2.08		
<u>1-bromotetradecane (G.O.T.P.) (6.9% by weight)</u>						
120.1	1746.11	1.95	0.30	0.6		
122.5	1034.89	2.18	0.42	0.7		
125.2	654.92	2.38	0.41	0.7		
129.0	444.12	2.55	0.35	0.7		
132.6	256.99	2.79	0.32	0.7		
136.8	122.51	3.11	0.32	0.7		
141.0	64.91	3.38	0.33	0.7		
144.0	47.07	3.52	0.35	0.7		
149.0	24.55	3.81	0.35	0.7		

TABLE V-5: continued...

T(K)	$10^6 \tau$ (s)	$\log v_{\max}$	β	$10^3 \epsilon''_{\max}$	ϵ_{∞}	μ (D)
<u>1-bromohexadecane (G.O.T.P.) (7.5% by weight)</u>						
117.2	1891.27	1.92	0.26	3.3		
119.5	1183.64	2.12	0.27	3.4		
121.5	758.23	2.32	0.27	3.4		
123.3	570.53	2.44	0.32	3.5		
126.0	304.52	2.71	0.29	3.5		
130.7	123.64	3.10	0.31	3.6		
135.0	61.45	3.41	0.34	3.7		
139.2	32.57	3.68	0.37	3.8		
142.7	21.69	3.86	0.39	3.8		
145.7	17.16	3.96	0.42	3.9		
149.4	12.61	4.10	0.46	3.9		

1-bromooctadecane (G.O.T.P.) (8.1% by weight)

112.1	4803.22	1.52	0.22	0.6		
113.7	3582.81	1.64	0.22	0.6		
117.5	1181.49	2.12	0.37	0.7		
119.4	1042.55	2.18	0.29	0.7		
121.1	889.32	2.25	0.31	0.7		
124.8	483.78	2.51	0.29	0.7		
129.4	251.74	2.80	0.27	0.7		
133.0	129.95	3.08	0.27	0.7		
138.0	76.03	3.32	0.26	0.8		
140.0	49.92	3.50	0.26	0.8		
147.0	27.90	3.75	0.23	0.8		

0.45 M 1-bromododecane (polypropylene) (lower temperature process)

107.2	3134.83	1.70	0.25	11.4		
110.8	1482.97	2.03	0.26	12.1		
113.8	714.03	2.34	0.26	12.5		
117.0	349.35	2.65	0.27	12.9		
119.0	231.99	2.83	0.28	13.2		
123.6	86.54	3.26	0.29	13.7		

TABLE V-5: continued...

T(K)	$10^6 \tau$ (s)	$\log v_{\max}$	β	$10^3 \epsilon''_{\max}$	ϵ_{∞}	μ (D)
<u>0.45M 1-bromododecane (polypropylene)(higher temperature process)</u>						
192.0	2355.26	1.83	0.19	20.4		
195.6	1355.53	2.07	0.18	19.6		
199.0	619.50	2.41	0.18	18.5		
202.3	348.37	2.66	0.16	17.8		
206.4	112.73	3.15	0.16	17.4		
210.6	24.66	3.81	0.15	17.2		

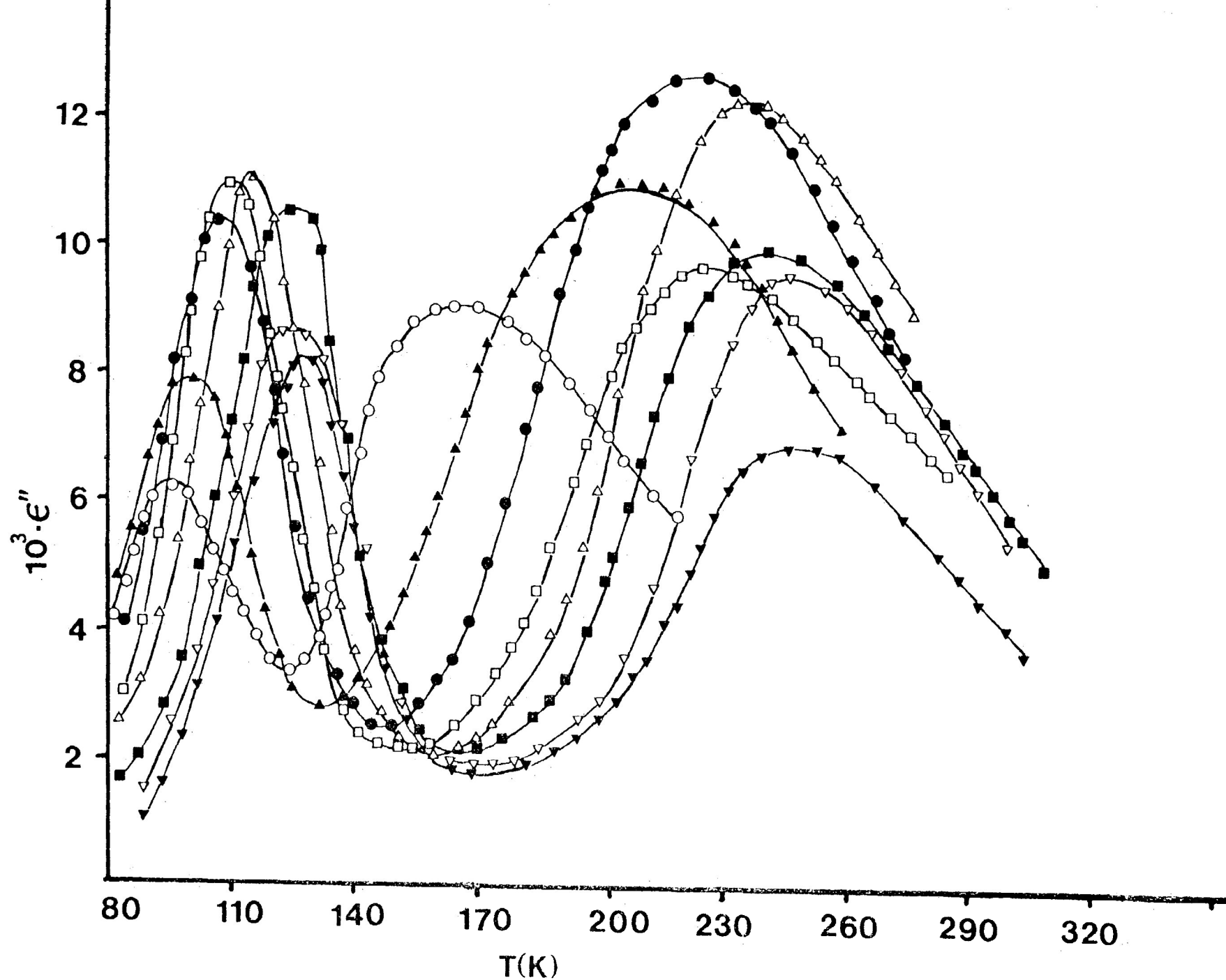


FIGURE V-1: Dielectric loss factor (at 50 Hz) as a function of temperature for 1-bromoalkanes in a polystyrene matrix: \circ $n=4$; \blacktriangle $n=6$; \bullet $n=8$; \square $n=10$; \triangle $n=12$; \blacksquare $n=14$; ∇ $n=16$; \blacktriangledown $n=20$.

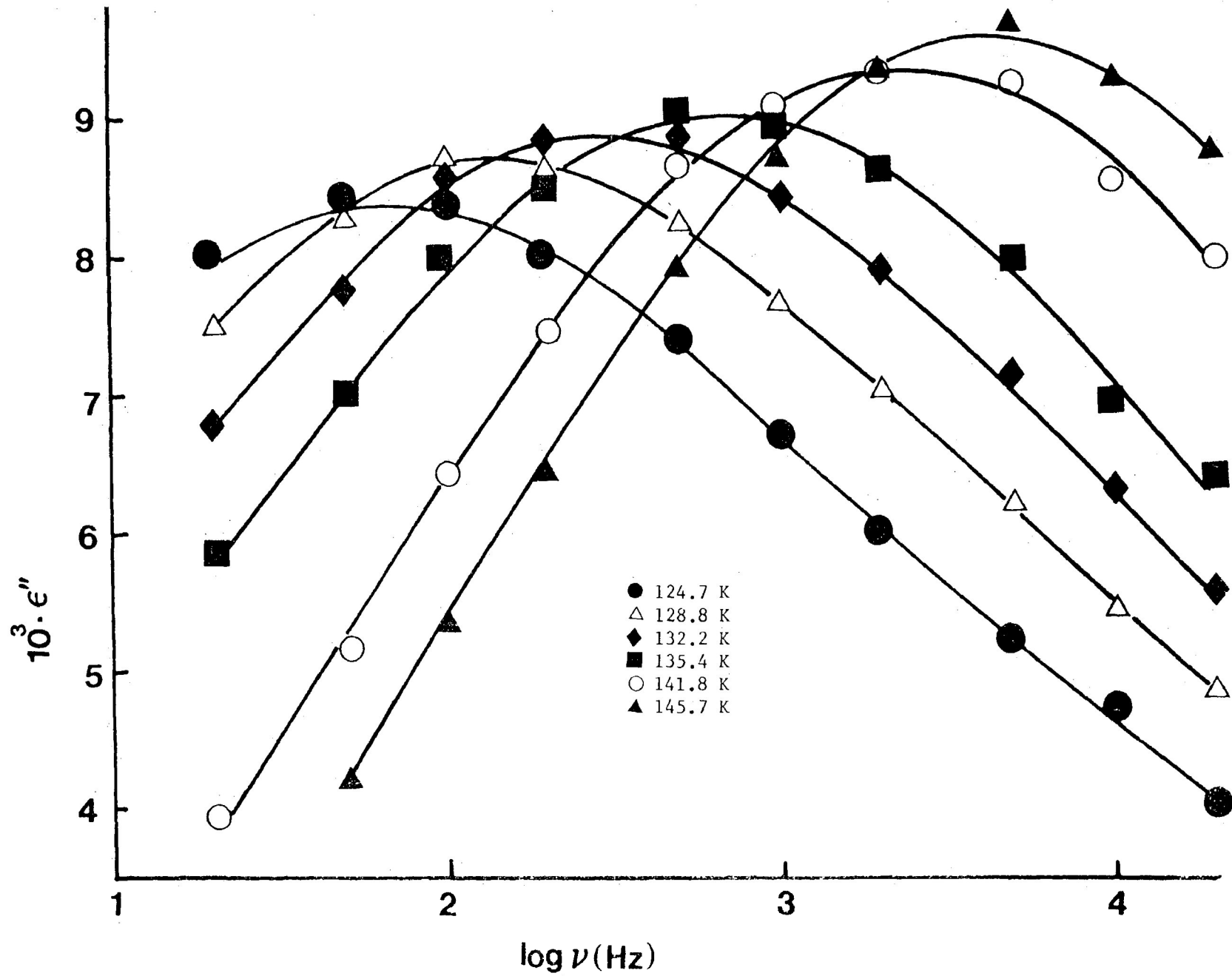


FIGURE V-2: Dielectric absorption for the lower temperature absorption process for 1-bromodocosane in a polystyrene matrix

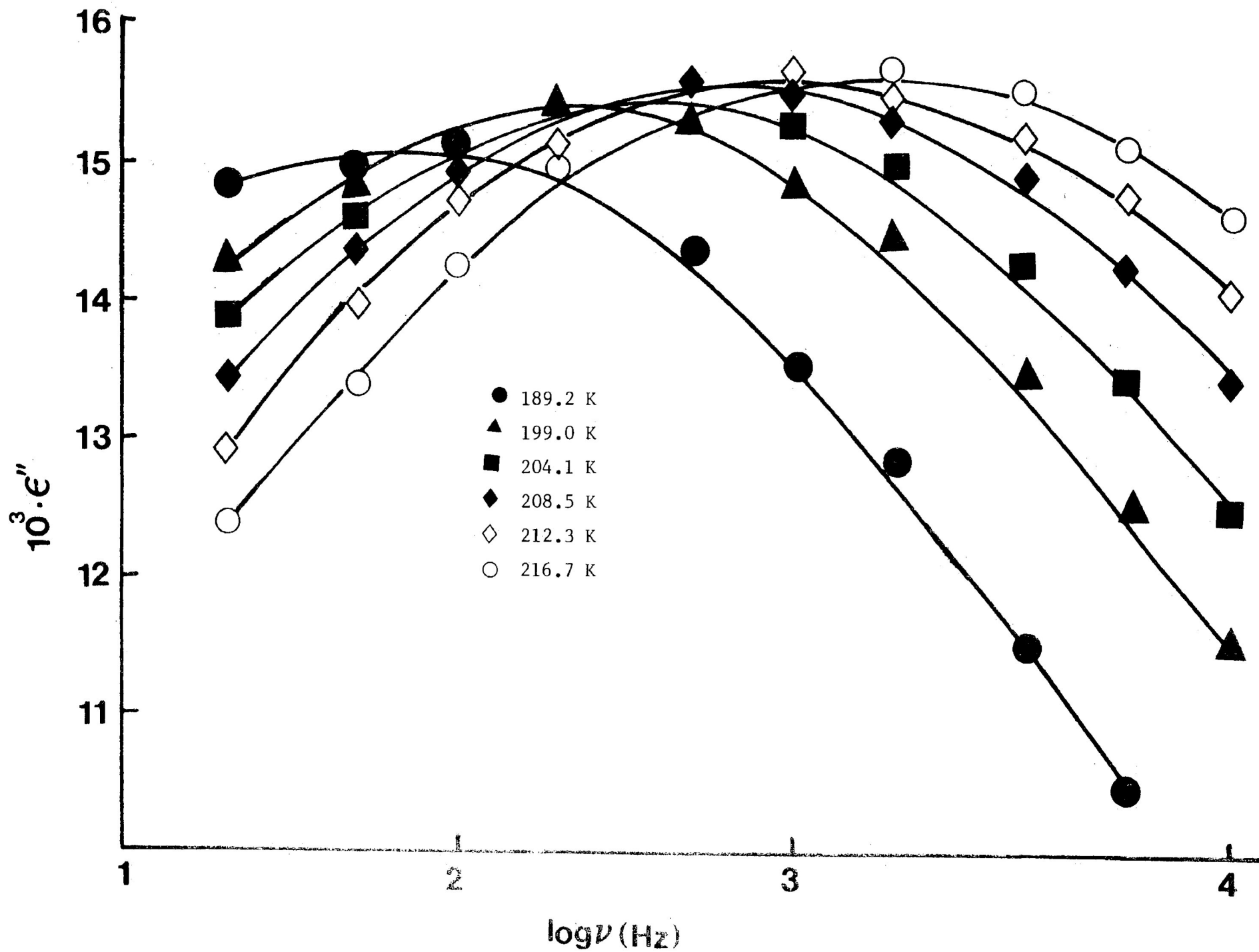
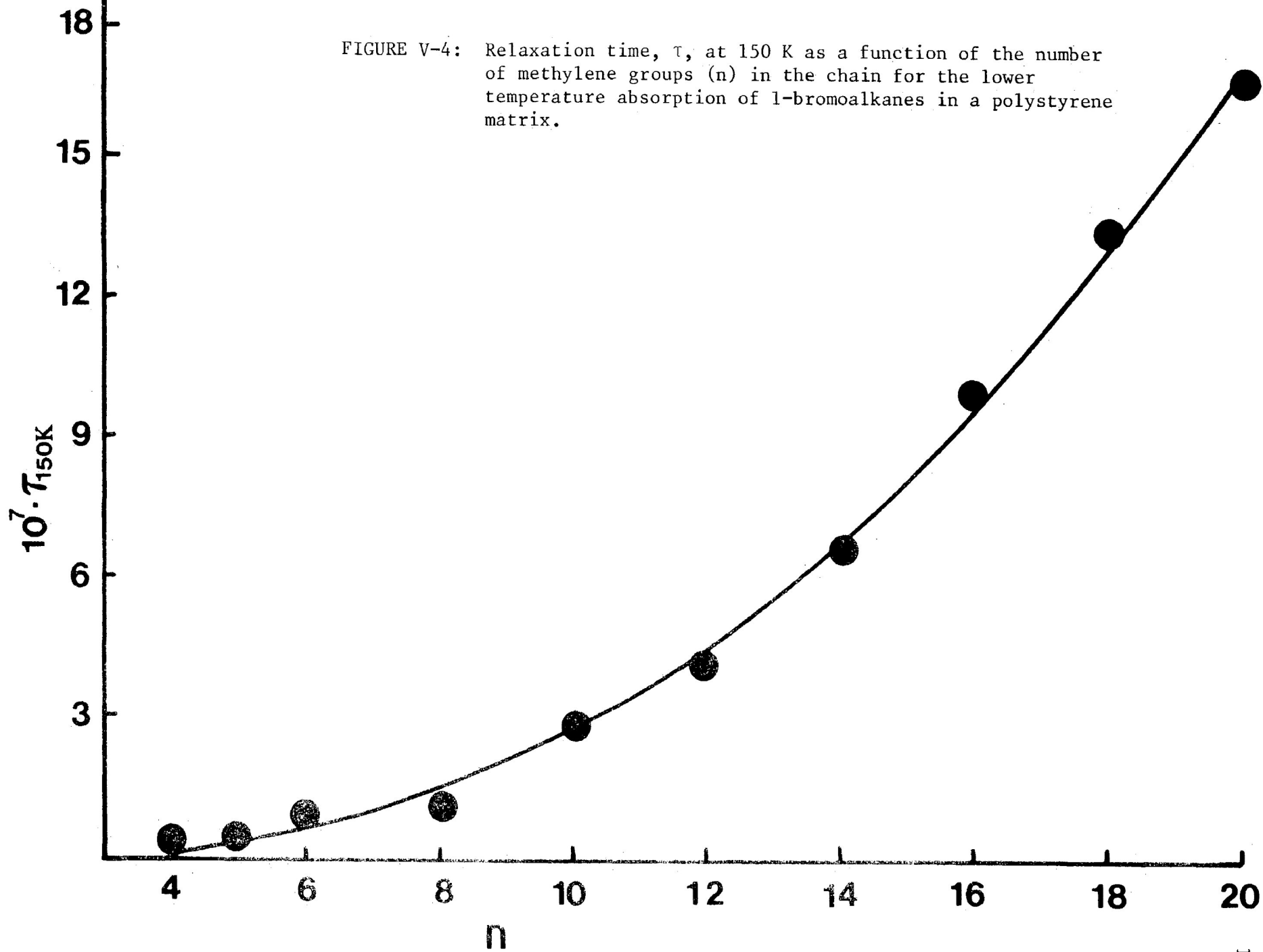


FIGURE V-3: Dielectric absorption for the higher temperature process of 1-bromoheptane in a polystyrene matrix

FIGURE V-4: Relaxation time, τ , at 150 K as a function of the number of methylene groups (n) in the chain for the lower temperature absorption of 1-bromoalkanes in a polystyrene matrix.



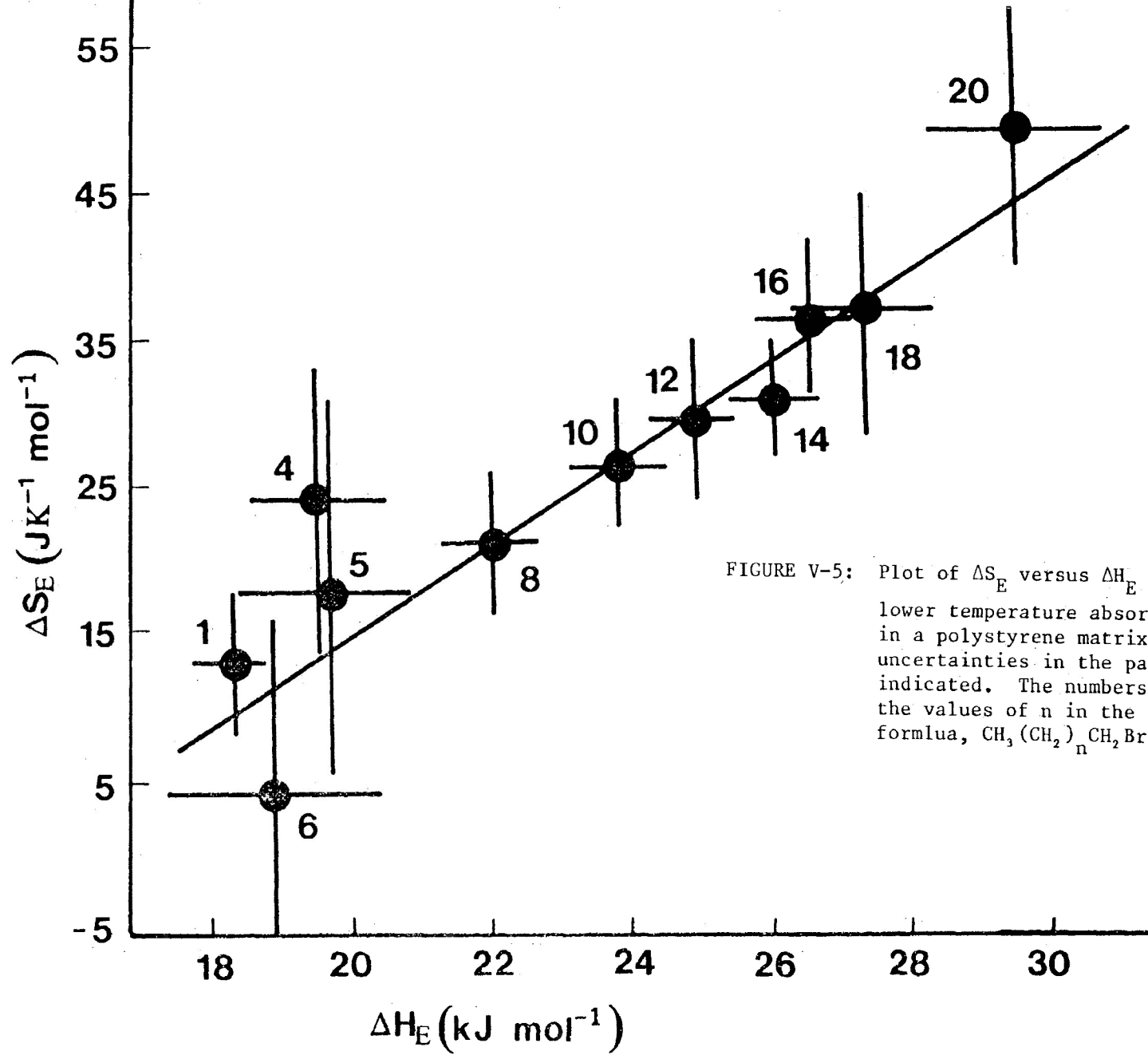
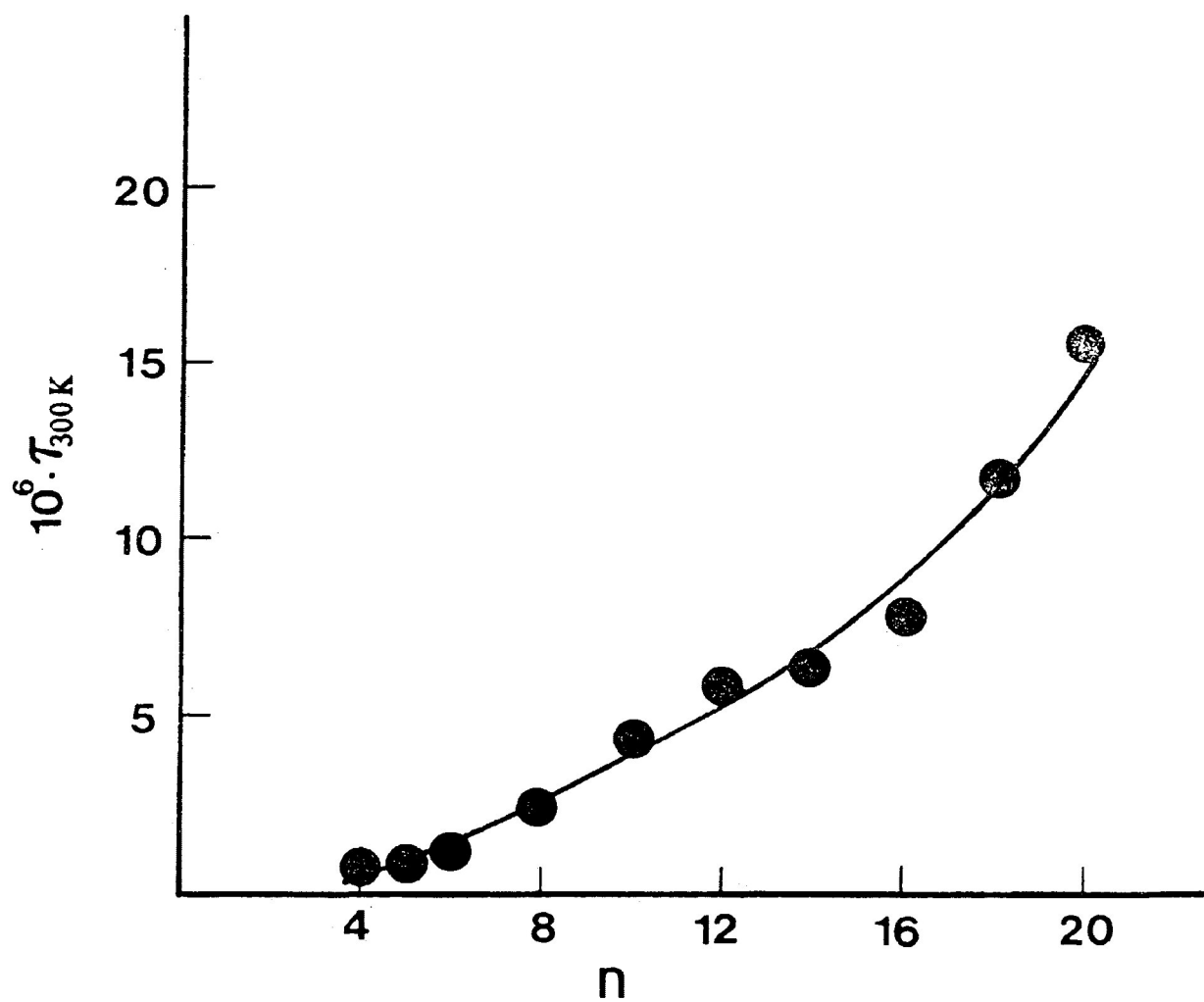


FIGURE V-5: Plot of ΔS_E versus ΔH_E for the lower temperature absorption process in a polystyrene matrix. The uncertainties in the parameters are indicated. The numbers indicate the values of n in the general formula, $\text{CH}_3(\text{CH}_2)_n\text{CH}_2\text{Br}$.

FIGURE V-6: Relaxation time, τ , at 300 K as a function of the number of methylene groups (n) for the higher temperature processes of 1-bromoalkanes in a polystyrene matrix.



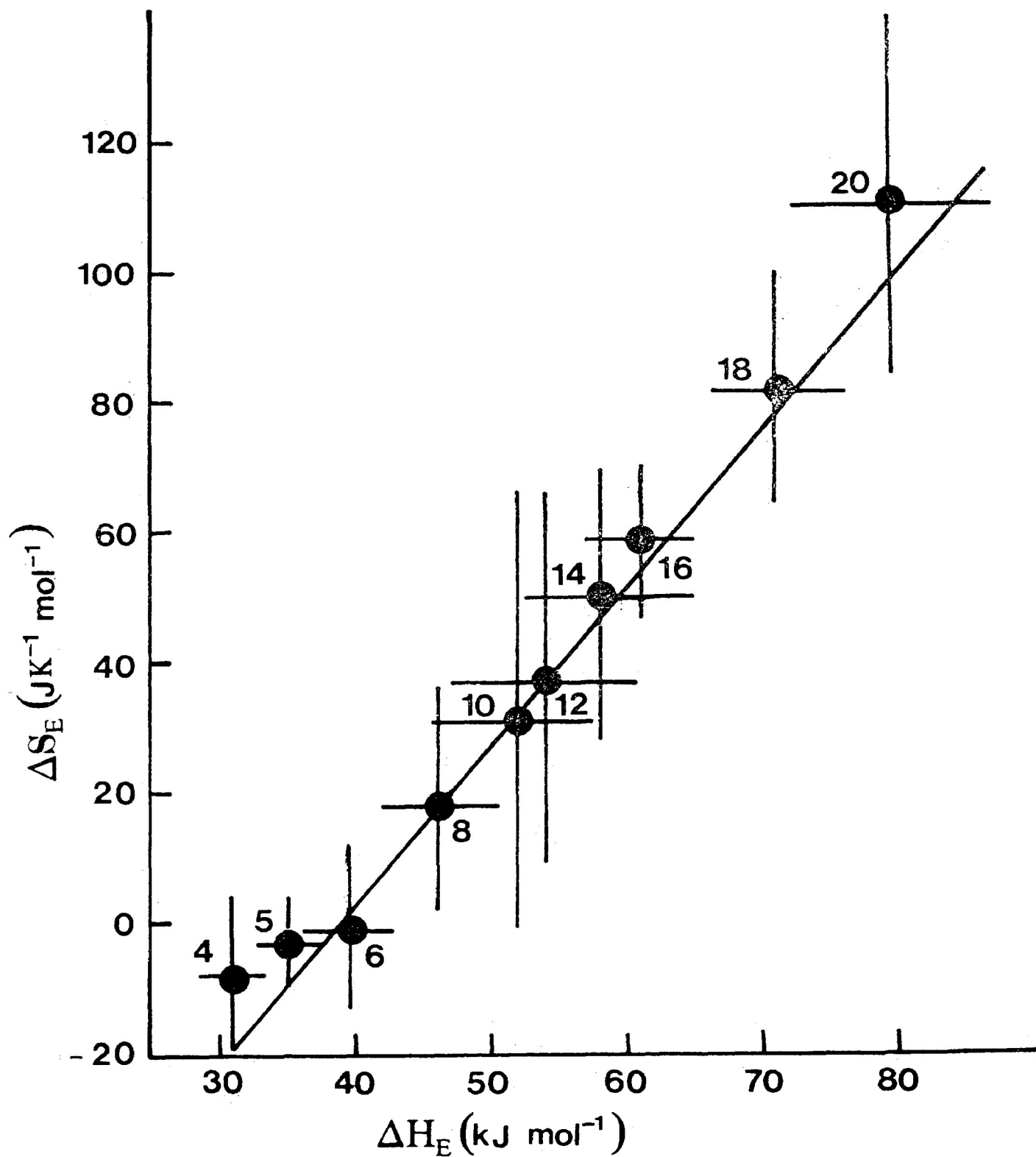


FIGURE V-7: Plot of ΔS_E versus ΔH_E for the higher temperature process of 1-bromoalkanes in a polystyrene matrix. The uncertainties in the factors are indicated.

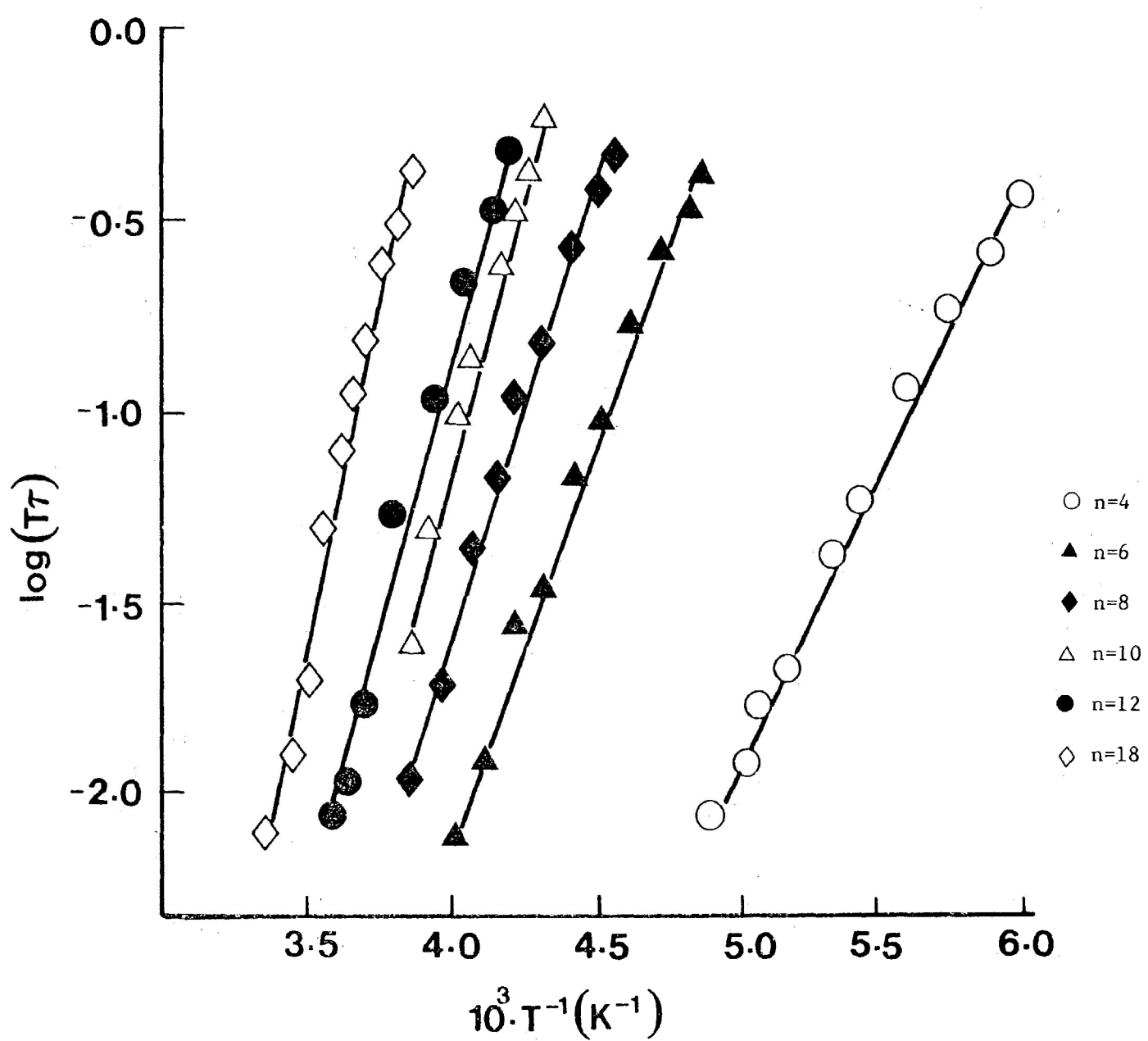


FIGURE V-8: Eyring plots for the higher temperature absorption process of 1-bromoalkanes in a polystyrene matrix

CHAPTER VI

DIELECTRIC STUDIES OF SOME

BROMOSUBSTITUTED ALKANES IN

POLYSTYRENE AND POLYPROPYLENE MATRICES

INTRODUCTION

A detailed dielectric study of 1-bromoalkanes has been presented in Chapter V. In this Chapter we investigate the effect of the variation of the position of dipoles along the hydrocarbon chain. Dielectric studies of the variation of the position of the dipole on relaxation parameters are incomplete in the literature. A few studies may be mentioned of Crossley et al (1) who measured dielectric constants and losses of 1,2, and 4-bromooctanes and 1,10-dibromodecanes in cyclohexane solution at 25°C. They were unable to obtain any sensible Budó analyses of the data in terms of two relaxation times. Their results suggested (a) the polar end group rotation is not a dominant mechanism of dipole reorientation for 1-bromoalkanes as it is for primary amines and 2-alkanones; (b) the mean relaxation time lengthens only slightly with increased molecular size from 1-bromodecane to 1-bromooctadecane; (c) the contribution from intramolecular rotation, especially for the larger molecules, is not negligible; (d) the intramolecular reorientation is dominated by smaller segments which contain CH_2Br ; (e) the relaxation times for 1,10-dibromodecane and 1-bromodecane are almost the same; and (f) the location of the dipole has little effect on the relaxation times for bromooctanes which is also the case

for the nonanones and nonylamines.

Anderson and Smyth (2) have studied the dielectric absorptions of three isomeric dibromobutanes and 1,4-dibromopentane at frequencies of 0.52 MHz, 9.3 GHz and 240 GHz and at 293 K, 310 K and 333 K as pure liquids. They observed that the Cole-Cole distribution parameter, α , was almost zero and the mean relaxation time for three isomeric dibromobutanes were identical within the accuracy of determinations but for 1,4-dibromopentane a "somewhat longer relaxation time than that of dibromobutanes has been found". They suggested that the dielectric absorptions in these molecules could be attributed to the whole molecule rotation and there was no indication of a second relaxation process as evident from zero values of distribution parameter, α .

Garg et al (3) measured the dielectric constants and losses of 1,4-, 1,6- 1,8- and 1,10-dibromoalkanes at frequencies of 9.3 GHz, 24 GHz, 69.8 GHz and 136.4 GHz as pure liquids. Their results could be represented by the Cole-Davidson Skewed-arc plot of dielectric loss against dielectric constant. The mean relaxation time increased with the increase of chain length. An analysis of the data in terms of two superimposed, non-interacting Debye

type absorptions was successful in representing the data by a Cole-Davidson type distribution function. The longer relaxation times, τ_1 , were found to increase with the increase in molecular size and were attributed to overall molecular rotation. The increase in the shorter relaxation times, τ_2 , with increased molecular size is not significant and is ascribed to rotational orientation of the two CH_2Br groups in each molecule.

Chandra and Prakash (4) reported the dielectric absorption studies on 1,3-, 1,4-, 1,5-, and 1,6-dibromoalkane at frequencies 1.8 MHz, 2 GHz, 4 GHz, 22 GHz and 37 GHz and at 303 K, 313 K, 323 K and 333 K as pure liquids. Their results could be equally well represented in terms of (i) the Cole-Davidson representation as a result of intramolecular co-operative relaxation and (ii) superposition of the two non-interacting Debye type absorptions. The longer relaxation time, τ_1 , increases with chain length which suggests that this corresponds to end-over-end rotation of the molecule as a whole. The shorter relaxation time, τ_2 , is found to be independent of the chain length within the experimental uncertainties and ascribed to terminal $-\text{CH}_2\text{Br}$ group rotation about the C-C bond.

It seemed worthwhile to carry out a systematic dielectric study of the variation of position of the dipole along the hydrocarbon chain in a polystyrene matrix with a view to separating the intramolecular processes from the molecular one and characterize by means of its Eyring parameters. Such a separation has been attained in 1-bromoalkanes where the low and high temperature absorptions have been interpreted as segmental reorientation involving the movement of the $-\text{CH}_2\text{Br}$ group whose size increases as n increases and molecular rotation respectively. It was thought that the variation of the location of the dipole along the hydrocarbon chain and the introduction of a second dipole at the end of the chain might produce some alteration in the dielectric behaviour which would facilitate the understanding of the mechanism of dielectric relaxation in long chain bromides.

EXPERIMENTAL RESULTS

The following molecules have been included in the present study.

<u>Number</u>	<u>Molecule</u>
1	2-Bromooctane
2	3-Bromooctane
3	4-Bromooctane
4	1-Bromopentane
5	3-Bromopentane
6	4-Bromoheptane
7	1,6-Dibromohexane
8	1,10-Dibromodecane

All of the compounds were obtained commercially. All of the compounds were measured as polystyrene matrices except 4-bromooctane and 4-bromoheptane which have been studied also in a polypropylene matrix. Tables VI-1 to VI-7 list the relaxation and Eyring parameters, extrapolated dipole moment, loss factors and Fuoss-Kirkwood parameters for all of the systems. Figures VI-1 to VI-17 show the dielectric loss factor, ϵ'' versus temperature plots,

plots of relaxation time versus location of the bromine atom along the n-octane chain, absorption curves and the Cole-Cole plots for some of the systems studied here.

The following symbols are employed:

$\Delta T(K)$	Temperature range in absolute scale
$\Delta \log_{10} \nu_m$	$\log_{10} \nu_m$ range
β -range	Range of variation in the Fuoss-Kirkwood distribution parameter, β
ΔG_E	Eyring free energy
ΔH_E	Eyring enthalpy of activation
ΔS_E	Eyring entropy of activation
$\mu_s(330 \text{ K})$	Extrapolated dipole moment at 330 K for low temperature absorption
$\mu_m(330 \text{ K})$	Extrapolated dipole moment at 330 K for high temperature absorption
μ_{eff}	Effective dipole moment calculated from $\mu_{\text{eff}} = (\mu_m^2 + \mu_s^2)^{\frac{1}{2}}$
μ_{lit}	Literature value of dipole moment usually for a benzene solution at 298 K

DISCUSSION

1, 2, 3 and 4-Bromooctanes

From the Figure VI-1 it is seen that when the dielectric loss, ϵ'' , is plotted against temperature at a fixed frequency, two absorption peaks appear. The absorption peaks that appeared in the temperature range 80 - 160 K and 180 - 250 K are termed as the low and high temperature absorption processes, respectively. It is interesting to note that the low temperature absorption peaks [$\epsilon''_{(\max)L}$] shift to the higher temperature region whereas the high temperature absorption peaks [$\epsilon''_{(\max)H}$] shift to the low temperature region as the bromine atom is moved from terminal carbon atom to a higher carbon number along the n-octane chain.

Figure VI-2 shows that the relaxation time $\tau_{100\text{ K}}$ for the low temperature absorption lengthens as the bromide atom is moved from the terminal carbon atom to higher carbon numbers along the n-octane chain. But the situation is different for the high temperature absorption. The relaxation time $\tau_{200\text{ K}}$ decreases as the bromine atom is moved along the n-octane chain.

The Fuoss-Kirkwood distribution parameters, β , for low temperature absorption, lie in the range 0.17-0.31 (see Table VI-1) at 98-161 K. The half-width, $\Delta T_{\frac{1}{2}}$, for low temperature absorption, is very similar and lies in the range 40-50 K. Such high β -values and short half width suggest that the low temperature absorption is an intramolecular process (see Chapter V). This is borne out by the fact that flexible aromatic molecules undergo intramolecular rotation with typical β -values 0.17-0.34 at 85-157 K (5).

It has been established for 1-bromoalkanes (Chapter V) that the low temperature absorption may be attributed to segmental rotation involving movement of the CH_2Br group. The enthalpy of activation, ΔH_E , increases in the order 18.7, 22.5, 24.9 and 25.9 kJ mol^{-1} when the bromine atom is moved from C-1 to C-2 to C-3 to C-4. The probable reasons for the increase of relaxation time, $\tau_{100 \text{ K}}$, and enthalpy of activation, ΔH_E are that (a) the size of the smallest reorientating unit responsible for low temperature absorption increases as the bromine atom is moved along the n-octane chain and (b) the steric effects increase when the bromine atom is moved from the end of the n-octane chain. With respect to (b), it is noticeable how the largest increase in ΔH_E between consecutive members occurs between

1- and 2-bromooctane in this series (see Table VI-1).

In 1-bromoalkanes, the high temperature absorption has been attributed to molecular rotation. The relaxation time, τ , at 200 K for the high temperature process decreases (though small in magnitude) as the bromine atom is moved along the n-octane chain. We have already established that the τ value increases with the increase in chain length of 1-bromoalkanes for the molecular rotation (Chapter V). It was advanced by Khwaja and Walker (6) for the relaxation of rigid molecules in a polystyrene matrix that the relaxation time increases linearly with the increase of volume swept out on molecular rotation. Thus it is reasonable to assume that the volume swept out on molecular reorientation decreases as the bromine atom is moved along the n-octane chain. In 4-bromooctane in a polystyrene matrix, though the high temperature absorption peak has been detected in the ϵ'' versus T plot (Figure VI-1), loss maxima have not been resolved. in the ϵ'' versus $\log \nu$ plot (Figure VI-3). The probable explanation is that the high temperature process overlapped with the low temperature absorption process. It follows from:

$$\tau = (h/kT) e^{\Delta G/RT}$$

that when two processes possess similar free energy of activation, ΔG_E , then the absorption curves will overlap. In fact, the extrapolated dipole moment, 1.52 D at 330 K for the low temperature absorption of 4-bromooctane (see Table VI-6 does not correspond with the literature value, 1.99 D suggesting another absorption in the high temperature region. To investigate the probable overlap of the two processes further, 4-bromooctane has also been investigated in a polypropylene matrix. The absorption curves are shown in Figure VI-4 and VI-17. In this case the intramolecular process has been completely separated from the molecular one. The enthalpy of activation, ΔH_E , for the low temperature absorption of 4-bromooctane in a polystyrene matrix is 24.9 kJ mol⁻¹ which is in good agreement with 26.1 kJ mol⁻¹ in a polypropylene matrix. The μ_{eff} obtained from the relation, $\mu_{\text{eff}} = (\mu_m^2 + \mu_s^2)^{\frac{1}{2}}$, (see Chapter V for details) for 4-bromooctane in a polypropylene matrix is 1.97 D which is in excellent agreement with the literature value, 1.99 D.

1-Bromoheptane and 4-bromoheptane / 1-bromopentane and 3-bromopentane

Two compounds, 3-bromopentane and 4-bromoheptane, in which the dipole is located at the centre of the chain, have been studied in a polystyrene matrix to investigate

thoroughly the effect of location of the dipole on the relaxation parameters. The absorption curves are given in Figures VI-5 and -6. The figures show that when the bromine atom is at the terminal carbon atom, the intramolecular processes are well separated from the molecular one, but when the dipole is located at the centre of the chain, the contribution of high temperature absorption to the total absorption significantly decreases. For both 3-bromopentane and 4-bromoheptane, a single absorption process has been studied and the loss maximum has not been resolved in the ϵ'' versus $\log \nu$ plot for the high temperature absorption of each of the molecules. The asymmetric loss curves for 3-bromopentane (Figure VI-5) and 4-bromoheptane (Figure-8) indicate that the low and high temperature processes merged. This is borne out by the fact that the extrapolated dipole moments, 0.85 and 1.52 D at 330 K for the single absorption process of 3-bromopentane and 4-bromoheptane in a polystyrene matrix, do not agree with the literature values, 2.09 and 2.02 D, respectively. 4-Bromoheptane has also been investigated in a polypropylene matrix. In this case the intramolecular process has been separated from the molecular one (Figure VI-9) and the μ_{eff} value, 1.90 D for 4-bromoheptane in a polypropylene matrix is in reasonable agreement with the literature value, 2.02 D (see Table VI-6).

The ΔH_E value for the molecular rotation of 1-bromoheptane ($\Delta H_E = 35.4 \text{ kJ mol}^{-1}$) in a polystyrene matrix is very close to that of 4-bromoheptane ($\Delta H_E = 33.5 \text{ kJ mol}^{-1}$) in a polypropylene matrix. This fact strongly supports the view that when the dipole moves away from the terminal carbon atom, the volume swept out on molecular reorientation becomes less and this is least when the bromine atom is located at the centre of the chain.

On closer examination of the loss factors presented in Table VI-5 several striking and interesting points can be made. First, the location of the dipole away from the n-octane chain end has negligible influence on the contribution of intramolecular and molecular processes to the total absorption and the contribution of the two processes to the total absorption is almost similar. The second point to be made is that the contribution of molecular rotation to the total absorption decreases significantly when the dipole is located at the centre of the chain.

Thus, our results show that the intramolecular process in 1, 2, and 3-bromooctanes, 1-bromopentane and 1-bromoheptane has been separated from the molecular one. 4-Bromooctane and 4-bromoheptane give clear separation of an intramolecular process from the molecular one in a polypropylene

matrix. Earlier investigations (1) could neither account for the increase of relaxation time for the low temperature absorption nor for the decrease of relaxation time for the high temperature absorption when the bromine atom is moved along the n-octane chain.

α,ω -Dibromoalkanes

1-6-Dibromohexane and 1,10-dibromodecane have also been studied in a polystyrene matrix to investigate the mechanism of dipole reorientation where the two dipoles are located at the terminal carbon atoms.

The absorption curves are shown in Figure VI-10 and Figure VI-11. The Cole-Cole plots for the low and high temperature absorption of 1,6-dibromohexane are given in Figures VI-12 and -13. the Cole-Cole plots being adequately represented by the depressed centre semicircular arc.

The ΔH_E value and relaxation time for the low temperature absorption of 1,6-dibromohexane are 21.4 kJ mol^{-1} and $3.6 \times 10^{-4} \text{ s}$ at 100 K, respectively. This ΔH_E value is slightly greater, and the relaxation time at 100 K slightly longer than that of 1-bromohexane. An examination of Table VI-5 will reveal that the maximum loss factors for the

high temperature absorption of 3-bromooctane and 1,6-dibromohexane in a polystyrene matrix is the same whereas the loss factor in 1,6-dibromohexane for the low temperature absorption approximately doubles the one in 3-bromooctane. This is due to the fact that when the number of $-\text{CH}_2\text{Br}$ groups is doubled, then the absorption doubles. In 1-bromoalkanes the low temperature absorption has been attributed to the segmental rotation involving the movement of the $-\text{CH}_2\text{Br}$ group.

Thus, it is reasonable to attribute low temperature absorption of 1,6-dibromohexane to rotational orientation of both ends involving the movement of $-\text{CH}_2\text{Br}$ groups. The ΔH_E values for the high temperature absorption of 1,6-dibromohexane is 32.1 kJ mol^{-1} which is in excellent agreement with 31.5 kJ mol^{-1} for the high temperature absorption of 1-bromohexane. This bears out that we are dealing with a molecular process of the same size in each of the two cases.

Table VI-5 shows that in 1,10-dibromodecane, the ϵ''_{max} of the intramolecular absorption approximately doubles the one for 1-bromodecane in a polystyrene matrix. The relaxation times at 150 K and ΔH_E for 1,10-dibromodecane are $1.2 \times 10^{-6} \text{ s}$ and 22.0 kJ mol^{-1} , respectively. This relaxation time is 10 times longer and the ΔH_E value is

slightly higher than that of 1-bromodecane. Thus, the low temperature absorption in 1,10-dibromodecane may be attributed to rotational reorientation of both ends involving the movement of the $-\text{CH}_2\text{Br}$ groups.

Altogether, the present work for the α,ω -dibromoalkanes in a viscous media bears out what was previously inferred by Garg et al (3) and Chandra et al (4) for the dielectric absorption of α,ω -dibromoalkanes as pure liquids. The conclusions differ, however, in that the low temperature absorption is a segmental reorientation involving rotation about the C-C bond and consequent movement of $-\text{CH}_2\text{Br}$ group and the size is not limited to $-\text{CH}_2\text{Br}$, also the relaxation time increases significantly with the increase of chain length while the plot of dielectric loss against dielectric permittivities does not show any asymmetry in either of the processes.

Our results are in disagreement with Crossley et al (1) who concluded that the dielectric relaxation in 1,10-dibromodecane is dominated by $-\text{CH}_2\text{Br}$ group rotation.

Our findings are not in agreement with Anderson et al (2) who concluded that the dipole reorientation in α,ω -dibromoalkanes is dominated by whole molecule rotation

and there was no indication of a second relaxation process. In the glassy media, however, the intramolecular process has been completely separated from the molecular one and characterized by means of its Eyring parameters whereas the work in the microwave region has led to mean relaxation times resulting from the overlap of molecular and intramolecular processes.

CONCLUSION

In most of the bromoalkanes studied the intramolecular process has been completely separated from the molecular ones in a polystyrene matrix. Polypropylene matrix seemed to be an effective medium for the separation of the intramolecular process from the molecular one in the case where the dipole is located near the centre of the chain.

The dielectric behaviour can be summarized as follows:

- (1) The increase of relaxation time for the low temperature absorption when the bromine atom is moved along the n-octane chain could be attributed to (a) the increase in the size of the reorientating unit and (b) the steric effects.
- (2) The decrease in volume swept out on molecular rotation accounts for the decrease in relaxation time at 200 K for the high temperature absorption when the bromine atom is moved along the n-octane chain.
- (3) The results of α,ω -dibromoalkanes bear out that (i) we are dealing with a molecular and intramolecular process,

(ii) both ends of the chain rotate involving $-\text{CH}_2\text{Br}$ groups, (iii) the α,ω -dibromoalkanes and 1-bromoalkanes for a given total number of carbon atoms sweep out similar volumes and have identical ΔH_E values and (iv) molecules with two $-\text{CH}_2\text{Br}$ groups have approximately double the ϵ''_{max} for the intramolecular absorption.

REFERENCES

1. S. P. Tay and J. Crossley, Can. J. Chem. 51(1972) 2549.
2. J. E. Anderson and C. P. Smyth, J. Phys. Chem., 77(1973)230.
3. S. K. Garg, W. S. Lovell, C. J. Clemett and C. P. Smyth. J. Phys. Chem. 77(1973)232.
4. S. Chandra and J. Prakash, J. Chem. Phys., 54(1971)5366.
5. J. Chao, M. A. Desando, D. L. Gourlay, D. E. Orr, and S. Walker. J. Phys. Chem., 88(1984)711.
6. H. A. Khwaja and S. Walker. Adv. Mol. Int. and Relax. Process. 19(1981)1.

TABLE VI-1: Eyring parameters for the low temperature absorption of bromooctanes

Molecule	ΔT (°K)	Medium	ϵ range	Relaxation Times τ (s)		ΔG_E (kJ mol ⁻¹)		ΔH_E	ΔS_E
				100 K	150 K	100 K	150 K	kJ mol ⁻¹	J K ⁻¹ mol ⁻¹
1-bromooctane	98-124	P.S.	0.25-0.31	1.68×10^{-3}	6.23×10^{-7}	18.3	18.1	18.7±1.3	4±12
2-bromooctane	108-130	P.S.	0.17-0.21	2.48×10^{-2}	1.99×10^{-6}	20.5	19.5	22.5±2.5	20±22
3-bromooctane	122-152	P.S.	0.18-0.30	1.25×10^0	3.76×10^{-5}	23.8	23.2	25.0±1.2	12±9
4-bromooctane	127-161	P.S.	0.20-0.27	3.68×10^0	7.04×10^{-5}	24.7	24.0	26.1±1.1	14±8
4-bromooctane	122-142	P.P.	0.23-0.30	8.22×10^{-1}	2.52×10^{-5}	23.4	22.8	24.9±1.5	15±11

TABLE VI-2:

Eyring parameters for the high temperature absorption of bromooctanes

Molecule	ΔT (°K)	Medium	β range	Relaxation Times τ (s)		ΔG_E (kJ mol ⁻¹)	ΔH_E kJ mol ⁻¹	ΔS_E J K ⁻¹ mol ⁻¹
				200 K	200 K			
1-bromooctane	205-249	P.S.	0.18-0.16	5.02×10^{-3}		39.5	39.3±3.3	-2±14
2-bromooctane	199-238	P.S.	0.14-0.16	3.56×10^{-3}		38.9	41.5±2.3	13±11
3-bromooctane	192-216	P.S.	0.12-0.16	1.01×10^{-3}		36.9	33.5±3.4	-17±17
4-bromooctane	185-213	P.P.	0.18-0.27	7.89×10^{-5}		32.6	42.2±3.6	48±18

TABLE VI-3: Eyring activation parameters for some bromopentanes and bromoheptanes in a polystyrene matrix

Molecule	$\Delta T(^{\circ}K)$	Medium	β -range	Relaxation Time $\tau(s)$			ΔG_E ($kJ\ mol^{-1}$)			ΔH_E $kJ\ mol^{-1}$	ΔS_E $J\ K^{-1}\ mol^{-1}$
				100 K	150 K	200 K	100 K	150 K	200 K		
1-bromoheptane	96-116	P.S.	0.22-0.27	1.10×10^{-3}	2.83×10^{-7}		17.9	17.1		19.6 ± 1.4	17 ± 13
1-bromoheptane	189-213	P.S.	0.15-0.20			6.05×10^{-4}			36.0	35.4 ± 2.8	-3 ± 7
4-bromoheptane	125-153	P.S.	0.22-0.25	2.42×10^0	5.38×10^{-5}		24.3	23.6		25.7 ± 0.9	14 ± 7
4-bromoheptane	119-138	P.P.	0.25-0.29	1.15×10^{-1}	2.45×10^{-5}		21.8	22.6		20.1 ± 0.7	-17 ± 5
4-bromoheptane	217-238	P.P.	0.15-0.22			1.41×10^{-2}			41.2	33.5 ± 3.8	-39 ± 17
1-bromopentane	95-106	P.S.	0.18-0.26	7.17×10^{-4}	7.28×10^{-7}		17.7	18.3		16.2 ± 1.6	-14 ± 16
3-bromopentane	122-139	P.S.	0.27-0.32	4.25×10^{-1}	1.14×10^{-5}		22.9	21.7		25.3 ± 1.7	24 ± 13
1-bromopentane	142-162	P.S.	0.11-0.15	8.50×10^0	4.38×10^{-4}		25.4	26.2		23.6 ± 1.8	-18 ± 12

TABLE VI:4 Comparison of Eyring activation parameters for 1-bromoalkanes and α,ω -dibromoalkanes in a polystyrene matrix

Molecule	$\Delta T(^{\circ}K)$	Medium	β -range	Relaxation Time τ (s)			ΔG_E (kJ mol ⁻¹)			ΔH_E kJ mol ⁻¹	ΔS_E J K ⁻¹ mol ⁻¹
				100 K	150 K	200 K	100 K	150 K	200 K		
1,6-dibromohexane	104-107	P.S.	0.25-0.32	9.69×10^{-3}	1.23×10^{-6}		19.7	18.9		21.4 \pm 0.6	16 \pm 5
1,6-dibromohexane	223-244	P.S.	0.10-0.16			1.53×10^{-2}			42.5	32.1 \pm 4.6	-46 \pm 20
1-bromohexane	95-117	P.S.	0.18-0.23	3.66×10^{-4}	1.00×10^{-7}		17.0	15.8		19.5 \pm 1.0	24 \pm 10
1-bromohexane	168-204	P.S.	0.16-0.17			6.60×10^{-5}			32.3	31.5 \pm 2.0	-4 \pm 11
1,10-dibromo- decane	113-138	P.S.	0.24-0.32	1.18×10^{-1}	4.33×10^{-6}		21.8	20.1		24.5 \pm 0.4	27 \pm 3
1,10-dibromo- decane	244-268	P.S.	0.20-0.24			3.16×10^{-1}			46.4	46.4 \pm 3.8	0 \pm 15
1-bromo- decane	106-130	P.S.	0.26-0.32	1.15×10^{-2}	1.13×10^{-6}		18.8	17.7		22.0 \pm 0.6	21 \pm 5
1-bromo- decane	220-260	P.S.	0.16-0.19			4.14×10^{-2}			43.0	46.9 \pm 4.5	19 \pm 19

TABLE VI-5: Maximum loss factors for some molecules in polystyrene and polypropylene at 50.2 Hz

Molecule	$\epsilon''_{\max(L)}$	$\epsilon''_{\max(H)}$
1-bromooctane	7.9×10^{-3}	11.0×10^{-3}
2-bromooctane	12.0×10^{-3}	11.0×10^{-3}
3-bromooctane	10.0×10^{-3}	7.0×10^{-3}
4-bromooctane	8.0×10^{-3}	9.2×10^{-3}
4-bromooctane (PP)	1.8×10^{-3}	1.3×10^{-3}
1-bromoheptane	10.0×10^{-3}	15.2×10^{-3}
4-bromoheptane	10.0×10^{-3}	5.1×10^{-3}
1-bromopentane	7.9×10^{-3}	8.0×10^{-3}
3-bromopentane	15.0×10^{-3}	1.3×10^{-3}
1-bromohexane	6.3×10^{-3}	8.9×10^{-3}
1,6-dibromohexane	21.0×10^{-3}	7.0×10^{-3}
1-bromodecane	12.9×10^{-3}	10.5×10^{-3}
1,10-dibromodecane	20.0×10^{-3}	5.0×10^{-3}

TABLE VI-6: μ_s and μ_m are extrapolated dipole moments at 330 K and μ_{eff} from $\mu_{\text{eff}} = (\mu_s^2 + \mu_m^2)^{\frac{1}{2}}$

Molecule	μ_s 330 (D)	μ_m 330 (D)	μ_{eff} (D)	$\mu_{\text{lit.}}$ (D)
1-bromooctane	1.2 ₅	1.4 ₆	1.9 ₂	1.99
2-bromooctane	1.3 ₁	1.2 ₉	1.8 ₄	
3-bromooctane	1.5 ₂	1.1 ₂	1.8 ₉	
4-bromooctane	1.5 ₂	-	-	
4-bromooctane (PP)	1.4 ₀	1.3 ₉	1.9 ₇	
1-bromopentane	1.3 ₁	1.4 ₁	1.9 ₂	2.09
3-bromopentane	0.8 ₅	-	-	
1-bromoheptane	1.1 ₈	1.5 ₉	1.9 ₂	2.02
4-bromoheptane	1.5 ₅	-	-	
4-bromoheptane (PP)	1.2 ₉	1.3 ₉	1.9 ₀	2.06
1,6-dibromohexane	1.9 ₀	1.4 ₃	2.3 ₈	2.40
1,10-dibromodecane	2.1 ₀	1.4 ₄	2.5 ₅	2.62

TABLE VI-7: Fuoss-Kirkwood parameters, ϵ_{∞} and μ at various temperatures for some bromoalkanes in a polystyrene and polypropylene matrix

T (K)	$10^6 \tau$ (s)	$\log v_{\max}$	β	$10^3 \epsilon''_{\max}$	ϵ_{∞}	μ (D)
0.44 M 2-Bromooctane (lower temperature process)						
108.6	2233.42	1.85	0.18	10.9	2.834	0.76
110.0	1798.02	1.95	0.18	11.1	2.833	0.78
115.6	619.12	2.40	0.18	11.7	2.826	0.84
118.6	366.70	2.64	0.17	12.0	2.821	0.88
122.4	148.45	3.03	0.17	12.5	2.816	0.91
125.5	78.12	3.31	0.17	12.7	2.814	0.92
129.4	33.32	3.68	0.20	13.2	2.820	0.88
0.44 M 2-Bromooctane (higher temperature process)						
199.7	4089.40	1.60	0.14	11.2	2.941	1.18
201.4	2527.06	1.80	0.15	11.2	2.944	1.14
204.1	1917.73	1.92	0.16	11.2	2.946	1.13
207.7	1327.63	2.08	0.16	11.3	2.953	1.14
213.2	731.66	2.34	0.16	11.3	2.941	1.16
218.3	418.14	2.58	0.16	11.3	2.943	1.17
223.6	268.53	2.77	0.16	11.2	2.941	1.19
228.4	141.82	3.05	0.15	11.1	2.934	1.24
234.4	75.05	3.33	0.14	11.1	2.963	1.27
238.0	44.87	3.55	0.14	11.1	2.926	1.30
0.56 M 3-Bromooctane (lower temperature process)						
122.2	4979.73	1.51	0.19	11.80	2.844	0.75
124.0	2328.71	1.83	0.21	12.02	2.858	0.73
128.4	1211.10	2.12	0.23	12.32	2.844	0.71
131.4	687.21	2.36	0.24	12.52	2.814	0.70
133.0	409.83	2.59	0.26	12.17	2.851	0.68
136.7	257.05	2.79	0.28	13.00	2.849	0.68
139.5	178.77	2.95	0.29	13.16	2.832	0.68
144.6	86.49	3.26	0.29	13.48	2.848	0.70
147.7	51.53	3.49	0.29	13.82	2.846	0.71
151.3	32.57	3.69	0.29	14.08	2.843	0.74

TABLE VI-7: continued...

T(K)	$10^6 \tau$ (s)	$\log v_{\max}$	β	$10^3 \epsilon''_{\max}$	ϵ_{∞}	μ (D)
<u>0.56 M 3-Bromooctane (lower temperature process)</u>						
122.2	4979.73	1.51	0.19	11.80	2.844	0.75
124.0	2328.71	1.83	0.21	12.02	2.858	0.73
128.4	1211.10	2.12	0.23	12.32	2.844	0.71
131.4	687.21	2.36	0.24	12.52	2.814	0.70
133.0	409.83	2.59	0.26	12.17	2.851	0.68
136.7	257.05	2.79	0.28	13.00	2.849	0.68
139.5	178.77	2.95	0.29	13.16	2.832	0.68
144.6	86.49	3.26	0.29	13.48	2.848	0.70
147.7	51.53	3.49	0.29	13.82	2.846	0.71
151.3	32.57	3.69	0.29	14.08	2.843	0.74
<u>0.56 M 3-Bromooctane (higher temperature process)</u>						
192.6	2379.30	1.82	0.14	8.76	2.891	0.93
194.9	1651.10	1.98	0.15	8.78	2.893	0.88
196.9	1477.81	2.03	0.15	8.82	2.800	0.91
199.8	1147.01	2.14	0.15	8.82	2.891	0.91
202.6	769.41	2.32	0.15	8.82	2.880	0.93
205.3	520.83	2.48	0.15	8.84	2.890	0.93
208.8	376.61	2.63	0.15	8.85	2.890	0.93
211.9	297.84	2.73	0.16	8.86	2.889	0.92
216.0	240.23	2.82	0.16	8.82	2.891	0.93
<u>0.36 M 4-Bromooctane in Polystyrene</u>						
128.0	2875.38	1.74	0.24	9.4	3.045	0.73
129.4	2106.92	1.88	0.27	9.6	3.047	0.70
132.0	1290.79	2.09	0.23	10.0	3.039	0.77
136.4	659.91	2.38	0.24	10.4	3.03	0.78
140.4	325.36	2.69	0.25	11.0	3.037	0.81
144.1	193.76	2.91	0.24	11.3	3.038	0.85
147.4	118.03	3.13	0.23	11.8	3.027	0.89
150.0	62.89	3.40	0.25	12.3	3.026	0.89
154.5	35.52	3.65	0.25	12.8	3.025	0.91
159.3	17.74	3.95	0.23	13.4	3.019	1.00

TABLE VI-7: continued...

T(K)	$10^6 \tau$ (s)	$\log v_{\max}$	β	$10^3 \epsilon''_{\max}$	ϵ_{∞}	μ (D)
<u>0.22 M 4-Bromooctane in polypropylene (lower temperature process)</u>						
122.1	3144.72	1.70	0.23	1.7	2.311	0.46
123.0	2012.18	1.90	0.23	1.8	2.309	0.48
127.0	1018.75	2.19	0.25	1.8	2.311	0.47
129.3	667.92	2.38	0.27	1.9	2.310	0.47
132.6	379.04	2.62	0.28	1.9	2.310	0.46
136.0	241.94	2.81	0.29	1.9	2.310	0.45
138.0	140.62	3.05	0.29	2.0	2.309	0.48
142.2	81.26	3.29	0.29	2.0	2.308	0.49
<u>0.22 M 4-Bromooctane in polypropylene (higher temperature process)</u>						
185.5	717.85	2.34	0.21	1.61	2.309	0.58
189.1	316.07	2.70	0.26	1.60	2.388	0.53
193.5	178.79	2.94	0.23	1.59	2.309	0.57
199.2	81.15	3.29	0.21	1.59	2.307	0.60
204.3	42.97	3.56	0.19	1.58	2.306	0.63
208.3	29.09	3.74	0.19	1.57	2.306	0.64
212.3	17.55	3.96	0.18	1.57	2.305	0.66
<u>0.54 M 1-Bromopentane (lower temperature process)</u>						
95.3	1821.81	1.94	0.20	9.7	2.764	0.60
96.4	1467.34	2.03	0.20	9.9	2.762	0.62
97.5	1292.77	2.09	0.23	10.9	2.767	0.60
100.0	712.57	2.54	0.18	10.3	2.749	0.67
102.7	428.18	2.57	0.18	10.6	2.757	0.69
106.0	215.06	2.87	0.19	10.8	2.791	0.69
<u>0.54 M 1-Bromopentane (higher temperature process)</u>						
142.7	1225.64	2.11	0.14	13.6	2.776	1.02
143.6	1054.31	2.18	0.11	13.8	2.75	1.16
147.4	622.07	2.41	0.13	14.0	2.761	1.12
150.7	390.86	2.61	0.14	14.2	2.766	1.10
151.0	301.77	2.72	0.14	14.4	2.766	1.10
155.4	229.01	2.84	0.14	14.5	2.766	1.12
161.2	109.76	3.16	0.13	14.7	2.752	1.15

TABLE VI-7: continued...

T(K)	$10^6 \tau$ (s)	$\log v_{\max}$	β	$10^3 \epsilon''_{\max}$	ϵ_{∞}	μ (D)
<u>0.34 M 3-Bromopentane (lower temperature process)</u>						
122.0	1387.80	2.06	0.24	15.84	2.733	1.01
124.7	843.57	2.28	0.26	15.89	2.740	0.97
127.5	480.39	2.52	0.31	16.00	2.747	0.91
129.5	329.88	2.68	0.32	15.87	2.748	0.90
132.2	215.86	2.87	0.36	16.05	2.754	0.86
135.0	111.14	3.16	0.35	16.05	2.641	0.90
138.2	67.67	3.37	0.37	16.02	2.748	0.87
<u>0.21 M 4-Bromoheptane in polypropylene (lower temperature process)</u>						
119.5	1854.43	1.93	0.25	4.9	2.471	0.74
122.2	1106.68	2.16	0.27	5.0	4.475	0.73
125.0	755.72	2.32	0.27	5.1	2.468	0.74
127.6	474.67	2.53	0.29	5.3	2.461	0.74
130.4	314.88	2.70	0.29	5.3	2.463	0.75
133.1	212.47	2.87	0.29	5.4	2.461	0.76
137.1	118.51	3.13	0.28	5.5	2.457	0.79
<u>0.21 M 4-Bromoheptane in polypropylene (higher temperature process)</u>						
217.4	2866.30	1.75	0.21	2.8	2.459	0.82
219.7	1983.91	1.90	0.18	2.6	2.457	0.86
223.0	1443.40	2.04	0.18	2.6	2.560	0.87
226.4	1200.71	2.12	0.18	2.6	2.455	0.88
232.0	689.62	2.36	0.17	2.6	2.452	0.91
235.5	580.16	2.44	0.17	2.6	2.451	0.92
238.0	454.77	2.54	0.14	2.5	2.446	1.00

TABLE VI-7: continued...

T(K)	$10^6 \tau$ (s)	$\log v_{\max}$	β	$10^3 \epsilon''_{\max}$	ϵ_{∞}	μ (D)
<u>0.21 M 4-Bromoheptane (lower temperature process)</u>						
125.6	3680.95	1.63	0.22	8.6	2.868	0.98
128.2	1819.57	1.94	0.24	8.9	2.570	0.96
131.5	1088.60	2.16	0.24	9.1	2.869	0.98
134.4	681.70	2.38	0.25	9.3	2.868	0.99
138.4	341.49	2.67	0.24	9.5	2.865	1.02
140.0	212.41	2.87	0.24	9.7	2.864	1.05
144.5	122.02	3.11	0.24	9.9	2.861	1.08
148.6	68.49	3.37	0.24	10.1	2.858	1.11
152.7	33.61	3.67	0.22	10.4	2.852	1.18
<u>0.51 M 1,6-dibromohexane (lower temperature process)</u>						
104.5	2859.90	1.75	0.25	19.9	2.915	0.80
106.7	1728.23	1.96	0.25	20.4	2.910	0.81
109.1	1077.43	2.17	0.25	20.8	2.912	0.82
113.1	433.96	2.56	0.26	21.5	2.910	0.86
117.0	211.32	2.88	0.27	22.1	2.908	0.86
120.3	99.51	3.20	0.28	22.5	2.907	0.87
123.6	55.40	3.46	0.30	23.1	2.910	0.86
127.6	28.71	3.75	0.31	23.6	2.909	0.87
<u>0.51 M 1,6-dibromohexane (higher temperature process)</u>						
223.3	1793.49	1.95	0.16	7.1	3.041	0.86
225.0	1527.84	2.02	0.15	7.2	3.039	0.90
229.3	1281.00	2.12	0.16	7.2	3.040	0.88
232.2	925.49	2.23	0.14	7.2	3.033	0.94
243.8	381.71	2.62	0.12	7.1	3.023	1.04
<u>0.39 M 1,10-dibromodecane (lower temperature process)</u>						
113.0	3588.14	1.65	0.25	19.6	2.847	0.95
114.6	2267.66	1.85	0.26	20.0	2.844	0.95
117.6	1243.95	2.11	0.26	20.6	2.847	0.97
121.0	487.08	2.51	0.27	21.3	2.844	1.00
125.7	235.07	2.83	0.28	21.7	2.844	1.01
129.2	113.25	3.15	0.29	22.3	2.849	1.01
133.2	56.28	3.45	0.35	22.9	2.859	0.96
137.3	28.51	3.75	0.32	23.5	2.926	0.99

TABLE VI-7: continued...

T(K)	$10^6 \tau$ (s)	$\log v_{\max}$	β	$10^3 \epsilon''_{\max}$	ϵ_{∞}	μ (D)
<u>0.39 M 1,10-dibromodecane (higher temperature process)</u>						
244.0	1503.61	2.02	0.20	12.9	3.037	1.22
250.0	859.61	2.27	0.21	13.3	2.985	1.23
256.0	536.39	2.47	0.22	13.3	2.984	1.24
262.0	293.21	2.75	0.22	13.7	2.982	1.24
268.0	180.28	2.95	0.25	14.0	2.894	1.21

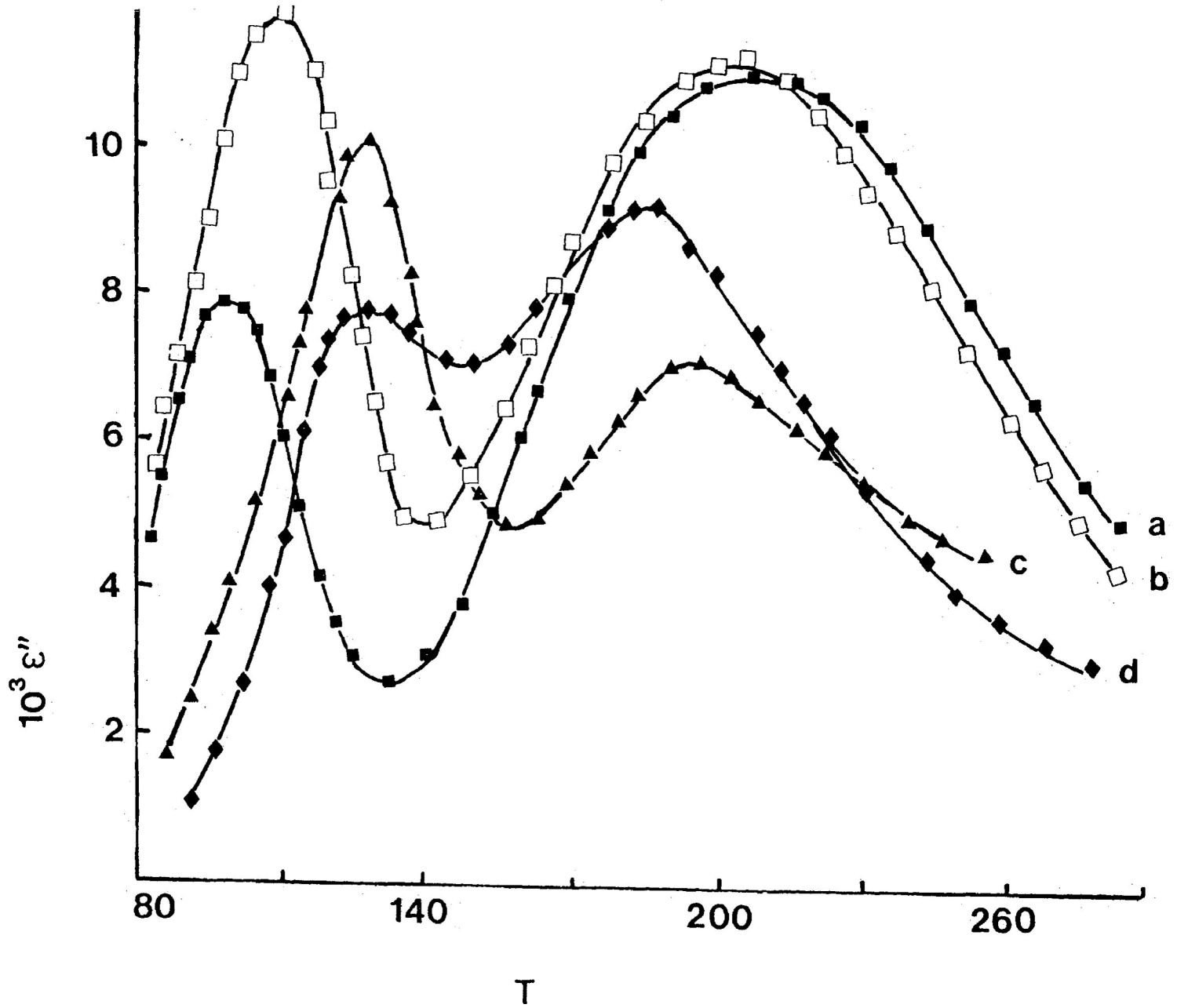


FIGURE VI-1: Dielectric loss factor, ϵ'' versus temperature (K) at 50.2 Hz in a polystyrene matrix
 a) 1-bromooctane, b) 2-bromooctane, c) 3-bromooctane and d) 4-bromooctane

FIGURE VI-2: Relaxation times at 100 K (low temperature absorption) and 200 K (high temperature absorption) versus location of the bromine atom along the n-octane chain in a polystyrene matrix. Point 1 in the diagram indicates the value of the relaxation time in polypropylene.

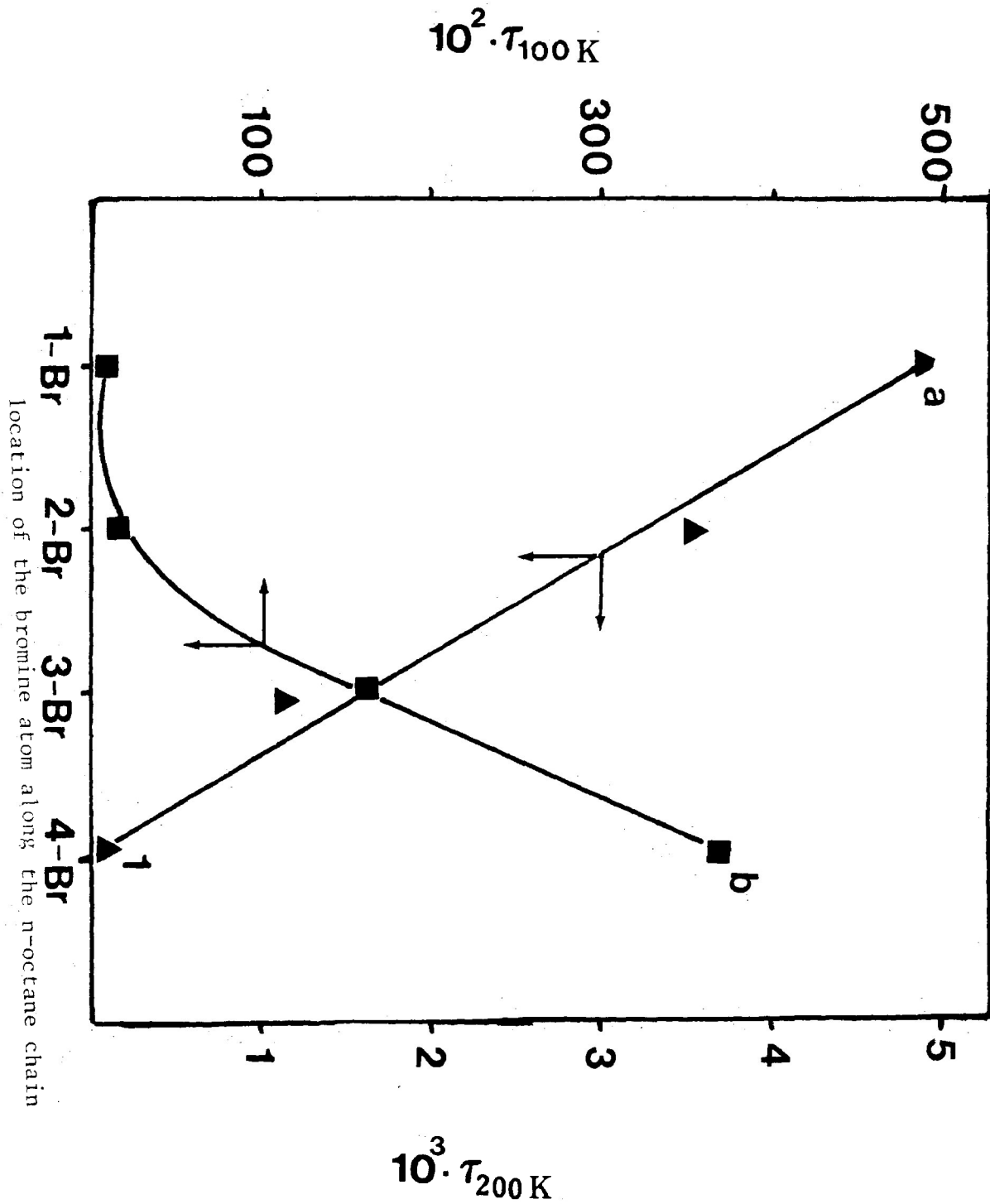
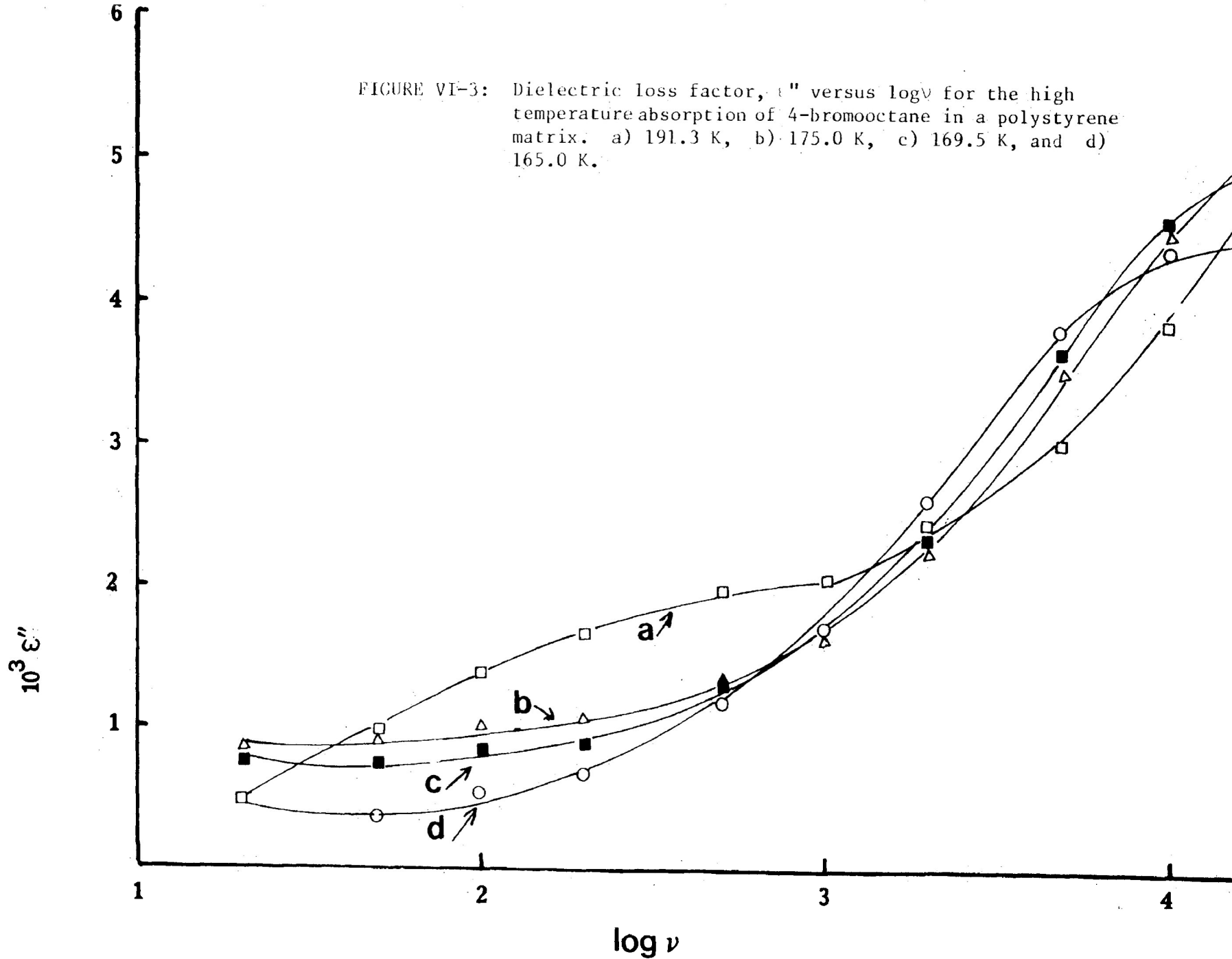


FIGURE VI-3: Dielectric loss factor, ϵ'' versus $\log \nu$ for the high temperature absorption of 4-bromooctane in a polystyrene matrix. a) 191.3 K, b) 175.0 K, c) 169.5 K, and d) 165.0 K.



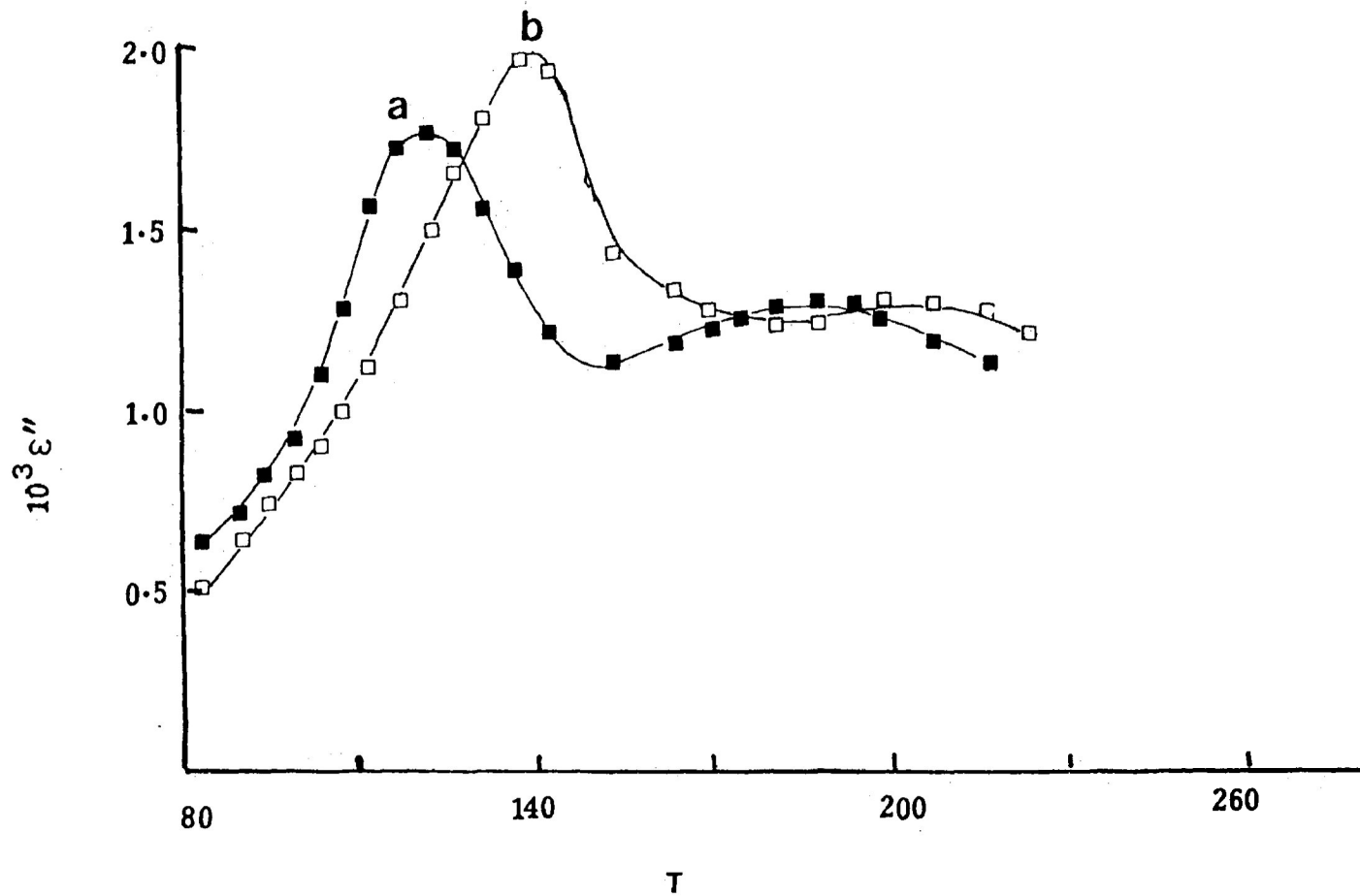


FIGURE VI-4: Dielectric loss factor, ϵ'' versus temperature (K) for 4-bromooctane in polypropylene
 a) 0.0502 kHz and b) 1.01 kHz

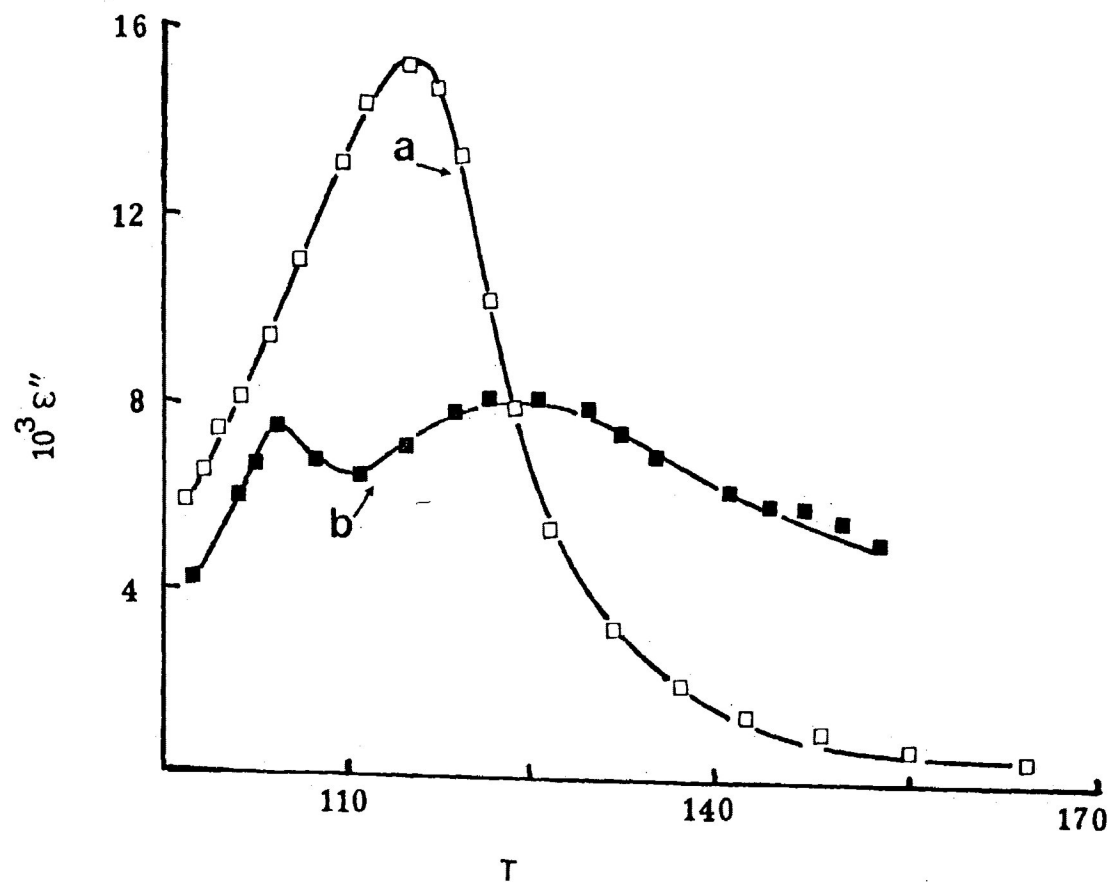


FIGURE VI-5: Dielectric loss factor, ϵ'' versus temperature (K) at 50.2 Hz in a polystyrene matrix

a) 3-bromopentane and b) 1-bromopentane

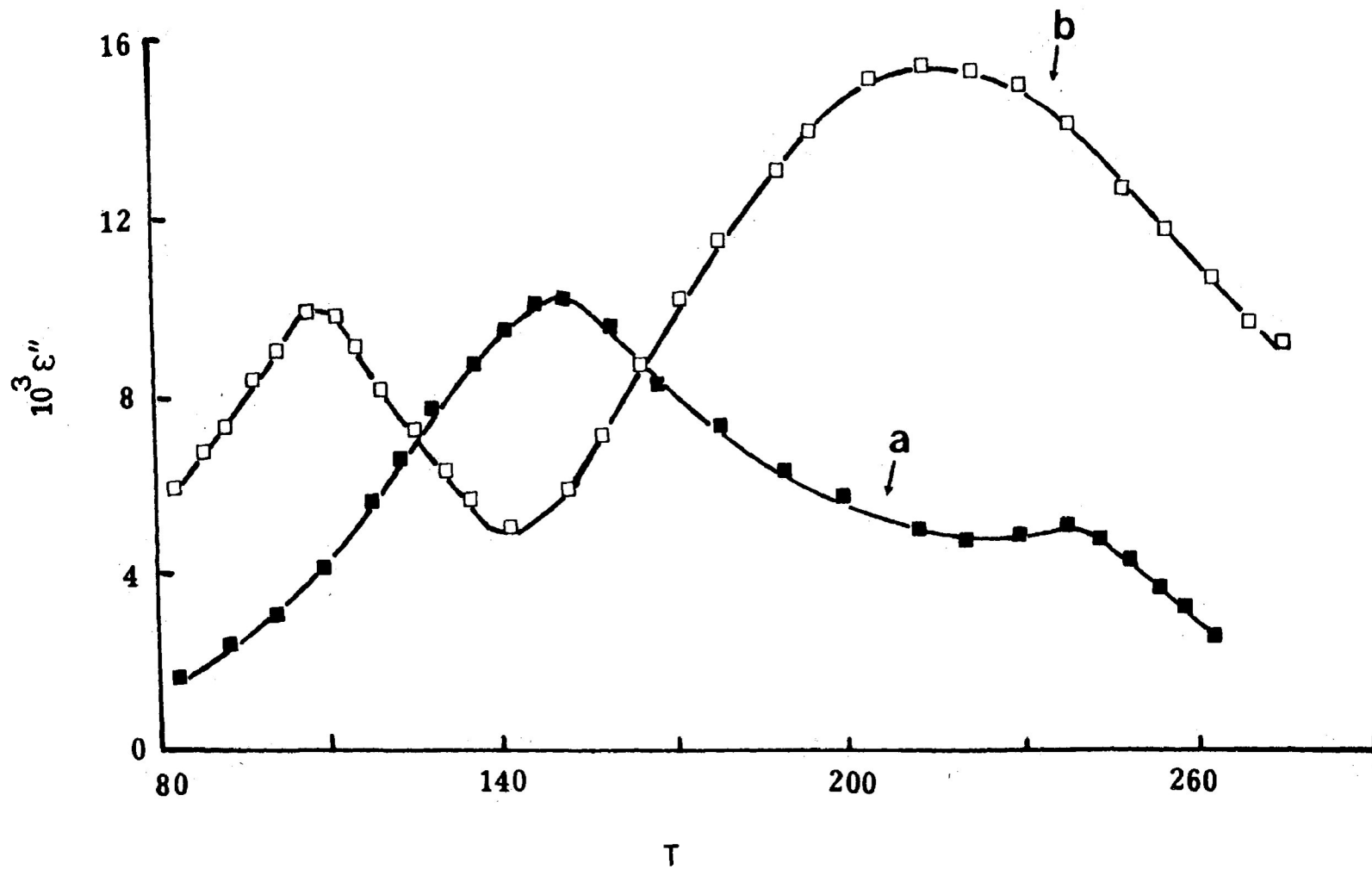
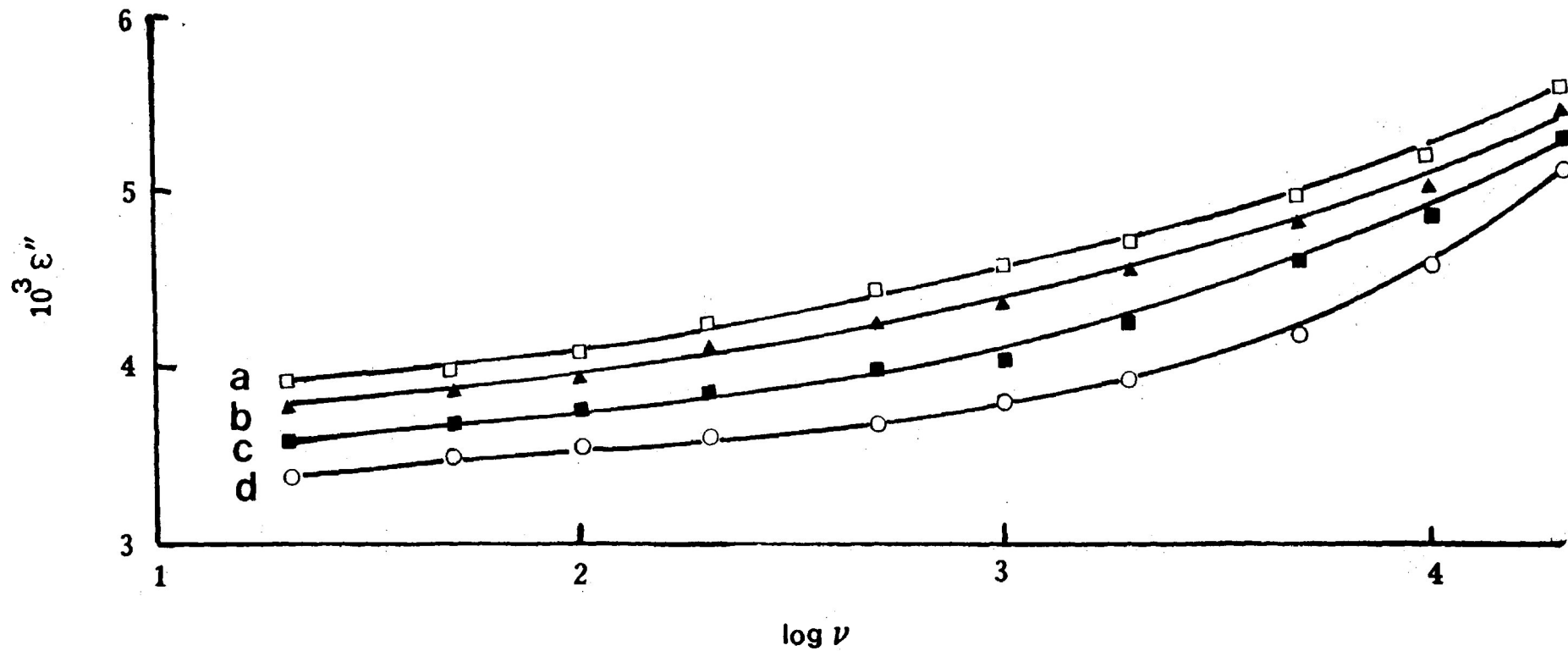


FIGURE VI-6: Dielectric loss factor, ϵ'' versus temperature (K) at 1.01 kHz in a polystyrene matrix
 a) 4-bromoheptane and b) 1-bromoheptane

FIGURE VII-7: Dielectric loss factor, ϵ'' versus $\log \nu$ for the high temperature absorption of 4-bromoheptane in a polystyrene matrix. a) 229.0 K, b) 239.7 K, c) 243.0 K and d) 251.6 K.



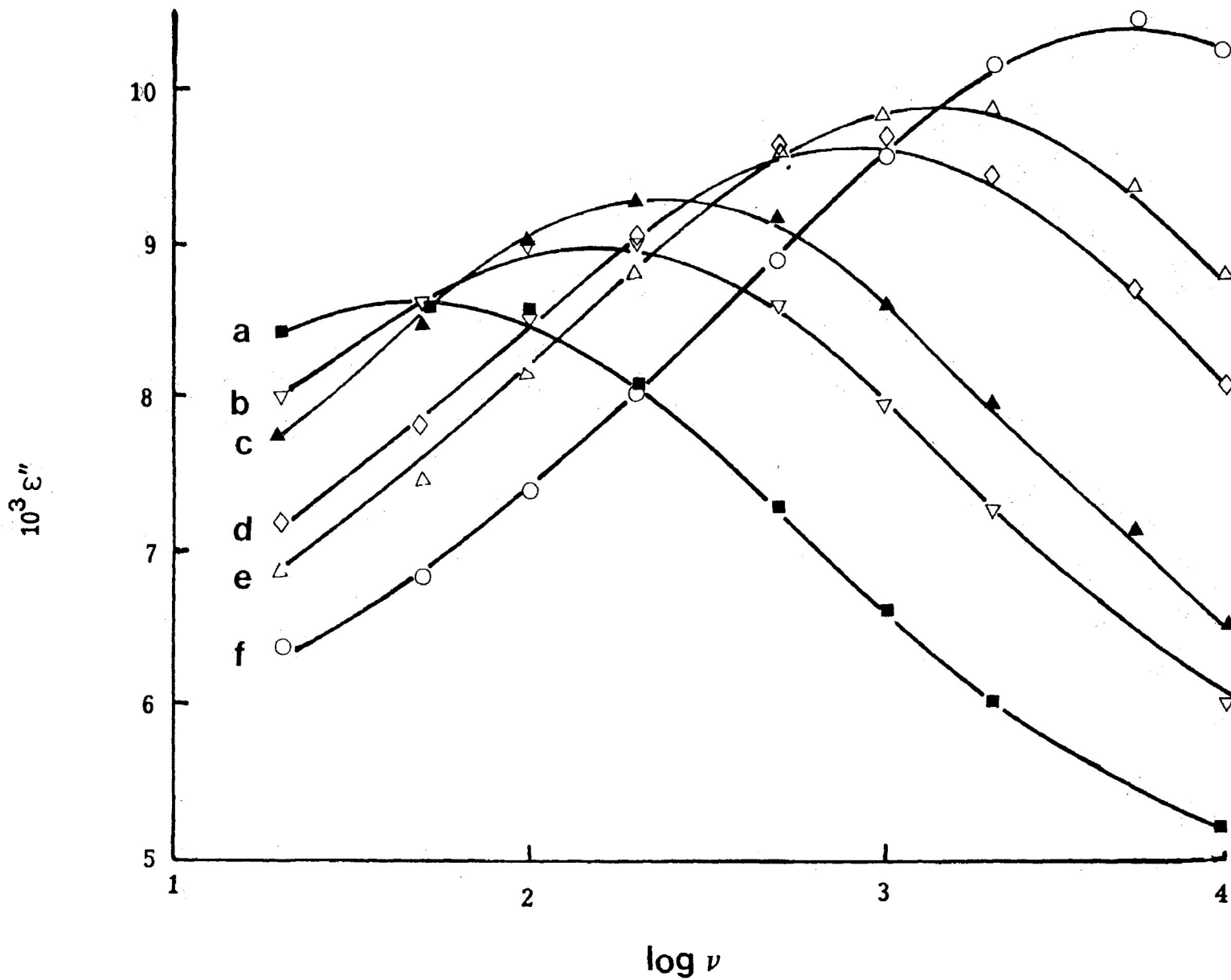


FIGURE VI-8: Dielectric loss factor, ϵ'' versus $\log \nu$ for the low temperature absorption of 4-bromoheptane in a polystyrene matrix. a) 125.7 K; b) 131.6 K; c) 134.5 K; d) 141.6 K; e) 144.6 K and f) 152.2 K.

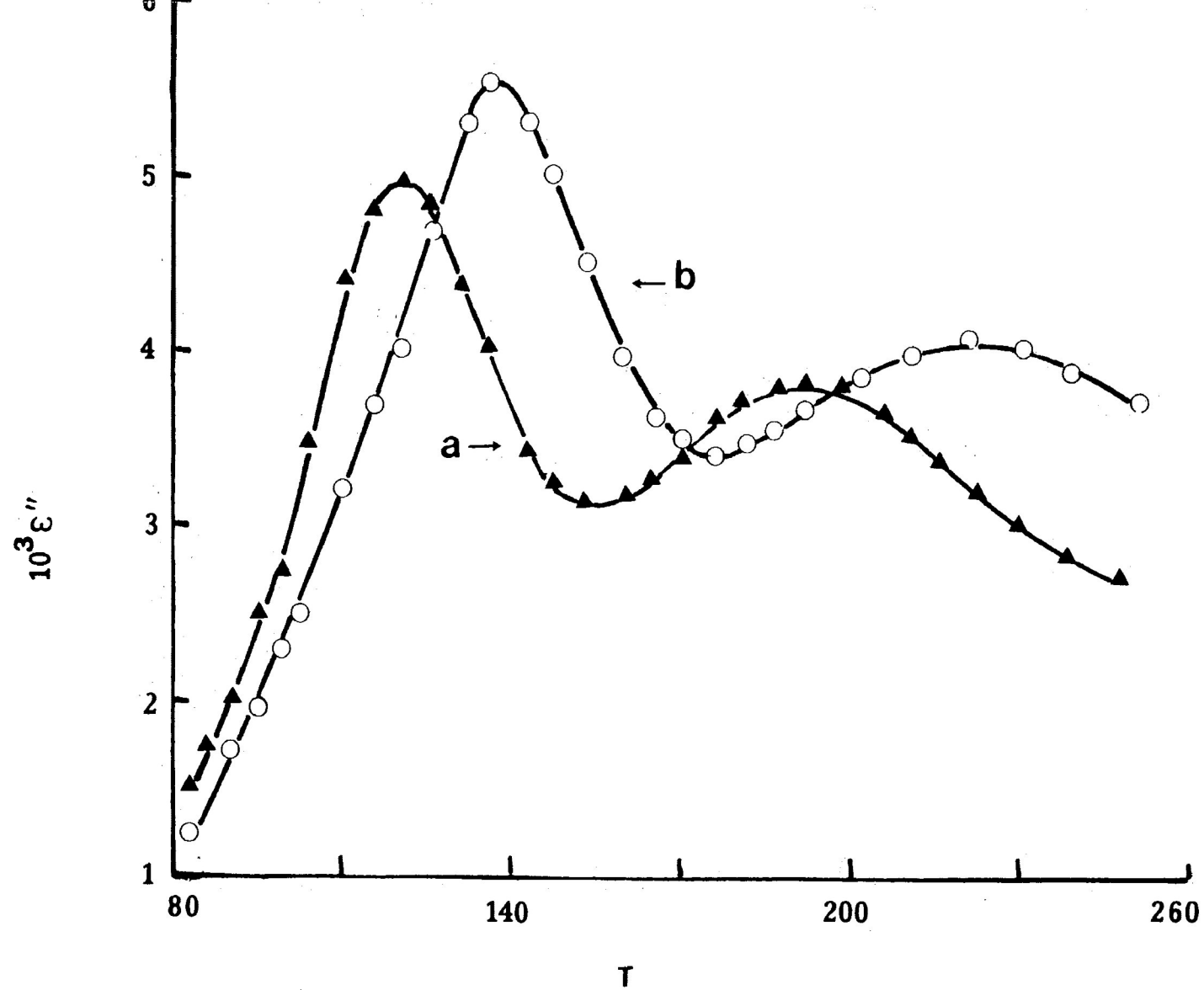


FIGURE VI-9: Dielectric loss factor, ϵ'' versus temperature (K) for 4-bromoheptane in a polypropylene matrix
 a) 0.0502 kHz and b) 1.01 kHz

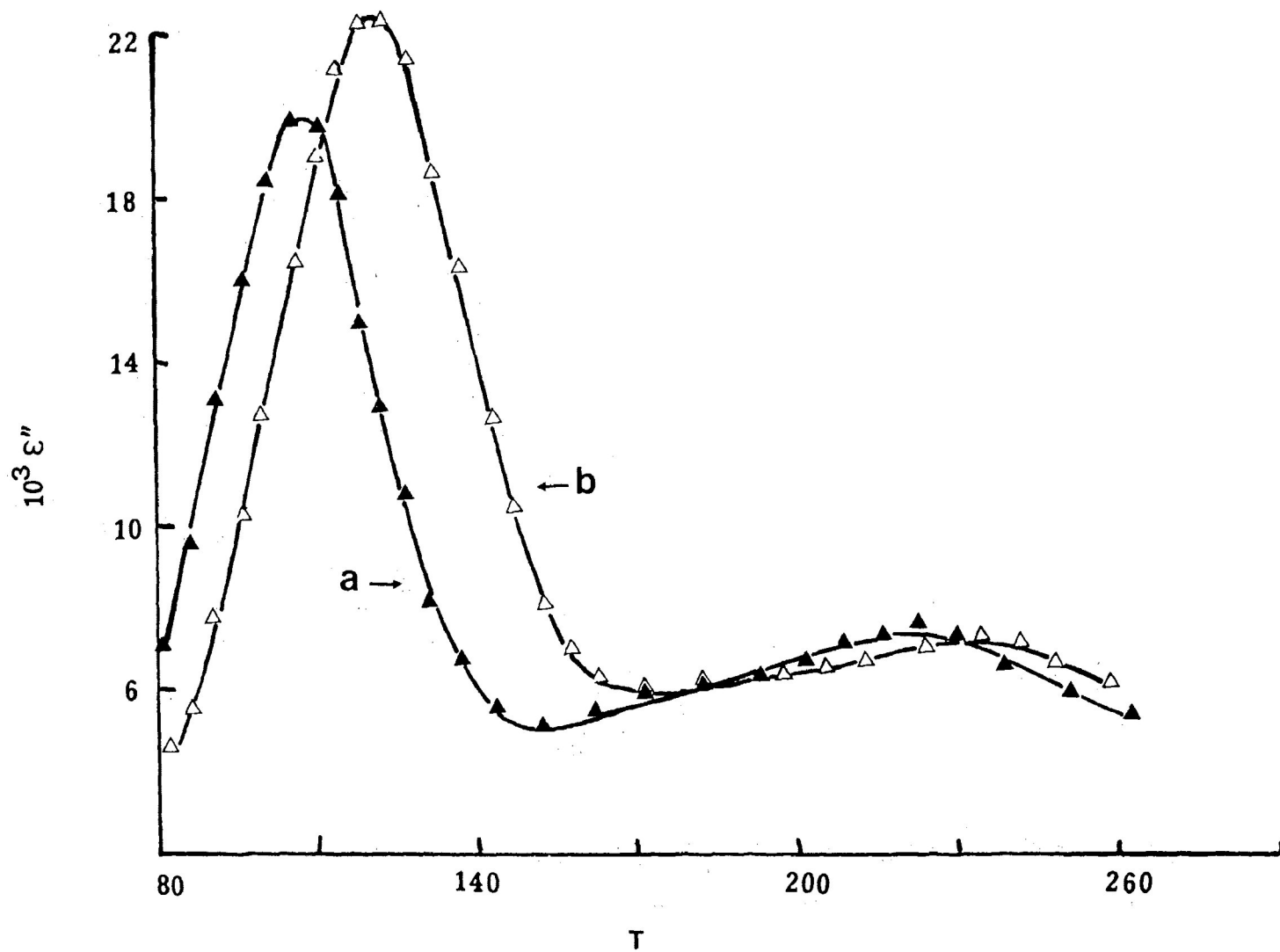


FIGURE VI-10: Dielectric loss factor, ϵ'' versus temperature (K) for 1,6-dibromohexane in a polystyrene matrix. a) 0.0502 kHz and b) 1.01 kHz

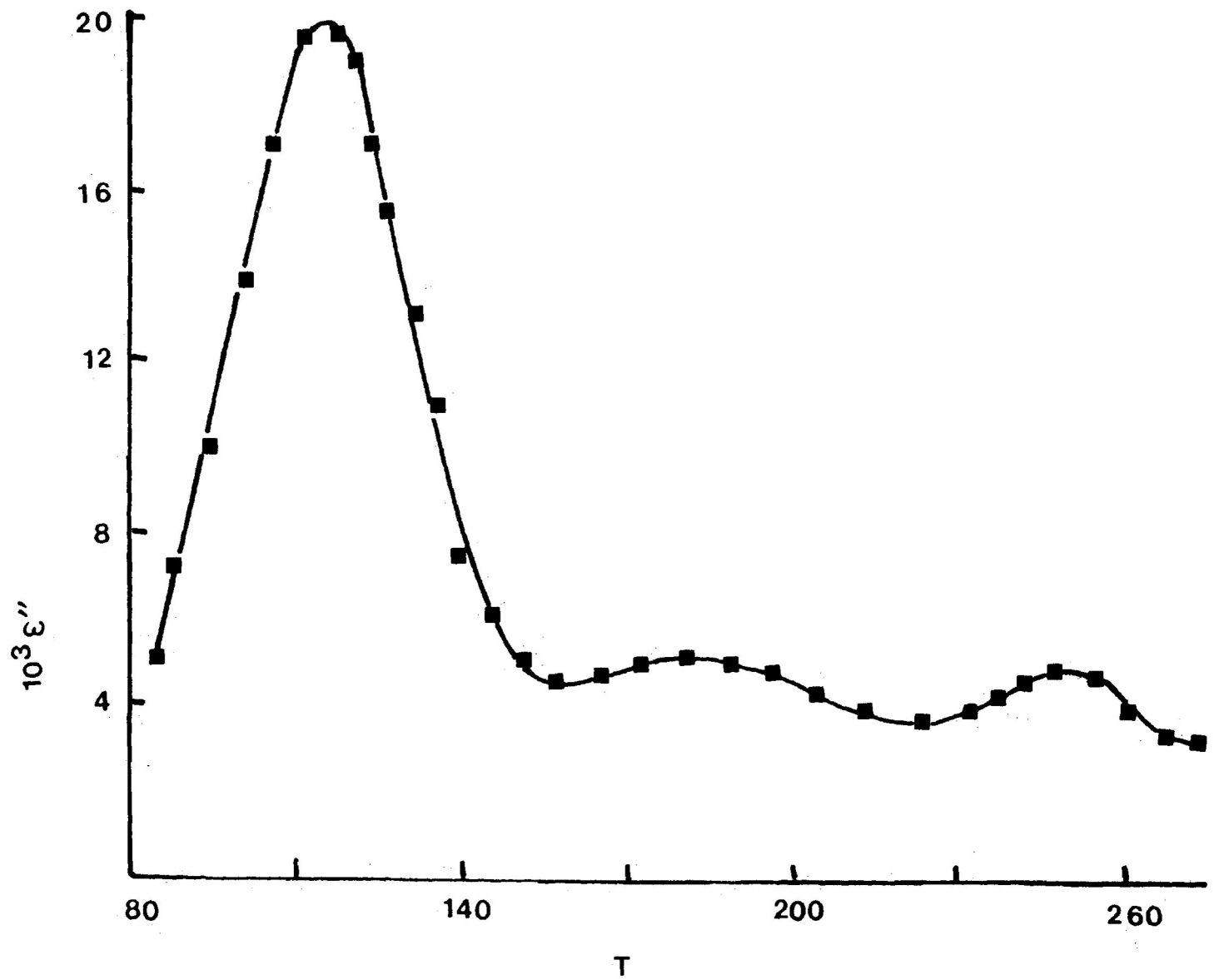


FIGURE VI-11: Dielectric loss factor, ϵ'' versus temperature (K) at 0.0502 kHz for 1,10-dibromodecane in a polystyrene matrix

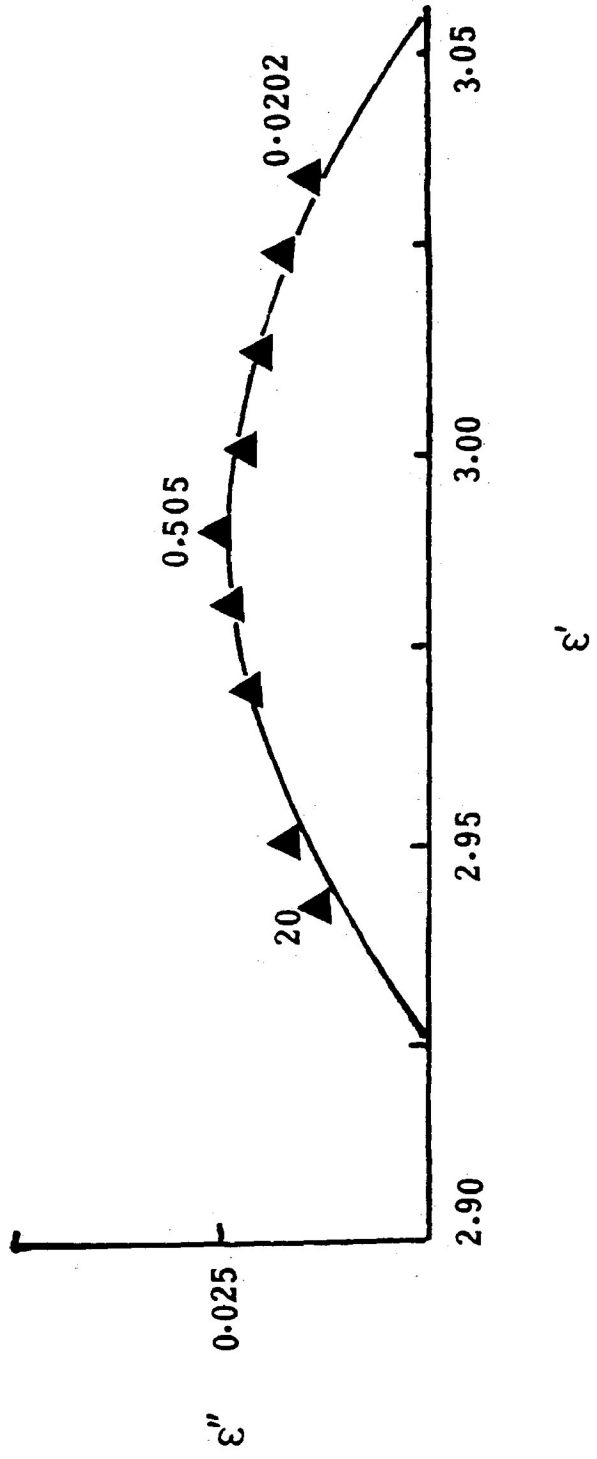


FIGURE VI-12: Cole-Cole plot for 1,6-dibromohexane at 117 K in polystyrene

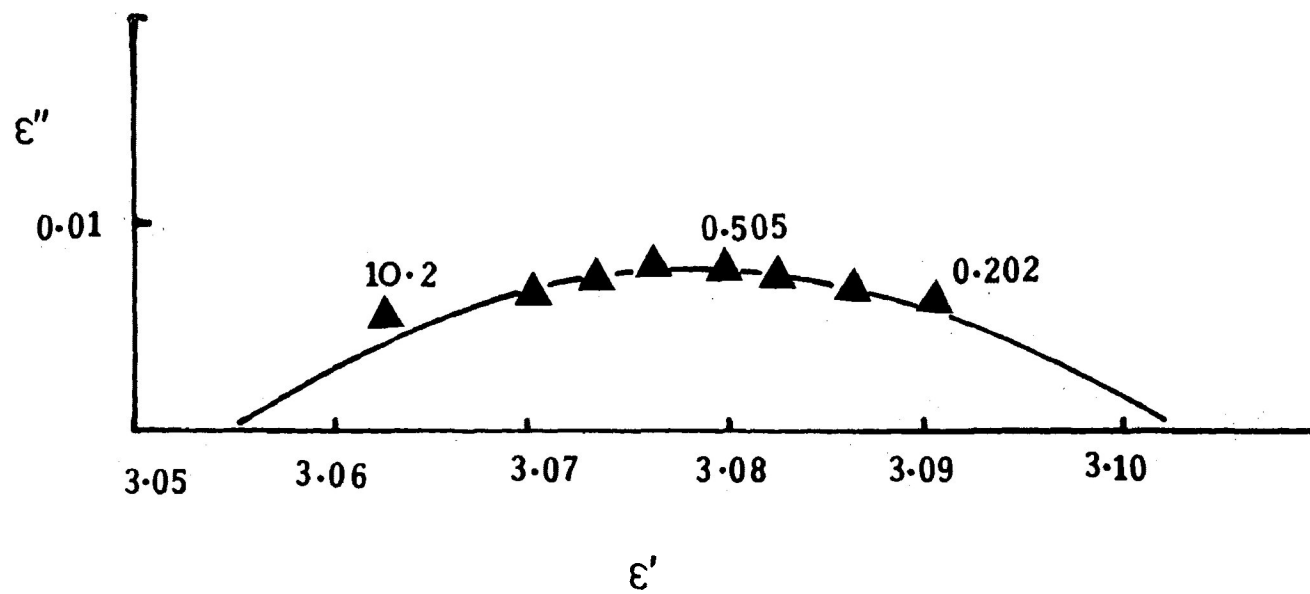


FIGURE VI-13: Cole-Cole plot for 1,6-dibromohexane at 232.2 K in polystyrene

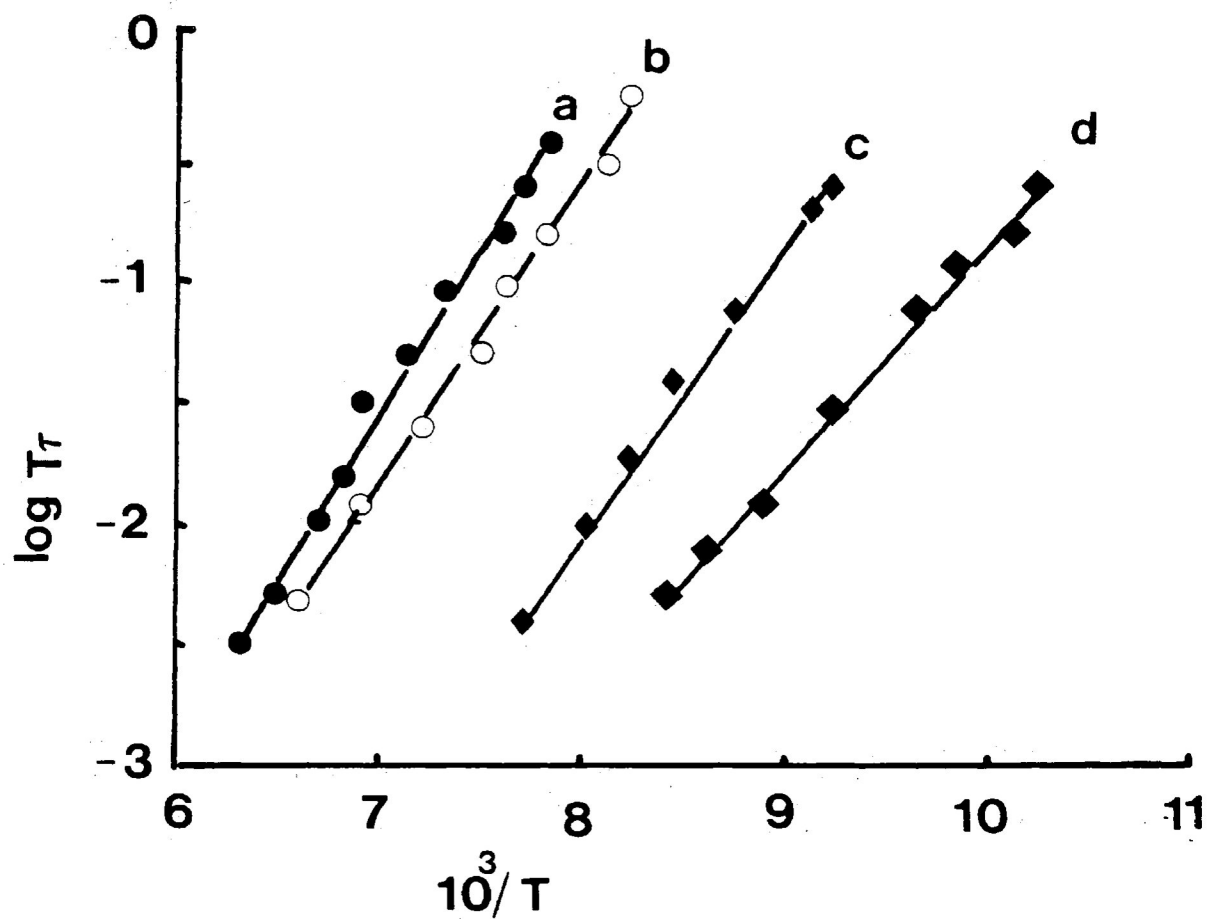


FIGURE VI-14: Eyring rate plot of $\log T\tau$ versus $1/T$ (K^{-1}) for the low temperature absorption in a polystyrene matrix

a) 4-bromooctane, b) 3-bromoocatne, c) 2-bromooctane and d) 1-bromooctane.

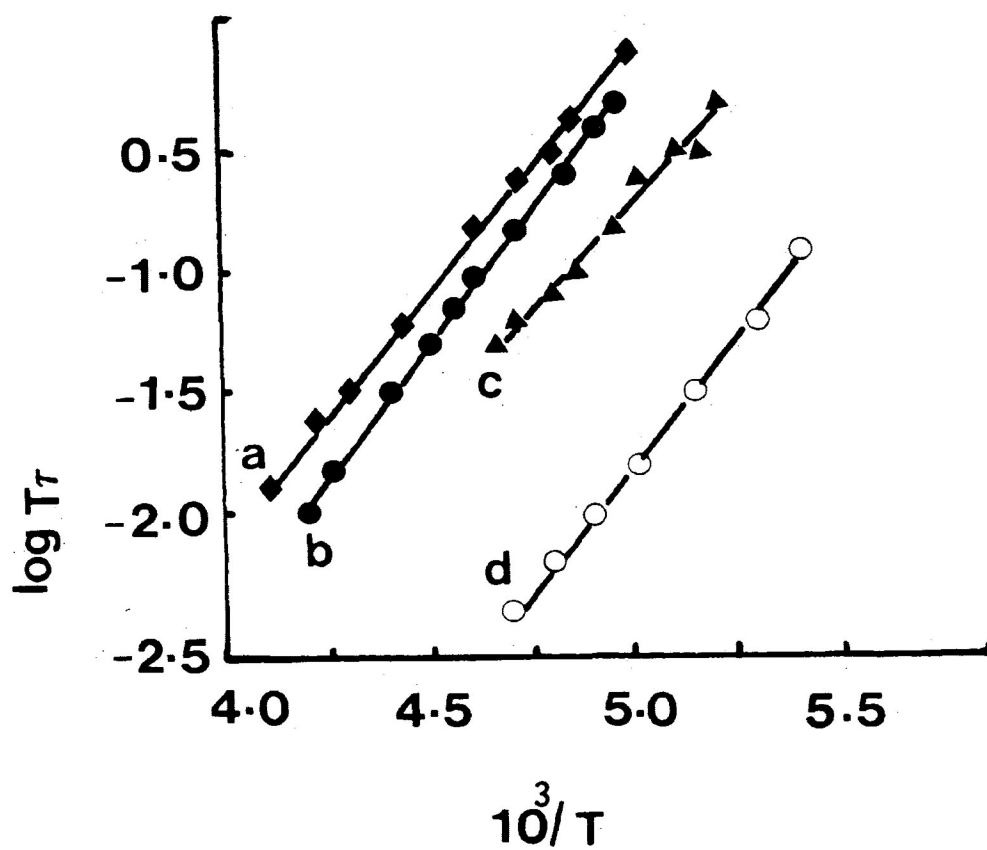


FIGURE VI-15: Eyring rate plots of $\log T\tau$ versus $1/T$ (K^{-1}) for the high temperature absorption. a) 1-bromooctane (polystyrene), b) 2-bromooctane (polystyrene) c) 3-bromooctane (polystyrene) and d) 4-bromooctane (polypropylene).

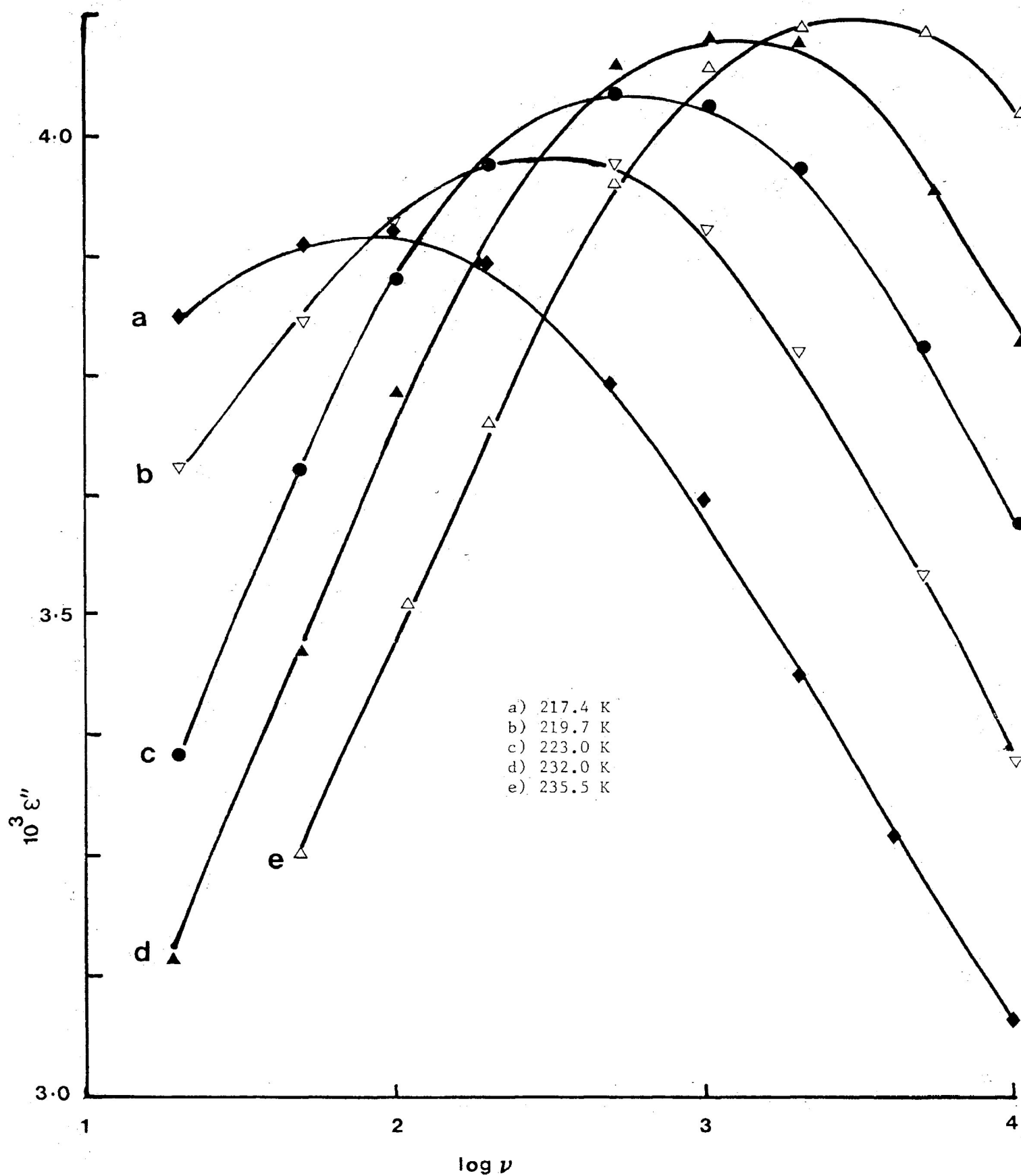


FIGURE VI-16: Dielectric loss factor, ϵ'' versus $\log \nu$ for the high temperature absorption of 4-bromoheptane in polypropylene

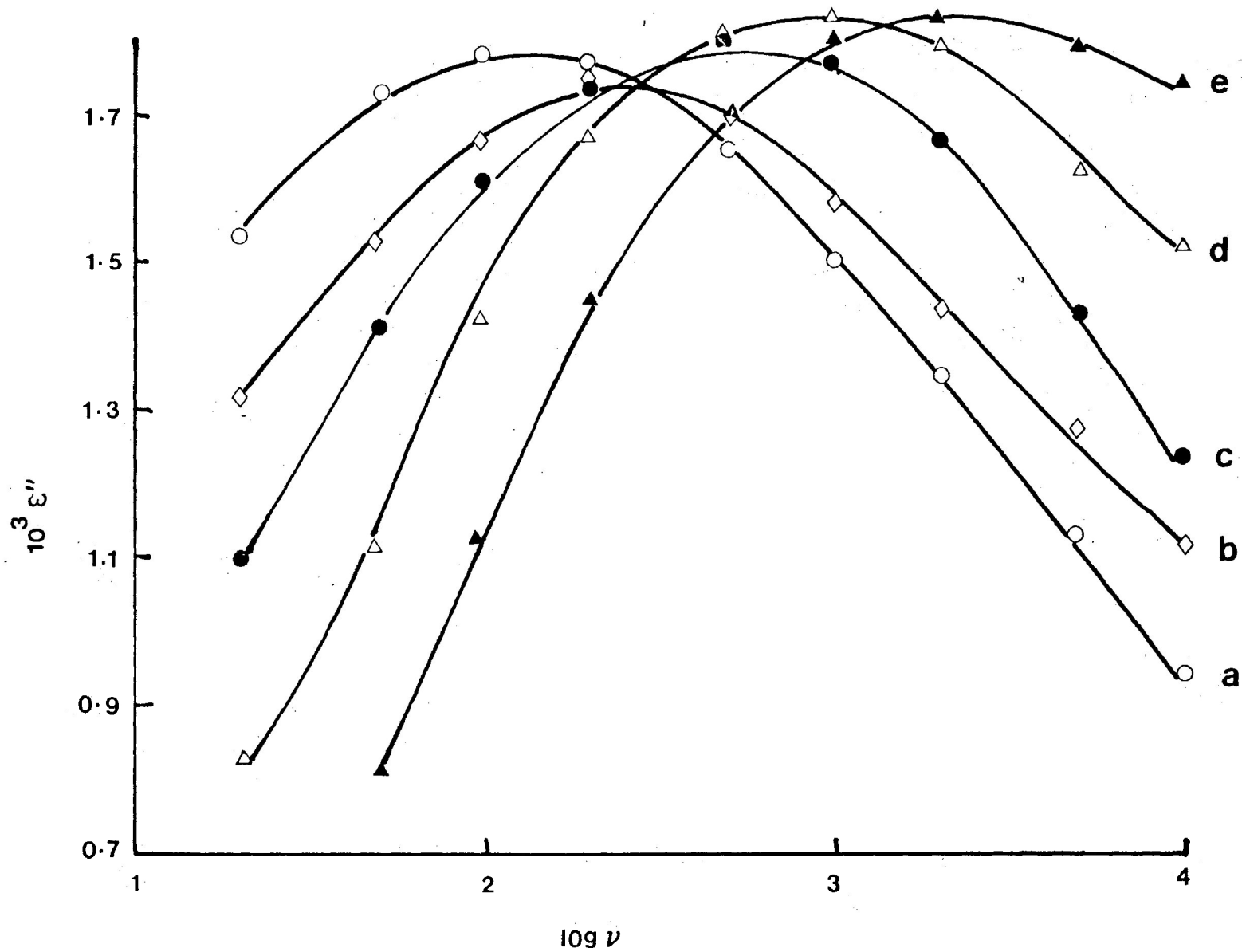


FIGURE VI-17: Dielectric loss factor, ϵ'' versus $\log \nu$ for the high temperature absorption of 4-bromooctane in polypropylene. a) 185.5 K; b) 189.1 K, c) 193.5 K, d) 204.3 K and e) 212.3 K.

CHAPTER VII

DIELECTRIC RELAXATION OF 2-ALKANONES AND 1-
AMINOALKANES IN A POLYSTYRENE MATRIX

INTRODUCTION

Smyth and co-workers (1) measured dielectric permittivities and losses of acetone, 2-heptanone, 4-heptanone, 8-pentadecanone and 9-heptadecanone as pure liquids between 274 to 363 K. The mean relaxation time is found to increase with the increase of chain length. The slightly greater values of relaxation time (17.0 ps at 274 K) for 4-heptanone compared to that of 2-heptanone (15.3 ps at 274 K) suggest the possibility that the location of the dipole at the centre of the carbon chain makes segmental reorientation more difficult than it is when at the end of the chain as in 2-heptanone. The results were interpreted in terms of dipole reorientation by the whole molecule rotation and an intramolecular process possibly twisting around the R-C and R'-C bonds of the ketones RCOR' .

Johari et al (2) studied the dielectric absorption of 2-octanone in n-heptane solution. The Cole-Cole plot could be represented by the two semicircular arcs. The data can be analyzed in terms of two relaxation times. The short τ_2 values can account for $-\text{COCH}_3$ group rotation and the τ_1 values to molecular rotation.

Crossley (3) measured dielectric permittivities

and losses of several ketones in which the location of the carbonyl group varied along the chain in the cyclohexane solution and at frequencies between 1.5 to 145 GHz at 298 K. It was possible for each system to draw a depressed centre, semi-circular arcs through most of the experimental points. His results suggested that (a) the mean relaxation time increases only slightly as the size of the alkyl group increases, acetyl group rotation being the dominant process of dipole relaxation for 2-alkanones, (b) the location of carbonyl group on the hydrocarbon backbone has relatively little effect on the relaxation time for the nonanones and decanones. In these molecules, the dipole reorientation may occur either by overall molecular reorientation or by twisting around the R-C or R'-C bond, (c) the relaxation times for pentadecanones and nonadecanones do lengthen significantly as the carbonyl group is further removed from the chain end. Crossley suggested that the intramolecular process is restricted when both R and R' are sufficiently long. Dipole reorientation by overall molecular rotation may then become more important, the contribution to the absorption increases with increased size of the R and R'. Alternatively, the increasing with increased size time may be due to the intramolecular rotation of molecular segments, (e.g. rotation of R CO- group around the R-C bond).

Vyas and Srivastava (4) examined some primary

amines as pure liquids and found the mean relaxation time to increase with the increase of chain length. Garg and Kadaba (5) measured dielectric constants and losses of several aliphatic amines from the 373 K downward in the solid state. The ΔF_0 values are found to be independent of the size of the molecules. They suggested that the dielectric relaxation in the primary amines is dominated by the rotation of small units.

Johari et al (2) examined n-octylamine in n-heptane solution in the microwave region. An asymmetric plot for the dielectric loss versus dielectric constant was obtained. Analysis of the results in terms of two relaxation times yields consistent parameters. The longer relaxation time, τ_1 , is attributed to the reorientation of the whole molecule, but the assignment of the shorter one is complicated by the possibility of inversion of the nitrogen atom as the contributing relaxation mechanism.

Dielectric absorption studies have been made by Tay and Crossley (6) on a number of primary amines, N-methyloctylamine, N,N-dimethyloctylamine, and N,N-diethyloctylamine in cyclohexane solutions. The plot of dielectric loss versus dielectric constant gives no clear indication of distinct separation into more than one dispersion region. It was possible to draw a relatively smooth depressed centre semicircular arc for

all the systems. The mean relaxation times of the primary amines do not increase significantly with increased size of the alkyl group or with the location of the amine group in the nonylamines. Their results suggest that the dipole reorientation in primary n-alkylamines occurs predominantly by a fast intramolecular process and rotational orientation of the whole molecule makes little or no detectable contribution to the absorption. In contrast, the mean relaxation times of N-methyl, N,N-dimethyl, and N,N-diethyloctylamines, which are considerably longer than those for the primary amines, lengthen with increased number and size of the N-alkyl groups. They suggested that the reorientation of dipole by intramolecular rotation may be restricted for secondary and tertiary amines, and the reorientation of the whole molecule appears to make a significant contribution to the absorption of secondary and tertiary amines. The contribution apparently increases with the increase of the size of the N-alkyl groups. Because of the short relaxation times the errors in the estimation of ϵ_{∞} and the Cole-Cole distribution parameter (α) values are considerable. Therefore, the analysis of the data in terms of two relaxation processes did not yield any consistent and physically significant results.

Very recently Solsona et al (7) reported the dielectric relaxation studies of ten primary amines (propylamine

to dodecylamine) as pure liquids. The Kirkwood co-relation factor, g , was found to decrease with increasing temperature and at the boiling point of the amines, the value approached unity. The Cole-Davidson model was found most suitable to describe the dielectric relaxation phenomena in those amines. They concluded that the intramolecular rotation was the predominant mechanism in the relaxation process, mainly the rotation of the $-NH_2$ group following the previous breaking of the hydrogen bondings.

Gilchrist (8) reported the dielectric absorption studies for a number of aliphatic primary amines in a polyethylene matrix. His results indicated that the inversion barrier of the nitrogen atom was low and appeared below liquid nitrogen temperature (at 4.2 K in the frequency range 10 to 100 kHz).

In Chapter V a detailed dielectric study of 1-bromoalkanes as a function of the number of carbon atoms in the chain have been presented. The major objective of the present investigation is to compare the influence of the different polar end groups in the relaxation mechanisms by substituting $-CH_2Br$ in 1-bromoalkanes by the $-COCH_3$ and $-NH_2$ groups. The interpretations of fast intramolecular processes

in 1-aminoalkanes have been complicated by the possibility of contributions from nitrogen inversion and the mechanism has never been studied precisely. Our present intent was to separate completely the absorption peaks of some or any of the relaxation processes. A separation into molecular and intramolecular processes has previously been achieved for a series of long chain bromides (see Chapter V) and aldehydes (9) in a polystyrene matrix.

EXPERIMENTAL RESULTS

The following compounds have been included in the present study:

2-Alkanones

<u>Number</u>	<u>Molecule</u>	<u>Structural Formula</u>
1	2-Heptanone	$\text{CH}_3(\text{CH}_2)_4\text{COCH}_3$
2	2-Octanone	$\text{CH}_3(\text{CH}_2)_5\text{COCH}_3$
3	2-Nonanone	$\text{CH}_3(\text{CH}_2)_6\text{COCH}_3$
4	2-Undecanone	$\text{CH}_3(\text{CH}_2)_8\text{COCH}_3$
5	2-Tridecanone	$\text{CH}_3(\text{CH}_2)_{10}\text{COCH}_3$
6	2-Pentadecanone	$\text{CH}_3(\text{CH}_2)_{12}\text{COCH}_3$
7	2-Heptadecanone	$\text{CH}_3(\text{CH}_2)_{14}\text{COCH}_3$
8	2-Nonadecanone	$\text{CH}_3(\text{CH}_2)_{16}\text{COCH}_3$

1-Aminoalkanes

9	1-Propylamine	$\text{CH}_3(\text{CH}_2)_2\text{NH}_2$
10	1-Butylamine	$\text{CH}_3(\text{CH}_2)_3\text{NH}_2$
11	1-Hexylamine	$\text{CH}_3(\text{CH}_2)_5\text{NH}_2$
12	1-Octylamine	$\text{CH}_3(\text{CH}_2)_7\text{NH}_2$
13	1-Nonylamine	$\text{CH}_3(\text{CH}_2)_8\text{NH}_2$
14	1-Decylamine	$\text{CH}_3(\text{CH}_2)_9\text{NH}_2$
15	1-Undecylamine	$\text{CH}_3(\text{CH}_2)_{10}\text{NH}_2$
16	1-Dodecylamine	$\text{CH}_3(\text{CH}_2)_{11}\text{NH}_2$

All of the compounds were obtained commercially and studied as received except 1-decylamine and 1-undecylamine which were dried by K_2CO_3 , distilled and a middle fraction collected.

All of the compounds were measured as polystyrene matrices in the temperature range 80-320 K and frequency range $10-10^5$ Hz. 2-Undecanone has also been studied in polypropylene o-terphenyl and polyphenyl ether to investigate thoroughly the lower temperature absorption.

Tables VII-1 to VII-5 show the relaxation and Eyring parameters, extrapolated dipole moment, energy difference between the equilibrium positions of the dipoles for 2-alkanones and 1-aminoalkanes. Table VII-6 lists the Fuoss-Kirkwood analysis parameters, ϵ_∞ , and dipole moments at various temperatures.

Figures VII-1 to VII-15 show the plots of dielectric loss factor, ϵ'' versus temperature, relaxation time versus number of methylene groups, plots of ΔS_E versus ΔH_E , absorption curves and Eyring rate plots of $\log T\tau$ versus $1/T$ for some of the systems of 2-alkanones and 1-aminoalkanes.

DISCUSSION

2-Alkanones having the general formula $\text{CH}_3(\text{CH}_2)_n\text{COCH}_3$ (where $n = 4, 5, 6, 8, 10, 12, 14$ and 16) have been dispersed in a polystyrene matrix. Two distinct absorption peaks appear when the loss factor is plotted against the temperature at 0.0202 kHz. The low temperature absorption peaks appear somewhere in the region between 80 - 148 K and the high temperature absorption peaks in the range between 160 - 290 K.

1-Aminoalkanes having the general formula $\text{CH}_3(\text{CH}_2)_n\text{NH}_2$ ($n = 2, 3, 5, 7, 8, 9, 10$ and 11) exhibited two distinct absorption peaks in a polystyrene matrix when loss factor, ϵ'' , is plotted against temperature at 1.01 kHz except for $n = 2$ and 3 where only the low temperature absorption peak has been detected.

Low temperature absorption

From Figures VII-1 and VII-2, it is evident that the half-width, $\Delta T_{\frac{1}{2}}$ values of the low temperature absorption of 2-alkanes and 1-aminoalkanes for a given value of n are almost similar and lie in the range 45 - 55 K. These $\Delta T_{\frac{1}{2}}$ values are

very similar to the one found for the low temperature absorption of 1-bromoalkanes (see Chapter V).

The β -values for the low temperature absorption of 2-alkanones and 1-aminoalkanes lie in the range 0.18-0.35 at 83-145 K and 0.20-0.32 at 80-126 K, respectively. These β -values for the low temperature absorption of 2-alkanones and 1-aminoalkanes compare favourably with 0.24-0.35 at 80-150 K for the low temperature absorption of 1-bromoalkanes. The similarity of $\Delta T_{\frac{1}{2}}$ and β -values for the low temperature absorption of 2-alkanones and 1-aminoalkanes with that of 1-bromoalkanes suggests that similar mechanisms are at work in the relaxation of 2-alkanones, 1-aminoalkanes and 1-bromoalkanes.

The relaxation times at 150 K (see Figures VII-3 and VII-4) and ΔH_E (see Figures VII-5 and VII-6) for the low temperature absorption of 2-alkanones and 1-aminoalkanes increase with the increase in the number of carbon atoms in the chain. It is observed from Figures VII-3 and VII-4 that the increase in relaxation time is slow for the lower values of n ($n < 6$) and then the increase is almost linear for the higher values of n . The probable reasons are that (a) the high temperature absorption has not been detected for some lower values of n (see Table VII-2), the low temperature absorption is either the intramolecular process (where the molecular process occurs

below that of liquid nitrogen temperature) or an overlapping of the molecular and intramolecular processes, (b) even though the intramolecular and molecular processes have been studied for some lower values of n , the separation of the two processes is not sufficient as to give accurate ν_{\max} . With larger values of n , the separation of the processes is increased. The increase in relaxation time and ΔH_E value with the increase in the number of carbon atoms suggests that the size of the reorientating unit also increases. Table VII-1 shows that the relaxation time at 150 K and ΔH_E values are almost similar for a given value of n and $X = -CH_2Br, -CH_2OH, -COCH_3$ and $-NH_2$. For example, $\tau_{150 K}$ and ΔH_E values for $n = 8$ and $X = -CH_2Br, -CH_2OH, -COCH_3$ and $-NH_2$ are 1.1×10^{-6} s and 22.0 kJ mol^{-1} , 1.0×10^{-6} s and 22.0 kJ mol^{-1} , 1.0×10^{-6} s and 22.4 kJ mol^{-1} and 2.9×10^{-7} s and 20.1 kJ mol^{-1} , respectively. These suggest that the polar end groups have negligible influence on the relaxation time and ΔH_E values for the low temperature absorption. The rotation about the C-C bonds is the main contributor to the low temperature absorption.

Dispersion of a substance in different media may permit characterization of a relaxation process as being intramolecular or molecular, for whereas the former is relatively insensitive to the viscosity of the medium, the barrier for rotation of a large dipole is dependent on its environment. This

has been demonstrated for 2-alkanones with $n = 8$ in the two different polymers and the two glassy forming solids, *o*-terphenyl and polyphenyl ether. In *o*-terphenyl and polyphenyl ether a low temperature absorption peak were detected whereas in polystyrene and polypropylene two distinct absorption peaks were found. The high temperature absorption peak in *o*-terphenyl and polyphenyl ether is most likely merged by the co-operative process of the dispersion medium. Not only does dielectric absorption occur at similar low temperatures but the relaxation times and Eyring activation parameters are in good agreement in the polystyrene matrix ($\tau_{100\text{ K}} = 1.2 \times 10^{-2}$ s, $\Delta G_{\text{E}(100\text{ K})} = 19.9$ kJ mol⁻¹ and $\Delta H_{\text{E}} = 22.4 \pm 0.4$ kJ mol⁻¹), polypropylene matrix ($\tau_{100\text{ K}} = 6.5 \times 10^{-4}$ s, $\Delta G_{\text{E}(100\text{ K})} = 17.5$ kJ mol⁻¹ and $\Delta H_{\text{E}} = 18.7 \pm 1.3$ kJ mol⁻¹), *o*-terphenyl ($\tau_{100\text{ K}} = 8.2 \times 10^{-3}$ s, $\Delta G_{\text{E}(100\text{ K})} = 19.6$ kJ mol⁻¹ and $\Delta H_{\text{E}} = 20.6 \pm 0.6$ kJ mol⁻¹) and polyphenylether ($\tau_{100\text{ K}} = 2.1 \times 10^{-2}$ s, $\Delta G_{\text{E}(100\text{ K})} = 20.4$ kJ mol⁻¹ and $\Delta H_{\text{E}} = 22.9 \pm 0.4$ kJ mol⁻¹).

Thus, it is reasonable to assume that the low temperature absorption in 2-alkanones and 1-aminoalkanes is the intramolecular rotation about the C-C bonds involving the movement of the polar end group, $-\text{COCH}_3$ and $-\text{NH}_2$ and is independent of the choice of solvent.

The possibilities of the inversion of the nitrogen atom and the intermolecular hydrogen bonding may be considered as relaxation candidates for the low temperature absorption of 1-aminoalkanes. Gilchrist (8) has shown that the inversion of the nitrogen atom appears below the liquid nitrogen temperature in the radio frequency range (4.2 K in the frequency range 10 to 100 kHz).

If there were an intermolecular hydrogen bonding in 1-aminoalkanes, the relaxation time and the Eyring activation parameters would be higher than that of the corresponding non-associated 1-bromoalkanes and 2-alkanones. Further, no significant increase in relaxation time and ΔH_E values with increased concentration is evident for nonylamine (n=8) in Table VII-1. Huque (10) could not detect H-bonding in alcohols at concentrations of about 5% (by weight) which are much stronger H-bonding systems in a polystyrene matrix.

Thus, it would seem that the inversion of the nitrogen atom and intermolecular H-bonding could not be considered as the relaxation candidates for the low temperature absorption of 1-aminoalkanes.

A linear relationship appears when ΔS_E is plotted against ΔH_E for the low temperature absorption of both 2-

alkanones (see Figure VII-7) and 1-aminoalkanes (see Figure VII-8). Within experimental error, there is a reasonable fit of the $\Delta S_{E(\text{obsd})}$ values for the low temperature absorption of 2-alkanones and 1-aminoalkanes to two quite similar empirical relations:

$$\Delta S_E = 3.3 \Delta H_E - 48 \quad \text{for 2-alkanones}$$

$$\Delta S_E = 3.7 \Delta H_E - 50 \quad \text{for 1-aminoalkanes}$$

Figure VII-1 shows that the contribution of the molecular and the intramolecular processes to the total absorption are similar for 2-alkanones whereas for 1-aminoalkanes, the intramolecular process is the dominant one (see Figure VII-2).

High temperature absorption

From Figures VII-1 and VII-2 it is evident that the half-width, $\Delta T_{\frac{1}{2}}$ for the high temperature absorption of 2-alkanones and 1-aminoalkanes for a given value of n is almost similar and only slightly increases with the increase in the number of carbon atoms in a particular series. The $\Delta T_{\frac{1}{2}}$ values lie in the range 80-140 K and 85-150 K for 2-alkanones and 1-aminoalkanes, respectively. Similar $\Delta T_{\frac{1}{2}}$ values (90-150 K) have been obtained for the molecular rotation of 1-bromoalkanes

in a polystyrene matrix.

The β -values for the high temperature absorption of 2-alkanones and 1-aminoalkanes lie in the range 0.14-0.24 at 160-290 K and 0.12-0.30 at 190-290 K, respectively. Such low β -values indicate a wide distribution of relaxation times. Similar β -values for the high temperature absorption of 1-bromoalkanes (0.18-0.24 at 160-300 K) have been observed in a polystyrene matrix where the high temperature absorption has been attributed to a molecular rotation.

Table VII-2 shows that the relaxation time at 200 K and ΔH_E values increases with the increase in the number of carbon atoms in the chain for both 2-alkanes and 1-aminoalkanes. These suggest that the size of the reorientating unit also increases with the increase in chain length.

In the plot of ΔS_E against the ΔH_E (see Figure VII-9) for the high temperature absorption of 1-bromoalkanes, 2-alkanones, 1-aminoalkanes and 1-alkanols, it is possible to draw a mean line according to the empirical relation

$$\Delta S_E = 2.2 \Delta H_E - 72$$

obtained by Khwaja and Walker (12) for the relaxation of rigid molecules in a polystyrene matrix. The deviation of the points from the mean line may be attributed to errors involved in the

estimation of ν_{\max} . This is because the loss difference between one frequency and another is very low especially for 2-alkanones and 1-aminoalkanes.

Thus, it is reasonable to assume that the high temperature absorption of 2-alkanones and 1-aminoalkanes may be assigned to a molecular rotation. This is supported by the fact that for 2-alkanone with $n=8$ dispersed in a polypropylene matrix yields significantly different Eyring parameters ($\Delta H_E = 68.3 \text{ kJ mol}^{-1}$, $\Delta S_E = 188.5 \text{ J K}^{-1} \text{ mol}^{-1}$) from that in a polystyrene matrix ($\Delta H_E = 54.0 \text{ kJ mol}^{-1}$, $\Delta S_E = 65.5 \text{ J K}^{-1} \text{ mol}^{-1}$).

The effective dipole moments (μ_{eff}) calculated from the relation, $\mu_{\text{eff}} = (\mu_s^2 + \mu_m^2)^{\frac{1}{2}}$ where μ_s and μ_m moments govern the segmental and molecular rotation, respectively, correspond well with the literature values (see Table VII-3 and Table VII-4). For example, the μ_{eff} value for 2-heptanone is $[(2.01)^2 + (1.48)^2]^{\frac{1}{2}} = 2.5_0 \text{ D}$ which is in reasonable agreement with the literature value 2.61 D (see Table VII-3). The estimates of μ_{eff} values for the molecules are given in Table VII-3 and Table VII-4. Tables VII-3 and VII-4 also show that the calculated ratio of C_1/C_2 is in rough agreement with the loss factor ratio $\epsilon''_{(\max)H} / \epsilon''_{(\max)L}$ in Figures VII-1 and VII-2.

Table VII-5 shows that the energy difference

between the equilibrium positions of dipole for 2-alkanones and 1-aminoalkanes are low and lie in the range 0-6 kJ mol⁻¹. Likewise for 1-bromoalkanes, the two sites, symmetric barrier model seems adequate for the results of 2-alkanones and 1-aminoalkanes in a polystyrene matrix.

Altogether the present work on 2-alkanones in a viscous medium bears out what was previously inferred by Johari et al (2) for the dielectric absorption of 2-octanone in the microwave region. Although their results can be analyzed in terms of two relaxation times, the values are unrealistic and the mean relaxation time ($\tau_0 = 4 \times 10^{-12}$ s) suggests that there is little contribution from larger segments - the acetyl group rotation being the dominant process. In the glassy media, however, we see that the intramolecular and molecular processes are well separated (see Figure VII-1) and the contribution of the intramolecular and the molecular process to the total absorption is very similar (see Table VII-3). Our present findings seem to be in contrast with Crossley (3) who suggested that the relaxation time in 2-alkanones increases slightly with the increase in chain length and that the dielectric absorption is dominated by the terminal acetyl group rotation. But Figures VII-3 and VII-5 clearly show that the relaxation time at 150 K and ΔH_E values for the low temperature absorption increases appreciably

with the increase in the number of carbon atoms in the chain. The sole rotation of acetyl group cannot account for the appreciable increase in relaxation time and ΔH_E value as postulated by Crossley.

The present work for 1-aminoalkanes in a polystyrene matrix bears out what was previously inferred by Johari et al (2) for the dielectric absorption of n-octylamine in the pure liquid state. However, our results show a clear separation of the two processes and that the fast intramolecular (see Figure VII-2) process is not due to nitrogen inversion; it is an intramolecular rotation about the C-C bonds involving increasing segmental motion as n increases. Our results are not in agreement with Tay et al (6) who concluded that the dielectric absorption in primary amines is dominated by the terminal $-NH_2$ group rotation. The sole rotation of the terminal $-NH_2$ group can neither accounts for the appreciable increase in ΔH_E (see Figure VII-6) and the relaxation time (see Figure VII-4) with increasing chain length, nor for the linear relationship between ΔS_E and ΔH_E (see Figure VII-8). The present results for 1-aminoalkanes do not show H-bonding in a polystyrene matrix as was found by previous workers (7).

CONCLUSIONS

In viscous media, including both polymer matrices and glass forming solids, 2-alkanones and 1-aminoalkanes exhibit considerable flexibility which gives rise to dielectric absorptions. The enthalpy of activation for the low temperature absorption of 2-alkanones and 1-aminoalkanes lie in the ranges $17-28 \text{ kJ mol}^{-1}$ at 80-147 K and $14-24 \text{ kJ mol}^{-1}$ at 80-126 K, respectively, and is identified as the intramolecular rotation about the C-C bonds involving the movement of the polar end groups. The enthalpy of activation for the high temperature absorption of 2-alkanones and 1-aminoalkanes lies in the ranges $40-80 \text{ kJ mol}^{-1}$ at 160-290 K and $45-70 \text{ kJ mol}^{-1}$ at 190-290 K, respectively, and is characterized by a molecular rotation.

In 1-bromoalkanes (see Chapter V) and 2-alkanones, the contribution of the molecular and intramolecular processes to the total absorption is very similar (see Figure VII-1) whereas in 1-aminoalkanes, the intramolecular process is the dominating one (see Figure VII-2).

The nature of the polar end groups has negligible influence on the relaxation time and ΔH_E values of low temperature absorption. The intramolecular rotation about the C-C

bonds involving the movement of the polar end groups is the main contributor to the low temperature absorption.

The results for 2-alkanones and 1-aminoalkanes may be successfully analyzed in terms of a model which involves a molecular relaxation process (governed by a μ_m moment) and segmental motion involving movement of the polar end groups (characterized by a μ_s dipole moment). The extrapolated values of μ_s and μ_m at 330 K lead to a molecular dipole moment in reasonable agreement with literature values.

The energy differences between the equilibrium positions of the dipoles, ΔE_0 , for 2-alkanones and 1-aminoalkanes are very low and the two sites, symmetric barrier model seems adequate for the long chain polar molecules in a polystyrene matrix.

REFERENCES

1. J. H. Calderwood and C. P. Smyth, J. Am. Chem. Soc., 78, 1295(1956).
2. G. P. Johari, J. Crossley and C. P. Smyth, 91, 1597(1969).
3. J. Crossley, J. Chem. Phys., 56, 2549(1972).
4. A. Vyas and K. K. Srivastava, Bull. Chem. Soc. Japan, 43, 21313(1970).
5. S. K. Garg and P. K. Kadaba, 68, 737(1964).
6. S. P. Tay and J. Crossley, J. Chem. Phys., 56, 4303(1972).
7. F. J. A. Solsona and F. M. F. Marquina, J. Phys. D, App. Phys., 15, 1783(1982).
8. J. Gilchrist, Chem. Phys., 65, 1(1982).
9. H. A. Khwaja and S. Walker, Ad. Mol. Inter. and Relax. Processes, 22, 27(1982).
10. M. E. Huque. Private Communication, this laboratory.
11. S. P. Tay, Ph.D. Thesis, University of Salford, 1977.
12. H. A. Khwaja and S. Walker, Adv. Mol. Inter. and Relax. Process., 19, 1(1981).

TABLE VII-1: Relaxation time and Eyring activation parameters for the low temperature absorption of $\text{CH}_3(\text{CH}_2)_n\text{X}$ (where X = $-\text{CH}_2\text{OH}$, $-\text{COCH}_3$, $-\text{NH}_2$ and $-\text{CH}_2\text{Br}$) in a polystyrene matrix

X	ΔT (°K)	β range	Relaxation Times τ (s)		ΔG_E (kJ mol ⁻¹)		ΔH_E	ΔS_E
			100 K	150 K	100 K	150 K	kJ mol ⁻¹	J K ⁻¹ mol ⁻¹
			<u>n=3</u>					
$-\text{CH}_2\text{OH}^{10}$	84-104	0.19-0.23	1.3×10^{-4}	1.3×10^{-7}	16.0	16.0	16.1 ± 1.3	-0.6 ± 13.0
$-\text{NH}_2$	82-94	0.21-0.23	7.5×10^{-6}	1.2×10^{-8}	13.8	13.1	15.1 ± 1.7	13.7 ± 19.1
			<u>n=4</u>					
$-\text{CH}_2\text{Br}$	95-117	0.18-0.23	3.7×10^{-4}	1.0×10^{-7}	17.0	15.8	19.5 ± 1.1	24.4 ± 10.1
$-\text{CH}_2\text{OH}$	87-106	0.21-0.23	1.8×10^{-4}	1.5×10^{-7}	16.0	16.0	17.0 ± 1.2	3.0 ± 12.7
$-\text{COCH}_3$	85-104	0.20-0.21	1.0×10^{-4}	1.1×10^{-7}	16.0	15.9	16.2 ± 1.0	2.0 ± 10.8
			<u>n=5</u>					
$-\text{CH}_2\text{Br}$	96-116	0.22-0.27	1.1×10^{-3}	2.8×10^{-7}	17.9	17.0	19.6 ± 1.4	16.9 ± 13.5
$-\text{CH}_2\text{OH}$	95-117	0.21-0.23	8.0×10^{-4}	2.0×10^{-7}	18.0	17.0	20.1 ± 1.0	19.1 ± 10.0
$-\text{COCH}_3$	90-112	0.21-0.25	3.0×10^{-4}	1.4×10^{-7}	16.9	16.2	18.2 ± 1.0	13.4 ± 10.3
$-\text{NH}_2$	84-100	0.23-0.25	3.8×10^{-5}	2.4×10^{-8}	15.2	14.0	17.4 ± 3.2	22.3 ± 20.5
			<u>n=6</u>					
$-\text{CH}_2\text{Br}$	98-124	0.25-0.31	1.7×10^{-3}	6.2×10^{-7}	18.3	18.1	18.7 ± 1.3	4.0 ± 11.5
$-\text{CH}_2\text{OH}$	99-120	0.22-0.23	1.6×10^{-3}	3.7×10^{-7}	18.0	17.0	20.1 ± 1.4	17.0 ± 12.0
$-\text{COCH}_3$	95-116	0.22-0.26	1.3×10^{-3}	4.2×10^{-7}	18.0	17.6	19.0 ± 0.5	9.4 ± 5.1

TABLE VII-1: continued...

X	ΔT (°K)	β range	Relaxation Times τ (s)		ΔG_E (kJ mol ⁻¹)		ΔH_E	ΔS_E
			100 K	150 K	100 K	150 K	kJ mol ⁻¹	J K ⁻¹ mol ⁻¹
			<u>n=7</u>					
-CH ₂ OH	98-120	0.22-0.25	2.2×10^{-3}	5.5×10^{-7}	19.0	18.0	20.1±1.9	12.1±9.8
-NH ₂	93-111	0.24-0.28	4.3×10^{-4}	1.3×10^{-7}	17.1	16.1	19.1±0.5	20.0±5.0
			<u>n=8</u>					
-CH ₂ Br	106-130	0.26-0.32	1.2×10^{-2}	1.1×10^{-6}	19.9	18.8	22.0±0.6	21.4±11.5
-CH ₂ OH	102-126	0.21-0.23	1.0×10^{-2}	1.0×10^{-6}	20.0	19.0	22.0±0.8	21.1±7.0
-COCH ₃	105-128	0.24-0.30	1.2×10^{-2}	1.0×10^{-6}	19.9	18.7	22.4±0.4	24.7±3.4
-COCH ₃ (PP)‡	96-112	0.22-0.25	6.5×10^{-4}	2.4×10^{-7}	17.5	16.9	18.7±1.3	12.1±12.5
-COCH ₃ (GOTP)*	105-123	0.25-0.29	8.2×10^{-3}	1.4×10^{-6}	19.6	19.1	20.6±0.6	10.2±5.7
-COCH ₃ (SV)#	109-126	0.25-0.36	2.5×10^{-2}	1.5×10^{-6}	20.4	19.1	22.9±0.4	24.7±3.6
-NH ₂ (0.45 M)	47-117	0.24-0.32	1.3×10^{-3}	2.9×10^{-7}	18.1	17.1	20.1±1.1	19.8±10.3
-NH ₂ (0.60 M) ¹¹	105-158	0.20-0.40		5.0×10^{-7}		17.0	23.3±1.0	37.1±7.2

‡ is polypropylene

* is glassy o-terphenyl

is polyphenyl ether

TABLE VII-1: continued...

X	ΔT (°K)	$\bar{\epsilon}$ range	Relaxation Times τ (s)		ΔG_E (kJ mol ⁻¹)		ΔH_E	ΔS_E
			100 K	150 K	100 K	150 K	kJ mol ⁻¹	J K ⁻¹ mol ⁻¹
			<u>n=10</u>					
-CH ₂ Br	114-136	0.27-0.36	6.0×10^{-2}	2.8×10^{-6}	21.3	20.0	23.9±0.5	26.2±4.5
-CH ₂ OH	104-129	0.20-0.25	2.1×10^{-2}	1.6×10^{-6}	20.0	19.0	23.1±1.2	22.1±10.7
-COCH ₃	111-132	0.25-0.36	2.5×10^{-2}	1.7×10^{-6}	20.5	19.3	23.2	24.4±4.7
-NH ₂	102-124	0.22-0.30	5.3×10^{-3}	4.8×10^{-7}	19.2	17.7	22.2±0.7	28.9±5.8
			<u>n=12</u>					
-CH ₂ Br	114-135	0.27-0.33	1.4×10^{-1}	$4. \times 10^{-6}$	21.9	20.4	24.9±0.8	28.6±6.2
-CH ₂ OH	116-142	0.20-0.23	1.2×10^{-1}	3.2×10^{-6}	22.0	20.0	25.0±0.9	35.3±7.1
-COCH ₃	113-136	0.25-0.34	1.2×10^{-1}	3.9×10^{-6}	21.8	20.4	24.7±0.3	28.8±2.7
			<u>n=14</u>					
-CH ₂ Br	116-144	0.25-0.35	4.2×10^{-1}	6.2×10^{-6}	22.9	21.0	26.5±0.8	36.7±5.4
-CH ₂ OH	115-133	0.18-0.22	2.2×10^{-1}	3.7×10^{-6}	22.0	20.0	26.0±1.4	41.3±11.5
-COCH ₃	116-141	0.26-0.34	3.6×10^{-1}	6.6×10^{-6}	22.7	4.0	26.2±0.6	34.7±4.4
			<u>n=16</u>					
-CH ₂ Br	119-147	0.25-0.35	5.3×10^{-1}	9.6×10^{-6}	23.1	21.5	26.2±0.5	31.4±4.2
-CH ₂ OH	116-139	0.19-0.28	1.1×10^{-1}	2.8×10^{-6}	22.0	20.0	25.1±1.5	36.4±11.7
-COCH ₃	124-144	0.27-0.36	1.1×10^0	1.2×10^{-5}	23.7	21.8	27.4±0.8	37.8±6.2
			<u>n=18</u>					
-CH ₂ Br	120-146	0.24-0.34	1.2×10^0	1.3×10^{-5}	23.7	21.8	27.4±1.1	27.4±8.5
-CH ₂ OH	114-137	0.15-0.27	3.3×10^{-1}	4.6×10^{-6}	23.0	21.0	27.4±2.1	42.3±16.5

TABLE VII-2: Relaxation time and Eyring parameters for the high temperature absorption of $\text{CH}_3(\text{CH}_2)_n\text{X}$
 (where X = $-\text{CH}_2\text{Br}$, $-\text{CH}_2\text{OH}$, $-\text{COCH}_3$ and $-\text{NH}_2$)

X	ΔT (°K)	E range	Relaxation Times τ (s)		ΔG_E (kJ mol ⁻¹)		ΔH_E kJ mol ⁻¹	ΔS_E J K ⁻¹ mol ⁻¹
			200 K	300 K	200 K	300 K		
			<u>n=4</u>					
$-\text{CH}_2\text{Br}$	168-204	0.16-0.17	6.6×10^{-5}	7.9×10^{-8}	32.3	30.7	31.6 ± 2.0	-4.0 ± 10.6
$-\text{COCH}_3$	169-196	0.14-0.19	2.9×10^{-5}	2.9×10^{-8}	30.9	30.2	41.9 ± 2.6	40.9 ± 31.6
			<u>n=5</u>					
$-\text{CH}_2\text{Br}$	189-213	0.15-0.20	6.1×10^{-4}	3.3×10^{-7}	36.0	36.3	35.4 ± 2.8	-3.2 ± 4.5
$-\text{CH}_2\text{OH}$	196-220	0.13-0.20	8.2×10^{-5}		33.0		59.0 ± 4.0	73.1 ± 30.9
$-\text{COCH}_3$	183-211	0.19-0.21	1.9×10^{-4}	9.9×10^{-9}	34.0	27.5	47.2 ± 3.2	65.6 ± 16.3
$-\text{NH}_2$	192-212	0.25-0.31	4.3×10^{-4}	3.0×10^{-8}	35.4	30.3	45.1 ± 3.7	51.1 ± 8.6
			<u>n=6</u>					
$-\text{CH}_2\text{Br}$	205-249	0.15-0.19	5.0×10^{-3}	1.3×10^{-6}	39.5	39.6	39.3 ± 3.3	-2.0 ± 14.0
$-\text{CH}_2\text{OH}$	196-220		1.6×10^{-3}		38.0		2.3 ± 6.3	73.4 ± 30.7
$-\text{COCH}_3$	187-212	0.16-0.22	3.3×10^{-4}	1.6×10^{-7}	35.0	28.7	47.5 ± 5.0	62.6 ± 25.8
			<u>n=7</u>					
$-\text{CH}_2\text{OH}$	198-234	0.19-0.23	5.3×10^{-3}		40.0		49.5 ± 3.3	48.3 ± 15.4
$-\text{NH}_2$	196-223	0.20-0.25	1.9×10^{-3}	5.1×10^{-8}	37.9	15.3	50.5 ± 6.0	62.9 ± 28.9
			<u>n=8</u>					
$-\text{CH}_2\text{Br}$	220-260	0.16-0.19	4.1×10^{-2}	2.3×10^{-6}	43.0	41.0	46.9 ± 4.5	19.3 ± 18.9
$-\text{CH}_2\text{OH}$	219-243	0.17-0.21	5.8×10^{-2}		44.0		62.3 ± 9.5	91.3 ± 39.4
$-\text{COCH}_3$	210-235	0.17-0.20	1.2×10^{-2}	1.6×10^{-7}	40.9	34.4	54.1 ± 2.8	65.6 ± 12.7
$-\text{COCH}_3$ (PP)	179-196	0.18-0.19	2.3×10^{-5}	1.8×10^{-11}	30.6	11.8	68.3 ± 3.2	188.5 ± 17.2
$-\text{NH}_2$	239-265	0.24-0.32	2.2×10^0	1.4×10^{-6}	49.6	39.8	69.4 ± 6.1	98.5 ± 12.5

TABLE VII-2: continued...

X	ΔT (°K)	E range	Relaxation Times τ (s)		ΔG_E (kJ mol ⁻¹)		ΔH_E	ΔS_E
			200 K	300 K	200 K	300 K	kJ mol ⁻¹	J K ⁻¹ mol ⁻¹
-NH ₂	210-235	0.16-0.23	1.4×10^{-2} ⁿ⁼⁹	3.1×10^{-7}	41.0	36.1	51.4±2.3	50.8±10.2
-CH ₂ Br	236-261	0.16-0.20	2.5×10^{-1} ⁿ⁼¹⁰	4.6×10^{-6}	46.0	42.8	52.4±6.8	31.8±28.0
-CH ₂ OH	239-261	0.20-0.25	3.4×10^0		50.0		74.3±7.4	119.4±28.5
-COCH ₃	252-269	0.15-0.16	1.4×10^0	9.5×10^{-6}	48.9	44.7	57.3±3.8	41.1±0.1
-NH ₂	217-240	0.13-0.18	6.4×10^{-2}	1.6×10^{-7}	43.8	34.4	62.4±8.8	93.2±38.7
-NH ₂	248-283	0.12-0.17	6.9×10^0 ⁿ⁼¹¹	6.8×10^{-6}	51.5	43.8	67.0±7.9	77.0±30.0
-CH ₂ Br	237-280	0.15-0.22	5.4×10^{-1} ⁿ⁼¹²	6.1×10^{-6}	47.3	43.6	54.7±6.5	37.3±25.1
-CH ₂ OH	229-256	0.20-0.23	1.3×10^0		49.0		64.2±3.3	74.3±13.8
-COCH ₃	221-233	0.15-0.24	8.0×10^{-2}	1.1×10^{-7}	44.0	33.6	65.2±5.2	105.2±23.0
-CH ₂ Br	238-279	0.13-0.20	1.3×10^1 ⁿ⁼¹⁴	6.7×10^{-6}	48.8	43.8	58.8±5.4	50.0±21.3
-CH ₂ OH	259-272	0.19-0.28	4.7×10^2		59.0		87.2±9.2	141.3±34.8
-COCH ₃	257-284	0.14-0.17	6.9×10^0	1.5×10^{-5}	51.5	45.8	63.0±2.9	57.0±11.0

TABLE VII-2 continued...

X	T (°K)	τ range	Relaxation Times τ (s)		ΔG _E (kJ mol ⁻¹)		ΔH _E	ΔS _E
			200 K	300 K	200 K	300 K	kJ mol ⁻¹	J K ⁻¹ mol ⁻¹
-CH ₂ Br	238-279	0.13-0.20	$1.3 \times 10^{\frac{n=14}{1}}$	6.7×10^{-6}	48.8	43.8	58.8±5.4	50.0±21.3
-CH ₂ OH	259-272	0.10-0.28	4.7×10^2		59.0		87.2±9.2	141.3±34.8
-COCH ₃	257-284	0.14-0.17	6.9×10^0	1.5×10^{-5}	51.5	45.8	63.0±2.9	57.0±11.0
-CH ₂ Br	245-299	0.16-0.21	$3.0 \times 10^{\frac{n=16}{1}}$	8.7×10^{-6}	50.1	44.4	61.6±3.7	57.1±11.7
-COCH ₃	262-278	0.13-0.16	5.2×10^1	5.6×10^{-6}	54.9	43.3	78.0±9.7	115.6±36.5
-CH ₂ Br	262-299	0.15-0.17	$6.2 \times 10^{\frac{n=18}{1}}$	1.2×10^{-5}	55.2	46.8	72.0±5.3	84.1±19.2
-CH ₂ Br	264-297	0.15-0.16	$2.1 \times 10^{\frac{n=20}{2}}$	1.7×10^{-5}	57.2	46.2	79.5±6.8	111.5±24.6

TABLE VII-3: μ_s and μ_m are extrapolated dipole moments at 330 K. μ_{eff} from $\mu_{\text{eff}} = (\mu_m^2 + \mu_s^2)^{1/2}$ and

$$C_2 = \mu_s^2 / (\mu_m^2 + \mu_s^2) \text{ for } \text{CH}_3(\text{CH}_2)_n\text{COCH}_3 \text{ in polystyrene}$$

n	μ_s 330 K (D)	μ_m 330 K (D)	μ_{eff} (D)	μ_{lit} (D)	C_2	$C_1/C_2 = \mu_m^2 / \mu_s^2$	$\epsilon''_{(\text{max})\text{H}} / \epsilon''_{(\text{max})\text{L}}$
4	2.0 ₁	1.4 ₈	2.5 ₀	2.61	0.64	0.54	1.50
5	1.7 ₅	2.1 ₂	2.6 ₉	2.72	0.41	1.65	2.27
6	1.7 ₆	1.9 ₅	2.6 ₃		0.45	1.23	1.29
8	1.9 ₅	1.8 ₅	2.6 ₉	2.71	0.53	0.90	0.89
10	1.9 ₈	1.5 ₁	2.4 ₅		0.63	0.58	0.53
12	1.9 ₃	1.7 ₈	2.6 ₃		0.54	0.85	0.77
14	1.7 ₈	1.4 ₅	2.3 ₀		0.60	0.66	0.65
16	1.8 ₀	1.8 ₉	2.6 ₁		0.48	1.10	1.00

TABLE VII-4: μ_m and μ_s are extrapolated dipole moments at 330 K. μ_{eff} from $\mu_{\text{eff}} = (\mu_m^2 + \mu_s^2)^{1/2}$ and $C_2 = \mu_s^2 / (\mu_m^2 + \mu_s^2)$ for $\text{CH}_3(\text{CH}_2)_n\text{NH}_2$ in polystyrene

n	μ_s 330 K (D)	μ_m 330 K (D)	μ_{eff} (D)	μ_{lit} (D)	C_2	$C_1/C_2 = \mu_m^2 / \mu_s^2$	$\epsilon''(\text{max})_H / \epsilon''(\text{max})_L$
5	1.3 ₅	0.3 ₀	1.3 ₈	1.32	0.95	0.16	0.84
7	1.3 ₀	0.5 ₅	1.4 ₁	1.42	0.85	0.18	0.47
8	1.1 ₃	0.9 ₇	1.4 ₉		0.58	0.83	1.42
9	1.1 ₀	0.6 ₃	1.2 ₇		0.75	0.33	0.24
10	1.2 ₀	0.5 ₁	1.3 ₀		0.85	0.18	0.42
11	1.2 ₆	0.8 ₀	1.4 ₉		0.71	0.40	0.59

TABLE VII-5: Energy differences, ΔE_0 between the equilibrium positions positions of the dipole for $\text{CH}_3(\text{CH}_2)_n\text{X}$ (where $\text{X} = -\text{COCH}_3$ and $-\text{NH}_2$) in a polystyrene matrix.

n	Temperature Region of Absorption	ΔE_0 (kJ mol ⁻¹)	
		X = COCH ₃	X = -NH ₂
2	LTA		4.40
	HTA		-
3	LTA		4.51
	HTA		-
4	LTA	0.71	0.00
	HTA	0.07	
5	LTA	4.75	0.38
	HTA	3.80	0.35
6	LTA	6.65	
	HTA	5.35	
7	LTA		0.30
	HTA		0.53
8	LTA	0.00	0.00
	HTA	5.38	5.08
9	LTA		4.85
	HTA		0.00
10	LTA	5.00	3.91
	HTA	2.93	0.29
11	LTA		4.85
	HTA		0.86
12	LTA	4.50	
	HTA	4.83	
14	LTA	4.62	
	HTA	4.84	
16	LTA	7.48	
	HTA	3.53	

TABLE VII-6: Fuoss-Kirkwood parameters, ϵ_{∞} and dipole moments at various temperatures for 2-alkanones and 1-aminoalkanes in a polystyrene matrix

T(K)	$10^6 \tau$ (s)	$\log v_{\max}$	β	$10^3 \epsilon''_{\max}$	ϵ_{∞}	μ (D)
<u>0.38 M 2-heptanone (lower temperature process)</u>						
85.3	2978.60	1.72	0.20	13.53	2.900	0.76
86.6	2227.10	1.85	0.20	13.83	2.899	0.78
87.9	1697.90	1.97	0.20	14.10	2.898	0.79
88.9	1390.10	2.05	0.20	14.25	2.895	0.81
90.3	1029.70	2.18	0.20	14.47	2.894	0.83
93.4	443.69	2.55	0.20	15.01	2.890	0.85
95.9	277.18	2.75	0.20	15.46	2.888	0.88
99.8	104.93	3.18	0.20	16.04	2.883	0.91
103.7	43.58	3.56	0.20	16.72	2.878	0.95
<u>0.38 M 2-heptanone (higher temperature process)</u>						
169.6	3495.40	1.65	0.14	20.93	2.999	1.52
173.7	1450.70	2.04	0.16	21.29	3.008	1.48
176.2	839.70	2.27	0.16	21.30	3.007	1.49
179.8	575.09	2.44	0.17	21.47	3.012	1.49
183.7	306.86	2.71	0.18	21.56	3.105	1.44
187.2	161.39	2.99	0.17	21.46	3.015	1.49
191.2	96.76	3.21	0.18	21.62	3.021	1.48
195.7	53.50	3.47	0.18	21.65	3.022	1.48
<u>0.77 M 2-octanone (lower temperature process)</u>						
90.7	2752.00	1.76	0.21	15.24	2.904	0.57
92.5	1876.70	1.92	0.21	15.65	2.902	0.59
95.2	1070.90	2.17	0.21	16.18	2.899	0.61
97.9	531.54	2.47	0.21	16.65	2.897	0.62
102.4	199.76	2.90	0.21	17.42	2.894	0.65
105.3	95.72	3.22	0.22	17.93	2.890	0.66
108.3	50.20	3.50	0.24	18.51	2.880	0.67
111.2	27.60	3.76	0.23	19.05	2.917	0.68

TABLE VII-6: continued...

T(K)	$10^6 \tau$ (s)	$\log v_{\max}$	β	$10^3 \epsilon''_{\max}$	ϵ_{∞}	μ (D)
<u>0.77 M 2-octanone (higher temperature process)</u>						
183.9	2212.20	1.85	0.20	33.92	3.066	1.18
187.5	1364.44	2.06	0.20	33.96	3.076	1.21
191.7	716.05	2.36	0.19	33.93	3.063	1.24
195.5	409.92	2.58	0.19	33.84	3.064	1.26
198.3	280.09	2.75	0.18	33.75	3.062	1.28
201.8	151.80	3.02	0.17	33.32	3.054	1.32
205.6	84.35	3.27	0.17	33.14	3.052	1.33
210.7	37.87	3.62	0.17	32.88	3.045	1.37
<u>0.69 M 2-nonanone (lower temperature process)</u>						
96.4	2898.20	1.74	0.23	22.79	2.823	0.74
98.9	1616.00	1.99	0.23	23.44	2.818	0.77
101.5	949.22	2.22	0.22	24.00	2.815	0.80
104.1	499.23	2.50	0.23	24.66	2.820	0.81
106.8	286.42	2.74	0.24	25.24	2.820	0.81
109.8	150.62	3.02	0.23	25.69	2.823	0.84
112.8	81.97	3.28	0.24	26.34	2.831	0.85
116.0	45.26	3.54	0.25	27.20	2.839	0.86
<u>0.69 M 2-nonanone (higher temperature process)</u>						
187.0	2806.60	1.75	0.21	27.30	3.018	1.34
189.5	1837.10	1.93	0.21	27.39	3.018	1.31
190.0	1252.50	2.10	0.21	27.20	3.028	1.28
194.2	823.37	2.28	0.20	26.87	3.027	1.23
196.0	572.07	2.44	0.20	26.80	3.027	1.19
198.5	412.24	2.58	0.20	26.59	3.024	1.18
203.7	269.66	2.77	0.19	26.16	3.019	1.17
205.6	169.67	2.97	0.17	25.62	3.072	1.15
209.0	03.99	3.27	0.16	25.33	3.013	1.14
212.0	50.14	3.50	0.16	24.98	3.001	1.33

TABLE VII-6: continued...

T(K)	$10^6 \tau$ (s)	$\log v_{\max}$	β	$10^3 \epsilon''_{\max}$	ϵ_{∞}	μ (D)
<u>0.67 M 2-undecanone (lower temperature process)</u>						
105.4	2707.60	1.76	0.24	23.76	2.881	0.78
106.5	2087.00	1.88	0.24	24.13	2.881	0.78
109.0	1215.80	2.11	0.24	24.72	2.879	0.85
111.7	626.96	2.40	0.25	25.31	2.876	0.81
114.3	358.55	2.64	0.25	25.87	2.876	0.83
117.2	204.04	2.89	0.26	26.44	2.874	0.84
119.8	113.78	3.14	0.26	26.91	2.874	0.84
123.4	56.71	3.44	0.28	27.79	2.875	0.85
127.3	28.35	3.74	0.29	28.60	2.875	0.86
<u>0.67 M 2-undecanone (higher temperature process)</u>						
210.4	2036.20	1.89	0.19	28.06	3.067	1.29
212.9	1556.90	2.01	0.19	27.92	3.071	1.30
216.6	979.95	2.21	0.18	27.44	3.067	1.33
219.3	632.89	2.40	0.18	27.10	3.068	1.33
222.0	429.66	2.56	0.18	26.78	3.070	1.32
225.9	259.95	2.78	0.17	26.48	3.070	1.36
229.6	147.82	3.03	0.17	25.74	3.064	1.39
239.3	83.91	3.27	0.17	25.08	3.069	1.34
<u>0.66 M 2-undecanone (polypropylene) (lower temperature process)</u>						
96.0	1533.38	2.01	0.22	7.5	2.458	0.48
98.3	961.68	2.21	0.22	7.7	2.457	0.50
100.8	533.33	2.47	0.23	7.9	2.456	0.50
103.4	314.17	2.70	0.23	8.1	2.456	0.52
106.0	182.45	2.94	0.23	8.3	2.455	0.53
190.1	85.84	3.26	0.23	8.5	2.452	0.54
111.3	53.85	3.47	0.24	8.7	2.452	0.54

TABLE VII-6: continued...

T(K)	$10^6 \tau$ (s)	$\log v_{\max}$	β	$10^3 \epsilon''_{\max}$	ϵ_{∞}	μ (D)
<u>0.66 M 2-undecanone (polypropylene) (higher temperature process)</u>						
179.5	2544.79	1.79	0.19	14.5	2.541	0.99
181.3	1735.30	1.96	0.19	14.7	2.510	1.01
183.1	1171.67	2.13	0.18	14.9	2.474	1.03
186.0	567.75	2.44	0.18	15.2	2.510	1.05
188.8	285.64	2.74	0.19	15.5	2.513	1.05
190.6	199.21	2.90	0.18	15.7	2.513	1.07
193.1	94.27	3.22	0.18	15.9	2.509	1.09
195.8	54.64	3.46	0.18	16.0	2.510	1.10
<u>9.1% (by wt.) 2-undecanone (Santovac)</u>						
109.8	1604.99	1.99	0.24	16.6		
111.6	1088.95	2.16	0.24	16.9		
112.1	948.57	2.22	0.24	16.9		
115.7	416.03	2.58	0.25	17.3		
118.0	278.84	2.75	0.26	17.6		
120.0	151.31	3.02	0.26	17.8		
122.4	110.87	3.15	0.26	17.9		
125.1	66.09	3.38	0.27	18.2		
<u>8.5% (by wt.) 2-undecanone (G.O.T.P.)</u>						
105.1	2174.45	1.86	0.25	5.9		
107.8	1259.58	2.10	0.25	6.1		
110.3	749.83	2.32	0.25	6.2		
112.8	440.71	2.55	0.26	6.3		
116.1	223.13	2.85	0.26	6.5		
119.0	132.38	3.07	0.27	6.5		
122.8	63.92	3.39	0.28	6.7		

TABLE VII-6: continued...

T(K)	$10^6 \tau$ (s)	$\log v_{\max}$	β	$10^3 \epsilon''_{\max}$	ϵ_{∞}	μ (D)
<u>0.37 M 2-tridecanone (lower temperature process)</u>						
111.6	1162.71	2.13	0.27	15.70	2.326	0.94
113.2	904.07	2.24	0.26	15.90	2.340	0.97
115.5	547.37	2.46	0.26	16.20	2.339	0.98
117.8	323.77	2.69	0.27	16.50	2.342	0.98
121.2	169.80	2.97	0.28	16.80	2.338	1.00
124.0	98.27	3.20	0.29	17.00	2.337	0.99
124.5	85.51	3.27	0.29	17.09	2.332	0.99
126.1	62.47	3.40	0.30	17.34	2.332	1.00
129.0	38.88	3.61	0.32	17.66	2.335	0.99
131.1	26.52	3.77	0.32	17.86	2.335	1.00
<u>0.37 M 2-tridecanone (higher temperature process)</u>						
239.8	2246.77	1.85	0.16	7.4	2.434	1.18
242.5	1695.75	1.97	0.17	7.3	2.434	1.18
246.2	1314.85	2.08	0.16	7.2	2.433	1.18
248.7	1155.45	2.13	0.16	7.2	2.431	1.20
252.3	846.12	2.27	0.16	7.1	2.431	1.21
254.3	680.36	2.36	0.16	7.0	2.430	1.22
258.0	466.56	2.53	0.16	6.9	2.429	1.20
260.0	376.33	2.62	0.15	6.8	2.425	1.24
263.1	260.43	2.78	0.15	6.7	2.425	1.23
268.3	159.62	2.99	0.15	6.4	2.421	1.22
<u>0.18 M 2-pentadecanone (lower temperature process)</u>						
113.0	3334.60	1.67	0.25	13.91	2.872	1.17
114.7	2239.90	1.85	0.26	14.20	2.871	1.18
116.5	1502.80	2.02	0.27	14.44	2.871	1.18
119.2	846.85	2.27	0.27	14.77	2.871	1.20
122.0	460.38	2.53	0.28	15.07	2.868	1.21
124.9	258.06	2.79	0.29	15.42	2.868	1.22
127.7	145.17	3.04	0.29	15.64	2.866	1.24
131.3	72.36	3.34	0.31	16.00	2.867	1.24
135.1	39.15	3.60	0.33	16.47	2.868	1.23

TABLE VII-6: continued...

T(K)	$10^6 \tau$ (s)	$\log v_{\max}$	β	$10^3 \epsilon''_{\max}$	ϵ_{∞}	μ (D)
<u>0.18 M 2-pentadecanone (higher temperature process)</u>						
220.9	1892.91	1.92	0.23	11.22	2.958	1.50
222.6	1314.30	2.08	0.22	11.19	2.955	1.54
224.4	969.66	2.21	0.21	11.11	2.951	1.60
228.0	408.78	2.59	0.17	10.79	2.936	1.78
230.1	558.36	2.45	0.19	11.03	2.948	1.68
233.0	278.74	2.75	0.15	10.65	2.991	1.87
<u>0.37 M 2-heptadecanone (lower temperature process)</u>						
116.1	3662.15	1.63	0.26	21.6	2.855	1.02
117.4	2826.00	1.75	0.26	21.8	2.790	1.03
119.1	1862.44	1.93	0.27	22.3	2.855	1.03
122.2	976.95	2.21	0.27	22.8	2.853	1.05
125.0	551.97	2.45	0.28	23.3	2.853	1.05
128.6	262.45	2.78	0.29	23.8	2.852	1.07
131.8	129.89	3.08	0.29	24.1	2.850	1.08
136.0	61.57	3.41	0.32	24.9	2.851	1.07
140.1	30.00	3.72	0.33	25.4	2.853	1.07
<u>0.37 M 2-heptadecanone (higher temperature process)</u>						
257.9	997.52	2.12	0.17	0.36	2.952	1.21
263.0	583.92	2.43	0.16	0.05	2.942	1.24
267.9	358.36	2.64	0.16	8.79	2.941	1.23
272.9	213.99	2.87	0.15	8.54	2.936	1.25
278.3	95.22	3.15	0.14	8.23	2.928	1.30
283.4	45.87	3.35	0.14	8.06	2.929	1.28

TABLE VII-6: continued...

T(K)	$10^6 \tau$ (s)	$\log v_{\max}$	β	$10^3 \epsilon''_{\max}$	ϵ_{∞}	μ (D)
<u>0.29 M 2-nonadecanone (lower temperature process)</u>						
124.3	1344.40	2.07	0.27	22.34	2.841	1.18
126.4	900.65	2.24	0.28	22.82	2.880	1.19
127.8	679.83	2.36	0.28	23.07	2.880	1.19
130.1	410.01	2.58	0.29	23.37	2.879	1.20
131.2	313.80	2.70	0.29	23.56	2.879	1.19
134.2	183.09	2.93	0.30	23.96	2.879	1.20
138.1	83.56	3.28	0.32	24.52	2.878	1.21
143.2	37.40	3.62	0.35	25.48	2.875	1.20
<u>0.29 M 2-nonadecanone (higher temperature process)</u>						
261.8	535.38	2.47	0.15	10.3	2.987	1.51
263.0	438.03	2.56	0.15	10.2	2.992	1.52
265.0	363.67	2.64	0.15	10.0	2.987	1.49
268.0	279.45	2.75	0.15	9.9	2.983	1.53
270.0	228.00	2.84	0.14	9.8	2.983	1.53
272.0	147.72	3.03	0.14	9.6	2.980	1.55
274.0	102.02	3.19	0.14	9.5	2.974	1.57
277.6	68.87	3.36	0.13	9.4	2.970	1.58
<u>0.40 M 1-propylamine (lower temperature process)</u>						
82.8	448.63	2.55	0.26	3.1	2.784	0.33
83.2	456.00	2.54	0.24	3.1	2.786	0.34
85.0	301.44	2.72	0.26	3.1	2.786	0.33
87.1	175.26	2.96	0.27	3.1	2.787	0.33
89.0	103.76	3.19	0.27	3.2	2.787	0.34
89.7	91.79	3.24	0.27	3.2	2.788	0.34
91.8	55.87	3.46	0.28	3.2	2.788	0.33
93.6	40.72	3.59	0.28	3.2	2.795	0.34

TABLE VII-6: continued...

T(K)	$10^6 \tau$ (s)	$\log v_{\max}$	β	$10^3 \epsilon''_{\max}$	ϵ_{∞}	μ (D)
<u>0.35 M 1-butylamine (lower temperature process)</u>						
81.8	502.44	2.50	0.23	2.9	2.783	0.36
83.8	293.34	2.73	0.23	3.0	2.784	0.37
85.2	224.91	2.85	0.22	3.0	2.797	0.38
87.6	141.23	3.05	0.24	3.1	2.786	0.37
88.9	71.93	3.35	0.22	3.1	2.796	0.39
91.0	44.81	3.55	0.22	3.2	2.784	0.40
92.8	34.03	3.67	0.23	3.2	2.784	0.40
94.0	26.25	3.78	0.22	3.2	2.791	0.41
<u>0.74 M 1-hexylamine (lower temperature process)</u>						
84.3	1934.20	1.91	0.23	3.4	2.883	0.26
85.4	1548.30	2.01	0.23	3.4	2.882	0.26
87.4	905.54	2.24	0.23	3.5	2.880	0.27
90.5	431.51	2.56	0.24	3.61	2.879	0.28
92.7	250.51	2.80	0.24	3.69	2.875	0.28
96.1	99.82	3.20	0.23	3.77	2.873	0.29
100.0	31.32	3.70	0.22	3.93	2.869	0.31
<u>0.74 M 1-hexylamine (higher temperature process)</u>						
190.8	2321.90	1.83	0.23	2.38	2.868	0.33
192.7	1349.60	2.07	0.25	2.35	2.867	0.32
195.2	850.53	2.27	0.26	2.32	2.865	0.31
197.6	610.01	2.41	0.27	2.29	2.865	0.31
200.2	389.95	2.61	0.28	2.33	2.851	0.30
200.8	273.89	2.76	0.30	2.31	2.851	0.29
206.6	192.61	2.91	0.31	2.27	2.850	0.29
211.6	89.79	3.24	0.32	2.28	2.851	0.29

TABLE VII-6: continued...

T(K)	$10^6 \tau$ (s)	$\log v_{\max}$	β	$10^3 \epsilon''_{\max}$	ϵ_{∞}	μ (D)
<u>0.60 M 1-octylamine (lower temperature process)</u>						
92.9	2544.61	1.79	0.24	9.0	2.882	0.48
95.0	1548.69	2.01	0.24	9.2	2.885	0.49
97.2	878.38	2.25	0.24	9.4	2.884	0.50
100.0	440.54	2.55	0.25	9.6	2.888	0.51
103.3	205.71	2.88	0.25	9.8	2.885	0.49
106.6	94.57	3.22	0.27	10.0	2.881	0.52
108.7	58.83	3.43	0.28	10.1	2.882	0.51
111.8	34.92	3.65	0.30	10.4	2.863	0.51
<u>0.60 M 1-n-octylamine (higher temperature process)</u>						
196.9	4432.87	1.55	0.21	5.40	2.929	0.58
198.9	1857.57	1.93	0.23	5.4	2.936	0.55
200.9	1434.14	2.04	0.24	5.3	2.928	0.54
203.5	997.48	2.20	0.23	5.2	2.917	0.55
206.3	698.87	2.35	0.23	5.2	2.915	0.55
210.7	368.34	2.63	0.24	5.1	2.933	0.54
214.5	241.63	2.81	0.22	5.0	2.909	0.57
217.7	162.25	2.99	0.21	4.9	2.907	0.57
222.4	77.94	3.31	0.20	4.8	2.901	0.59
227.4	38.95	3.61	0.18	4.7	2.897	0.65
<u>0.45 M 1-nonylamine (lower temperature process)</u>						
97.3	2571.66	1.79	0.24	6.9	2.960	0.50
99.2	1799.57	1.95	0.24	7.2	2.959	0.51
100.0	1381.06	2.06	0.24	7.3	2.68	0.52
101.5	808.36	2.29	0.24	7.4	2.956	0.53
104.4	517.01	2.49	0.31	8.3	2.963	0.50
197.2	240.48	2.82	0.25	7.7	2.955	0.54
112.6	79.80	3.30	0.25	7.8	2.949	0.56
116.3	39.14	3.60	0.27	8.1	2.945	0.56

TABLE VII-6: continued...

T(K)	$10^6 \tau$ (s)	$\log v_{\max}$	β	$10^3 \epsilon''_{\max}$	ϵ_{∞}	μ (D)
<u>0.45 M 1-nonylamine (higher temperature process)</u>						
239.0	1981.52	1.91	0.29	10.3	2.743	0.90
244.0	970.44	2.22	2.80	10.0	2.740	0.91
249.0	501.36	2.50	0.25	9.8	2.733	0.97
252.0	341.39	2.67	0.23	9.4	2.731	1.00
256.0	189.25	2.93	0.18	9.2	2.722	1.12
265.0	57.85	3.45	0.21	9.3	2.724	1.06
<u>0.47 M 1-decylamine (lower temperature process)</u>						
104.0	962.02	2.22	0.24	9.8	2.733	0.56
105.2	745.41	2.33	0.24	9.9	2.732	0.63
106.8	497.75	2.51	0.25	10.0	2.730	0.63
109.0	291.72	2.74	0.26	10.2	2.731	0.63
120.0	139.30	3.05	0.25	10.2	2.732	0.65
115.0	74.75	3.33	0.28	10.5	2.733	0.63
117.2	44.70	3.55	0.29	10.7	2.731	0.63
<u>0.47 M 1-decylamine (higher temperature process)</u>						
210.0	2882.25	1.74	0.23	3.0	2.759	0.50
212.8	2412.29	1.89	0.22	2.9	2.788	0.50
215.9	1904.02	2.08	0.22	2.9	2.759	0.51
218.8	1030.76	2.25	0.21	2.8	2.755	0.53
222.8	907.65	2.48	0.20	2.8	2.753	0.54
226.5	759.66	2.65	0.19	2.7	2.752	0.54
230.6	493.35	2.89	0.17	2.7	2.743	0.44
234.7	446.74	3.15	0.16	2.6	2.744	0.59

TABLE VII-6: continued...

T(K)	$10^6 \tau$ (s)	$\log v_{\max}$	β	$10^3 \epsilon''_{\max}$	ϵ_{∞}	μ (D)
<u>0.56 M 1-undecylamine (lower temperature process)</u>						
102.0	2955.90	1.73	0.22	9.38	2.869	0.55
105.8	1250.30	2.10	0.23	9.72	2.869	0.56
109.7	478.39	2.52	0.24	9.89	2.866	0.57
112.6	231.87	2.83	0.25	10.10	2.864	0.58
115.3	130.09	3.08	0.26	10.23	2.884	0.57
118.1	70.79	3.35	0.27	10.39	2.864	0.57
121.0	43.48	3.56	0.29	10.56	2.864	0.57
123.8	26.10	3.78	0.30	10.69	2.863	0.56
<u>0.56 M 1-undecylamine (higher temperature process)</u>						
217.5	2753.6	1.75	0.20	2.75	3.036	0.45
219.8	1983.9	1.98	0.17	2.64	2.890	0.49
223.1	1443.4	2.13	0.17	2.63	2.873	0.49
226.5	1200.7	2.29	0.17	2.61	2.871	0.50
230.0	737.1	2.49	0.18	2.60	2.867	0.51
233.0	689.6	2.69	0.16	2.57	2.864	0.51
235.6	580.1	2.99	0.16	2.57	2.861	0.52
239.5	454.8	3.23	0.13	2.52	2.854	0.57
<u>0.51 M 1-dodecylamine (lower temperature process)</u>						
105.8	2289.00	1.84	0.22	8.22	2.741	0.57
107.7	1444.70	2.04	0.22	8.39	2.885	0.56
109.9	966.71	2.21	0.22	8.42	2.734	0.59
111.5	602.83	2.42	0.23	8.54	2.884	0.57
114.8	276.52	2.76	0.24	8.73	2.884	0.57
116.5	208.28	2.88	0.24	8.78	2.883	0.57
119.2	101.17	3.19	0.25	8.90	2.882	0.58
123.3	45.65	3.54	0.27	9.15	2.879	0.57
125.9	29.86	3.72	0.28	0.26	2.876	0.59

TABLE VII-6: continued...

T(K)	$10^6 \tau$ (s)	$\log v_{\max}$	β	$10^3 \epsilon''_{\max}$	ϵ_{∞}	μ (D)
<u>0.51 M 1-dodecylamine (higher temperature process)</u>						
248.1	1827.20	1.94	0.14	4.60	2.877	0.78
250.9	1327.11	2.07	0.15	4.70	2.876	0.78
254.7	944.56	2.22	0.14	4.61	2.871	0.82
258.8	736.49	2.33	0.13	4.59	2.869	0.84
262.8	396.14	2.60	0.13	4.57	2.898	0.85
265.9	286.75	2.74	0.16	4.71	2.868	0.78
269.0	209.80	2.88	0.13	4.56	2.737	0.89
272.9	105.89	3.17	0.12	4.56	2.854	0.90
276.7	55.70	3.45	0.12	4.60	2.853	0.90

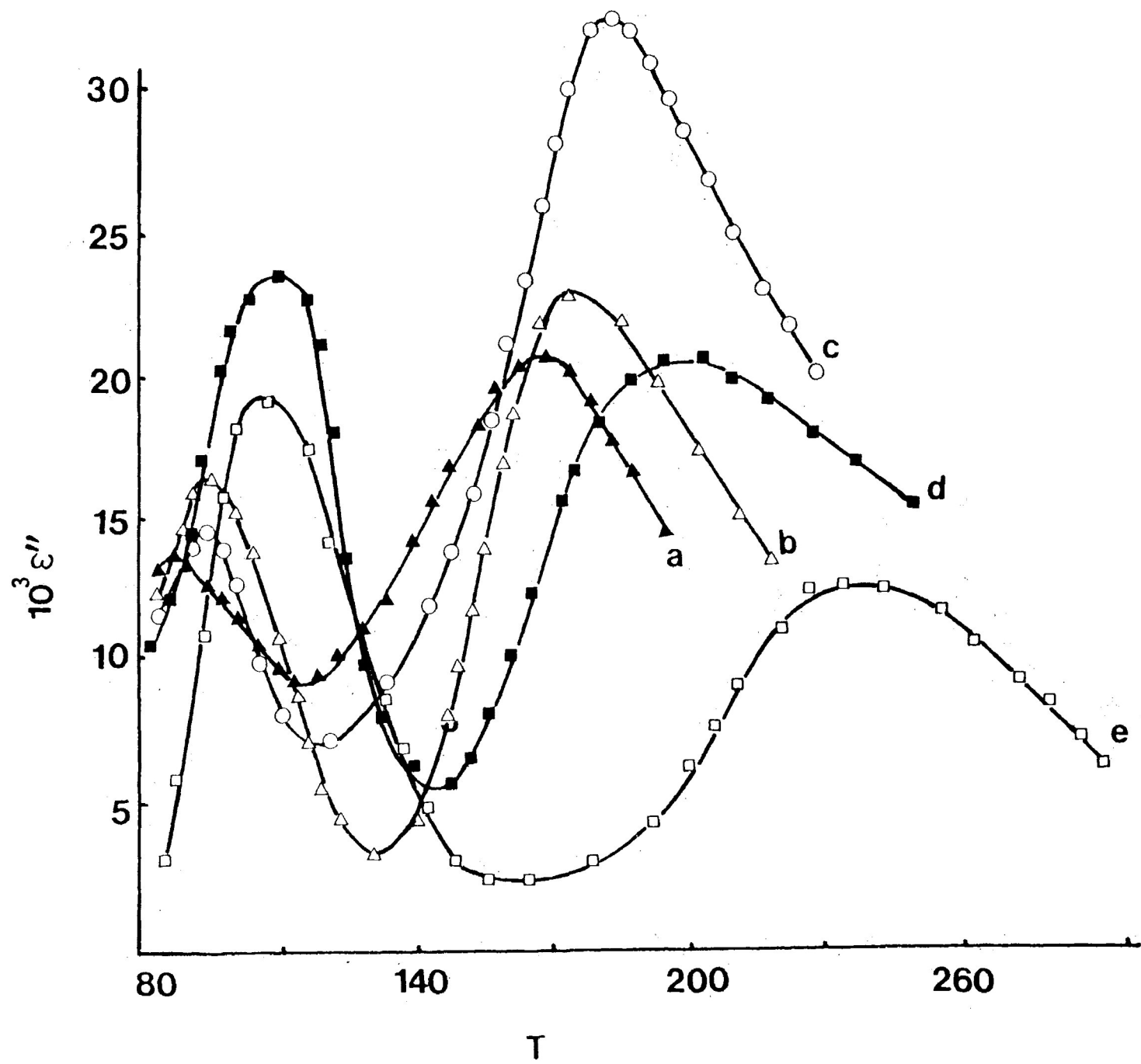


FIGURE VII-1: Dielectric loss factor, ϵ'' versus temperature (K) at 0.0202 kHz for $\text{CH}_2(\text{CH}_2)_n\text{COCH}_3$ in a polystyrene matrix. a) $n=4$; b) $n=5$; c) $n=6$; d) $n=8$ and e) $n=14$.

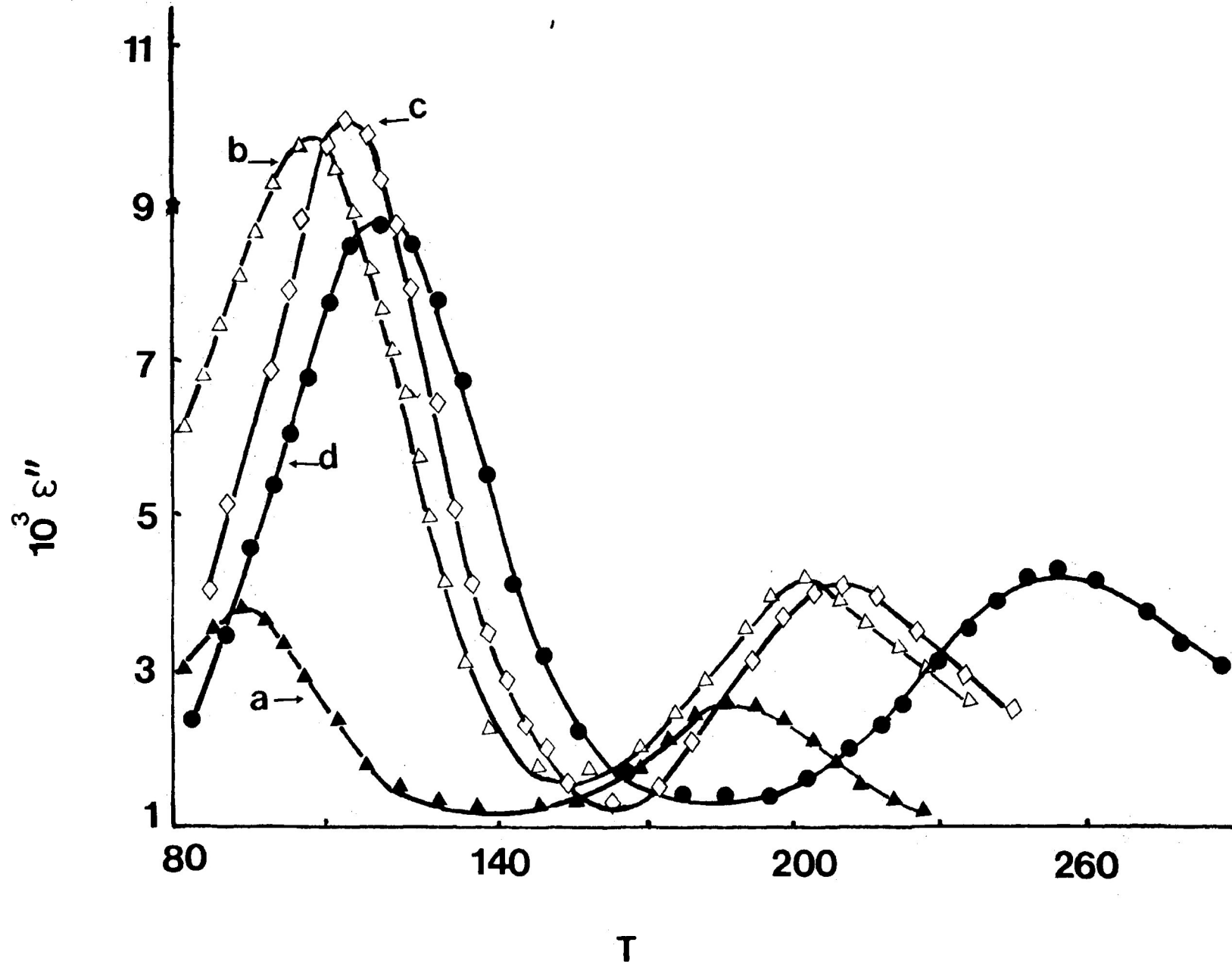


FIGURE VII-2: Dielectric loss factor, ϵ'' versus temperature (K) at 1.01 kHz for $\text{CH}_3(\text{CH}_2)_n\text{NH}_2$ in a polystyrene matrix. a) $n=5$; b) $n=7$; c) $n=10$ and d) $n=11$.

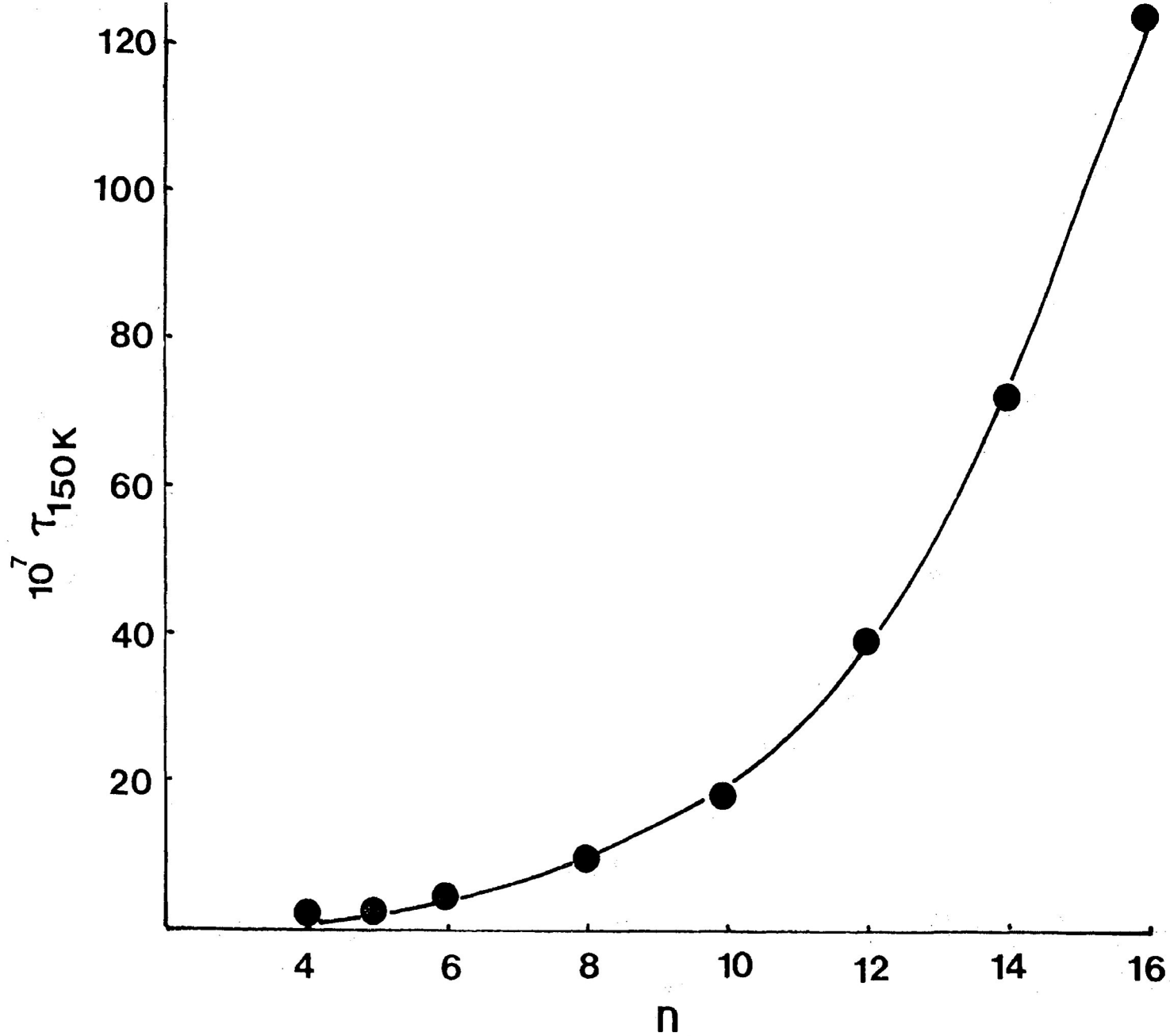


FIGURE VII-3: Relaxation time (in seconds) at 150 K versus number of methylene groups (n) for the low temperature absorption of $\text{CH}_3(\text{CH}_2)_n\text{COCH}_3$ in a polystyrene matrix.

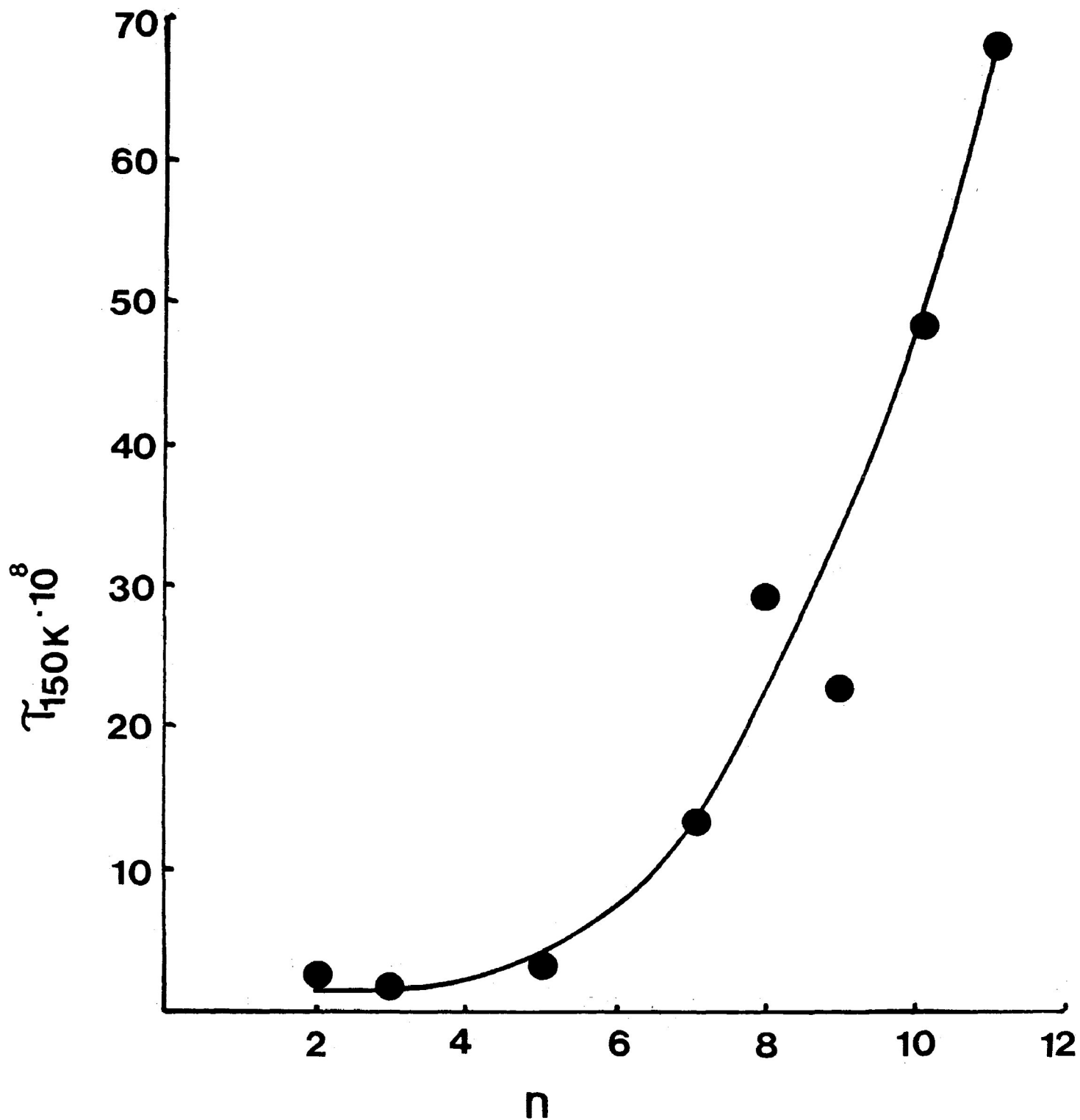


FIGURE VII-4: Relaxation time (in seconds) at 150 K versus number of methylene groups (n) for the low temperature absorption of $\text{CH}_3(\text{CH}_2)_n\text{NH}_2$ in a polystyrene matrix.

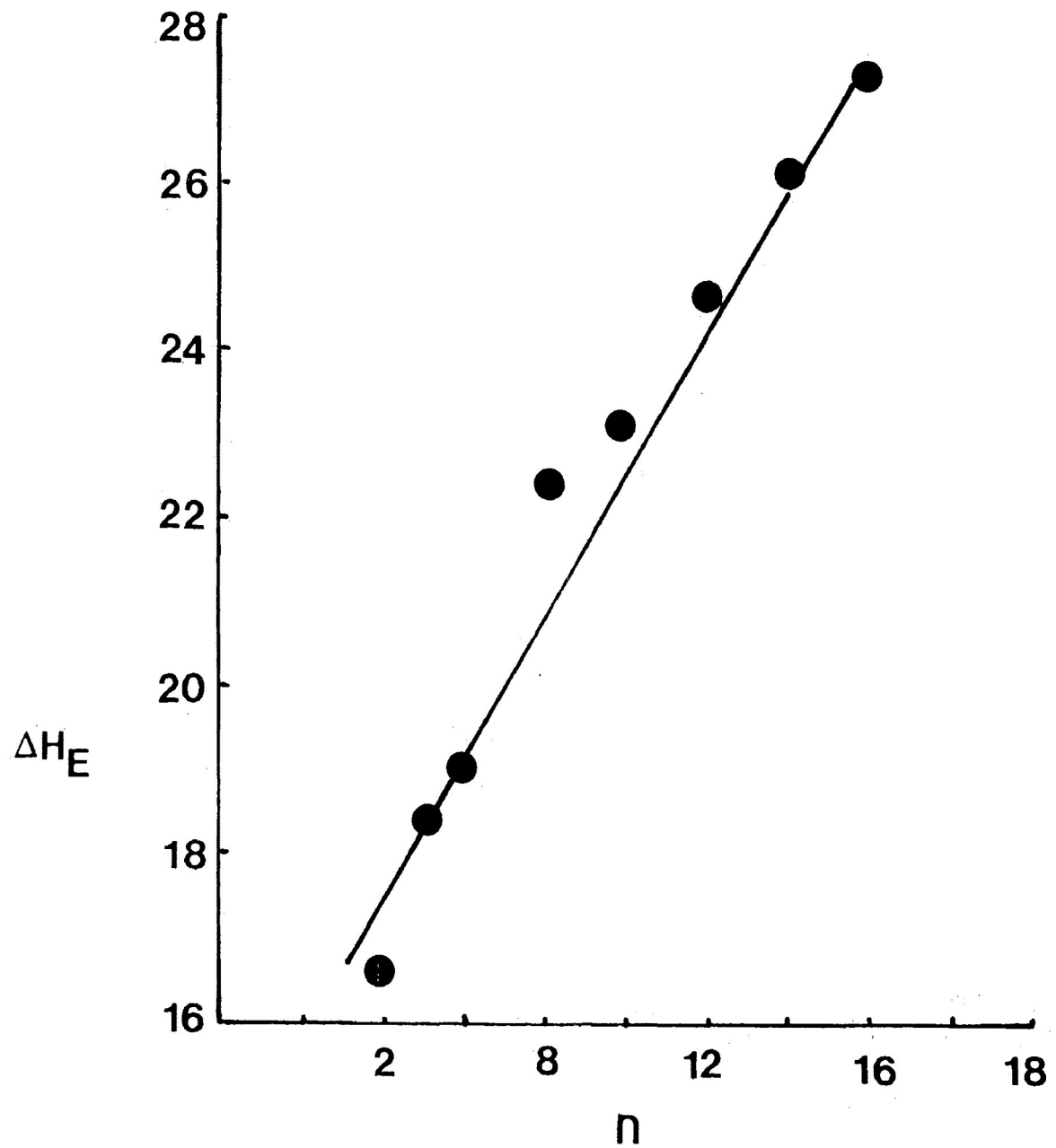


FIGURE VII-5: Enthalpy of activation (in kJ mol^{-1}) versus the number of methylene groups (n) of $\text{CH}_3(\text{CH}_2)_n\text{COCH}_3$ in a polystyrene matrix

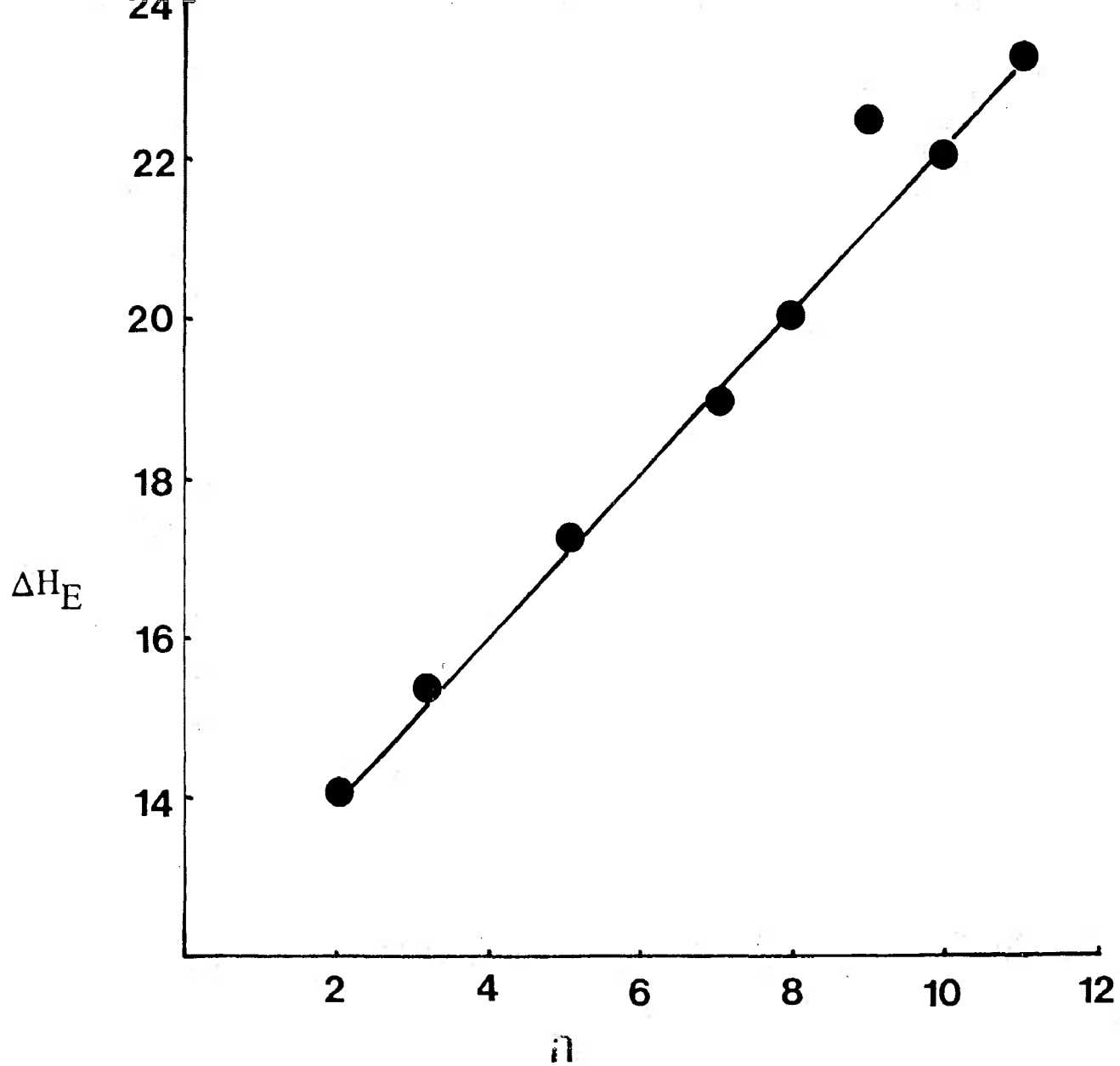


FIGURE VII-6: Enthalpy of activation (in kJ mol^{-1}) versus the number of methylene groups (n) for the low temperature absorption of $\text{CH}_3(\text{CH}_2)_n\text{NH}_2$ in a polystyrene matrix

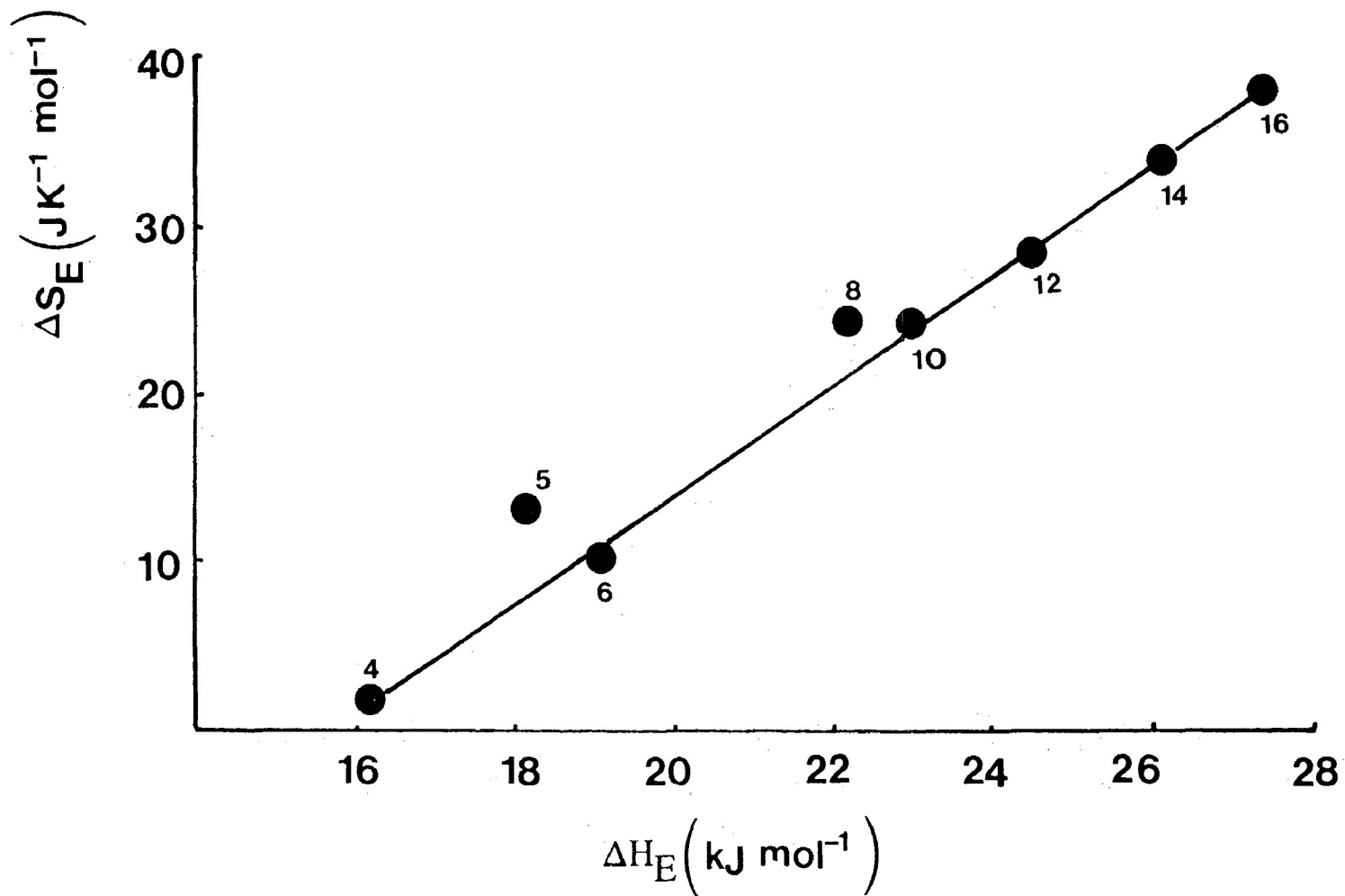


FIGURE VII-7: Plot of entropy of activation (in $\text{J K}^{-1} \text{mol}^{-1}$) versus enthalpy of activation (in kJ mol^{-1}) for the low temperature absorption of $\text{CH}_3(\text{CH}_2)_n\text{COCH}_3$ in a polystyrene matrix. The numbers beside the points indicate the values of n in the general formulae $\text{CH}_3(\text{H}_n)_n\text{COCH}_3$.

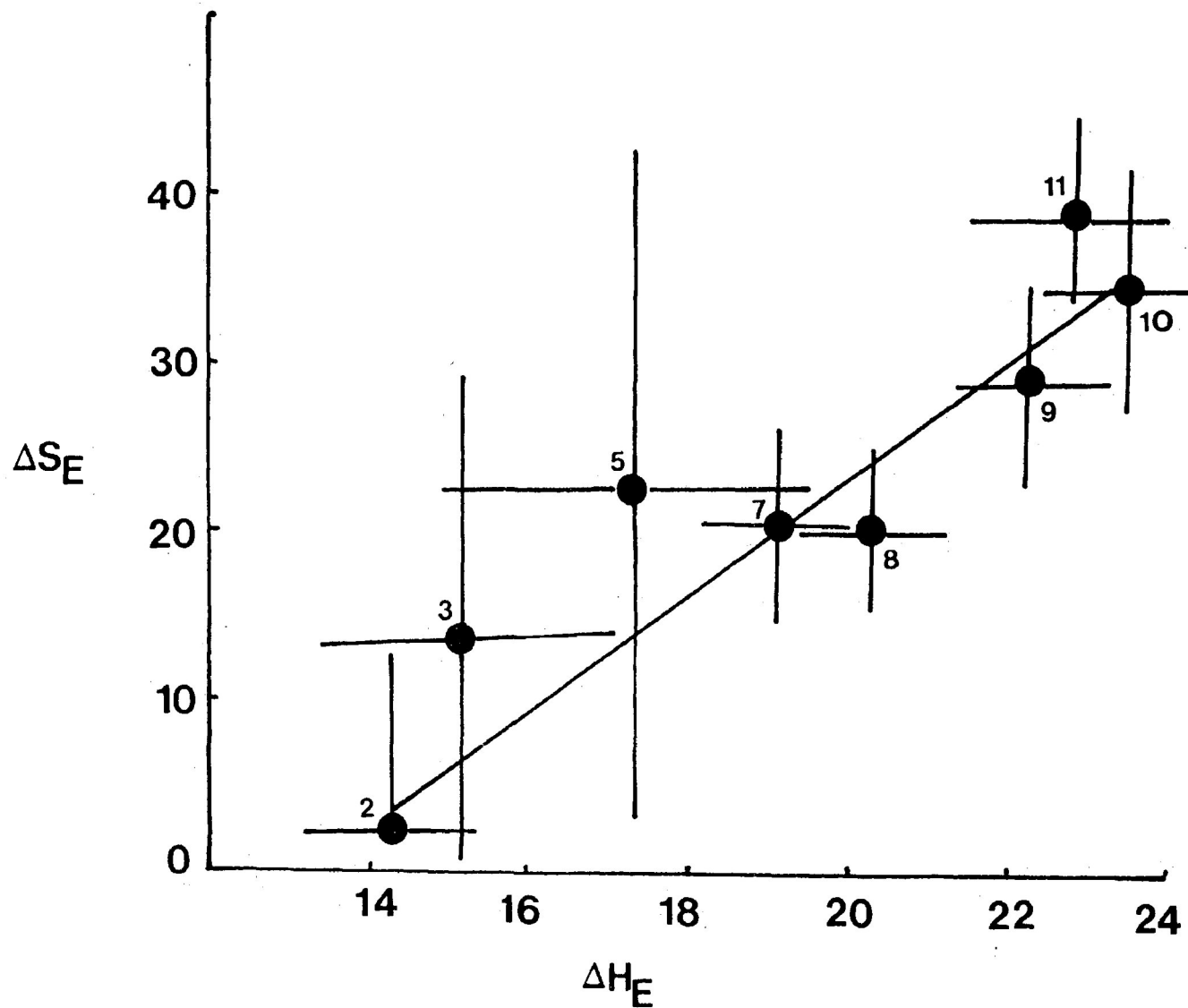


FIGURE VII-8: Plot of entropy of activation (in JK⁻¹ mol⁻¹) versus enthalpy of activation (in kJ mol⁻¹) for the low temperature absorption of CH₃(CH₂)_nNH₂ in a polystyrene matrix. The uncertainties in the parameters are indicated. The numbers beside the points indicate the values of n in the general formula CH₃(CH₂)_nNH₂.

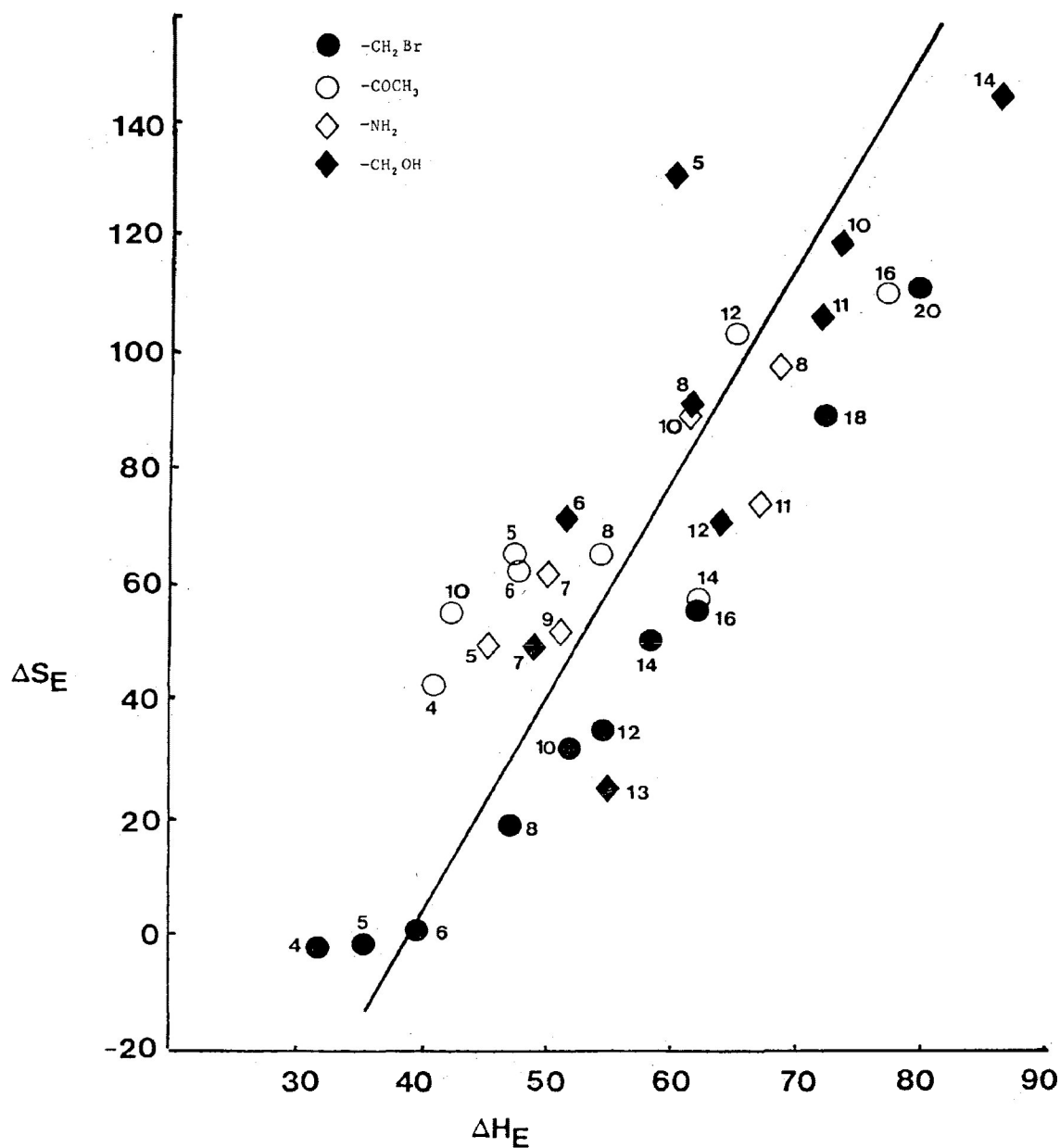


FIGURE VII-9: Plot of entropy of activation ($\text{J K}^{-1} \text{mol}^{-1}$) versus enthalpy of activation (kJ mol^{-1}) for the higher temperature absorption of $\text{CH}_3(\text{CH}_2)_n\text{X}$ (where $\text{X} = -\text{CH}_2\text{Br}$, $-\text{COCH}_3$, $-\text{NH}_2$ and $-\text{CH}_2\text{OH}$) in a polystyrene matrix. The numbers beside the points indicate the values of n in the general formula $\text{CH}_3(\text{CH}_2)_n\text{X}$.

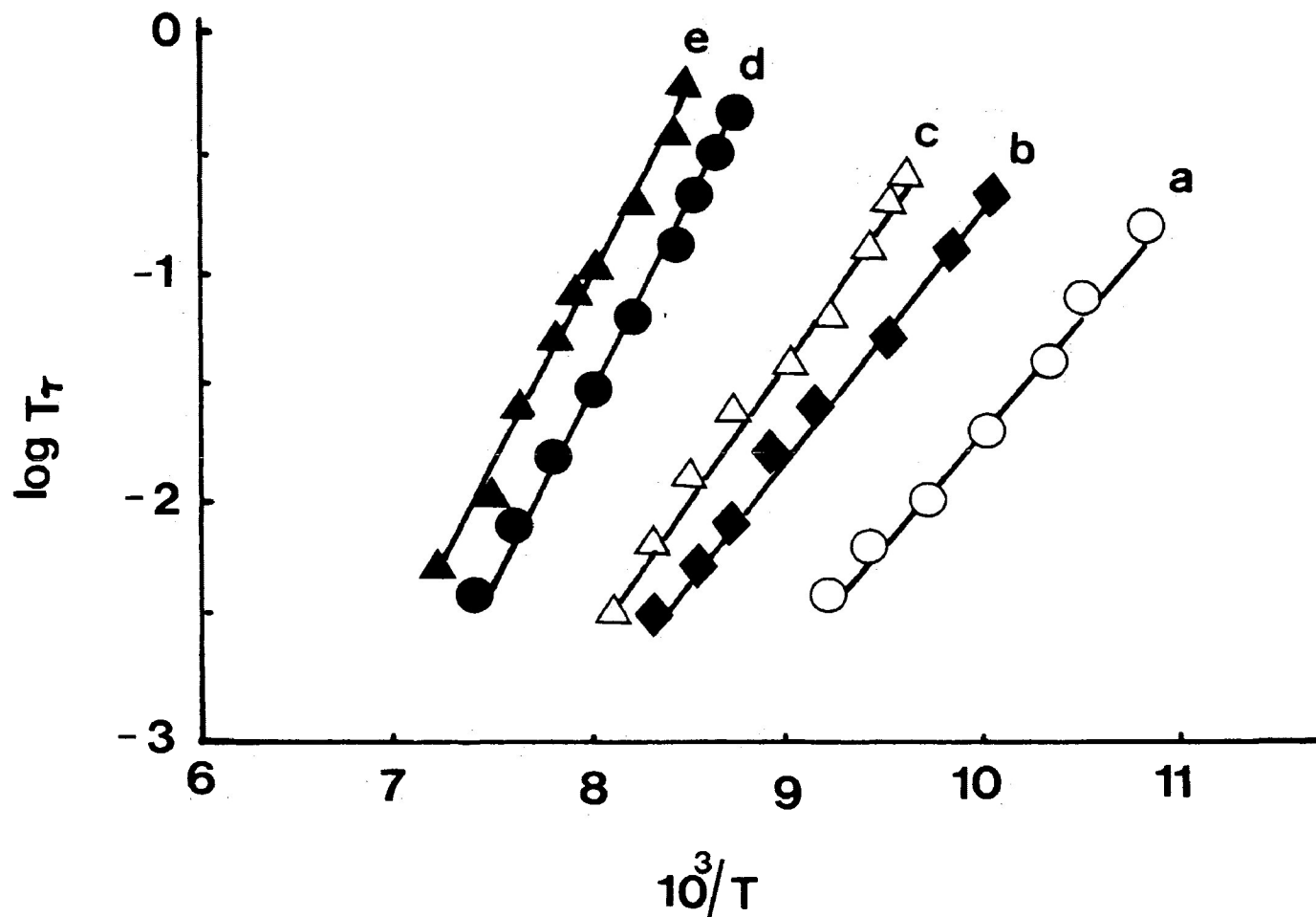


FIGURE VII-10: Eyring rate plot of $\log T\tau$ versus $1/T$ (K^{-1}) for the low temperature absorption of $CH_3(CH_2)_nX$ (where $X = -COCH_3$, and $-NH_2$) in a polystyreneⁿ matrix.

- a) $X = -NH_2$, $n=7$
- b) $X = -NH_2$, $n=10$
- c) $X = -COCH_3$, $n=8$
- d) $X = -COCH_3$, $n=14$
- e) $X = -COCH_3$, $n=16$

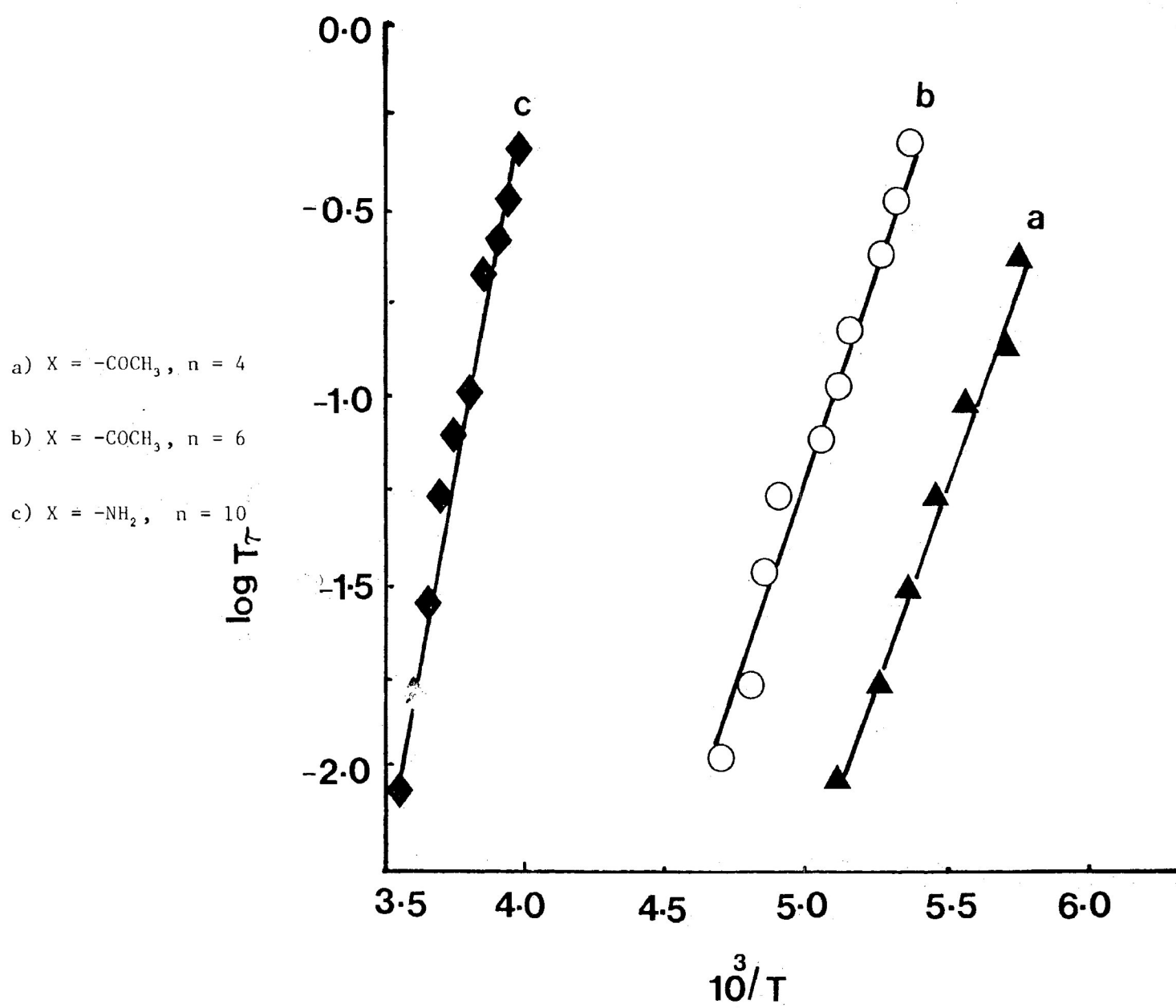


FIGURE VII-11: Eyring rate plot of $\log T\tau$ versus $1/T$ for the high temperature absorption of $\text{CH}_3(\text{CH}_2)_n\text{X}$ (where X = -COCH₃ and -NH₂) in a polystyrene matrix

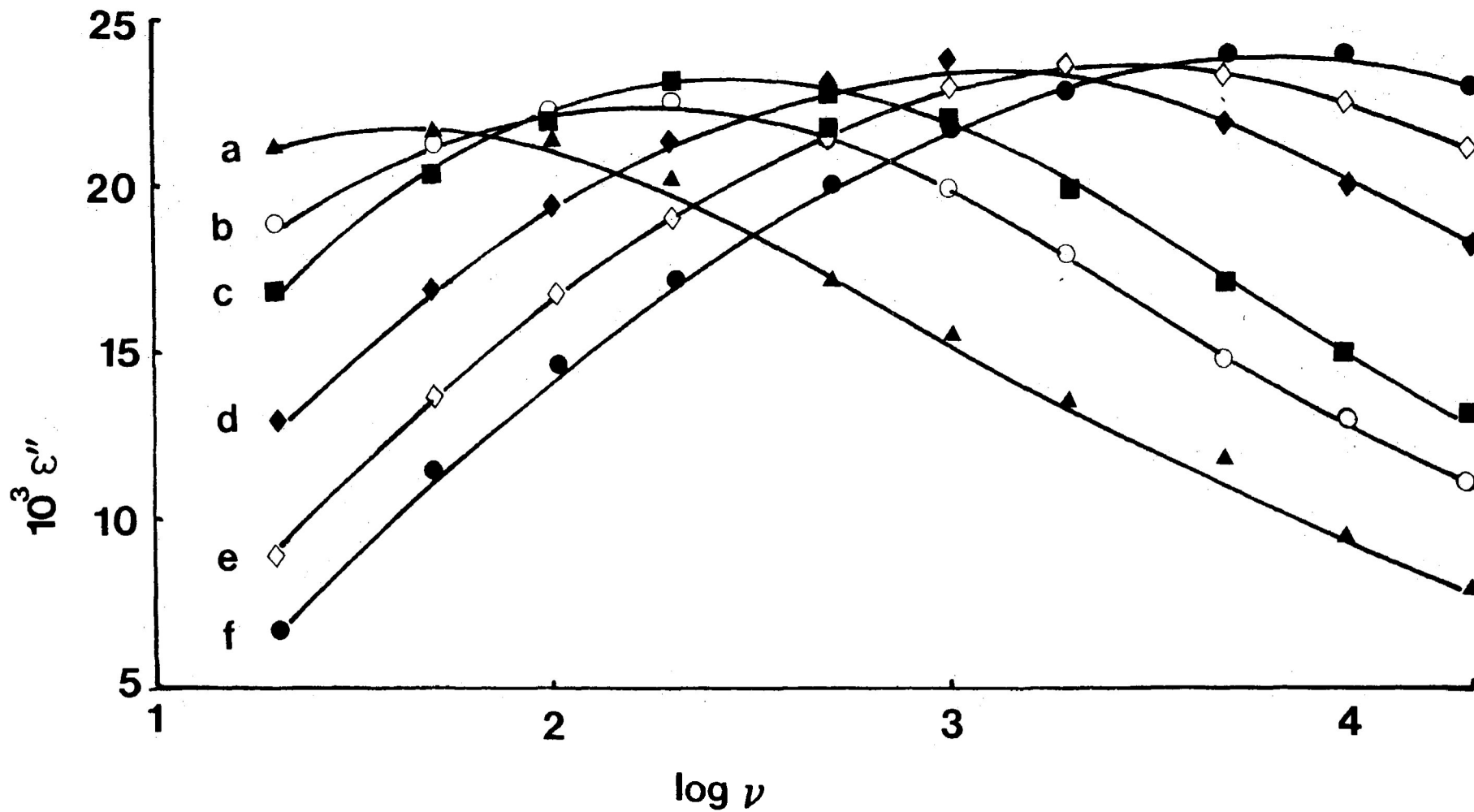


FIGURE VII-12: Dielectric loss factor, ϵ'' versus $\log \nu$ for the low temperature absorption of $\text{CH}_3(\text{CH}_2)_{14}\text{COCH}_3$ in a polystyrene matrix. a) 117.4 K, b) 119.1 K, c) 125.0 K, d) 131.8 K, e) 136.0 K, f) 140.1 K.

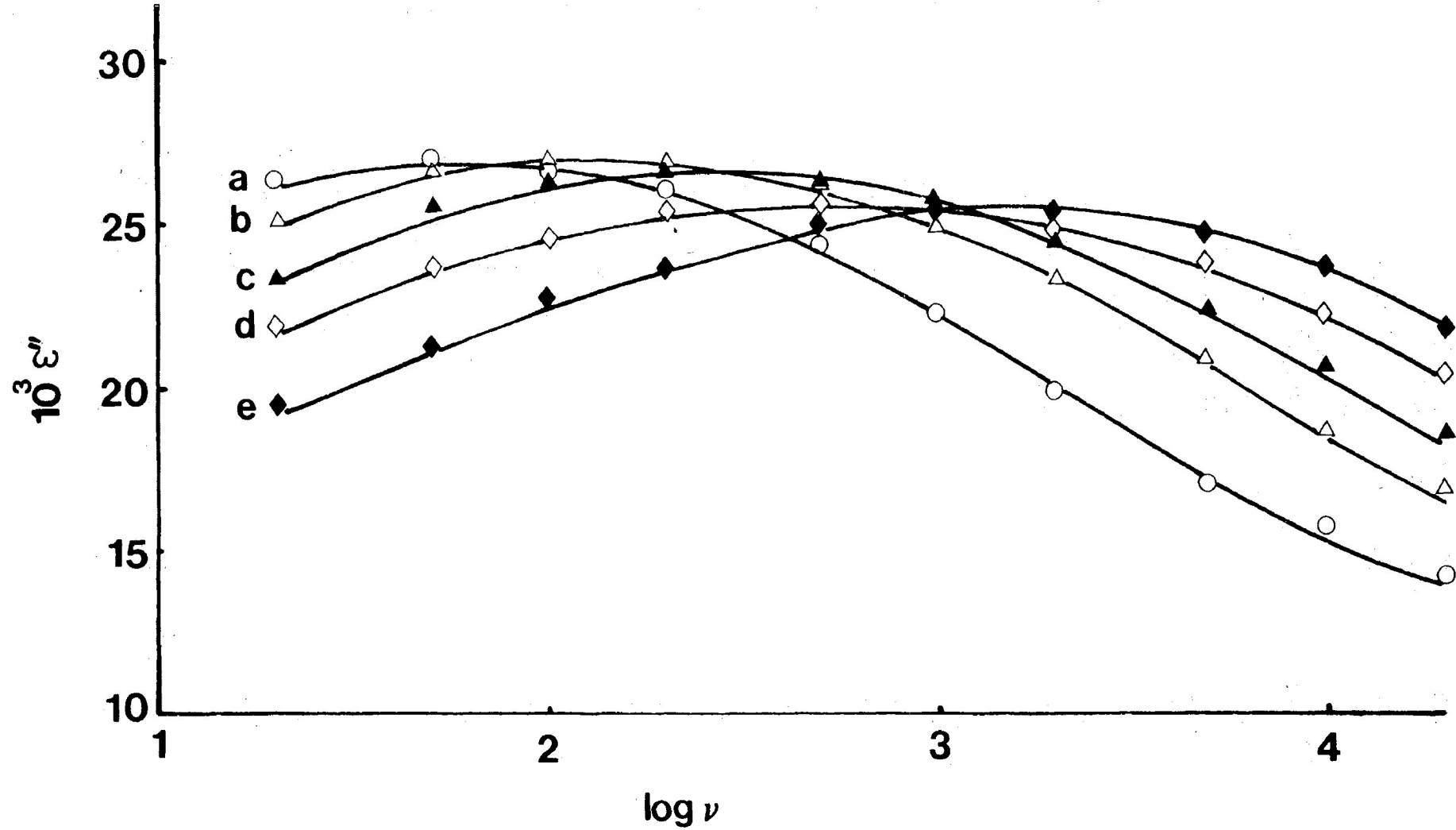


FIGURE VII-13: Dielectric loss factor, ϵ'' versus $\log \nu$ for the high temperature absorption of $\text{CH}_3(\text{CH}_2)_6\text{COCH}_3$ in a polystyrene matrix. a) 189.9 K, b) 190.0 K, c) 196.0 K, d) 205.6 K, e) 209.0 K.

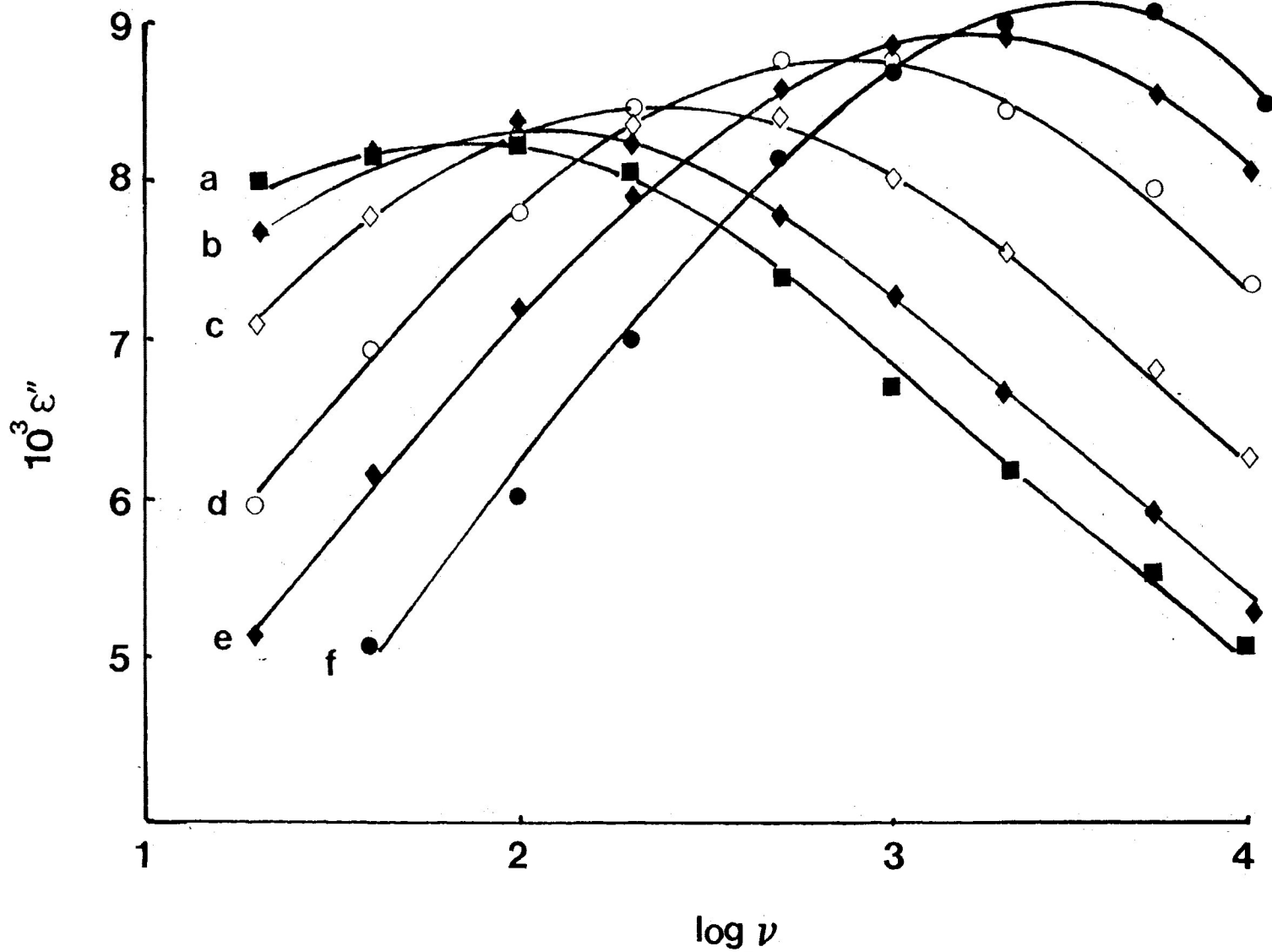


FIGURE VII-14: Dielectric loss factor, ϵ'' versus $\log \nu$ for the low temperature absorption of $\text{CH}_3(\text{CH}_2)_{11}\text{NH}_2$ in a polystyrene matrix. a) 105.8 K, b) 107.7 K, c) 111.5 K, d) 116.5 K, e) 119.2 K, and f) 123.3 K.

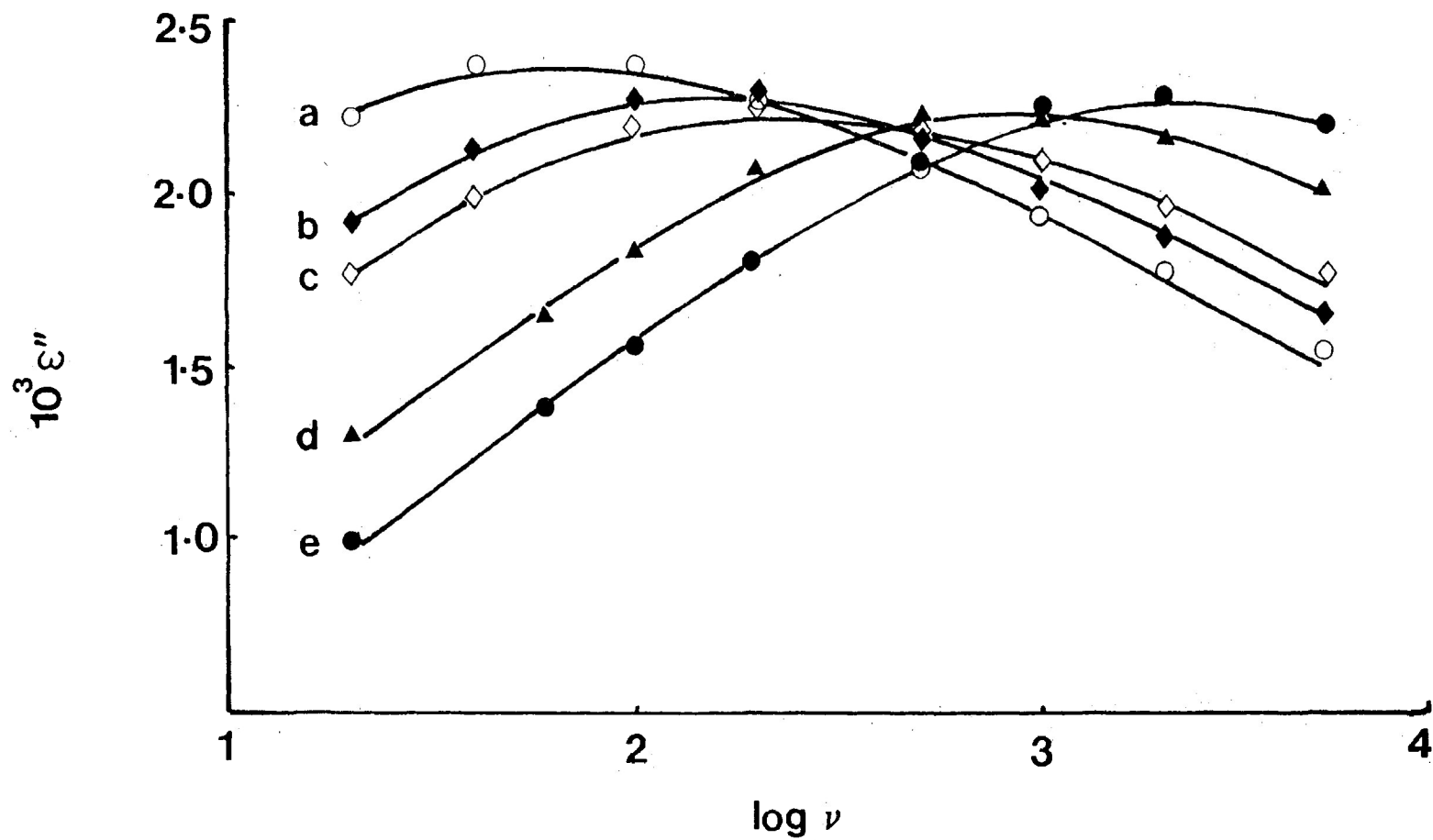


FIGURE VII-15: Dielectric loss factor, ϵ'' versus $\log \nu$ for the high temperature absorption of $\text{CH}_3(\text{CH}_2)_5\text{NH}_2$ in a polystyrene matrix.

a) 2116. K; b) 206.6 K; c) 197.6 K; d) 180.2 K; and e) 195.2 K.

CHAPTER VIII

DIELECTRIC STUDIES OF SOME
SYMMETRICALLY SUBSTITUTED KETONES, ETHERS, SULFIDES AND
AMINES IN A POLYSTYRENE MATRIX

INTRODUCTION

Dielectric absorption studies have been carried out by Dasgupta et al. (1) on n-heptane solutions of diethyl, dihexyl, didodecyl and dodecyl methyl ether and didodecyl sulfide at frequencies of 100 kHz, 1.2, 3.0, 9.4, 25 and 150 GHz at temperatures between 279 and 323 K. The Cole-Cole arcs for these molecules could be represented by two semicircles with the exception of dihexyl ether in which the Cole-Cole arc is a semi-circle indicating a single relaxation process or processes differing so little from one another in relaxation times as to be indistinguishable in these data. For the other ethers it was possible to analyze the data in terms of two discrete relaxation times which were assigned to the whole molecule rotation, τ_1 , and intramolecular rotation, τ_2 , by twisting about the C-O or C-S bonds. The increase of τ_2 with increased molecular size may be due to the increase in the size of the twisting segment. The slightly longer relaxation time of didodecyl sulfide than that of didodecyl ether has been attributed to increased size and polarizability of the sulfur atom as compared to an oxygen atom.

Hasan and Klages (2) reported the dielectric constants and loss measurements of several symmetrically substituted ethers of the general formula

$(C_n H_{2n+1})_2 O$ where n varies from 3 to 17 in cyclohexane and mesitylene solution at 11 frequencies between 0.3 and 300 GHz at 298 K. The relaxation time, τ_0 , of the symmetric ethers increases with increasing molecular size from dipropyl to dihexadecyl ether. The falling off of slope in the plot of τ versus $2n$ (the total number of carbon atoms in the molecule) for molecules with more than twenty carbon atoms has been interpreted by (a) segmental rotations faster than overall rotation of the molecule, and (b) coiling of the hydrocarbon chains. Their results have been analyzed by the Fröhlich distribution function into two limiting relaxation times. The upper limit, τ_a , of relaxation time is an almost linear function of chain length. The increase in chain length adds larger segments to the relaxation process, and τ_a corresponds to the largest unit taking part in it. The lower limit, τ_b , of the Fröhlich distribution on the other hand, is not independent of chain length, but also increases slowly. The intramolecular rotation about the C-O bonds has been suggested as the possible mechanism of intramolecular dielectric relaxation.

Crossley (4) measured dielectric permitivities and losses of several ketones in which the location of the carbonyl group varied along the chain in cyclohexane solution and at frequencies between 1.5 to 145 GHz at 298 K.

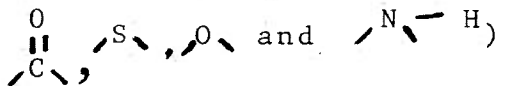
It was possible for each system to draw depressed centre semicircular arcs through most of the experimental points. His results suggested that (a) the mean relaxation time increases only slightly as the size of the alkyl group increases, acetyl group rotation being the dominant process of dipole relaxation for 2-alkanones, (b) the location of the carbonyl group on the hydrocarbon backbone has relatively little effect on the relaxation time for the nonanones and decanones. In the molecules, the dipole reorientation may occur either by overall molecular reorientation or by twisting around the R-C or R'-C bonds in the ketones, RCOR', (c) the relaxation times for pentadecanones and nonadecanones lengthen significantly as the carbonyl group is further removed from the chain end. Crossley suggested that the intramolecular process is restricted when both R and R' are sufficiently long. Dipole reorientation by overall molecular rotation may then become more important, the contribution to the absorption increasing with increased size of R and R'. Alternatively, the increase in relaxation time may be due to the intramolecular rotation of molecular segments, e.g. rotation of R-CO- group around the R-C bond.

Tay and Crossley (5) reported the dielectric absorption studies on a number of primary amines, N-methyl octylamine, N,N-dimethyloctylamine and N,N-diethyloctylamine

in cyclohexane solutions. The plot of dielectric loss versus dielectric constant gives no clear indication of distinct separations into more than one dispersion region. It was possible to draw a relatively smooth depressed centre for all the systems. The mean relaxation times of the primary amines does not increase significantly with increased size of the alkyl group or with the location of the amine group in the nonylamines. Their results suggested that the dipole reorientation in primary n-alkylamines occurs predominantly by a fast intramolecular process and rotational orientation of the whole molecule makes little or no detectable contribution to the absorption. In contrast, the mean relaxation times of N-methyl, N,N-dimethyl, and N,N-diethyloctylamines, which are considerably longer than those for primary amines, lengthen with increased number and size of the N-alkyl groups. They suggested that the reorientation of the dipole by intramolecular rotation may be restricted for secondary and tertiary amines, and the reorientation of the whole molecule appears to make a significant contribution to the absorption of secondary and tertiary amines. The contribution apparently increases with the increase of the size of N-alkyl groups. Because of the short relaxation times, the errors in the estimation of ϵ_{∞} and the Cole-Cole distribution parameters (α) values are considerable. The analysis of the data in

terms of the two relaxation processes did not yield any consistent and physically significant results.

From the preceding review, though a considerable amount of experimental work has been carried out on the investigation of the mechanisms of dielectric relaxation in these molecules in which the dipoles are located at the centre of the hydrocarbon backbone, it seems that the mechanisms of dielectric relaxation are not settled yet and in most of the cases the intramolecular process has not been separated from the molecular one. The previous interpretations are based on the mean relaxation time resulting from the overlap of molecular and intramolecular processes, and distribution parameters, α .

Therefore, it seemed highly desirable to investigate further the dielectric relaxation studies in these symmetrically substituted molecules having the general formula $[\text{CH}_3(\text{CH}_2)_n]_2\text{X}$ (where X = ) in a polystyrene matrix. Our present intent was to separate completely the absorption peaks of some or any of the relaxation processes. A separation into molecular and intramolecular processes has previously been achieved for 1-bromoalkane (see Chapter V), 2-alkanones, and 1-aminoalkane (see Chapter VII) and long chain aldehydes (6) in a polystyrene matrix. In

Chapter V and Chapter VII, it has been demonstrated that the nature of polar end group has negligible influence on the Eyring and relaxation parameters for the low temperature absorption. The main objective of the present investigation is to examine whether the nature of polar end group located at the centre of the hydrocarbon chain influence the relaxation parameters.

EXPERIMENTAL RESULTS

The following molecules have been included in the present study.

Ketones

<u>Number</u>	<u>Name</u>	<u>Structural formula</u>
1	4-Heptanone	$[\text{CH}_3(\text{CH}_2)_2]_2\text{CO}$
2	5-Nonanone	$[\text{CH}_3(\text{CH}_2)_3]_2\text{CO}$
3	6-Undecanone	$[\text{CH}_3(\text{CH}_2)_4]_2\text{CO}$
4	8-Pentadecanone	$[\text{CH}_3(\text{CH}_2)_6]_2\text{CO}$
5	9-Heptadecanone	$[\text{CH}_3(\text{CH}_2)_7]_2\text{CO}$
6	10-Nonadecanone	$[\text{CH}_3(\text{CH}_2)_8]_2\text{CO}$
7	11-Heneicosanone	$[\text{CH}_3(\text{CH}_2)_9]_2\text{CO}$
8	12-Tricosanone	$[\text{CH}_3(\text{CH}_2)_{10}]_2\text{CO}$
9	14-Heptacosanone	$[\text{CH}_3(\text{CH}_2)_{12}]_2\text{CO}$

Ethers

10	Di-n-butylether	$[\text{CH}_3(\text{CH}_2)_3]_2\text{O}$
11	Di-n-hexylether	$[\text{CH}_3(\text{CH}_2)_5]_2\text{O}$
12	Di-n-heptyl ether	$[\text{CH}_3(\text{CH}_2)_6]_2\text{O}$
13	Di-n-octyl ether	$[\text{CH}_3(\text{CH}_2)_7]_2\text{O}$
14	Di-n-decyl ether	$[\text{CH}_3(\text{CH}_2)_9]_2\text{O}$
15	Di-n-hexadecyl ether	$[\text{CH}_3(\text{CH}_2)_{16}]_2\text{O}$

Amines

16	Di-n-propylamine	$[\text{CH}_3(\text{CH}_2)_2]_2\text{NH}$
17	Di-n-butylamine	$[\text{CH}_3(\text{CH}_2)_3]_3\text{NH}$
18	Di-n-hexylamine	$[\text{CH}_3(\text{CH}_2)_5]_2\text{NH}$
19	Di-n-heptylamine	$[\text{CH}_3(\text{CH}_2)_6]_2\text{NH}$
20	Di-n-octylamine	$[\text{CH}_3(\text{CH}_2)_7]_2\text{NH}$
21	Di-n-decylamine	$[\text{CH}_3(\text{CH}_2)_9]_2\text{NH}$
22	Di-n-dodecylamine	$[\text{CH}_3(\text{CH}_2)_{11}]_2\text{NH}$
23	Di-n-octadecylamine	$[\text{CH}_3(\text{CH}_2)_{17}]_2\text{NH}$

Sulfides

24	Di-n-butylsulfide	$[\text{CH}_3(\text{CH}_2)_3]_2\text{S}$
25	Di-n-hexylsulfide	$[\text{CH}_3(\text{CH}_2)_5]_2\text{S}$
26	Di-n-octylsulfide	$[\text{CH}_3(\text{CH}_2)_7]_2\text{S}$
27	Di-n-undecylsulfide	$[\text{CH}_3(\text{CH}_2)_{10}]_2\text{S}$
28	Di-n-dodecylsulfide	$[\text{CH}_3(\text{CH}_2)_{11}]_2\text{S}$
29	Di-n-octadecylsulfide	$[\text{CH}_3(\text{CH}_2)_{17}]_2\text{S}$

All of the compounds were obtained commercially.

All of the compounds were measured as polystyrene matrices in the temperature range 80-320 K and frequency range $10-10^5$ Hz. Tables VIII-1 to VIII-5 summarize the relaxation parameters, Eyring activation parameters and extrapolated dipole moment data for

all of the systems. Table VIII-6 lists the energy differences between the equilibrium positions of the dipoles for the symmetrically substituted ketones. Table VIII-7 lists the results from the Fuoss-Kirkwood analyses, the ϵ_{∞} values and the experimental dipole moments at various temperatures.

Figures VIII-1 to VIII-18 show the dielectric loss factor versus temperature plots, relaxation time versus number of methylene groups, ΔS_E versus ΔH_E plot, Eyring rate plots and absorption curves for some of the compounds studied here.

DISCUSSION

Dielectric absorption studies have been made on symmetrically substituted alkanes having the general formulae $[\text{CH}_3(\text{CH}_2)_n]_2\text{X}$ (where $\text{X} = \begin{array}{c} \text{O} \\ \parallel \\ \text{C} \end{array}$, S , O and N^{H} and n varies from 2 to 20) in a polystyrene matrix. Two absorption peaks appear in each type of molecule when dielectric loss factor, ϵ'' is plotted against the temperature at a fixed frequency. The low temperature absorption has been studied in all the symmetrically substituted molecules and appears somewhere in the range between 80 to 150 K. The high temperature absorption process has been studied only for the symmetrically substituted ketones and occurs somewhere in the range between 200 to 290 K.

LOW TEMPERATURE ABSORPTION

From Figures VIII-1 - VIII-4, it is evident that the $\Delta T_{\frac{1}{2}}$ values for the low temperature absorption of symmetrically substituted molecules having the general formula $[\text{CH}_3(\text{CH}_2)_n]_2\text{X}$ where $\text{X} = \begin{array}{c} \text{O} \\ \parallel \\ \text{C} \end{array}$, S , O and $\begin{array}{c} \text{H} \\ \diagup \\ \text{N} \end{array}$ are very similar and lie in the range 45-55 K which are very similar to the $\Delta T_{\frac{1}{2}}$ values of the 1-bromoalkanes (40-50 K at 85-150 K).

The β -values for the low temperature absorptions of symmetrically substituted alkanes are very close and lie in the range 0.24-0.40 at 80-150 K. The β -values for the low temperature absorption of 1-bromoalkanes lie in the range 0.24-0.35 at 80-150 K. The similarities in β -values suggest that the low temperature absorption of symmetrically substituted alkanes is intramolecular in nature.

The low temperature absorption in 1-bromoalkanes has been attributed to the segmental rotation about the C-C bonds involving the movement of $-\text{CH}_2\text{Br}$ group. Alkyl group rotation cannot give rise to substantial absorption since the absorption is directly proportional to the square of the electric dipole moment perpendicular to the axis of rotation and the value is either zero or nearly so. So the segmental

rotation in symmetrically substituted alkanes must be detected by the corresponding movement of the polar group.

Figures VIII-5 to VIII-8 show that the relaxation time at 150 K and ΔH_E (Figure VIII-9) increases with the increase in the number of carbon atoms. It is observed in Figures VIII-5 to VIII-8 that the increase in relaxation time is slow for the lower values of n ($n < 6$) and then increases almost linearly for the higher values of n . The probable reasons are that (a) the high temperature absorption has not been detected for some lower values of n - the low temperature absorption is either the intramolecular process (where the molecular process occurs below that of liquid nitrogen temperature) or an overlap of the molecular and intramolecular processes, (b) even though the intramolecular and molecular processes have been studied for some lower values of n , the separation of the two processes is not sufficient as to give accurate ν_{\max} . With larger values of n , the separation of the two processes increases. The increase in relaxation time and ΔH_E values with the increase in the number of carbon atoms in the chain means that the size of the relaxing unit also increases.

A survey of Table VIII-1 shows that for a given value of n and when $X = \begin{array}{c} \text{O} \\ \parallel \\ \text{C} \end{array}$, S , O and $\begin{array}{c} \text{H} \\ \diagup \\ \text{N} \end{array}$

the relaxation time at 100 K and ΔH_E are similar within the limits of experimental error. For example, when $n = 7$ and $X = \begin{array}{c} \text{O} \\ \parallel \\ \text{C} \end{array}$, S , O and $\text{N}-\text{H}$, the relaxation time and ΔH_E values are 6.3×10^{-2} s and 23.9 ± 4.6 kJ mol $^{-1}$, 1.5×10^{-1} s and 25.0 ± 0.8 kJ mol $^{-1}$, 5.0×10^{-2} s and 23.8 ± 0.8 kJ mol $^{-1}$ and 3.7×10^{-1} s and 28.0 ± 1.4 kJ mol $^{-1}$, respectively. This bears out that the polar group has negligible influence on the Eyring and relaxation parameters of symmetrically substituted alkanes. Therefore, the intramolecular rotation in these symmetrically substituted molecules must occur about the C-C bond on either side of X in addition to any flexibility in the polar group itself.

When the carbonyl group is removed away from the 2-position to the centre of the chain, the relaxation time and ΔH_E values do not alter appreciably. For example, the relaxation time at 100 K and ΔH_E values (see Table VIII-2) for the low temperature absorption of $[\text{CH}_3(\text{CH}_2)_6]_2\text{CO}$ and $\text{CH}_3(\text{CH}_2)_{12}\text{COCH}_3$ are 2.4×10^{-6} s and 22.6 ± 6.1 kJ mol $^{-1}$, and 3.9×10^{-6} s and 24.7 ± 0.3 kJ mol $^{-1}$, respectively. This suggests that the location of the carbonyl group has negligible effect on the relaxation time and ΔH_E values of low temperature absorption.

In the case of long chain amines the location

of the dipole has relatively little effect on the relaxation time and ΔH_E values. For example, the relaxation time at 100 K and ΔH_E (see Table VIII-3) values for the low temperature absorption of $\text{CH}_3(\text{CH}_2)_{11}\text{NH}_2$ and $[\text{CH}_3(\text{CH}_2)_5]_2\text{NH}$ are 1.2×10^{-2} s and 23.4 kJ mol^{-1} and 2.9×10^{-2} s and 26.3 kJ mol^{-1} , respectively.

A linear relationship appears when ΔH_E is plotted against the ΔS_E for the low temperature absorption of symmetrically substituted alkanes. A typical plot of ΔS_E versus ΔH_E for the low temperature absorption of symmetrically substituted ethers is given in Figure VIII-10. Within experimental error there is a reasonable fit of the $\Delta S_{E(\text{obsd})}$ value for the low temperature absorption of symmetrically substituted alkanes in Table VII-1 to the empirical relation:

$$\Delta S_E = 1.5 \Delta H_E - 15$$

Thus, the low temperature absorption in symmetrically substituted alkanes may be attributed to an intramolecular rotation about the C-C bonds involving the movement of the polar groups.

High temperature absorption

The high temperature absorption has been studied

only for the symmetrically substituted ketones. The β -values for the high temperature absorption of symmetrically substituted ketones are relatively low and lie in the range between 0.10-0.26 at 200-290 K. Such low β -values as 0.10 testify to the broad distribution of relaxation times. Similar β -values for the high temperature absorption of 1-bromoalkanes (0.17-0.24 at 160-300 K), 2-alkanones (0.14-0.24 at 160-290 K) and 1-aminoalkanes (0.12-0.31 at 190-290 K) have been obtained in a polystyrene matrix. Clearly the mechanism of dielectric relaxation for the high temperature absorption of $[\text{CH}_3(\text{CH}_2)_n]_2\text{CO}$ is of a similar nature as it is in $\text{CH}_3(\text{CH}_2)_n\text{X}$ (where $\text{X} = -\text{CH}_2\text{Br}$, $-\text{COCH}_3$, and $-\text{NH}_2$).

The relaxation time at 300 K increases with the increase in the number of carbon atoms in the chain (see Figure VIII-11). This means that the size of the reorientating unit also increases.

Table VIII-4 shows that there is an increasing trend in ΔH_E values with the increase in the number of carbon atoms in the chain. But unlike 1-bromoalkanes, 2-alkanones and 1-aminoalkanes, the ΔH_E values do not increase in a regular fashion with the increase in the number of carbon atoms in the chain. The probable reasons are that the high temperature absorption peaks are very broad (see Figure VIII-1)

and the loss difference between one frequency and another is so low that the resolution of the loss peak and hence the estimation of ν_{\max} is inaccurate. Moreover, the ratio $\epsilon''_{(\max)H} / \epsilon''_{(\max)L}$ decreases with the increase in the number of carbon atoms (see Table VIII-5).

In view of what has been discussed for the high temperature absorption of 1-bromoalkanes (see Chapter V), 2-alkanones and 1-aminoalkanes (see Chapter VII), the high temperature absorption of $[\text{CH}_3(\text{CH}_2)_n]_2\text{CO}$ may be attributed to a molecular rotation process.

The μ_{eff} (effective dipole moment) values calculated from the relation:

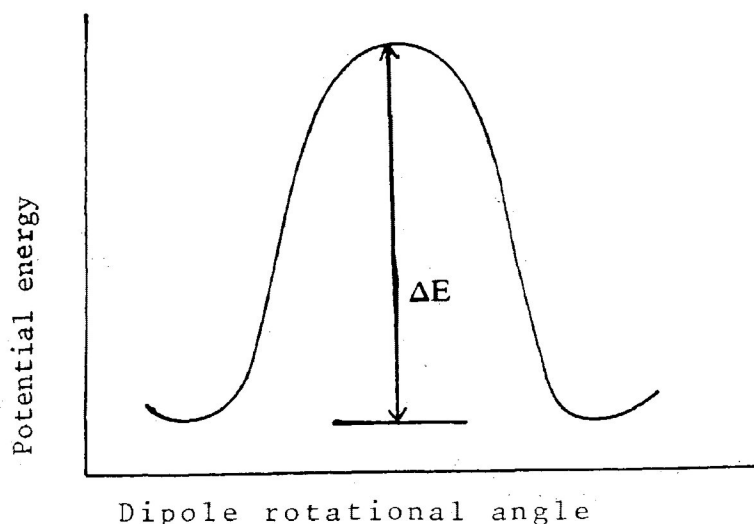
$$\mu_{\text{eff}} = [\mu_m^2 + \mu_s^2]^{\frac{1}{2}}$$

where μ_m governs the molecular relaxation process and μ_s governs the intramolecular process (segmental). The μ_{eff} value for 4-heptanone in a polystyrene matrix at 330 K is $[(1.02)^2 + (2.39)^2]^{\frac{1}{2}} = 2.6_0$ D which is in reasonable agreement with the literature value 2.74 D. Estimates of μ_{eff} for the other molecules are given in Table VIII-5. Table VIII-5 also shows that the weight factor due to intramolecular rotation lies in the range 0.70-0.90. This means that

the intramolecular process is dominant. This is true for other symmetrically substituted molecules such as $[\text{CH}_3(\text{CH}_2)_n]_2\text{S}$, $[\text{CH}_3(\text{CH}_2)_n]_2\text{O}$ and $[\text{CH}_3(\text{CH}_2)_n\text{NH}]$ (see Figures VIII-2-4).

Table VIII-6 lists the calculated values of ΔE_0 (energy difference between the equilibrium positions of the dipoles for the long chain polar molecules in a polystyrene matrix). It is apparent from Table VIII-6 that the ΔE_0 values lie between 0 to 6 kJ mol^{-1} . Such low ΔE_0 values have been observed for 1-bromoalkanes (see Chapter V), and 2-alkanones and 1-aminoalkanes (see Chapter VII) in a polystyrene matrix. A two sites symmetrical barrier model

FIGURE VIII-19:
Two sites symmetric
barrier model



could equally well apply to these long chain polar molecules.

Altogether the present results for the symmetrically substituted ethers and sulfides in a polystyrene matrix bear out what was previously inferred by Dasgupta

et al (1) and Johari et al (3) for the dielectric absorption of these molecules in non-polar solvent who concluded that (a) the Cole-Cole plot indicates two distinct dispersion regions, (b) separation of the intramolecular process from the molecular one increases as the size of the molecule increases; (c) both τ_1 and τ_2 increase with the increase of molecular size and (d) the intramolecular process is a dominant one. Our results (see Figure VIII-2 and Figure VIII-3) show that the intramolecular process is completely separated from the molecular one for the molecules with $n > 6$ and the dielectric absorption is dominated by an intramolecular process (see Table VIII-5). Our conclusion, however, differs from Dasgupta et al (1) and Johari et al (3) in that the rotation about the C-C bond is the main contributor to the low temperature absorption whereas Dasgupta et al and Johari et al suggested that the rotation about the C-O or C-S bonds is the principal mechanism of dielectric intramolecular rotation.

Our results for the symmetrically substituted ketones and amines in a polystyrene matrix do not lend support to the findings of Crossley (4) and Tay et al (5) for the dielectric absorption of the molecules in non-polar solvents who concluded that (a) the dielectric relaxation in these molecules is described by the distribution

of relaxation times (b) when R or R' in RCOR' and RNHR' becomes longer, the intramolecular rotation is restricted and the contribution from molecular rotation increases. But Figures VIII-1 and -2 show a clear separation of the two processes and that the intramolecular process is a dominant one. The weight factor, C_2 , governing the intramolecular rotation lies in the range 0.7-0.9 regardless of the value of n between 2 to 12 (see Table VIII-5). Moreover, the ratio of the $\epsilon''_{(\max)H} / \epsilon''_{(\max)L}$ decreases with the increase in the number of carbon atoms in the chain.

CONCLUSION

(1) Collectively the data presented in this work establish that the symmetrically substituted alkanes in a polystyrene matrix exhibit two distinct relaxation processes. The enthalpy of activation for the low temperature absorption lies in the range 17-27 kJ mol⁻¹ at 80-147 K and is identified as the rotation about the C-C bond, in addition to any flexibility in the polar group itself. The enthalpy of activation for the high temperature absorption of symmetrically substituted ketones lies in the range 40-61 kJ mol⁻¹ at 200-290 K and is characterized by a molecular rotation process.

(2) The dielectric absorption in symmetrically substituted ethers, sulfides, ketones and amines is dominated by intramolecular rotation (see Figures VIII-1-4).

(3) A relaxation model involving a molecular relaxation process (governed by a μ_m moment) and a segmental rotation (characterized by a μ_s movement) which govern the effective dipole moment, where $\mu_{\text{eff}} = (\mu_m^2 + \mu_s^2)^{\frac{1}{2}}$, seems adequate to explain the results of symmetrically substituted alkanes.

(4) The location of the carbonyl group away from the chain end has negligible influence on the relaxation time.

and ΔH_E values of low temperature absorption (see Table VIII-2). The relaxation time and ΔH_E values for the low temperature absorption of primary amines and secondary amines for a given total number of carbon atoms are identified (see Table VIII-3).

(5) The nature of the polar group in symmetrically substituted ethers, sulfides, ketones and amines would appear to have little influence on the relaxation time and ΔH_E values for the low temperature absorption.

(6) The energy difference between the equilibrium positions of dipoles, ΔE_0 , is very low and the two sites, symmetrical barrier model seems adequate for the long chain (see Table VIII-6) polar molecules in a polystyrene matrix.

REFERENCES

1. S. Dasgupta, K. M. Abdul-El Nour and C.P. Smyth, J. Chem. Phys., 50, 4810(1969).
2. A. Hasan and G. Klages, Z. Naturforsch, 33a, 687(1978).
3. G. P. Johari, J. Crossley and C.P. Smyth, J. Am. Chem. Soc., 91, 1597(1969).
4. J. Crossley, J. Chem. Phys., 56, 2549(1972).
5. S. P. Tay and J. Crossley, J. Chem. Phys., 56, 4303(1972).
6. H. A. Khwaja and S. Walker, Adv. Mol. Interact. and Relax. Processes, 22, 27(1982).

TABLE VIII-1: Eyring activation parameters for the low temperature absorption of $[\text{CH}_3(\text{CH}_2)_n]_2\text{X}$ (where $\text{X} = \begin{matrix} \text{O} \\ \parallel \\ \text{C} \end{matrix}$, $\begin{matrix} \text{S} \\ \diagdown \\ \diagup \end{matrix}$, $\begin{matrix} \text{O} \\ \diagdown \\ \diagup \end{matrix}$ and $\begin{matrix} \text{H} \\ \diagdown \\ \text{N} \end{matrix}$) in a polystyrene matrix

X	ΔT (°K)	T range	Relaxation times τ (s)		ΔG_E (kJ mol ⁻¹)		ΔH_E	ΔS_E
			100 K	150 K	100 K	150 K	kJ mol ⁻¹	J K ⁻¹ mol ⁻¹
<u>n=2</u>								
$\begin{matrix} \text{O} \\ \parallel \\ \text{C} \end{matrix}$	83-99	0.20-0.26	1.6×10^{-5}	2.0×10^{-8}	14.4	13.8	15.6 ± 0.8	12.3 ± 8.8
$\begin{matrix} \text{H} \\ \diagdown \\ \text{N} \end{matrix}$	83-98	0.20-0.24	3.2×10^{-5}	1.4×10^{-8}	15.0	13.4	18.3 ± 1.6	33.0 ± 17.9
<u>n=3</u>								
$\begin{matrix} \text{O} \\ \parallel \\ \text{C} \end{matrix}$	89-107	0.23-0.26	1.8×10^{-4}	9.2×10^{-8}	16.4	15.7	17.9 ± 0.5	15.0 ± 5.5
$\begin{matrix} \text{S} \\ \diagdown \\ \diagup \end{matrix}$	92-108	0.26-0.29	3.4×10^{-4}	1.3×10^{-7}	16.9	16.1	18.6 ± 1.2	16.8 ± 11.8
$\begin{matrix} \text{H} \\ \diagdown \\ \text{N} \end{matrix}$	93-113	0.18-0.29	4.0×10^{-4}	3.8×10^{-8}	17.1	14.6	22.1 ± 1.0	50.5 ± 9.5
$\begin{matrix} \text{O} \\ \diagdown \\ \diagup \end{matrix}$	86-104	0.21-0.26	7.0×10^{-5}	1.3×10^{-8}	15.6	13.3	20.4 ± 0.6	47.4 ± 6.7
<u>n=5</u>								
$\begin{matrix} \text{S} \\ \diagdown \\ \diagup \end{matrix}$	104-123	0.29-0.33	1.2×10^{-2}	1.0×10^{-6}	20.0	18.7	22.4 ± 1.5	24.8 ± 13.3
$\begin{matrix} \text{O} \\ \diagdown \\ \diagup \end{matrix}$	108-123	0.23-0.28	5.5×10^{-3}	4.8×10^{-7}	19.3	17.7	22.3 ± 0.6	30.3 ± 3.3
$\begin{matrix} \text{H} \\ \diagdown \\ \text{N} \end{matrix}$	105-128	0.17-0.30	2.9×10^{-2}	5.1×10^{-7}	20.6	17.8	26.3 ± 1.3	56.2 ± 10.5

TABLE VIII-1: continued...

X	ΔT (°K)	range	Relaxation Times τ (s)		ΔG_E (kJ mol ⁻¹)		ΔH_E	ΔS_E
			100 K	150 K	100 K	150 K	kJ mol ⁻¹	J K ⁻¹ mol ⁻¹
			<u>n=6</u>					
	110-131	0.27-0.32	3.1×10^{-2}	2.4×10^{-6}	20.7	19.7	22.6 ± 0.6	19.1 ± 5.1
	110-128	0.25-0.33	7.0×10^{-2}	9.8×10^{-7}	21.4	18.6	26.9 ± 1.5	54.9 ± 12.6
	109-129	0.24-0.29	1.2×10^{-2}	1.1×10^{-6}	19.9	18.8	22.1 ± 1.0	22.0 ± 8.5
			<u>n=7</u>					
	114-135	0.29-0.32	6.3×10^{-2}	3.6×10^{-6}	21.3	20.2	23.9 ± 4.6	20.9 ± 4.6
	114-138	0.31-0.40	1.5×10^{-1}	4.6×10^{-6}	22.0	20.7	25.0 ± 0.8	29.1 ± 6.6
	113-136	0.27-0.41	5.0×10^{-2}	2.4×10^{-6}	21.1	19.7	23.8 ± 0.8	27.3 ± 6.0
	114-135	0.20-0.34	3.7×10^{-1}	3.3×10^{-6}	22.8	22.8	28.0 ± 0.4	52.7 ± 11.0
			<u>n=9</u>					
	122-139	0.30-0.35	5.4×10^{-1}	1.0×10^{-5}	23.1	21.6	26.1 ± 0.4	30.1 ± 6.8
	118-140	0.26-0.40	8.6×10^{-1}	1.9×10^{-5}	23.5	23.3	25.8 ± 2.3	23.0 ± 18.4
	117-138	0.25-0.33	3.5×10^{-1}	5.1×10^{-6}	22.8	20.7	26.8 ± 3.4	40.9 ± 9.8

TABLE VIII-1: continued...


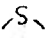
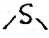
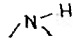

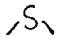
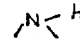
X	ΔT (°K)	range	Relaxation Times τ (s)		ΔG_F (kJ mol ⁻¹)		ΔH_F	ΔS_F
			100 K	150 K	100 K	150 K	kJ mol ⁻¹	J K ⁻¹ mol ⁻¹
	124-146	0.31-0.38	1.1×10^0 ⁿ⁼¹⁰	1.7×10^{-5}	23.6	22.2	26.6±0.6	29.5±4.5
	123-146	0.26-0.29	1.8×10^0	2.6×10^{-5}	24.1	21.4	26.8±0.9	27.3±6.8
	122-145	0.32-0.45	2.5×10^0 ⁿ⁼¹¹	2.2×10^{-5}	24.3	23.1	28.0±1.2	36.9±9.3
	123-134	0.25-0.40	3.1×10^0	7.3×10^{-6}	25.1	21.1	28.4±2.7	67.9±28.0
	127-150	0.27-0.41	9.8×10^0 ⁿ⁼¹⁶	3.3×10^{-5}	25.5	23.0	30.4±1.6	49.2±8.5
	126-149	0.27-0.48	1.1×10^1 ⁿ⁼¹⁷	3.4×10^{-5}	25.6	23.1	30.7±1.6	50.6±11.8
	132-149	0.22-0.29	6.5×10^0	4.8×10^{-5}	25.1	23.5	28.4±2.7	33.0±19.3

TABLE VIII-2: Comparison of Eyring activation parameters for $\text{CH}_3(\text{CH}_2)_n\text{COCH}_3$ and $[\text{CH}_3(\text{CH}_2)_n]_2\text{CO}$ for a given total number of carbon atoms in a polystyrene matrix.

Molecule	ΔT (°K)	T range	Relaxation Times τ (s)		ΔG_E (kJ mol ⁻¹)		ΔH_E kJ mol ⁻¹	ΔS_E J K ⁻¹ mol ⁻¹
			100 K	150 K	100 K	150 K		
$\text{CH}_3(\text{CH}_2)_4\text{COCH}_3$	85-104	0.20-0.21	1.0×10^{-4}	1.1×10^{-7}	16.0	15.9	16.2±1.0	2.0±10.8
$\text{CH}_3(\text{CH}_2)_2]_2\text{CO}$	83-99	0.23-0.26	1.8×10^{-4}	9.2×10^{-8}	15.4	15.7	17.9±5.5	15.0±5.5
$\text{CH}_3(\text{CH}_2)_6\text{COCH}_3$	95-116	0.22-0.26	1.3×10^{-3}	4.2×10^{-7}	18.0	17.6	19.0±0.5	9.4±5.1
$[\text{CH}_3(\text{CH}_2)_4]_2\text{CO}$	89-107	0.24-0.27	2.5×10^{-3}	3.8×10^{-7}	17.5	16.3	20.9±0.8	23.0±7.7
$\text{CH}_3(\text{CH}_2)_8\text{COCH}_3$	105-128	0.24-0.30	1.2×10^{-2}	1.0×10^{-6}	19.9	17.4	22.4±0.4	24.7±3.4
$[\text{CH}_3(\text{CH}_2)_4]_2\text{CO}$	102-118	0.24-0.27	2.5×10^{-3}	3.9×10^{-7}	18.6	17.5	20.9±0.8	23.0±7.7
$\text{CH}_3(\text{CH}_2)_{12}\text{COCH}_3$	113-136	0.25-0.34	1.2×10^{-1}	3.9×10^{-6}	21.8	20.4	24.7±0.3	28.8±2.7
$[\text{CH}_3(\text{CH}_2)_6]_2\text{CO}$	110-131	0.27-0.32	3.1×10^{-2}	2.4×10^{-6}	20.7	19.7	22.6±6.1	19.1±5.1
$\text{CH}_3(\text{CH}_2)_{16}\text{COCH}_3$	124-144	0.27-0.36	1.1×10^0	1.2×10^{-5}	23.7	21.8	27.4±0.8	37.9±6.2
$[\text{CH}_3(\text{CH}_2)_8]_2\text{CO}$	117-137	0.30-0.34	2.6×10^{-1}	7.9×10^{-6}	22.5	21.2	25.0±1.7	24.9±0.0

TABLE VIII-3: Comparison of Eyring activation parameters for $\text{CH}_3(\text{CH}_2)_n\text{NH}_2$ and $[\text{CH}_3(\text{CH}_2)_n]_2\text{NH}$ in a polystyrene matrix

Molecule	ΔT (°K)	T range	Relaxation Times τ (s)		ΔG_F (kJ mol ⁻¹)		ΔH_E kJ mol ⁻¹	ΔS_E J K ⁻¹ mol ⁻¹
			100 K	150 K	100 K	150 K		
$[\text{CH}_3(\text{CH}_2)_2]_2\text{NH}$	89-98	0.20-0.24	3.2×10^{-5}	1.4×10^{-8}	15.0	63.9	18.3±1.6	33.0±17.9
$\text{CH}_3(\text{CH}_2)_5\text{NH}_2$	84-100	0.23-0.25	3.8×10^{-5}	2.4×10^{-8}	15.2	14.0	17.4±3.2	22.4±20.5
$[\text{CH}_3(\text{CH}_2)_5]_2\text{NH}$	105-128	0.17-0.30	2.9×10^{-2}	5.2×10^{-7}	20.6	17.8	26.3±1.3	56.2±10.5
$\text{CH}_3(\text{CH}_2)_{11}\text{NH}_2$	105-126	0.22-0.29	1.2×10^{-2}	6.7×10^{-7}	19.9	16.4	23.4±0.8	35.1±7.7

TABLE VIII-4: Eyring Activation parameters for the High Temperature absorption of $[\text{CH}_3(\text{CH}_2)_n]_2\text{CO}$ in a polystyrene matrix

Molecule n	ΔT (°K)	β range	Relaxation Times τ (s)		ΔG_E (kJ mol ⁻¹)		ΔH_E	ΔS_E
			225 K	300 K	225 K	300 K	kJ mol ⁻¹	J K ⁻¹ mol ⁻¹
2	214-249	0.09-0.14	1.2×10^{-3}	1.1×10^{-6}	41.9	39.2	50.4±4.6	37.5±20.1
3	202-227	0.09-0.10	9.4×10^{-5}	5.7×10^{-8}	37.2	31.8	53.3±2.5	71.4±11.8
4	207-242	0.10-0.14	2.8×10^{-4}	3.1×10^{-7}	39.3	36.1	48.8±1.5	42.2±7
6	220-248	0.11-0.14	7.3×10^{-4}	3.1×10^{-4}	41.0	36.6	56.0±4.0	66.5±17.1
7	254-267	0.11-0.17	3.6×10^{-2}	2.7×10^{-5}	48.4	47.2	51.8±2.2	15.4±8.4
8	235-276	0.14-0.17	1.1×10^{-2}	3.2×10^{-6}	46.0	41.9	58.6±3.0	55.6±12
9	244-268	0.14-0.19	2.4×10^{-2}	5.5×10^{-6}	47.6	43.3	60.6±3.5	57.6±5.7
10	254-288	0.15-0.18	6.0×10^{-2}	2.7×10^{-5}	49.3	47.2	55.6±3.1	27.8±11.7
12	252-278	0.14-0.20	5.4×10^{-2}	3.9×10^{-5}	49.1	48.2	52.0±5.8	12.4±21.8

TABLE VIII-5: μ_s and μ_m are extrapolated dipole moments at 330 K. μ_{eff} from $\mu_{eff} = (\mu_m^2 + \mu_s^2)^{1/2}$ and

$$C_2 = \mu_s^2 / (\mu_m^2 + \mu_s^2) \text{ for } [\text{CH}_3(\text{CH}_2)_n]_2\text{CO in a polystyrene matrix}$$

n	μ_s 330 K (D)	μ_m 330 K (D)	μ_{eff} (D)	μ_{lit} (D)	C_2	$C_1/C_2 = \mu_m^2 / \mu_s^2$	$\epsilon''(\text{max})_H / \epsilon''(\text{max})_L$
2	2.3 ₉	1.0 ₂	2.6 ₀	2.74 (B)	0.85	0.18	0.60
3	2.3 ₅	1.0 ₅	2.5 ₇	2.69 (B)	0.83	0.20	0.27
4	2.3 ₀	1.0 ₁	2.5 ₁	2.68 (B)	0.84	0.19	0.42
6	2.4 ₁	1.1 ₂	2.6 ₃	2.73 (B)	0.82	0.22	0.22
7	2.2 ₉	0.8 ₅	2.4 ₄	2.40 (L)	0.74	0.14	0.20
8	2.2 ₆	0.9 ₂	2.4 ₄		0.86	0.17	0.16
9	2.2 ₃	1.0 ₅	2.4 ₆		0.82	0.22	0.25
10	2.3 ₆	0.8 ₉	2.5 ₂		0.88	0.14	0.15
12	2.2 ₀	0.9 ₈	2.4 ₁		0.83	0.20	0.16

B is Dipole moment in benzene solution

L is Dipole moment in pure liquid state

TABLE VIII-6: Energy differences, ΔE_0 between the equilibrium positions of dipoles for symmetrically substituted ketones in a polystyrene matrix

n	Temperature Region of Absorption	ΔE_0 kJ mol ⁻¹
2	LTP	4.15
	HTP	3.30
3	LTP	0.50
	HTP	4.61
4	LTP	0.41
	HTP	0.21
6	LTP	0.12
	HTP	0.09
7	LTP	1.11
	HTP	0.00
8	LTP	0.51
	HTP	0.23
9	LTP	0.04
	HTP	0.50
10	LTP	0.58
	HTP	0.04
12	LTP	0.55
	HTP	0.25

LTP is Low temperature absorption
HTP is High temperature absorption

TABLE VIII-7: Fuoss-Kirkwood parameters, ϵ_∞ and μ at various temperatures for $[\text{CH}_3(\text{CH}_2)_n\text{X}]$ (Where X = $\begin{array}{c} \text{O} \\ \parallel \\ \text{C} \end{array}$, $\begin{array}{c} \text{H} \\ | \\ \text{N} \end{array}$, S and O) in a polystyrene matrix.

T (K)	$10^6 \tau$ (s)	$\log v_{\text{max}}$	β	$10^3 \epsilon''_{\text{max}}$	ϵ_∞	μ (D)
<u>0.64 M 4-heptanone (lower temperature absorption)</u>						
83.2	854.24	2.27	0.20	16.41	2.925	0.64
84.1	641.34	2.39	0.20	16.58	2.920	0.65
85.5	456.66	2.54	0.20	16.85	2.920	0.65
88.5	200.96	2.89	0.21	17.44	2.917	0.67
91.1	101.04	3.19	0.21	17.86	2.913	0.68
93.3	60.28	3.42	0.22	18.31	2.920	0.68
95.5	37.27	3.63	0.23	18.72	2.909	0.69
98.1	25.91	3.78	0.25	19.21	2.921	0.68
<u>0.64 M 4-heptanone (higher temperature absorption)</u>						
214.2	4881.90	1.54	0.10	7.38	2.934	1.00
217.4	3464.00	1.66	0.10	7.37	2.933	0.99
221.6	1659.81	1.98	0.11	7.30	2.937	0.96
226.7	1070.00	2.17	0.12	7.25	2.948	0.93
230.7	548.37	2.46	0.12	7.16	2.955	0.90
237.5	308.03	2.71	0.13	7.05	2.965	0.87
242.3	189.49	2.92	0.12	6.92	2.965	0.89
248.2	72.35	3.34	0.13	6.79	2.969	0.89
<u>0.76 M 5-nonanone (lower temperature absorption)</u>						
88.5	3329.40	1.68	0.24	30.48	2.914	0.75
89.3	2561.41	1.79	0.24	30.86	2.871	0.76
90.4	1931.50	1.91	0.24	31.42	2.867	0.78
92.2	1277.50	2.09	0.24	32.14	2.866	0.79
95.1	634.09	2.40	0.23	33.12	2.859	0.83
98.5	273.55	2.76	0.24	34.42	2.856	0.85
101.1	145.08	3.04	0.24	35.03	2.846	0.87
103.9	75.58	3.22	0.24	36.09	2.847	0.89
106.8	41.22	3.58	0.25	37.25	2.845	0.90

TABLE VIII-7: continued...

T (K)	$10^6 \tau$ (s)	$\log v_{\max}$	β	$10^3 \epsilon''_{\max}$	ϵ_{∞}	μ (D)
<u>5-nonanone (higher temperature absorption)</u>						
202.0	2519.00	1.80	0.08	5.00	2.940	0.81
206.7	1261.20	2.10	0.08	4.99	2.899	0.82
209.3	931.20	2.23	0.08	4.98	2.901	0.83
211.0	663.31	2.38	0.10	4.96	2.923	0.74
217.0	290.39	2.74	0.09	4.94	2.929	0.79
221.0	52.73	3.02	0.09	4.93	2.939	0.79
227.0	70.65	3.35	0.08	4.92	2.947	0.85
<u>0.49 M 6-undecanone (lower temperature absorption)</u>						
102.3	1301.03	2.08	0.24	24.67	2.855	0.91
104.9	780.95	2.30	0.24	25.14	2.828	1.01
106.2	559.57	2.45	0.24	25.54	2.850	0.95
108.4	350.84	2.65	0.24	26.07	2.848	0.97
110.1	237.18	2.82	0.25	26.45	2.846	0.98
113.0	123.71	3.10	0.25	27.70	2.841	0.10
115.2	76.44	3.31	0.25	27.56	2.841	1.01
118.0	45.92	3.54	0.26	28.35	2.841	1.02
<u>0.49 M 6-undecanone (higher temperature absorption)</u>						
207.8	2594.80	1.79	0.13	7.05	2.895	0.98
212.9	1362.90	2.07	0.13	7.04	2.871	0.98
218.0	652.00	2.39	0.13	7.02	2.889	0.96
225.0	297.87	2.73	0.14	7.01	2.902	0.96
231.4	131.61	3.08	0.13	6.98	2.899	1.01
242.0	41.61	3.58	0.11	6.92	2.895	1.12

TABLE VIII-7: continued...

T(K)	$10^6 \tau$ (S)	$\log v_{\max}$	β	$10^3 \epsilon''_{\max}$	ϵ_{∞}	$\mu(D)$
<u>0.41 M 9-heptadecanone (lower temperature absorption)</u>						
114.0	1647.66	1.98	0.29	15.8	2.878	0.78
116.0	1143.56	2.14	0.29	16.1	2.878	0.80
118.6	665.51	2.37	0.29	16.4	2.856	0.81
120.6	428.52	2.57	0.29	16.7	2.850	0.83
122.8	28.15	2.75	0.29	17.0	2.841	0.84
126.0	150.56	3.02	0.29	17.3	2.832	0.86
129.3	80.01	3.29	0.31	17.7	2.819	0.86
134.3	35.66	3.65	0.32	18.4	2.809	0.88
<u>0.41 M 9-heptadecanone (higher temperature absorption)</u>						
254.7	1265.88	2.10	0.14	2.6	2.898	0.68
257.6	944.06	2.23	0.14	2.6	2.890	0.69
258.2	877.44	2.26	0.14	2.6	2.885	0.69
262.7	573.41	2.44	0.14	2.6	2.881	0.70
265.0	476.87	2.52	0.16	2.6	2.877	0.66
267.0	384.42	2.62	0.16	2.6	2.879	0.66
<u>0.38 M 8-pentadecanone (lower temperature absorption)</u>						
110.9	1842.45	1.93	0.27	23.4	2.894	0.98
113.0	1276.83	2.09	0.27	24.1	2.877	1.01
115.0	766.53	2.31	0.27	24.2	2.862	1.03
118.0	426.25	2.57	0.28	24.8	2.841	1.06
120.2	271.41	2.76	0.28	25.3	2.892	1.07
123.5	140.88	3.05	0.28	25.8	2.811	1.09
126.1	91.37	3.24	0.29	26.5	2.733	1.11
130.7	38.98	3.61	0.31	27.4	2.782	1.12

TABLE VIII-7: continued...

T (K)	$10^6 \tau$ (s)	$\log v_{\max}$	β	$10^3 \epsilon''_{\max}$	ϵ_{∞}	μ (D)
<u>0.38 M 8-pentadecanone (higher temperature absorption)</u>						
220.0	1769.29	1.95	0.14	7.01	2.949	1.07
222.0	1014.23	2.20	0.13	7.00	2.894	1.12
225.5	655.29	2.39	0.12	6.95	2.882	1.18
230.0	360.26	2.65	0.12	6.94	2.869	1.19
234.0	202.85	2.90	0.13	6.93	2.867	1.16
239.0	119.55	3.12	0.11	6.92	2.847	1.27
244.0	68.87	3.36	0.11	6.92	2.840	1.29
248.0	42.96	3.57	0.11	6.91	2.839	1.29
<u>0.49 M 10-nonadecanone (higher temperature absorption)</u>						
235.0	4021.01	1.75	0.15	4.02	2.917	0.72
241.0	1310.00	2.09	0.16	4.00	2.909	0.71
247.0	572.03	2.44	0.16	3.96	2.901	0.71
254.0	241.54	2.81	0.17	3.93	2.896	0.70
264.0	87.31	3.26	0.15	3.92	2.886	0.76
276.0	28.50	3.25	0.14	3.92	2.875	0.80
<u>0.49 M 10-Nonadecanone (lower temperature absorption)</u>						
117.1	2612.70	1.78	0.30	19.01	2.898	0.78
119.7	1553.70	2.01	0.30	19.48	2.887	0.79
122.2	954.69	2.22	0.30	19.85	2.874	0.81
124.9	544.85	2.46	0.30	20.30	2.867	0.83
127.6	318.15	2.69	0.31	20.64	2.851	0.84
130.3	189.69	2.92	0.31	20.98	2.839	0.86
133.1	110.29	3.15	0.32	21.40	2.828	0.86
136.9	56.02	3.45	0.33	22.04	2.817	0.87

TABLE VIII-7: continued...

T (K)	$10^6 \tau$ (s)	$\log v_{\max}$	β	$10^3 \epsilon''_{\max}$	ϵ_{∞}	μ (D)
<u>0.33 M 11-heneicosanone (higher temperature absorption)</u>						
244.0	1918.50	1.92	0.11	3.85	2.877	1.03
248.0	1061.57	2.18	0.12	3.84	2.891	0.99
251.0	723.80	2.34	0.10	3.83	2.864	1.09
254.3	508.74	2.50	0.11	3.83	2.863	1.05
258.0	331.05	2.68	0.13	3.82	2.853	0.97
262.0	204.15	2.89	0.14	3.81	2.863	0.94
268.0	119.55	3.13	0.13	3.81	2.857	0.99
<u>0.33 M 11-heneicosanone (lower temperature absorption)</u>						
122.1	1483.89	2.03	0.30	13.6	2.873	0.82
125.0	833.56	2.28	0.31	13.9	2.867	0.84
127.7	457.55	2.54	0.31	14.2	2.858	0.96
129.6	325.89	2.68	0.32	14.3	2.851	0.85
132.6	184.56	2.93	0.32	14.6	2.831	0.87
135.3	112.25	3.15	0.33	15.0	2.837	0.87
138.6	62.12	3.40	0.34	15.2	2.828	0.88
141.4	38.73	3.61	0.34	15.5	2.825	0.89
<u>0.30 M 12-tricosanone (lower temperature absorption)</u>						
124.7	1517.30	2.02	0.32	14.46	2.857	0.88
127.3	900.89	2.24	0.31	14.68	2.858	0.90
129.9	525.65	2.48	0.33	14.93	2.852	0.90
132.5	320.48	2.69	0.32	15.19	2.854	0.92
135.1	194.59	2.91	0.33	15.42	2.855	0.93
138.1	111.57	3.15	0.34	15.70	2.853	0.93
141.1	65.33	3.38	0.34	16.04	2.851	0.94
145.4	35.64	3.65	0.37	16.45	2.851	0.93

TABLE VIII-7: continued...

T (K)	$10^6 \tau$ (s)	$\log v_{\max}$	β	$10^3 \epsilon''_{\max}$	ϵ_{∞}	μ (D)
<u>0.30 M 12-tricosanone (higher temperature absorption)</u>						
254.0	1878.09	1.92	0.16	1.7	2.880	0.60
258.0	1206.14	2.12	0.16	1.6	2.883	0.59
261.0	720.93	2.34	0.17	1.6	2.885	0.57
264.8	541.67	2.46	0.17	1.6	2.890	0.59
268.0	393.95	2.60	0.17	1.6	2.897	0.58
273.8	223.10	2.85	0.17	1.6	2.898	0.59
281.8	122.15	3.11	0.17	1.6	2.902	0.59
288.0	67.67	3.37	0.15	1.5	2.903	0.61
<u>0.23 M 14-heptacosanone (lower temperature absorption)</u>						
126.2	1801.48	1.94	0.33	10.0	2.677	0.85
128.1	1455.63	2.03	0.32	10.1	2.701	0.88
130.7	828.90	2.28	0.33	10.2	2.700	0.87
134.4	387.68	2.61	0.34	10.5	2.700	0.89
138.1	199.16	2.90	0.34	10.7	2.692	0.90
141.0	100.18	3.20	0.36	10.9	2.696	0.90
145.3	57.49	3.44	0.37	11.2	2.690	0.92
<u>0.23 M 14-heptacosanone (higher temperature absorption)</u>						
252.0	2179.81	1.86	0.14	1.40	2.710	0.60
260.0	1064.00	2.17	0.17	1.40	2.720	0.63
265.0	627.01	2.40	0.18	1.40	2.712	0.62
268.0	507.60	2.49	0.20	1.40	2.722	0.60
273.1	352.24	2.65	0.18	1.30	2.730	0.61
278.3	200.97	2.89	0.20	1.30	2.724	0.59

TABLE VIII-7: continued...

T (K)	$10^6 \tau$ (s)	$\log \nu_{\max}$	β	$10^3 \epsilon''_{\max}$	ϵ_{∞}	μ (D)
<u>0.35 M di-n-butylsulfide (lower temperature absorption)</u>						
92.7	1840.53	1.94	0.28	16.3	2.725	0.81
95.4	1145.79	2.14	0.27	16.7	2.721	0.85
96.0	913.80	2.24	0.27	16.9	2.719	0.86
97.6	626.62	2.40	0.27	17.1	2.723	0.87
98.7	451.83	2.54	0.28	17.5	2.720	0.87
101.3	256.31	2.79	0.27	17.9	2.718	0.91
101.0	195.11	2.91	0.28	18.0	2.715	0.89
105.0	105.45	3.18	0.27	18.5	2.711	0.94
108.0	61.26	3.42	0.29	18.9	2.715	0.93
<u>0.47 M di-n-hexylsulfide (lower temperature absorption)</u>						
104.8	3083.00	1.71	0.30	11.3	2.713	0.61
106.5	1674.50	1.98	0.31	11.5	2.715	0.61
109.4	1294.41	2.10	0.30	11.8	2.711	0.63
111.5	718.39	2.35	0.30	12.2	2.709	0.65
114.7	341.51	2.67	0.31	12.6	2.709	0.66
117.0	214.38	2.87	0.31	12.8	2.708	0.67
120.6	99.01	3.21	0.32	13.1	2.707	0.68
123.0	64.44	3.40	0.33	13.4	2.707	0.68
<u>0.36 M di-n-octylsulfide (lower temperature absorption)</u>						
114.5	2704.57	1.77	0.31	11.3	2.840	0.68
117.4	1517.77	2.02	0.32	11.6	2.839	0.69
119.6	946.12	2.22	0.32	11.8	2.837	0.71
121.6	626.69	2.40	0.32	12.0	2.835	0.72
123.6	453.35	2.54	0.40	12.8	2.840	0.67
126.0	245.15	2.81	0.33	12.5	2.833	0.73
127.6	175.37	2.95	0.33	12.5	2.832	0.74
131.1	90.25	3.24	0.35	12.9	2.831	0.74
134.2	52.01	3.48	0.37	13.3	2.831	0.74
138.3	27.31	3.76	0.39	13.6	2.831	0.74

TABLE VIII-7: continued...

T (K)	$10^6 \tau$ (s)	$\log v_{\max}$	β	$10^3 \epsilon''_{\max}$	ϵ_{∞}	μ (D)
<u>0.45 M di-n-undecylsulfide (lower temperature absorption)</u>						
123.3	3360.04	1.67	0.26	5.5	2.815	0.49
124.8	2310.00	1.83	0.27	5.7	2.815	0.50
127.0	1483.47	2.03	0.27	5.8	2.814	0.51
129.6	857.80	2.26	0.27	5.9	2.813	0.51
132.0	583.01	2.43	0.27	6.0	2.811	0.52
134.8	330.07	2.68	0.27	6.2	2.831	0.54
137.9	203.86	2.89	0.28	6.3	2.809	0.54
141.4	104.46	3.18	0.27	6.6	2.799	0.57
145.8	45.49	3.54	0.26	6.9	2.798	0.60
<u>0.45 M di-n-dodecylsulfide (lower temperature absorption)</u>						
122.0	3531.30	1.65	0.33	8.5	2.855	0.54
124.8	2276.02	1.84	0.34	8.7	2.859	0.54
126.0	1853.31	1.94	0.35	8.8	2.860	0.54
128.5	1273.90	2.10	0.35	8.8	2.859	0.55
131.4	580.61	2.44	0.38	9.1	2.858	0.54
134.4	335.05	2.68	0.36	9.3	2.854	0.56
137.2	187.39	2.93	0.37	9.4	2.853	0.57
141.0	90.23	3.25	0.39	9.6	2.852	0.57
145.0	49.22	3.51	0.44	10.2	2.852	0.56
<u>0.55 M di-n-octadecylsulfide (lower temperature absorption)</u>						
126.3	4020.50	1.60	0.28	2.3	2.724	0.29
128.5	2677.40	1.77	0.27	2.3	2.721	0.30
130.5	1690.81	1.97	0.29	2.3	2.721	0.29
132.5	891.02	2.25	0.30	2.4	2.721	0.29
135.2	551.67	2.46	0.32	2.4	2.719	0.29
138.2	282.51	2.75	0.35	2.5	2.719	0.28
141.3	139.79	3.06	0.34	2.5	2.716	0.29
144.4	92.79	3.23	0.38	2.6	2.716	0.28
148.4	49.56	3.50	0.47	2.8	2.787	0.26

TABLE VIII-7: continued...

T (K)	$10^6 \tau$ (s)	$\log v_{\max}$	β	$10^3 \epsilon''_{\max}$	ϵ_{∞}	μ (D)
<u>0.45 M di-propylamine (lower temperature absorption)</u>						
83.1	2870.71	1.74	0.20	5.1	2.770	0.50
85.7	1682.00	1.98	0.21	5.4	2.269	0.46
86.2	1309.50	2.08	0.22	5.5	2.769	0.45
90.8	346.90	2.66	0.20	5.8	2.762	0.50
92.2	245.25	2.81	0.21	6.0	2.762	0.50
95.0	111.21	3.16	0.22	6.2	2.761	0.51
97.8	47.67	3.52	0.23	6.5	2.758	0.51
<u>0.61 M di-n0butylamine (lower temperature absorption)</u>						
93.0	3674.59	1.63	0.18	8.6	2.900	0.54
93.9	2415.38	1.81	0.19	8.7	2.900	0.53
96.8	1033.21	2.18	0.20	9.1	2.898	0.54
98.7	571.85	2.44	0.20	9.3	2.896	0.55
100.5	340.29	2.67	0.21	9.5	2.897	0.55
102.0	192.6	2.91	0.23	9.9	2.894	0.54
104.8	112.88	3.14	0.23	10.2	2.893	0.54
106.5	70.90	3.35	0.23	10.3	2.891	0.56
108.0	49.64	3.50	0.25	10.6	2.892	0.55
110.8	27.39	3.76	0.26	11.0	2.889	0.55
112.8	20.89	3.88	0.28	11.4	2.891	0.55
<u>0.36 M di-n-hexylamine (lower temperature absorption)</u>						
105.3	6560.80	1.38	0.17	7.7	2.851	0.71
107.4	3438.72	1.66	0.18	7.9	2.849	0.72
109.0	1807.07	1.94	0.20	8.1	2.849	0.70
111.0	1070.29	2.17	0.21	8.3	2.849	0.71
112.4	715.18	2.34	0.21	8.4	2.848	0.70
115.2	358.04	2.64	0.22	8.6	2.845	0.71
117.5	211.55	2.87	0.24	8.8	2.847	0.69
120.5	109.23	3.16	0.26	9.1	2.846	0.69
123.4	61.03	3.41	0.27	9.4	2.844	0.70
127.1	31.13	3.70	0.29	9.7	2.844	0.69

TABLE VIII-7: continued...

T (K)	$10^6 \tau$ (s)	$\log \nu_{\max}$	β	$10^3 \epsilon''_{\max}$	ϵ_{∞}	μ (D)
<u>0.45 M diheptylamine (lower temperature absorption)</u>						
110.4	3560.10	1.65	0.19	5.1	2.716	0.54
112.4	1639.81	1.98	0.24	5.2	2.719	0.48
113.8	117.70	2.13	0.24	5.3	2.718	0.49
115.7	727.79	2.34	0.25	5.4	2.717	0.49
116.9	549.46	2.46	0.26	5.5	2.717	0.49
119.1	553.79	2.71	0.26	5.5	2.718	0.50
121.7	195.29	2.91	0.27	5.7	2.714	0.50
124.2	100.19	3.20	0.29	5.8	2.714	0.49
127.4	56.47	3.45	0.30	6.0	2.714	0.50
<u>0.46 M di-n-octylamine (lower temperature absorption)</u>						
114.2	5191.95	1.48	0.22	6.5	2.849	0.55
116.4	2976.82	1.72	0.20	6.6	2.844	0.54
119.0	1421.31	2.04	0.24	7.1	2.845	0.56
121.2	733.13	2.33	0.23	7.0	2.844	0.57
125.3	311.20	2.70	0.25	7.2	2.841	0.57
128.0	178.84	2.94	0.27	7.4	2.841	0.56
131.9	82.45	3.28	0.30	7.6	2.840	0.55
135.9	41.44	3.58	0.33	8.0	2.840	0.54
<u>0.46 M di-n-octylamine (higher temperature absorption)</u>						
214.3	721.19	2.34	0.26	3.90	2.850	0.57
217.7	512.91	2.49	0.25	3.91	2.848	0.59
220.8	349.58	2.65	0.23	3.86	2.844	0.61
224.5	194.93	2.91	0.19	3.78	2.859	0.68
226.6	125.15	3.10	0.17	3.75	2.835	0.70
229.3	100.51	3.20	0.18	3.71	2.835	0.68
232.3	60.45	3.42	0.18	3.82	2.832	0.70

TABLE VIII-7: continued...

T (K)	$10^6 \tau$ (s)	$\log \nu_{\max}$	β	$10^3 \epsilon''_{\max}$	ϵ_{∞}	μ (D)
<u>0.29 M di-n-decylamine (lower temperature absorption)</u>						
118.4	4908.83	1.51	0.28	1.7	2.477	0.35
120.0	3585.27	1.65	0.28	1.7	2.476	0.35
123.1	1282.28	1.81	0.27	1.8	2.475	0.37
125.7	3585.27	2.09	0.28	1.7	2.473	0.36
128.2	620.88	2.41	0.30	1.7	2.472	0.35
131.5	342.27	2.67	0.31	1.8	2.471	0.36
135.6	180.93	2.94	0.36	1.9	2.469	0.35
139.7	96.38	3.22	0.42	1.9	2.524	0.32
<u>0.31 M didodecylamine (lower temperature absorption)</u>						
123.8	1865.16	1.93	0.24	1.7	2.718	0.35
125.5	1127.75	2.15	0.25	1.7	2.717	0.35
127.4	720.11	2.34	0.26	1.7	2.717	0.34
130.1	347.26	2.66	0.29	1.7	2.717	0.33
131.7	261.18	2.78	0.31	1.7	2.716	0.32
133.3	90.83	2.89	0.39	1.8	2.716	0.30
<u>0.37 M di-n-octadecylamine</u>						
132.0	1106.79	2.15	0.22	1.1	2.501	0.29
135.5	565.97	2.45	0.24	1.1	2.500	0.29
137.3	415.23	2.58	0.25	1.1	2.500	0.28
139.4	279.46	2.76	0.28	1.1	2.500	0.27
142.4	170.35	2.97	0.29	1.1	2.499	0.27
145.4	90.46	3.24	0.28	1.1	2.497	0.27
148.7	65.18	3.39	0.32	1.2	2.496	0.27

TABLE VIII-7: continued.....

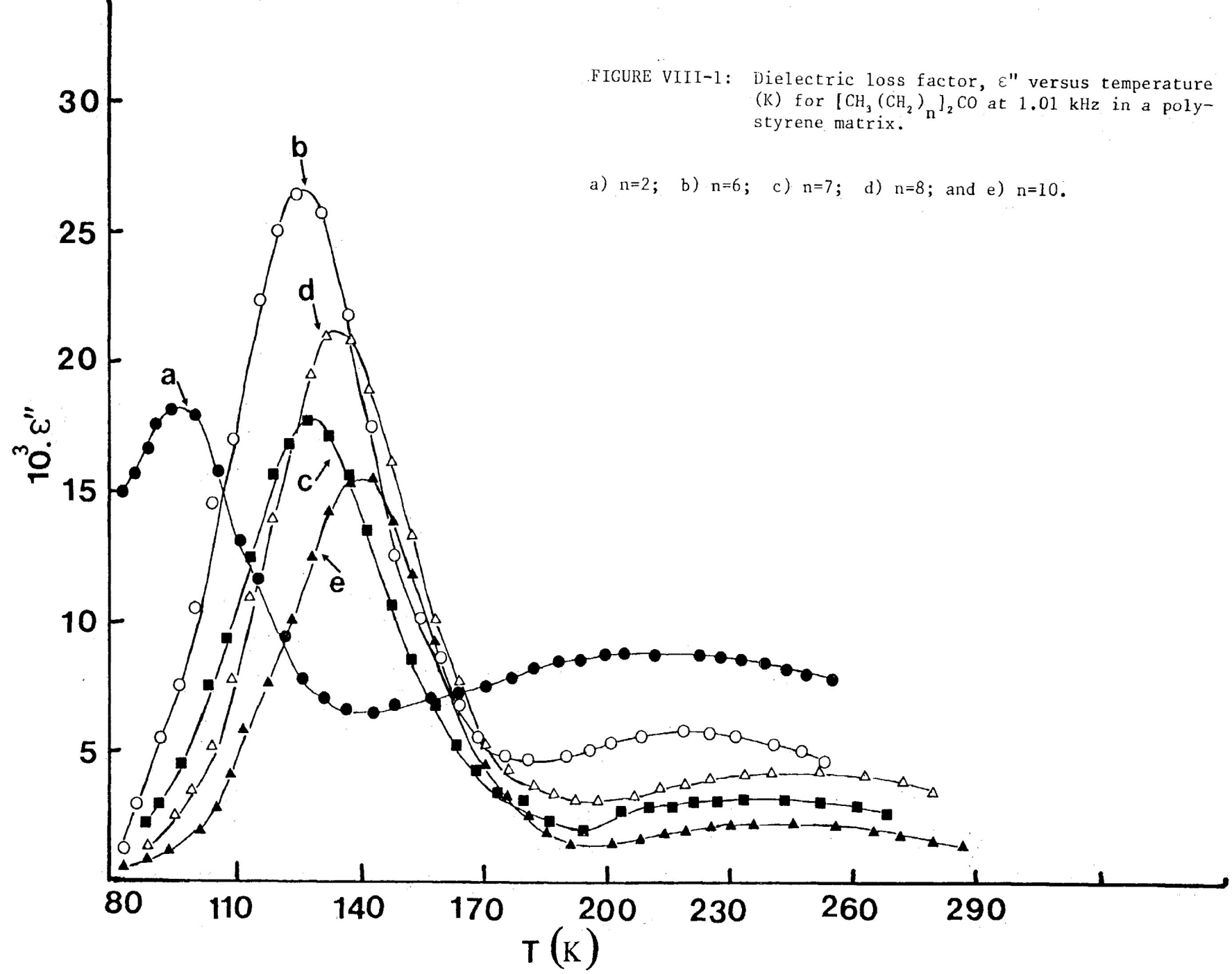
T (K)	$10^6 \tau$ (s)	$\log v_{\max}$	β	$10^3 \epsilon''_{\max}$	ϵ_{∞}	μ (D)
<u>0.55 M di-n-butylether (lower temperature absorption)</u>						
86.2	4254.30	1.58	0.21	3.6	2.865	0.33
88.8	1697.17	1.97	0.22	3.7	2.860	0.33
91.0	787.76	2.31	0.24	3.9	2.856	0.33
92.9	494.48	2.51	0.24	3.9	2.854	0.34
95.4	254.25	2.80	0.24	4.0	2.851	0.35
97.6	136.31	3.06	0.24	4.1	2.848	0.36
101.1	50.52	3.50	0.25	4.2	2.845	0.36
103.9	26.50	3.78	0.25	4.4	2.842	0.37
<u>0.37 M di-n-hexylether (lower temperature absorption)</u>						
108.0	705.70	2.35	0.25	6.1	2.826	0.55
109.6	467.23	2.53	0.26	6.2	2.849	0.54
110.9	357.57	2.64	0.26	6.2	2.849	0.55
112.5	254.82	2.80	0.27	6.3	2.825	0.55
114.9	156.00	3.00	0.27	6.4	2.823	0.56
117.5	81.32	3.28	0.28	6.6	2.819	0.56
120.3	49.60	3.51	0.29	6.7	2.822	0.56
122.2	34.96	3.66	0.30	6.9	2.821	0.57
<u>0.54 M di-n-heptylether (lower temperature absorption)</u>						
108.9	1311.20	2.08	0.24	5.20	2.749	0.43
111.9	620.90	2.41	0.26	5.40	2.749	0.43
114.0	403.94	2.60	0.26	5.50	2.749	0.44
115.4	310.40	2.71	0.28	5.60	2.750	0.43
118.3	144.07	3.04	0.27	5.70	2.748	0.45
120.8	104.84	3.18	0.27	5.70	2.748	0.45
122.6	70.83	3.35	0.28	5.90	2.747	0.46
124.9	47.39	3.53	0.28	6.00	2.747	0.46
128.7	26.38	3.78	0.29	6.20	2.746	0.47

TABLE VIII-7: continued...

T (K)	$10^6 \tau$ (s)	$\log v_{\max}$	β	$10^3 \epsilon''_{\max}$	ϵ_{∞}	μ (D)
<u>0.45 M di-n-octylether (lower temperature absorption)</u>						
113.4	1578.30	2.00	0.27	5.20	2.843	0.45
114.7	1143.80	2.14	0.28	5.30	2.843	0.45
117.6	591.77	2.43	0.29	5.40	2.842	0.45
119.6	345.41	2.65	0.30	5.50	2.841	0.45
121.9	229.87	2.84	0.31	5.60	2.840	0.45
124.8	137.19	3.06	0.31	5.70	2.839	0.46
126.8	86.12	3.26	0.33	5.80	2.839	0.45
129.7	50.98	3.50	0.36	6.00	2.838	0.45
132.7	33.20	3.68	0.38	6.10	2.838	0.44
135.8	21.11	3.88	0.41	6.30	2.838	0.44
<u>0.55 M di-decylether (lower temperature absorption)</u>						
117.0	2917.20	1.74	0.25	4.70	2.839	0.41
119.0	1694.60	1.98	0.28	4.70	2.840	0.39
120.5	1212.40	2.12	0.28	4.80	2.839	0.40
123.5	629.15	2.40	0.28	4.90	2.837	0.40
126.0	344.80	2.66	0.28	5.01	2.832	0.41
128.9	199.71	2.90	0.30	5.10	2.835	0.41
131.6	108.90	3.17	0.31	5.10	2.834	0.41
134.3	64.34	3.40	0.31	5.20	2.833	0.41
137.7	42.19	3.58	0.33	5.40	2.832	0.41
<u>0.35 M di-n-hexadecylether (lower temperature absorption)</u>						
127.0	3675.80	1.64	0.28	2.90	2.834	0.40
129.0	2044.30	1.89	0.28	2.82	2.830	0.40
131.6	1196.30	2.12	0.28	2.89	2.827	0.40
134.8	524.07	2.48	0.29	2.99	2.824	0.41
138.1	433.58	2.79	0.17	2.88	2.821	0.53
141.6	137.62	3.06	0.33	3.08	2.817	0.40
144.5	90.02	3.25	0.35	3.15	2.815	0.40
147.7	49.22	3.51	0.40	3.25	2.813	0.38
149.9	39.14	3.61	0.41	3.29	2.811	0.38

FIGURE VIII-1: Dielectric loss factor, ϵ'' versus temperature (K) for $[\text{CH}_3(\text{CH}_2)_n]_2\text{CO}$ at 1.01 kHz in a polystyrene matrix.

a) $n=2$; b) $n=6$; c) $n=7$; d) $n=8$; and e) $n=10$.



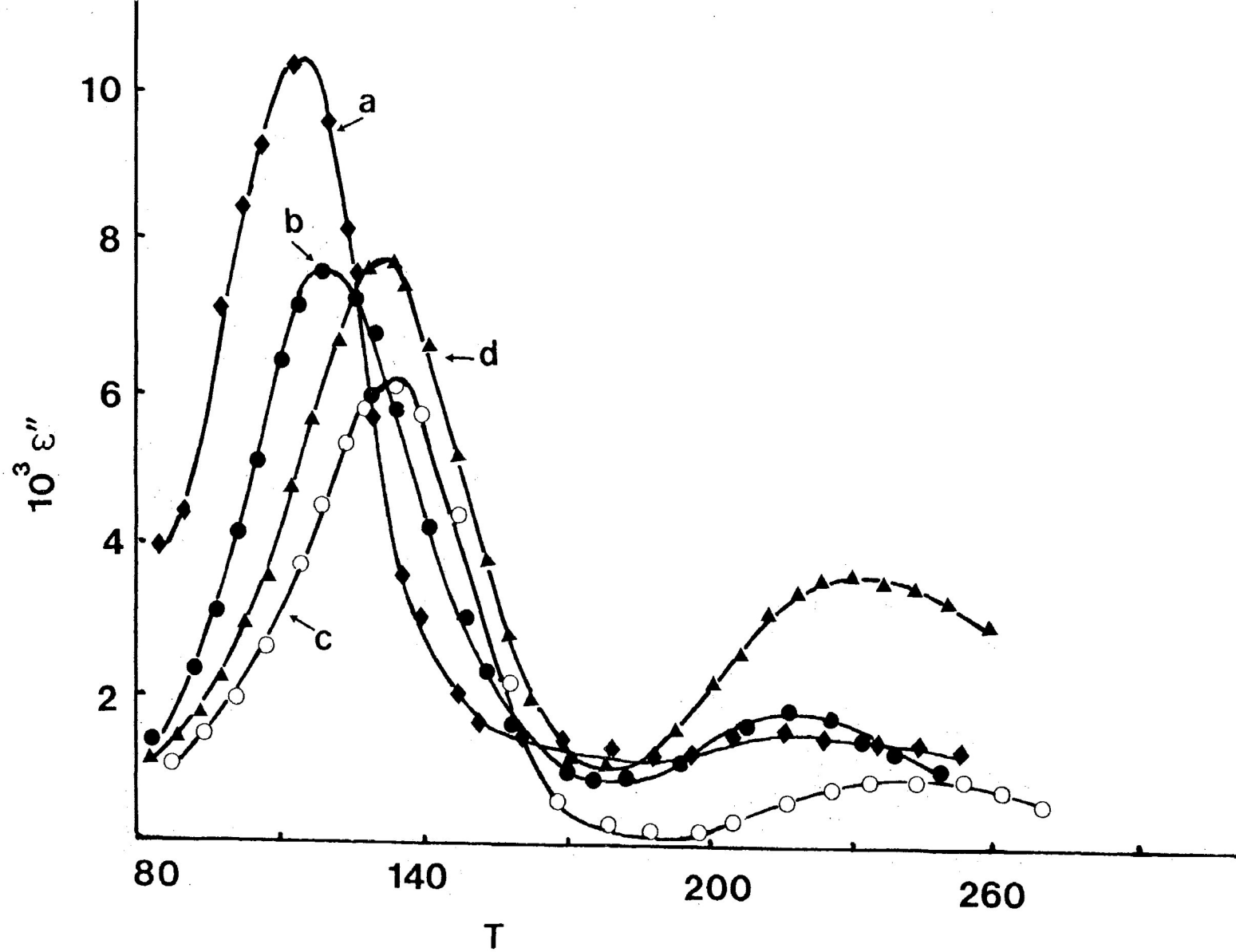


FIGURE VIII-2: Dielectric loss factor, ϵ'' versus temperature (K) for $[\text{CH}_3(\text{CH}_2)_n\text{NH}]$ at 1.01 kHz in a polystyrene matrix. a) $n=3$; b) $n=5$; c) $n=6$; and d) $n=7$.

FIGURE VIII-3: Dielectric loss, ϵ'' versus temperature (K) for $[\text{CH}_3(\text{CH}_2)_n]_2\text{S}$ at 1.01 kHz in a polystyrene matrix.

a) $n=7$; b) $n=10$ and c) $n=11$.

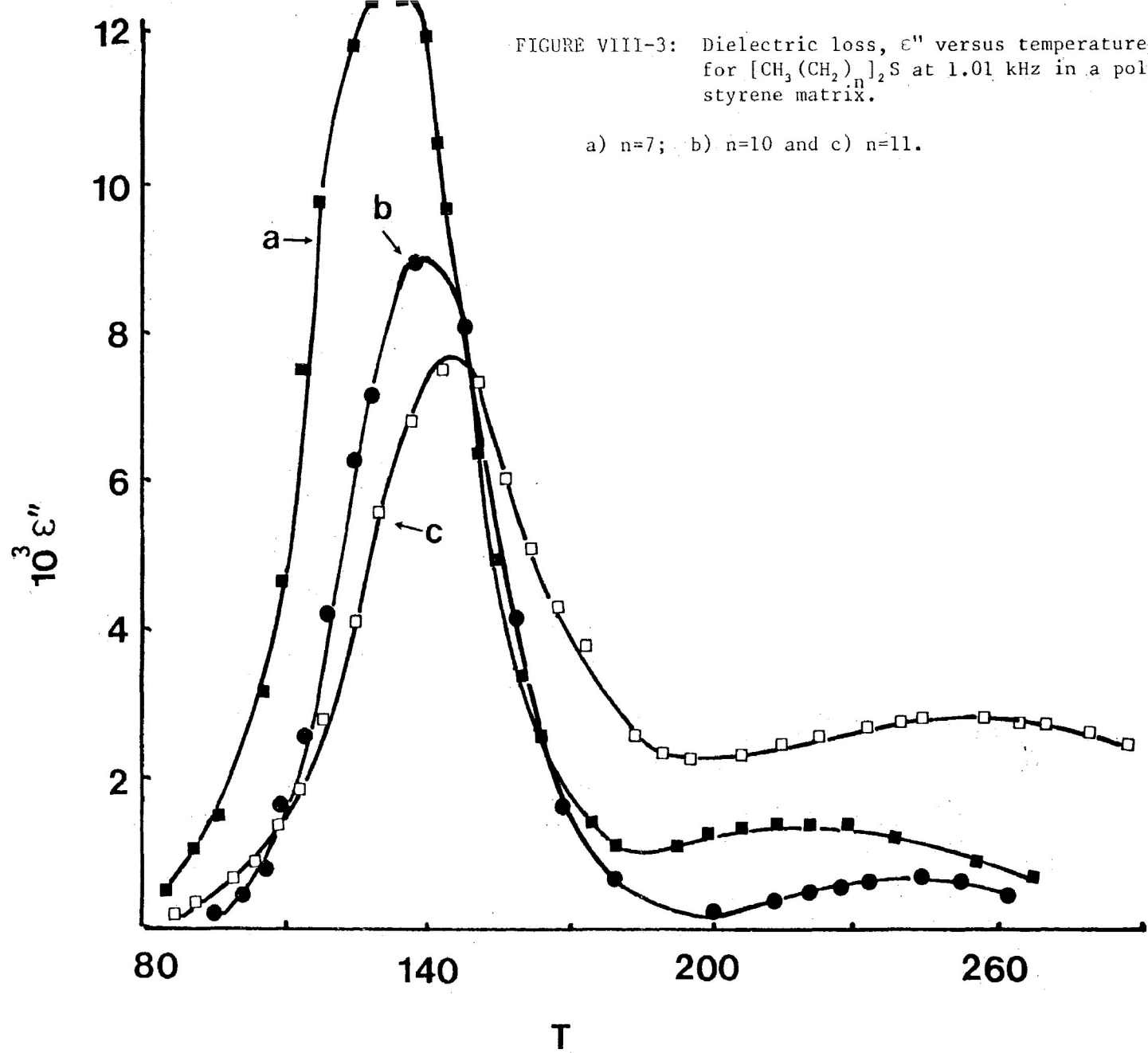
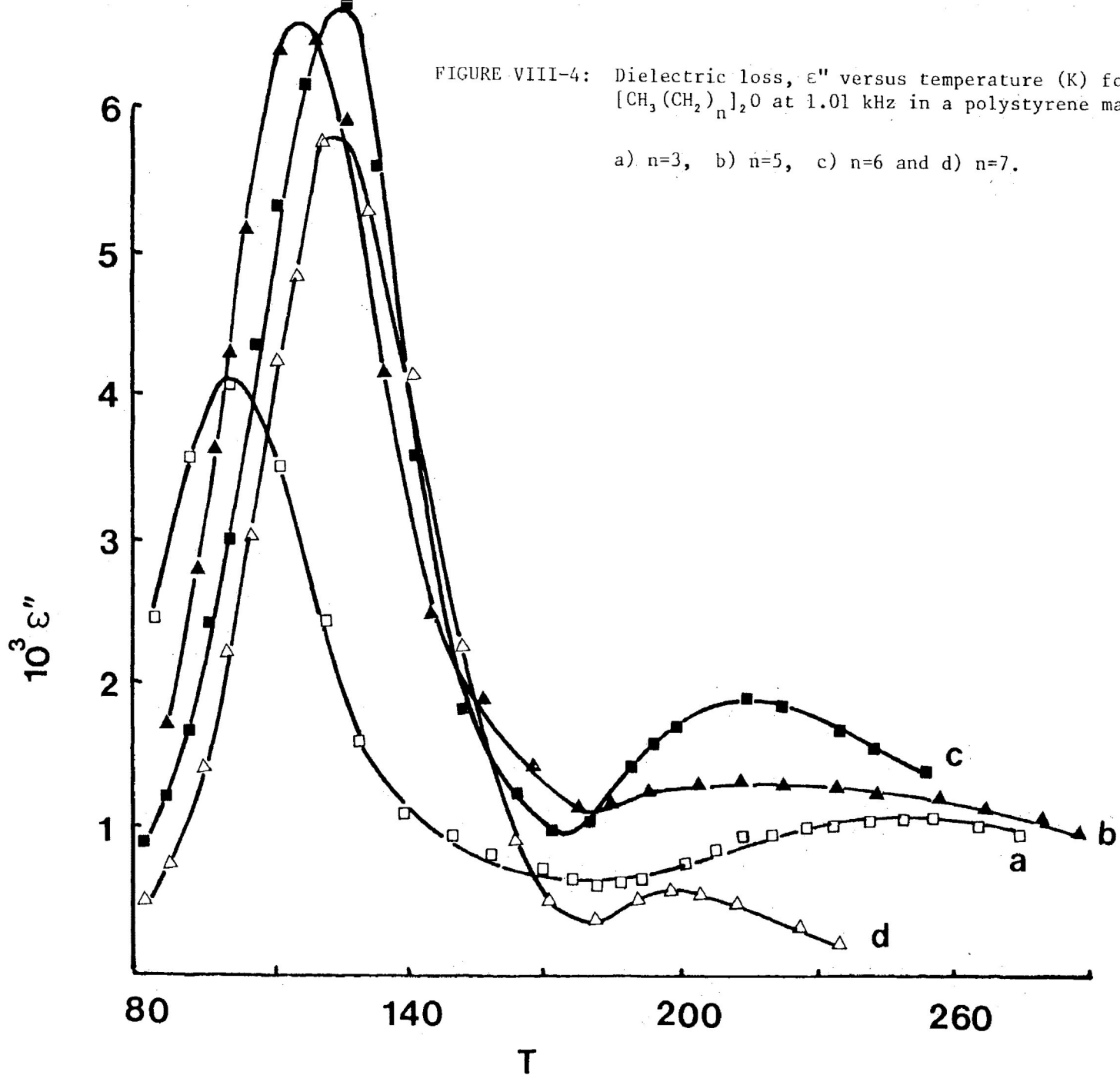


FIGURE VIII-4: Dielectric loss, ϵ'' versus temperature (K) for $[\text{CH}_3(\text{CH}_2)_n\text{O}]_2$ at 1.01 kHz in a polystyrene matrix.

a) $n=3$, b) $n=5$, c) $n=6$ and d) $n=7$.



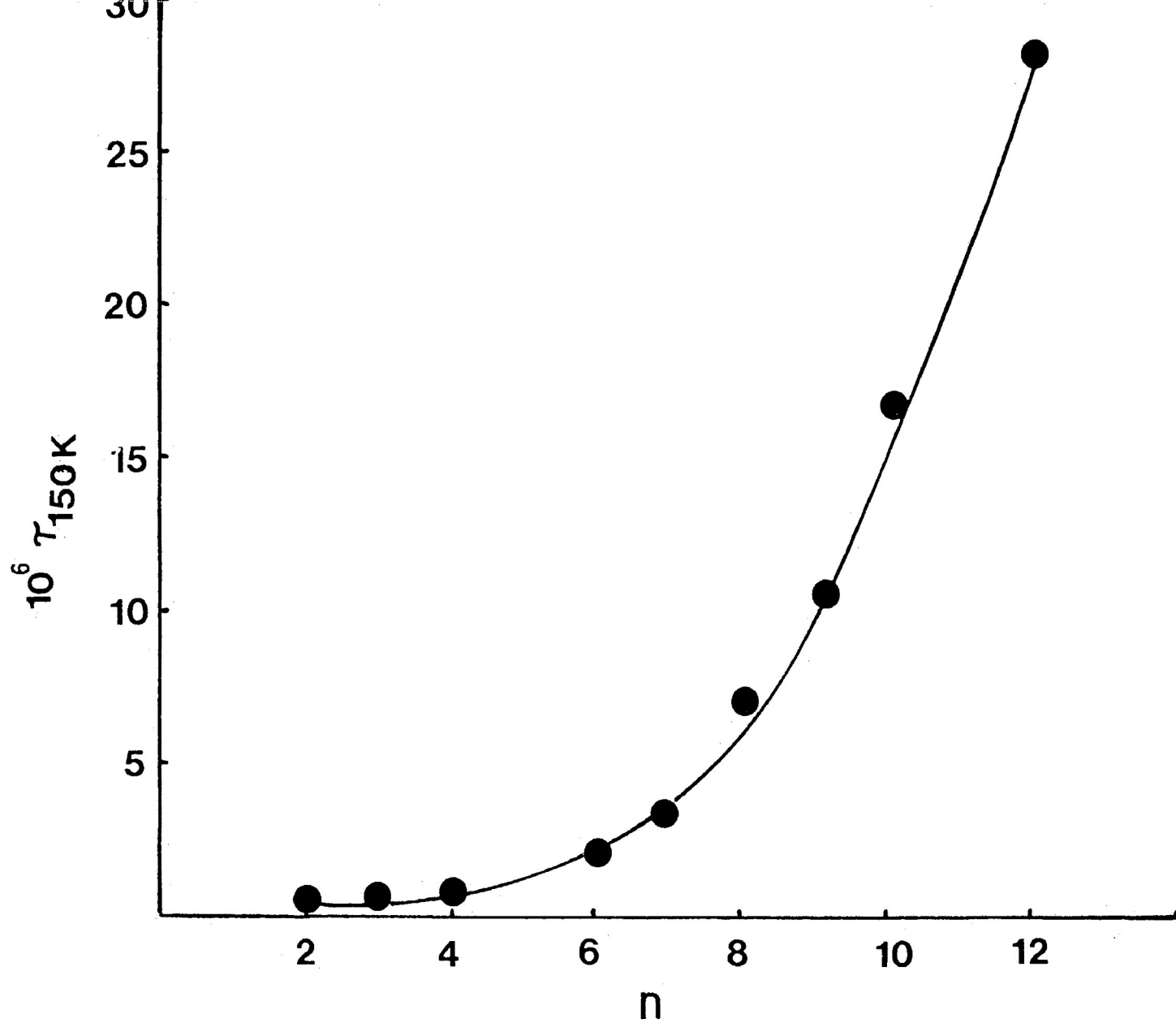


FIGURE VIII-5: Relaxation time at 150 K versus number of methylene groups (n) for the low temperature absorption of $[\text{CH}_3(\text{CH}_2)_n]_2\text{CO}$ in a polystyrene matrix

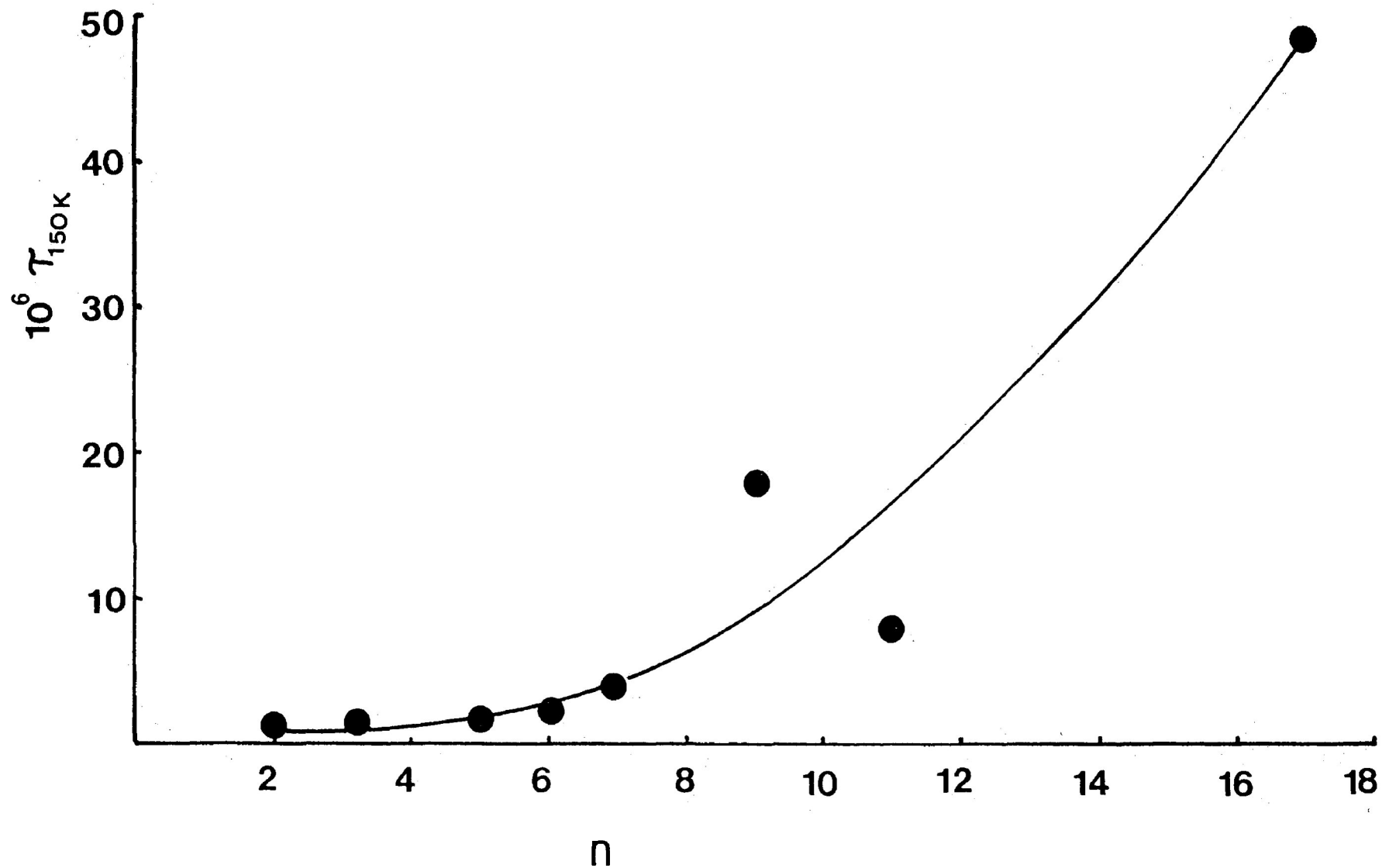


FIGURE VIII-6: Relaxation time at 150 K versus number of methylene groups (n) for the low temperature absorption of $[\text{CH}_3(\text{CH}_2)_n]_2\text{NH}$ in a polystyrene matrix.

for the low temperature absorption of $[\text{CH}_3(\text{CH}_2)_n]_2\text{S}$ in a polystyrene matrix.

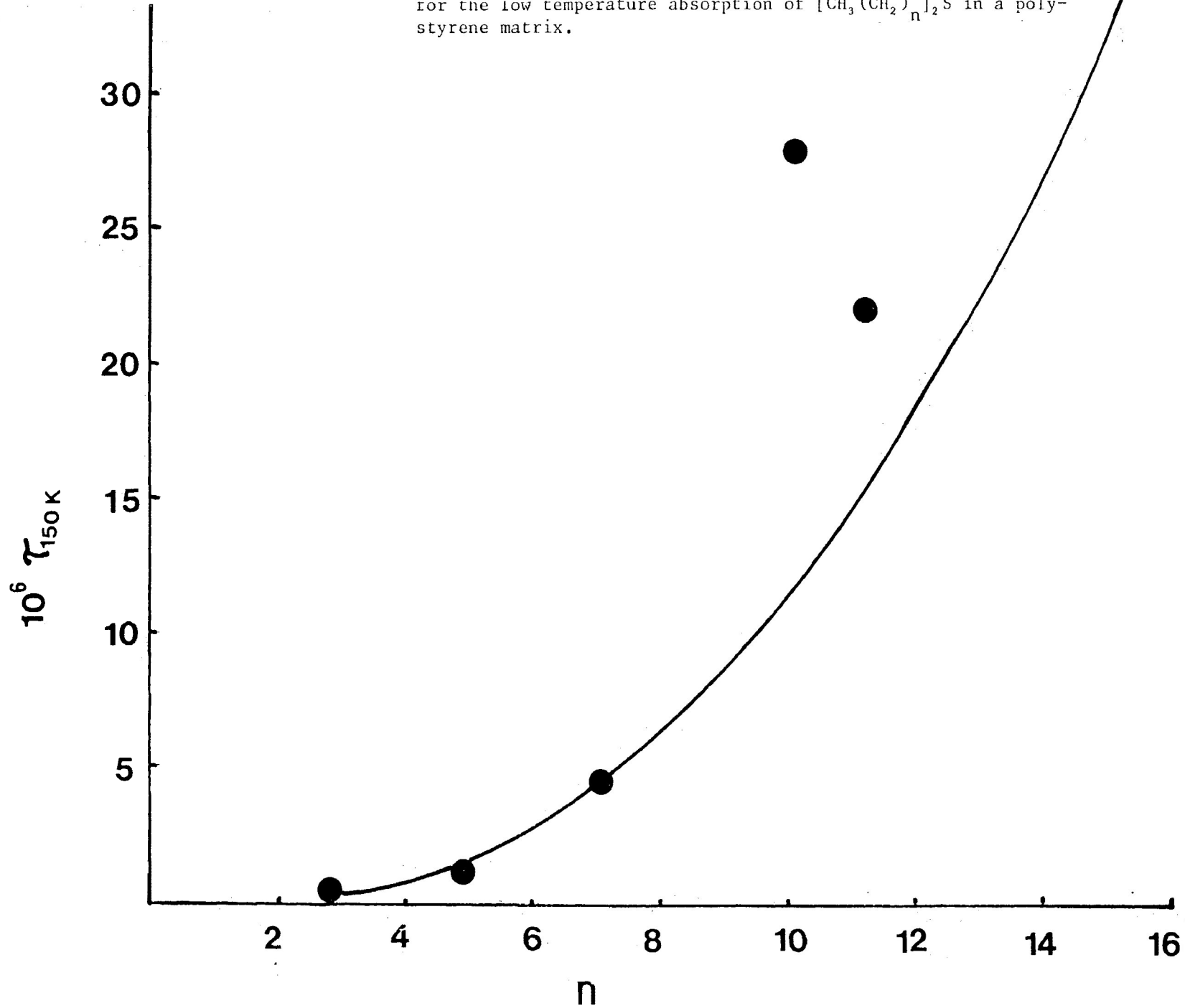


FIGURE VIII-8: Relaxation time at 150 K versus the number of methylene groups (n) for the low temperature absorption of $[\text{CH}_3(\text{CH}_2)_n]_2\text{O}$ in a polystyrene matrix

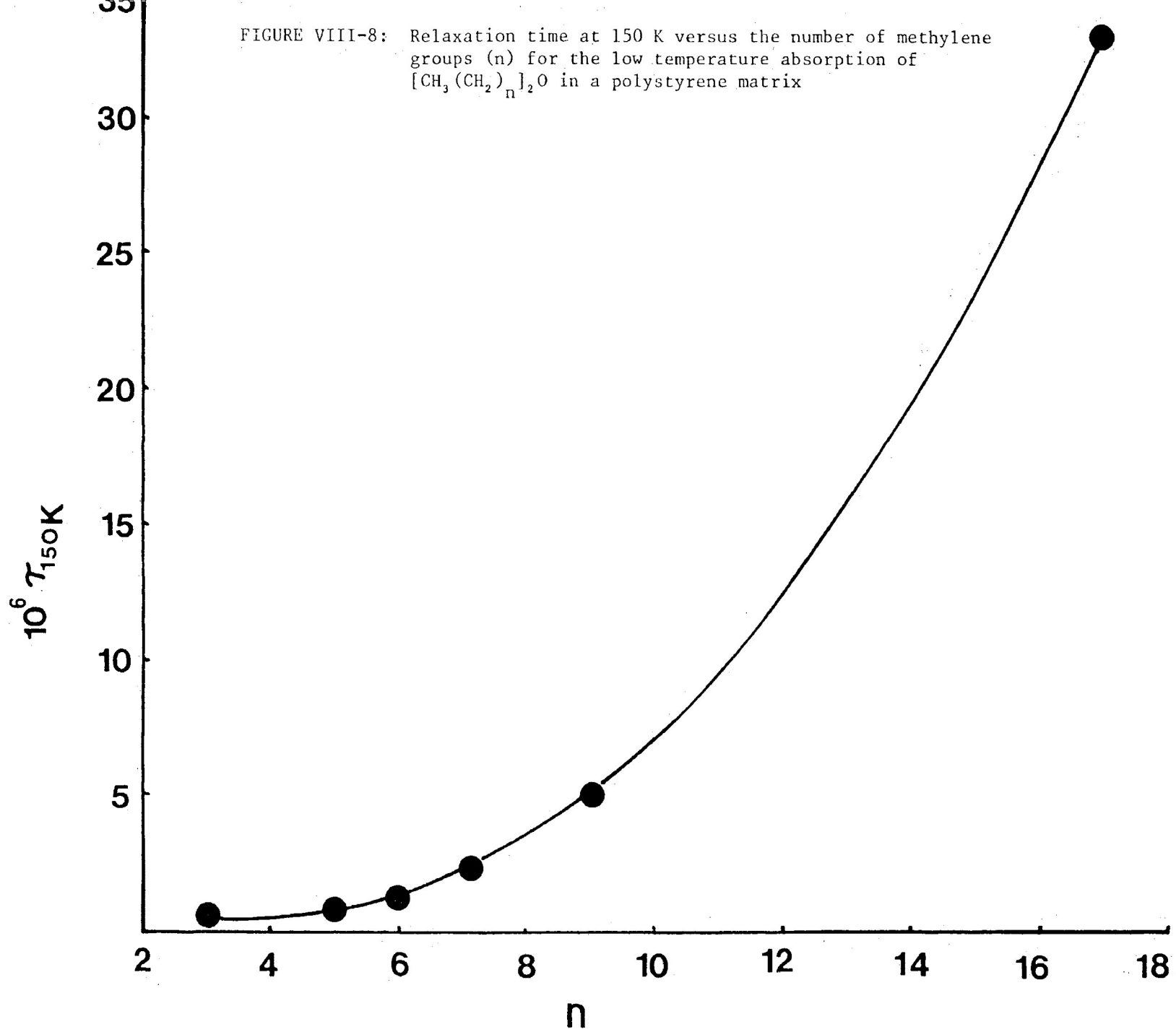


FIGURE VIII-9: Enthalpy of activation versus number of methylene groups for the low temperature absorption of $[\text{CH}_3(\text{CH}_2)_n]_2\text{X}$ in a polystyrene matrix.

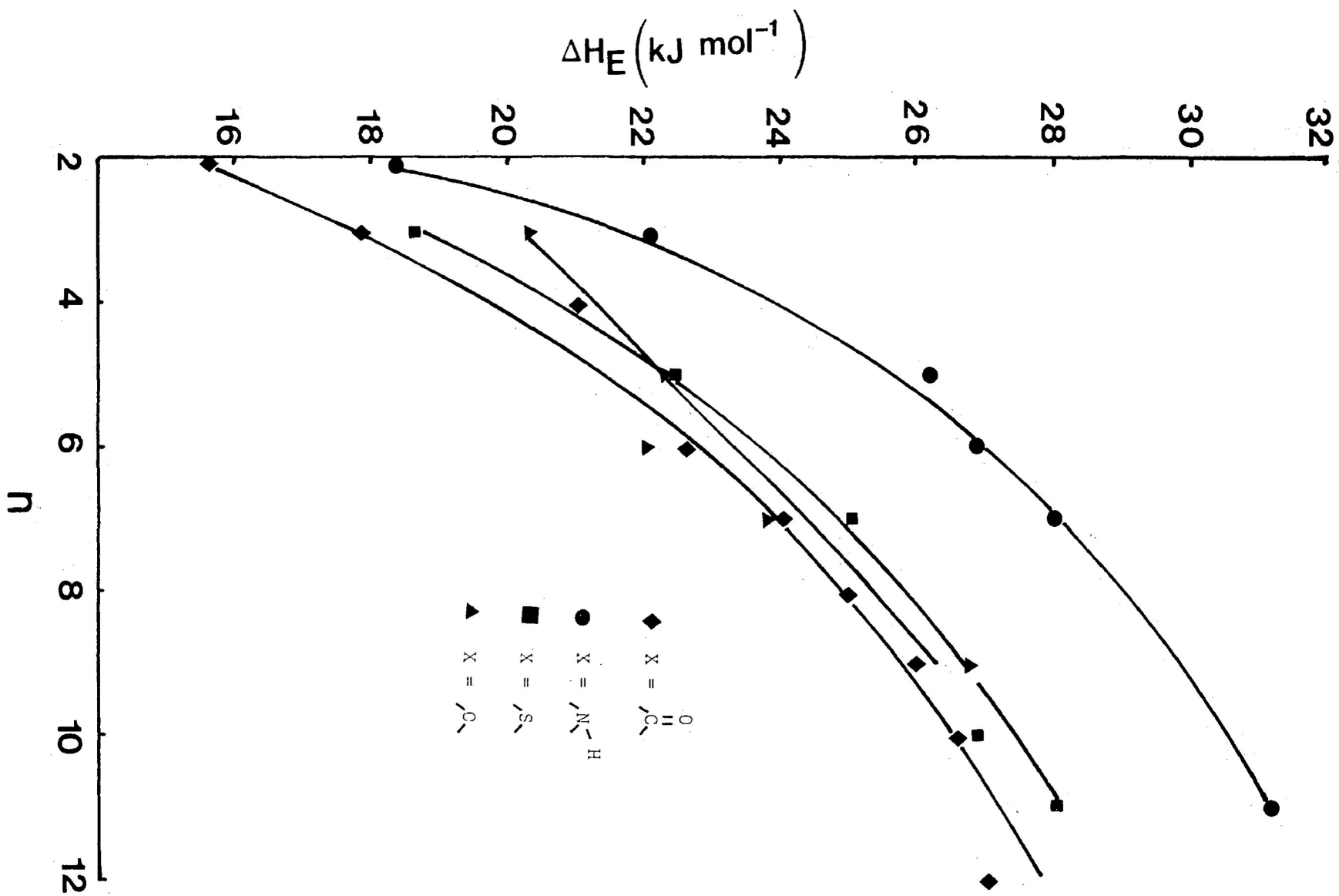
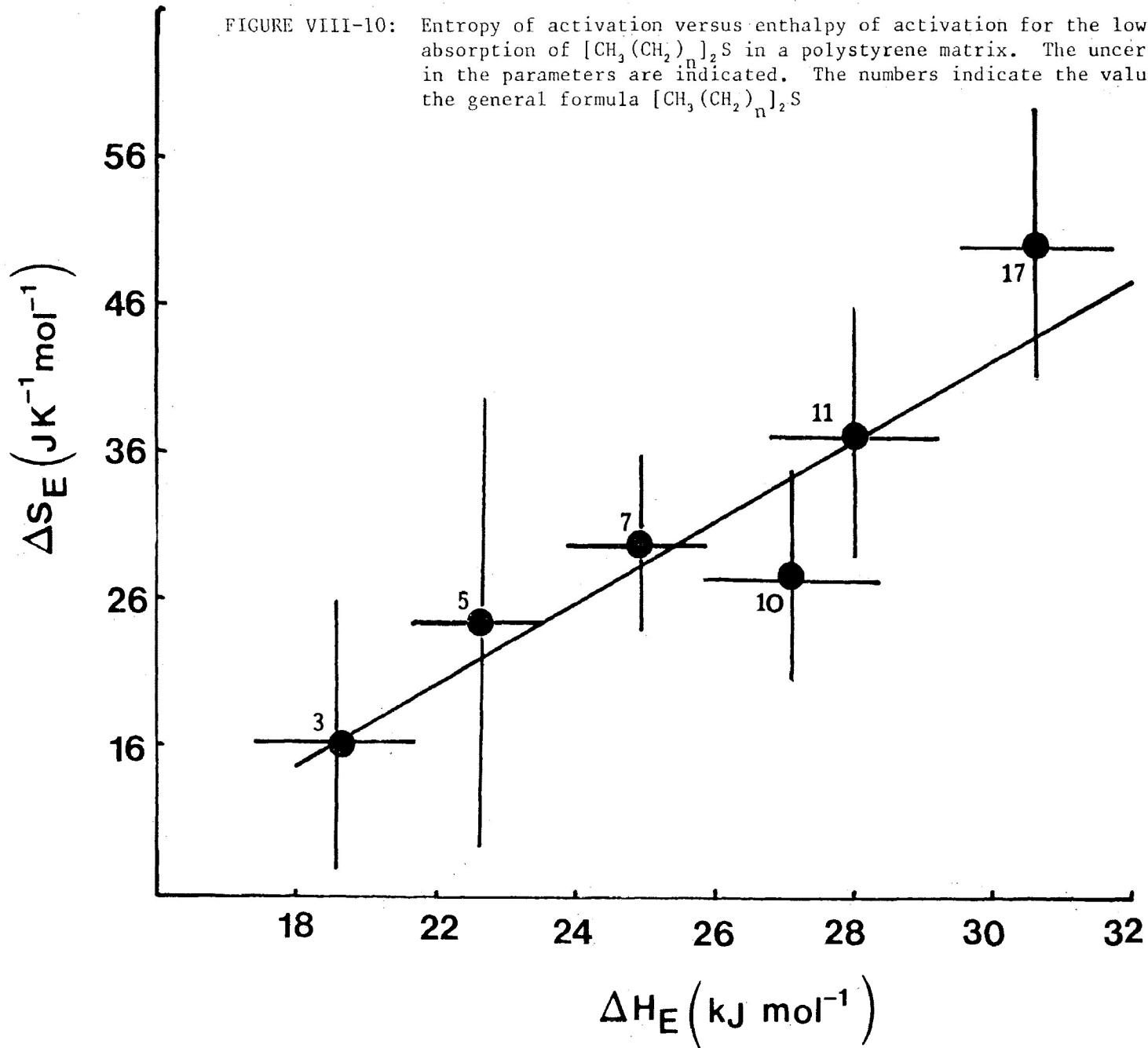


FIGURE VIII-10: Entropy of activation versus enthalpy of activation for the low temperature absorption of $[\text{CH}_3(\text{CH}_2)_n]_2\text{S}$ in a polystyrene matrix. The uncertainties in the parameters are indicated. The numbers indicate the value of n in the general formula $[\text{CH}_3(\text{CH}_2)_n]_2\text{S}$



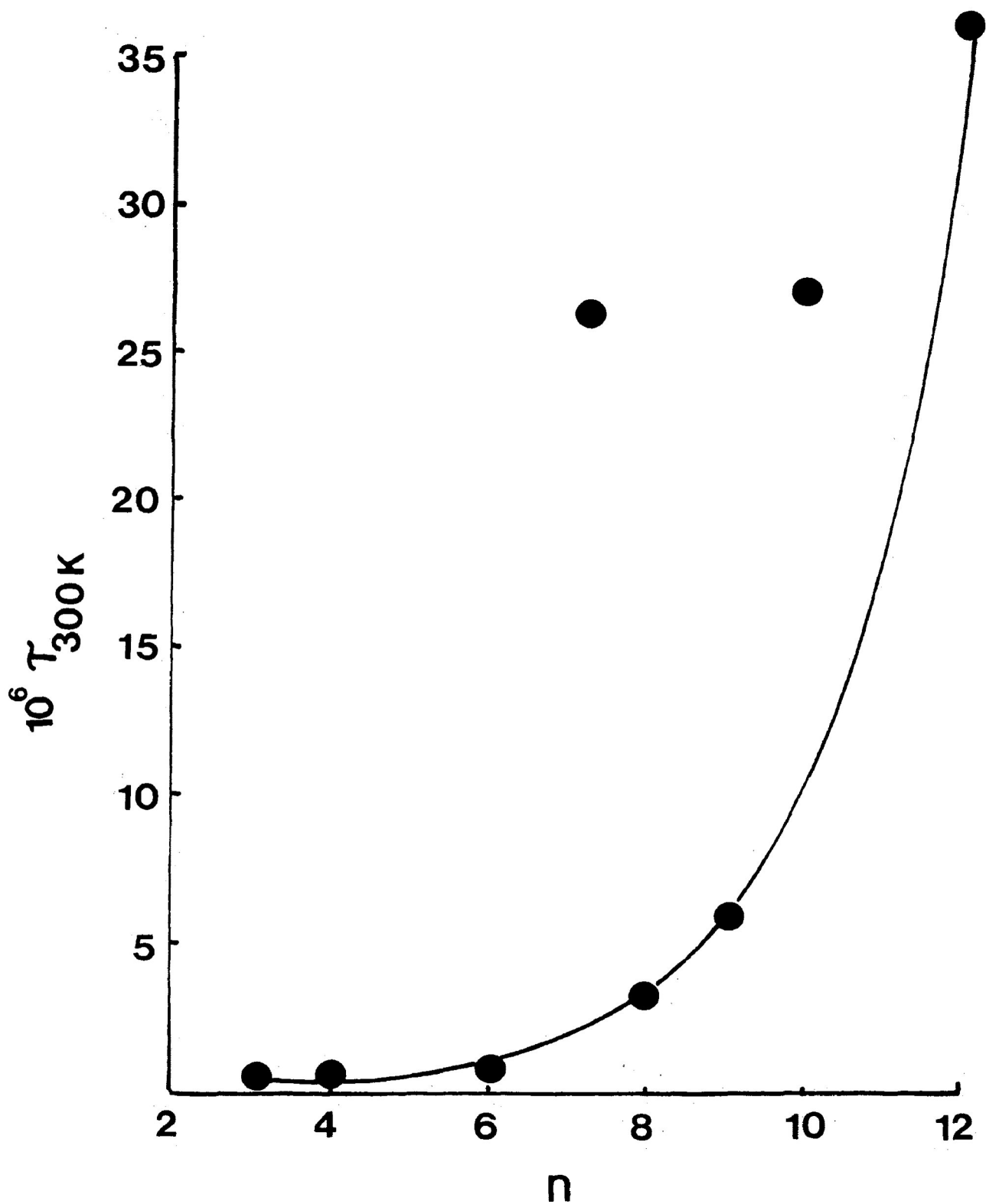


FIGURE VIII-11: Relaxation time at 300 K versus number of methylene groups for the high temperature absorption of $[\text{CH}_3(\text{CH}_2)_n]\text{CH}$ in a polystyrene matrix.

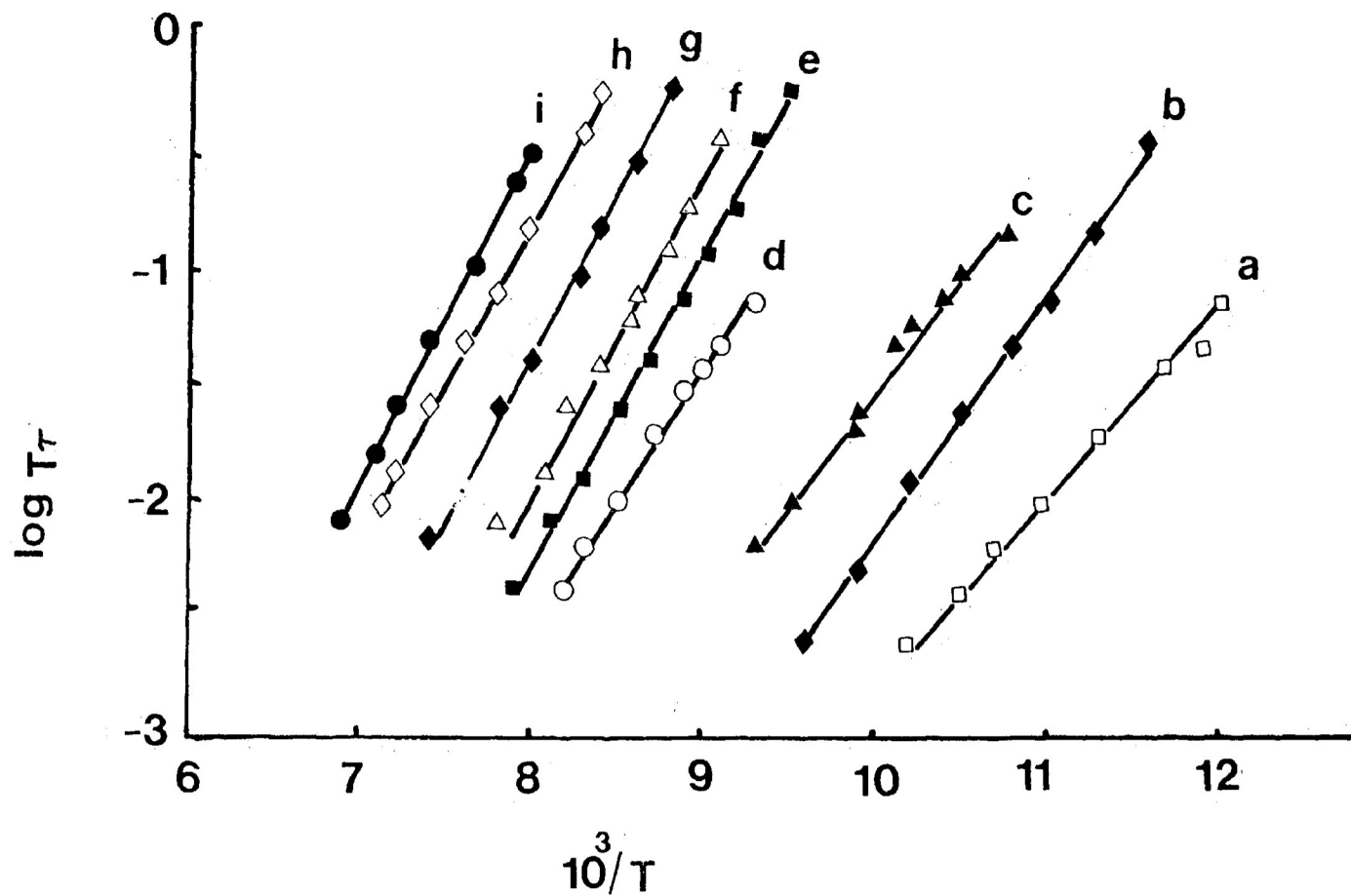
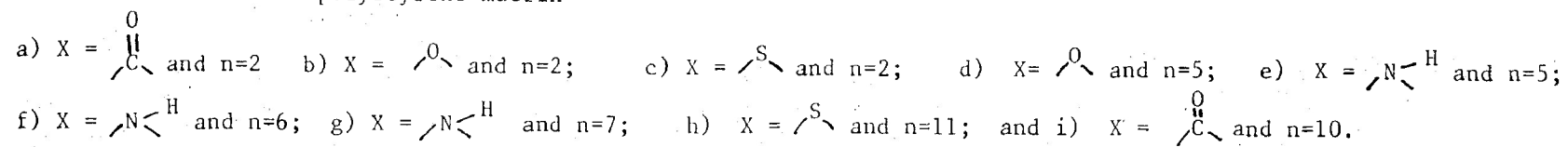


FIGURE VIII-12: Eyring rate plots of $\log T\tau$ versus $1/T$ for the low temperature absorption of $[\text{CH}_2(\text{CH}_2)_n]_2\text{X}$ in a polystyrene matrix



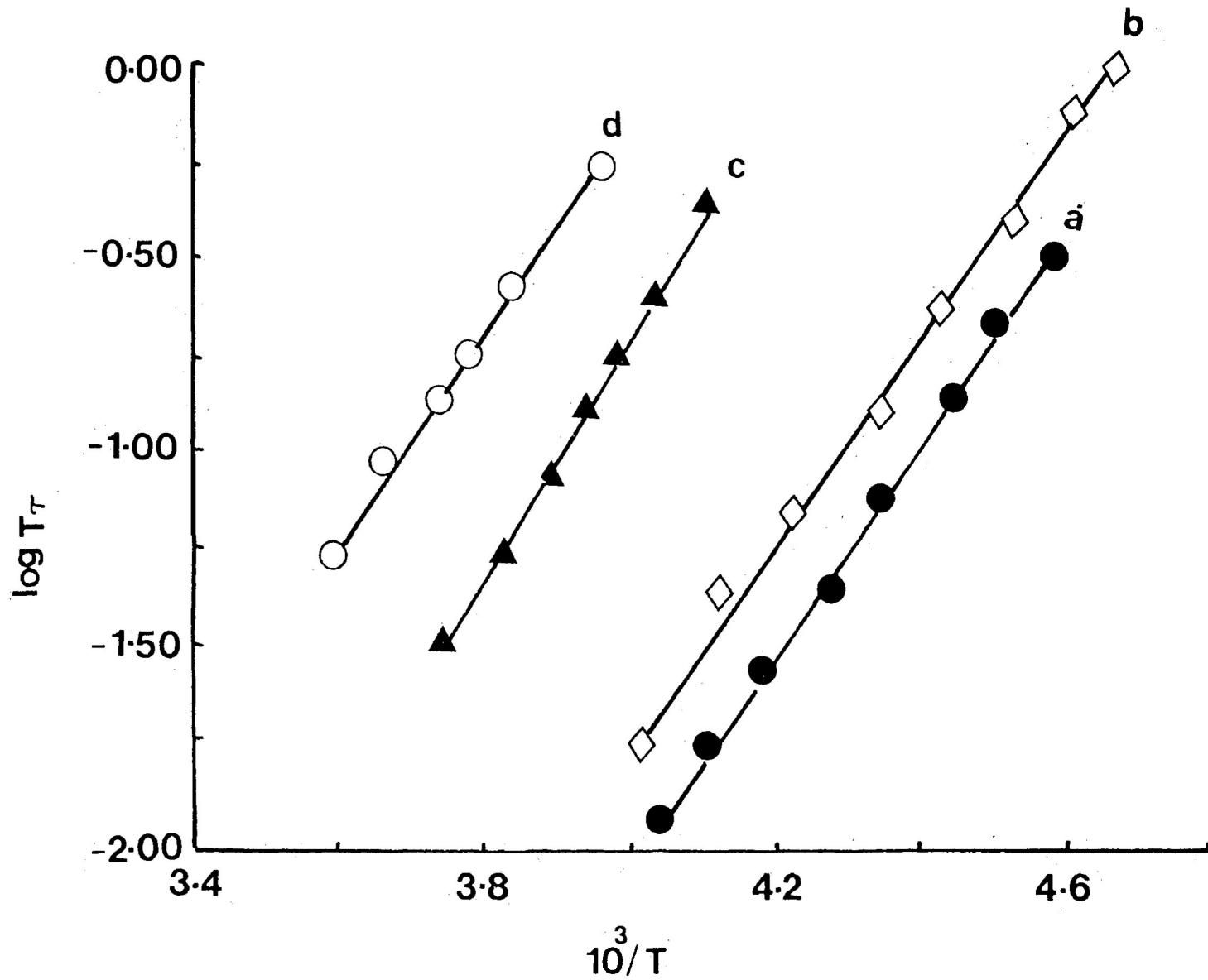


FIGURE VIII-13: Eyring rate plots of $\log T\tau$ versus $1/T$ for the high temperature absorption of $[\text{CH}_2(\text{CH}_2)_n]_2 \text{CO}$ in a polystyrene matrix. a) $n=2$; b) $n=6$; c) $n=9$ and d) $n=12$.

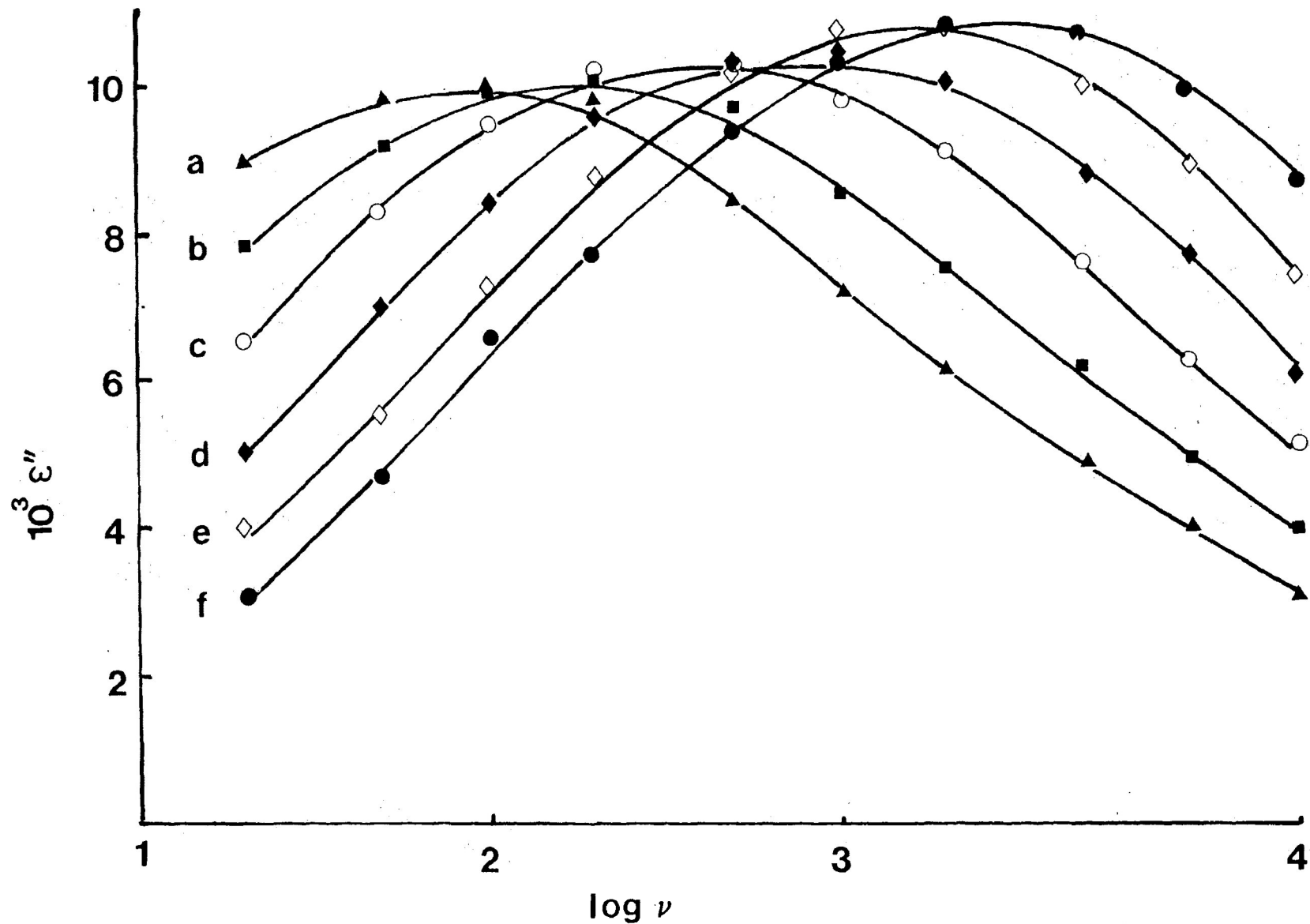


FIGURE VIII-14: Dielectric loss factor, ϵ'' versus $\log \nu$ for the low temperature absorption of $[\text{CH}_3(\text{CH}_2)_{10}]_2\text{CO}$ in a polystyrene matrix
 a) 126.3 K; b) 130.8 K; c) 134.5 K; d) 138.2 K; e) 142.0 K and f) 145.5 K.

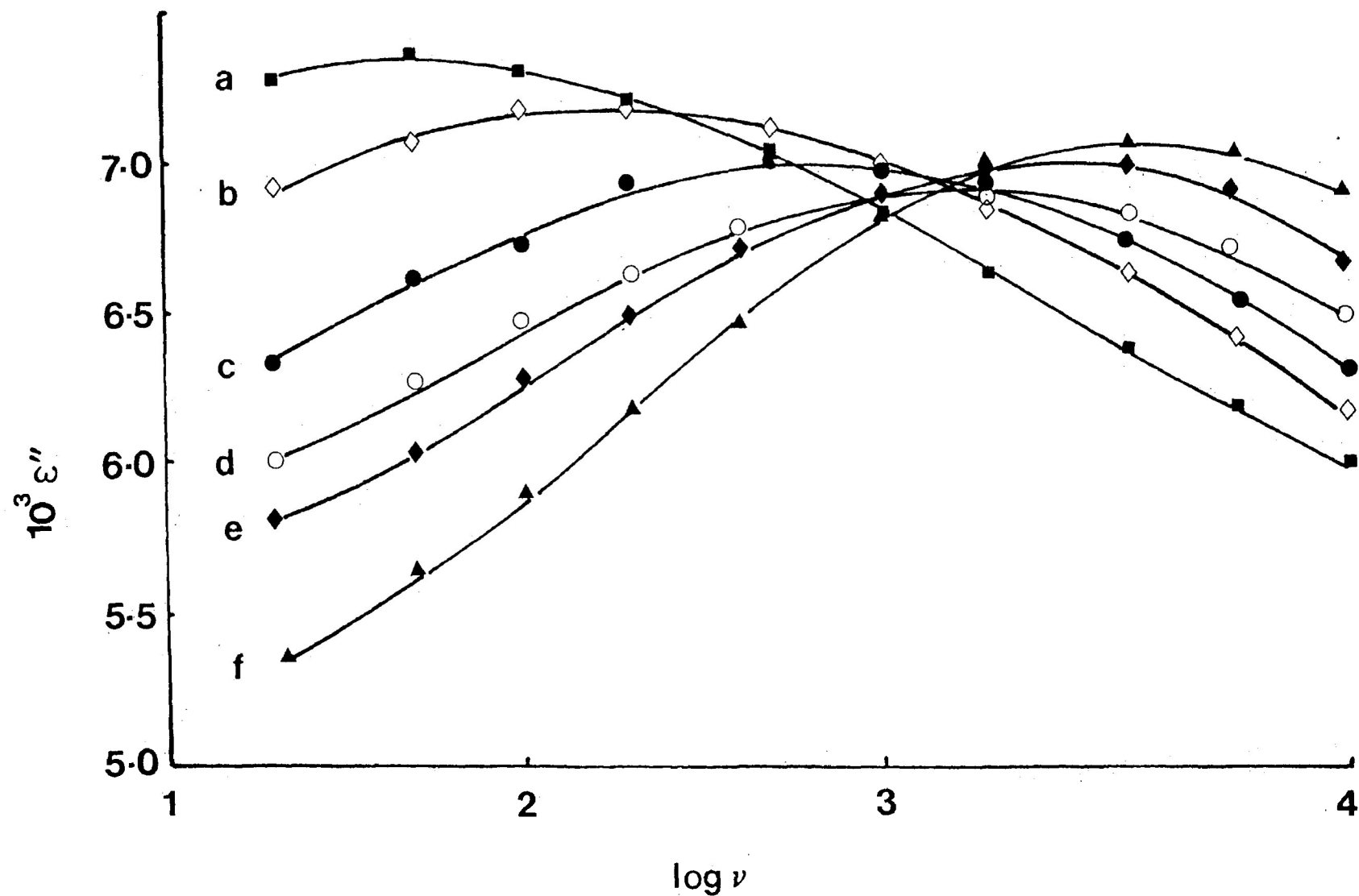


FIGURE VIII-15: Dielectric loss factor, ϵ'' versus $\log \nu$ for the high temperature absorption of $[\text{CH}_3(\text{CH}_2)_2]_2\text{CO}$ in a polystyrene matrix.

a) 214.2 K; b) 217.4 K, c) 221.6 K; d) 226.7 K; e) 230.4 K; and f) 237.4 K.

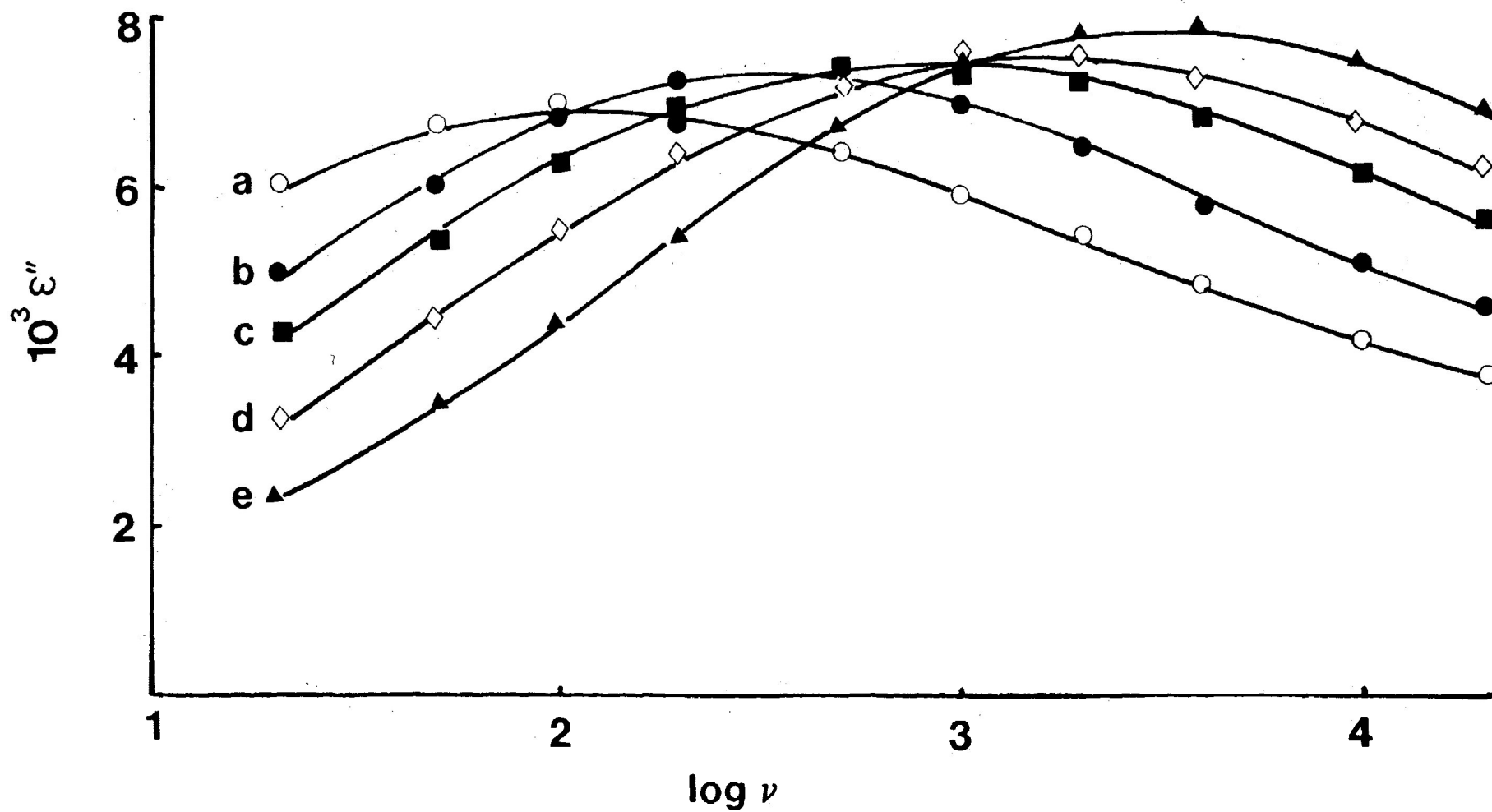


FIGURE VIII-16: Dielectric loss factor, ϵ'' versus $\log \nu$ for the low temperature absorption of $[\text{CH}_3(\text{CH}_2)_7]_2\text{NH}$
 a) 116.4 K; b) 121.2 K; c) 125.3 K; d) 131.6 K; and e) 135.9 K.

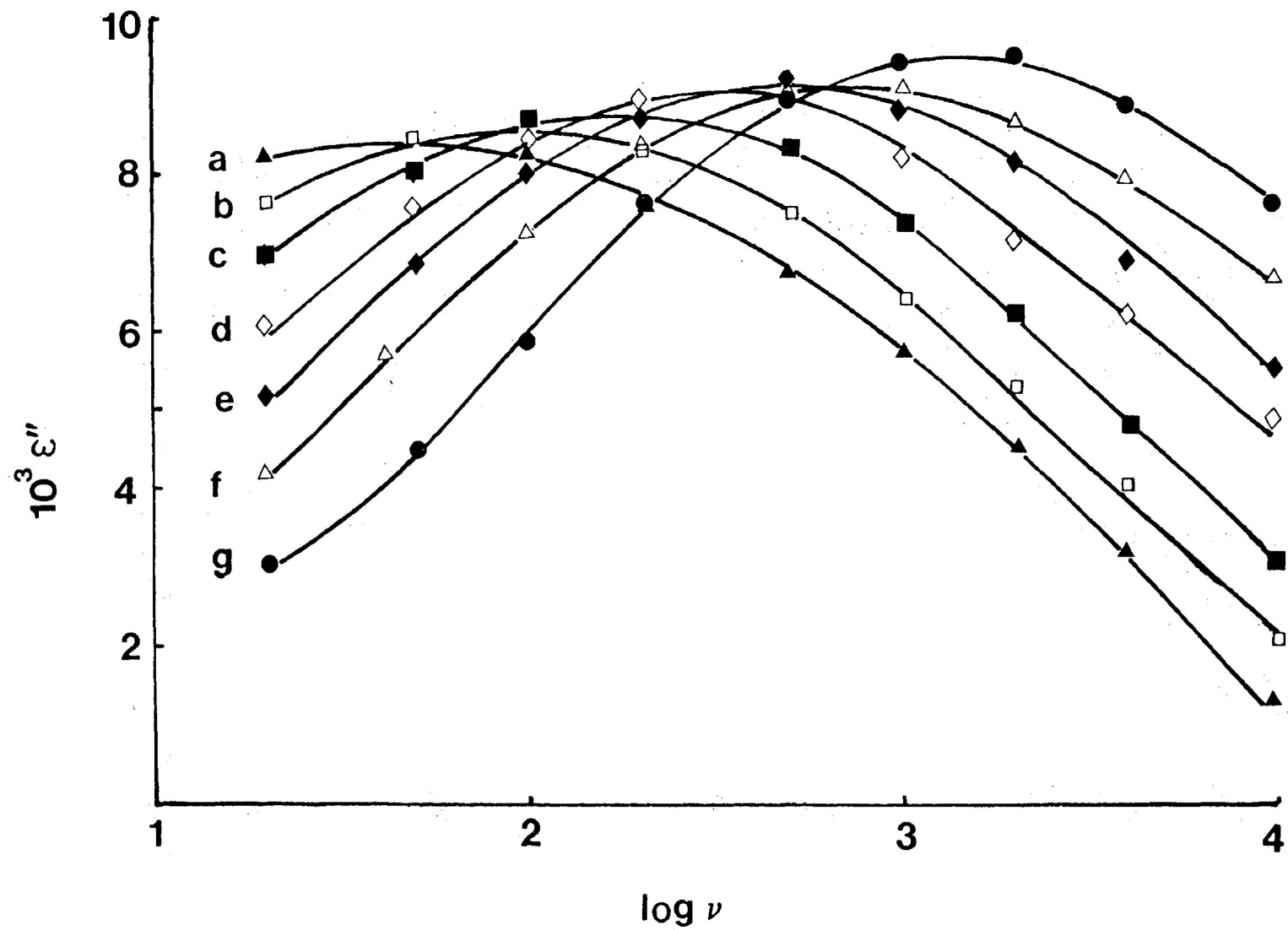


FIGURE VIII-17: Dielectric loss factor, ϵ'' versus $\log \nu$ for the low temperature absorption of $[\text{CH}_3(\text{CH}_2)_{11}]_2\text{S}$ in a polystyrene matrix.

a) 123.0 K; b) 126.1 K; c) 131.5 K; d) 134.5 K; e) 137.3 K; f) 141.1 K and g) 145.1 K.

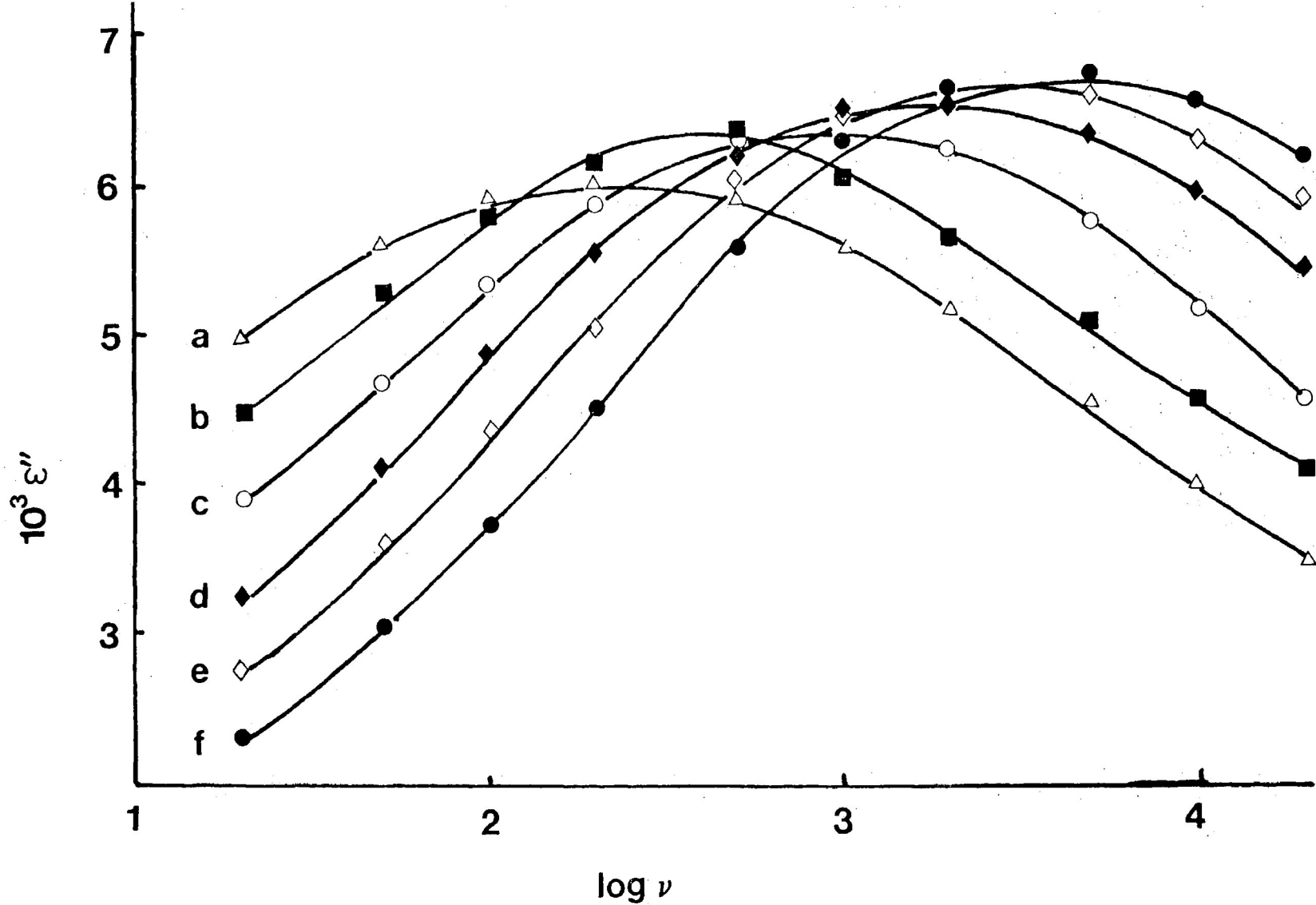


FIGURE VIII-18: Dielectric loss factor, ϵ'' versus $\log \nu$ for the low temperature absorption of $[\text{CH}_3(\text{CH}_2)_5]_2\text{O}$ in a polystyrene matrix.

a) 108.0 K; b) 110.9 K; c) 114.9 K; d) 117.5 K; e) 120.3 K; and f) 122.2 K.

CHAPTER IX

CONCLUSIONS AND SUGGESTIONS FOR FURTHER WORK

CONCLUSIONS

To conclude this thesis, the three major aspects examined will be summarized. Clearly, one of the purposes of this research work was to explore the nature of β -relaxation in the glassy forming solids of the rigid molecules. In general, the ΔH_E values for each solute in a particular solvent show an increase with increased molecular size (see Table III-1). The reasonable correspondence of each of the ΔH_E values for the o-dichlorobenzene, 4-methylpyridien and bromoform in cis-decalin, o-terphenyl and polyphenyl ether with polystyrene indicate the molecular nature of the process. An attempt has been made to extend the concept of the single solute molecule (at low concentration) in the polystyrene cavity to that of the solvents - the model being that there is a trapped solute molecule (in what is effectively a cavity) where the molecular relaxation takes place between equilibrium positions. On the time scale of the relaxation process the "solvent cavity" does not need to alter appreciably to permit a solute molecule to rotate. Our systems which seem to lead to a "solvent cavity" model, for somewhat limited types of systems, would seem in harmony with the more general model conceived by Johari.

The second aspect of this study involved

aromatic flexible molecules (see Chapter IV) capable of exhibiting molecular and intramolecular processes. In most cases comparisons were made between results obtained in cis-decalin and media such as glassy o-terphenyl, polyphenyl ether and polystyrene. Generally, Eyring and relaxation parameters determined were in excellent agreement within experimental error with those determined by other workers using glassy o-terphenyl and other solvent systems. In the systems studied methoxy group relaxation is the main contributor to the dielectric relaxation except for para-fluoroanisole. The barrier to methoxy group rotation is independent of para-substitution and the choice of solvent. The work establishes that for most of the anisoles in these various glassy media, the β -relaxation is an intramolecular one.

The third aspect of this thesis, which is to investigate long chain polar molecules, explores to a great extent, the dielectric mechanisms through which these molecules relax. Long chain polar molecules having the general formulae $\text{CH}_3(\text{CH}_2)_n\text{X}$ (where $\text{X} = -\text{CH}_2\text{Br}$, $-\text{COCH}_3$ and $-\text{NH}_2$) and $[\text{CH}_3(\text{CH}_2)_n]_2\text{Y}$ (where $\text{Y} = \begin{array}{c} \text{O} \\ \parallel \\ \text{C} \end{array}$, S , O and $\text{N} \begin{array}{l} \diagup \\ \diagdown \end{array} \text{H}$) exhibited two distinct relaxation processes for molecules with $n > 6$. The long chain polar molecule theme of this thesis work has been divided into two types of study. The first of these in Chapters V and VII is an attempt to characterize

the mechanisms of dipole reorientation for the low temperature absorption processes for molecules of the type $\text{CH}_3(\text{CH}_2)_n\text{X}$ (where $\text{X} = -\text{CH}_2\text{Br}$, $-\text{COCH}_3$ and $-\text{NH}_2$). Both the relaxation time at 150 K and ΔH_E values increase appreciably with the increase in the number of carbon atoms in the chain (see Figures V-4, VII-3 and VII-4) for the low temperature absorption of 1-bromoalkanes, 2-alkanones and 1-aminoalkanes. The following three quite similar empirical relationships were obtained for the low temperature absorption of $\text{CH}_3(\text{CH}_2)_n\text{X}$:

$$\Delta S_E = 4.1 \quad \Delta H_E - 70 \text{ for } \text{X} = -\text{CH}_2\text{Br}$$

$$\Delta S_E = 3.3 \quad \Delta H_E - 48 \text{ for } \text{X} = -\text{COCH}_3$$

$$\Delta S_E = 3.7 \quad \Delta H_E - 50 \text{ for } \text{X} = -\text{NH}_2$$

The nature of polar end groups has negligible influence on the Eyring and relaxation parameters for the low temperature absorption (see Table VII-1). The intramolecular rotation about the C-C bonds involving the movement of the polar end group has been suggested as the most likely mechanism of dipole reorientation for the low temperature absorption and the size of the reorientating unit increases as n increases.

In the case of high temperature absorption

NOTE: In the equations in this chapter where ΔS_E is related to ΔH_E the former is expressed in $\text{JK}^{-1} \text{mol}^{-1}$ and the latter in kJ mol^{-1}

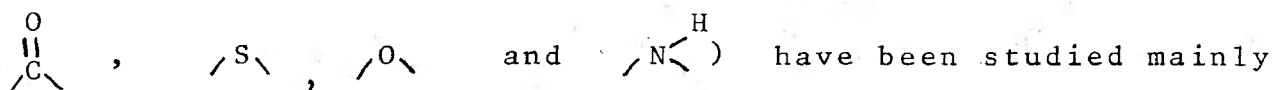
of these molecules, both ΔH_E values and relaxation time are found to increase significantly with the increase in the number of carbon atoms in the chain (see Figure V-6 and Table VII-2). The data (see Table VII-2) for the high temperature process follow the relationship:

$$\Delta S_E = 2.2 \Delta H_E - 72$$

within experimental error (see Figure VII-9) which has been obtained by Khwaja and Walker for the molecular relaxation of rigid molecules in a polystyrene matrix. Thus the high temperature absorption process for 1-bromoalkanes, 2-alkanones and 1-aminoalkanes may be attributed to a molecular rotation process.

The contribution of intramolecular and molecular processes to the total absorption is very similar for 1-bromoalkanes (see Figure V-1) and 2-alkanones (see Figure VII-1) whereas for 1-aminoalkanes (see Figure VII-2) intramolecular process is a dominant one.

The second area of long chain polar molecule study is found in Chapter VIII in which symmetrically substituted alkanes of the general formula $[\text{CH}_3(\text{CH}_2)_n]_2\text{Y}$ (where Y=



to show the influence of (a) the location of dipole and different polar groups on the Eyring and relaxation parameters for the low temperature absorption. The data for the low temperature absorption of $[\text{CH}_3(\text{CH}_2)_n]_2\text{Y}$ can be represented by the following empirical relationship:

$$\Delta S_E = 1.5 \Delta H_E - 5$$

within experimental errors (see Figure VIII-10). The nature of the polar group Y has negligible effect on the ΔH_E values and relaxation time for the low temperature absorption of $[\text{CH}_3(\text{CH}_2)_n]_2\text{Y}$ (see Table VIII-1). The low temperature absorption is attributed to intramolecular rotation about the C-C bonds involving the movements of the polar groups in addition to any flexibility in the polar group itself. The high temperature absorption of symmetrically substituted ketones may be attributed to a molecular rotation.

The location of the dipole away from the chain end has negligible effect on the relaxation time and ΔH_E values for the low temperature absorption of long chain amines and ketones in a polystyrene matrix (see Tables VII-2 and VII-3). The dielectric relaxations in these symmetrically substituted molecules are dominated by an intramolecular rotation (see Figures VIII-1 to 4).

The location of the bromine atom along the n-octane chain has significant effects on both the relaxation time and the ΔH_E values (see Chapter VI). The increase in ΔH_E values and relaxation time for the low temperature absorption as the bromine atom is moved along the n-octane chain may be attributed to the (a) increase in the size of the reorientating unit and (b) the steric effects. The decrease in relaxation time, as the bromine atom is moved along the n-octane chain for the high temperature absorption, is attributed to the decrease in volume swept out on molecular rotation.

For all long chain polar molecules, regardless of dipole location, the data can be analyzed by a relaxation model which involves a molecular relaxation process (governed by a μ_m moment) and segmental motion involving movement of the polar group (characterized by a μ_s moment). The extrapolated values of μ_m and μ_s at 330 K lead to a molecular dipole moment in reasonable agreement with literature values.

For all long chain polar molecules studied, the energy difference, ΔE_0 , between the equilibrium positions of dipole has been found to be very low, 0-6 kJ mol⁻¹ and the two sites, symmetrical barrier model in which dipoles

rotate from one equilibrium position to the other through an angle of 180° seems adequate in a polystyrene matrix. The summaries of the results of long chain polar molecules are given in Table IX-1 and IX-2.

TABLE IX-1

Summary of results for the long chain polar molecules in a polystyrene matrix
(low temperature absorption)

Type of molecules studied	$T_{150\text{ K}}$ increases with the increase in the number of carbon atoms	ΔH_E increases with the increase in the number of carbon atoms	Plot of ΔS_E versus ΔH_E is linear and represented by the empirical relationship:	Mechanism of dielectric relaxation: intramolecular rotation about the C-C bond involving the movement of the polar group	Similar contribution of the intramolecular and molecular processes to the total absorption	Intramolecular process in a dominant one
$\text{CH}_3(\text{CH}_2)_n\text{CH}_2\text{Br}$	x	x	$\Delta S_E = 4.1 \Delta H_E - 70$	x	x	
$\text{CH}_3(\text{CH}_2)_n\text{COCH}_3$	x	x	$\Delta S_E = 3.3 \Delta H_E - 48$	x	x	
$\text{CH}_3(\text{CH}_2)_n\text{NH}_2$	x	x	$\Delta S_E = 3.7 \Delta H_E - 50$	x		x
$[\text{CH}_3(\text{CH}_2)_n]_2\text{CO}$	x	x	$\Delta S_E = 1.5 \Delta H_E - 5$	x		x
$[\text{CH}_3(\text{CH}_2)_n]_2\text{S}$	x	x		x		x
$[\text{CH}_3(\text{CH}_2)_n]_2\text{O}$	x	x		x		x
$[\text{CH}_3(\text{CH}_2)_n]_2\text{NH}$	x	x		x		x
$\text{BrCH}_2(\text{CH}_2)_n\text{CH}_2\text{Br}$				x		x

x indicates agreement

TABLE IX-2:

Summary of results for the long chain polar molecules in a polystyrene matrix
(high temperature absorption)

Types of molecules studied	Relaxation time increases with the increase in the number of carbon atoms	ΔH_E values increase with the increase in the number of carbon atoms	Plot of ΔS_E versus ΔH_E is almost linear and represented by the empirical relationship: $\Delta S_E = 2.2 \Delta H_E - 72$	Mechanism of dielectric relaxation molecular motion
$\text{CH}_3(\text{CH}_2)_n\text{CH}_2\text{Br}$	x	x	x	x
$\text{CH}_3(\text{CH}_2)_n\text{COCH}_3$	x	x	x	x
$\text{CH}_3(\text{CH}_2)_n\text{NH}_2$	x	x	x	x
$[\text{CH}_3(\text{CH}_2)_n]_2\text{CO}$	x	x	x	x

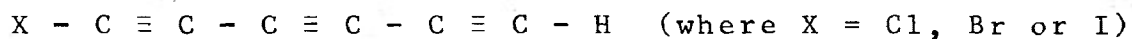
x indicates agreement

SUGGESTIONS FOR FURTHER WORK

The technique of examining the dielectric relaxations of a solute in an amorphous polymer matrix would appear very useful for the investigation of long chain polar molecules. Some further work is being carried out in this laboratory somewhat along these lines.

The low temperature absorption of the long chain polar molecules in a polystyrene matrix has been identified as the intramolecular rotation about the C-C bonds involving the movement of the polar groups. The size of the segmental unit increases as the number of carbon atoms in the chain increases. But the number of carbon atoms involved in the various segmental units of differing length has not been determined. It would be interesting to examine these long chain polar molecules by n.m.r. relaxation techniques to determine which C-C bond rotation is responsible for the low temperature absorption. The high temperature absorption process in these long chain polar molecules has been attributed to a molecular rotation. What is perhaps the most important question in the dielectric relaxation of long chain polar molecules whether the hydrocarbon chain is fully extended or coiled, remains largely unanswered. A partial

understanding of this problem would require a synthesis of long chain rigid polar molecules of the type



which is capable of exhibiting molecular rotation only. It would be of interest to compare Eyring and relaxation parameters of these long chain rigid polar molecules with those of similar-sized, long chain, flexible polar molecules.

A comparison of the Eyring and relaxation parameters of aromatic rigid polar molecules with total volume swept out on molecular rotation similar to those of long chain polar molecules may shed some light on the extent of coiling of the hydrocarbon chain.

It would be worth studying, for example, a large range of sizes of long chain polar molecules to determine whether there is an upper limit to the size of a molecule which may rotate in the polymer matrix.

Investigations of molecular relaxation in polymer matrices above the glass transition temperature could provide useful information. Such studies could yield values of the activation energy of the glass transition temperature process itself and possibly shed some light on the nature of this process.

PUBLICATIONS

This section includes a reprint of one publication by the author. In addition, the following three papers have been submitted for publication:

1. "Dielectric Studies of β -Relaxation Processes of Some Anisoles in a Variety of Organic Glasses", submitted to the Journal of Physical Chemistry.

2. "Co-operative Motion of Some Simple Hydrocarbons", accepted for publication in the Journal of Chemical Society Faraday, Transaction, II.

3. "Two Resolved Dielectric Absorption Peaks of the 1-Bromoalkanes", submitted to the Journal of Chemical Society Faraday, Transactions, II.